Biofouling Mitigation of Reverse Osmosis (RO) Membranes via Surface Modification with Nanoparticles and Polymer Brushes

Wen Ma

A Thesis

In the Department

of

Building, Civil and Environmental Engineering

Presented in Partial Fulfillment of the Requirements

For the Degree of

Doctor of Philosophy (Civil Engineering) at

Concordia University

Montreal, Quebec, Canada

August 2018

CONCORDIA UNIVERSITY

SCHOOL OF GRADUATE STUDIES

This is to certify that the thesis prepared

By: Wen Ma

Entitled: Biofouling mitigaiton of reverse osmosis (RO) membranes via surface modification with nanocomposites and polymer brushes

and submitted in partial fulfillment of the requirements for the degree of

Doctor of Philosophy (Civil Engineering)

complies with the regulations of the University and meets the accepted standards with respect to originality and quality.

Signed by the final examining committee:

_____ Chair
Dr. Alex de Visscher

_____ External Examiner
Dr. Baoqiang Liao

_____ External to Program
Dr. Muthukumaran Packirisamy

_____ Examiner
Dr. Michelle Nokken

_____ Examiner
Dr. Maria Elektorowicz

_____ Thesis Supervisor
Dr. Saifur Rahaman

Approved by _____
Dr. Fariborz Haghighat, Graduate Program Director

Friday, September 28, 2018

_____
Dr. Amir Asif, Dean
Gina Cody School of Engineering and Computer Science

Abstract

Biofouling Mitigation of Reverse Osmosis (RO) Membranes via Surface Modification with Nanoparticles and Polymer Brushes

Wen Ma, Ph.D.

Concordia University, 2018

The reverse osmosis (RO) filtration process, which uses semi-permeable membranes to achieve selective mass transport, has become the most versatile and efficient technique to produce fresh water from saline water and wastewater sources. A major challenge facing the widespread application of RO technology is membrane biofouling which is caused by the deposition and multiplication of microorganisms on the surface of the membranes required for the filtration process. Biofouling not only deteriorates membrane materials but also adds an energy burden to the system, increasing the operational cost of the RO technique. Modifying membrane surfaces with antibacterial materials is an effective technique to prevent the growth of biofilms while maintaining the original water purification capabilities of the membrane.

In this study, three district types of membrane-surface modifications were proposed as potential methods for mitigating biofouling on the RO membrane: (i) bacteria/biofilm-"defending" strategy: coating with zwitterionic and low-surface-energy polymers to prevent microorganism/protein deposition; (ii) bacteria/biofilm-"attacking" strategy: anchoring CuNPs to inhibit the propagation of microorganisms and (iii) combined bacteria/biofilm-"defending and attacking" strategy: grafting polymers and natural antibiofouling materials to not only prevent foulant deposition but potentially inhibit biofilm formation.

Hydrophilic compounds (polysulfonbetain, PSB) and low surface energy polymers (polydimethylsiloxane, PDMS) were grafted in combination to the membrane to control biofouling via the bacteria/biofilm-"defending" strategy. Results showed that surface hydrophilicity is critical

for the deposition of bacteria and protein. Combining functionalization of different fouling-resistant materials (PDMS and pSB) achieved an enhanced antibiofouling performance.

CuNPs were proposed as a cost-efficient and quality-competitive material for fabricating antibiofouling membranes with bacteria-"attacking" functions. CuNPs modified membranes exhibited bacterial inactivation comparable to the widely used silver NPs. The multiple layers of CuNPs coating on surface mitigated the permeate flux decline caused by biofouling and the flux of the modified membrane was 20% higher than the control under the same experimental conditions.

The fouling resistant membrane with a combined bacteria/biofilm-"defending" and -"attacking" function was fabricated by grafting a fouling-resistant polymer (poly(sulfobetaine methacrylate), PSBMA) and a biofilm inhibiting amino acid (poly methacryloyl-L-Lysine, PLysMA) to the membrane via a polymer length controlling technique, electron transfer-atom transfer radical polymerization atom (ARGET-ATRP). When the defending moieties (PSBMA) were predominant on the exposed top of surface with the biofilm inhibiting material (PLysMA) underneath, the membrane significantly mitigated the flux decline caused by bacterial deposition and biofilm formation (50% higher than the control). Furthermore, complete flux recovery was observed on the former after two cycles of "fouling-cleaning", while the control membrane only maintained 94% of initial flux under the same condition.

This study proposes cost-effective modifiers (CuNPs and PLysMA) for the fabrication of anti-biofouling membranes, enriches the knowledge around the application of GO in modification of anti-biofouling membranes and proposes controllable functionalization methods for the development of antibiofouling membranes. The strategies proposed in this study contribute to the investigation of novel anti-biofouling membranes and the development of facile membrane modification methods, which can further broaden the applicability of membrane processes in wastewater reclamation and increase the future fresh water supply.

Key words: reverse osmosis membrane, biofouling, nanoparticles, polymer brush

Acknowledgements

I want to acknowledge the support of Helene Linder Doctoral Fellowship from Concordia University to offer the funding support for my PhD study and NSERC as well as FRQNT for the financial support of this project. In addition, I would like to express my special acknowledgements to people who give me lots of help during my PhD study.

Most importantly, my supervisor, Dr. Saifur Rahaman, for offering me the opportunity to study in Concordia University, continuously encouraging, supporting and guiding me during the research study. His high requirement and expectation towards the research quality encouraged me to continuously improving myself. Dr. Rahaman valued collaboration with experts in different fields and sharing ideas in conferences, from which, I had opportunities to practice presenting myself and improve the communication skills. Moreover, I really appreciate his patience on me for improving both oral and writing English during five years' study. The instruction and guidance of Dr. Rahaman shaped my view in research study.

Furthermore, I appreciate Dr. Nathalie Tufenkji (Chemical Engineering, McGill University) and Dr. Zhibin Ye (Material and Chemical Engineering, Concordia University) for giving professional suggestion and instruction on biological and organic chemistry part of my experiment, respectively. They helped correcting part of the writing in this thesis. I would like to thank Dr. Michelle Nokken for borrowing us the glove box which is very important for of one my experiment. I appreciate the members of my thesis committee, for their precious comments and suggestions, which are not only valuable in polishing this thesis but also treasures for my future research.

Moreover, I would like to thank the technicians of BCEE department, especially Hong Guan and Joseph Hrib. They helped us for the building, installation, training and maintenance of most setups in our lab. Joseph helped for the design and manufactory of one special polymerization reactor used in my work, I could not finish the experiment in time without his help.

In addition, I would like to extend my regards to my friends and colleagues, especially Sharmin Sultana, Tiantian Chen and TranVan Anh Luong, for their friendship and knowledge.

Finally, my deepest gratitude goes to my husband, Ruibiao Song, who has been always there for me; to my parents and my younger sister, for their unconditional love and support.

Co-authorship Statement

Chapter 3 Controlling biofouling via "defending" strategy: surface modification via grafting patterned polymer brushes

This chapter is part of the published article：

Controlling biofouling of reverse osmosis membranes through surface modification via grafting patterned polymer brushes

Author(s): Wen Ma[1], Md. Saifur Rahaman[1*] and Heloise Therien-Aubin[2]

[1] Department of Building Civil and Environmental Engineering, Concordia University, Montreal, Quebec, Canada H3G 1M8,

[2] Department of Chemistry, University of Toronto, 80 St. George Street, Toronto, ON, M5S 3H6, Canada

[*] *The corresponding author*

Wen Ma organized the experiment data, constructed the graph and wrote the manuscript. Dr. Saifur Rahaman conducted the membrane performance evaluation tests and revised the manuscript. Dr. Heloise Therien-Aubin fabricated all the membranes required in this paper.

Chapter 4 Controlling biofouling via "attacking" strategy: spray- and spin-assisted layer-by-layer assembly of copper nanoparticles on membrane for biofouling mitigation

The following subsections, "materials and discussion", "results and discussion" as well as "conclusions" are from the published article：

Spray-and spin-assisted layer-by-layer assembly of copper nanoparticles on thin-film composite reverse osmosis membrane for biofouling mitigation

Author(s): Wen Ma[1], Adel Soroush[1], Tran Van Anh Luong[1], Gregory Brennan[1], Md Saifur Rahaman[1*], Bahareh Asadishad[2], Nathalie Tufenkji[2]

[1] Department of Building Civil and Environmental Engineering, Concordia University, Montreal, Quebec, Canada H3G 1M8,

[2] Department of Chemical Engineering, McGill University, Montreal, QC, H3A 0C5, Canada

[*] *The corresponding author*

Wen Ma participated in all the experiment conduction, material characterization, graph construction and manuscript preparation. Adel Soroush (master student) helped for the antimicrobial-performance evaluation and manuscript revision. Tran Van Anh Luong (undergraduate student) helped for the membrane modification and characterization. Gregory Brennan (undergraduate student) helped the equipment installation. Dr. Saifur Rahaman proposed and supported this project and critically reviewed the manuscript. Dr. Bahareh Asadishad offered the training of bacterial experiment. Dr. Nathalie Tufenkji critically reviewed the manuscript.

Chapter 5 Controlling biofouling via "attacking" strategy: cysteamine- and graphene oxide mediated copper nanoparticle decoration on membrane for enhanced anti-microbial performance

The following subsection: "materials and discussion", "results and discussion" as well as "conclusions" are from the published article：

Cysteamine-and graphene oxide-mediated copper nanoparticle decoration on reverse osmosis membrane for enhanced anti-microbial performance

Author(s): Wen Ma[1], Adel Soroush[1], Tran Van Anh Luong[1], Md Saifur Rahaman[1*]

[1] *Department of Building Civil and Environmental Engineering, Concordia University, Montreal, Quebec, Canada H3G 1M8*

[*] *The corresponding author*

Wen Ma participated in all the experiment measurement, material characterization, graph construction and manuscript preparation. Adel Soroush (master student) revised the manuscript. Tran Van Anh Luong (undergraduate student) helped for the membrane modification, characterization and performance evaluation. Dr. Saifur Rahaman proposed and supported this project and critically reviewed the manuscript.

Chapter 6 Controlling biofouling via "defending and attacking" combining strategy: surface modification with fouling-resistant/biofilm inhibition polymer

Wen Ma participated in all the experiment measurement, material characterization, graph construction and manuscript preparation. Dr. Zhibin Ye (Chemical and Materials Engineering) offered the instruction on polymerization process. Dr. Nathalie Tufenkji kindly provide the Gram-positive bacteria (B. subtilis, ATCC6633). Dr.

Saifur Rahaman proposed and supported this project and critically reviewed the writing.

Table of Contents

List of Figures

List of Tables

List of Abbreviations

RO	Reverse osmosis	TFC	Thin Film Composite
NF	Nanofiltration	PA	Polyamide
UF	Ultrafiltration	GO	Graphene oxide
MF	Microfiltration	CNT	Carbon nanotubes
NPs	Nanoparticles	Cys	Cysteamine
CuNPs	Copper nanoparticles	EPS	Extracellular polysaccharide substances
PSB	Polysulfonbetain	NOM	Natural organic matter
PDMS	Polydimethylsiloxane	PEG	Poly(ethylene glycol)
LbL	Layer-by-layer	MPD	Phenylene diamine
PLysMA	Poly (methacryloyl-L-Lysine)	TMC	Trimesoyl chloride
SSLbL	Spray- and spin-assisted layer-by-layer	ROS	Reactive oxygen species
PLL	Poly L-Lysine	PVA	Carbon nanotubes
PEI	Polyethyleneimine	PEI	Polyethyleneimine
PAA	Poly(acrylic acid)	PAH	Poly(allylamine) hydrochloride
G^+	Gram-positive	PSS	Poly(sodium- 4-styrene sulfonate)
G^-	Gram-negative	QS	Quorum sensing
PVDF	Polyvinylidene fluoride	DI	Deionized water
PES	Poly(ether sulfones)	PAA	Poly(acrylic acid)
APTES	3-Aminopropyl)triethoxysilane	PSBMA	poly(sulfobetaine methacrylate)
PDA	Polydopamine	CFU	Colony forming unit

XPS	X-ray Photoelectron Spectroscopy	LB	Luria-Bertani broth
EKA	Electrokinetic analyzer	BSA	Bovine serum albumin
AFM	Atomic force microscope	*E.coli*	*Escherichia coli*
SEM	Scanning electron microscope	*E. Faecalis*	*Enterococcus faecalis*
TGA	Thermogravimetric analysis	*B. subtilis*	*Bacillus subtilis*
TEM	Transmission electron microscopy	OD	Optical density
ICP-MS	Inductively coupled plasma mass spectroscopy	PI	Propidium iodide
CLSM	Confocal laser scanning microscope	ED	Ethylenediamine
ARGET-ATRP	Activators regenerated by electron transfer-atom transfer radical polymerization	NHS	N-Hydroxysuccinimide
EDX	Energy-dispersive X-ray spectroscopy	EDC	N-(3-dimethylaminopropyl)-N′-ethylcarbodiimide hydrochloride
FTIR-ATR	Fourier transform infrared pectroscopy equipped with an attenuated total reflectance single logic accessory	HEPES	4-(2-hydroxyethyl)-1-piperazineethanesulfonic acid
BiBB	α- bromoisobutyryl bromide	MES	2-(N-morpholino)ethanesulfonic acid
EDTA	Ethylenediaminetetraacetic acid	SDS	Sodium dodecyl sulfate

Chapter 1. Introduction

1.1 Problem statement

The global fresh water crisis is widely considered to be one of the most critical challenges currently faced by mankind [1]. Water reuse and desalination are considered the most feasible ways to alleviate the issue. Through a superior water purification performance, the smaller physical footprints, and a lower construction cost [2], reverse osmosis (RO) has proven to be a competitive technology for various types of wastewater treatment and desalination of brackish water/seawater. With a decrease in required energy [3], this technology is more appealing and the number of desalination plants using the RO process continues to increase. Therefore, it is apparent that that RO will play an important role in securing fresh water supplies into the future.

Since their development in the 1970s, thin film composites (TFC) have served as the core component of RO membranes [4]. The standard material [3], polyamide (PA), with a thickness of only 50-230 nm, is used as the top active layer of TFC membranes, contributing to their exceptional water permeation and salt rejection performance[5]. However, the major drawback of the polyamide membrane is biofouling, which limits its widespread application [6]. Biological substances are ubiquitous in any water treatment environment, and once they adhere to a membrane, bacteria and metabolites generated during cell growth lead to biofilm formation on the membrane surface, causing irreversible degradation of the membrane material. Biofouling not only affects the membrane's lifespan but also adds an energy burden, consequently becoming a major constraint to broader application current RO desalination techniques [7].

Developing an effective, biofouling-resistant TFC membrane is crucial to increasing the widespread application of RO and its broader contribution to relieving the global water crisis. With this goal in mind, selecting effective antibiofouling material sand facile modification methods for fabricating fouling-resistant membranes have become attractive topics of study in membrane community.

Many studies have been conducted to investigate the prevention of polyamide membrane biofouling via incorporation of antibiofouling materials. The main concept is to make membranes able to "defend" and "attack" bacteria or biofilms. The bacteria/biofilm-"defending" surface refers to a membrane surface which has a low interaction with bacteria. Since it is generally accepted

that surface charge, hydrophilicity, and roughness are closely related to irreversible fouling [6], investigation related to a membrane anti-fouling property has mainly aimed at enhancing hydrophilicity [8], reducing roughness [9] and decreasing charge density [10] to reduce microorganismal adhesion. The bacteria/biofilm-"attacking" surface could either inhibit the propagation of bacteria by inactivating cells or disrupt the biofilm structure to prevent biofouling.

Traditional polymers with certain fouling resistant functionalities are materials which have been widely studied for membrane surface modification. Since bacterial cell adhesion and their growth on the membrane surface are the promoters of biofouling, different polymers have been used to reduce attachment propensity and the viability of bacteria on surfaces. According to the antimicrobial mechanism, the polymeric coatings are divided into "biocidal coatings" (to kill bacteria, such as quaternary ammonium), "antifouling coatings" (to reduce bacteria adhesion, such as zwitterionic polymer), and "fouling release coatings" (to provide weak foulant/surface adhesion thus allowing foulants to be easily washed off). Currently, investigating natural antibiofouling materials to prevent the biofouling in an environmentally friendly manner has been gaining growing interest.

Aside from exploring those effective and green polymeric materials, nanotechnology offers a different route to address the problem of biofouling. Because of their ultra-small size, the variety of functional units, free energy, and active reaction sites found with nanoparticles (NPs) are amplified thousands of times. Thus, NPs with antibiofouling function could enhance the biofouling-resistance with little effect on the performance of the original membrane. Furthermore, NPs modification could render the polyamide membrane with combined properties of both organic and inorganic materials, and supply specific novel advantages in respect to chemical resistance, fouling mitigation and protection from the harsh wastewater environments [11]. Therefore, NPs with antibiofouling functions are now attracting great interest in the membrane community.

Incorporating bacterial/biofilm-"defending"/"attacking" polymers or NPs into the membrane structure to develop antibiofouling membranes is another challenge of our work. Blending modification materials directly into membrane casting solution has been the convenient, low cost method for modification; however, since most of the functional agents are buried in the inner structure of the membrane, the anti-biofouling effect was largely compromised.

Recently, direct surface modification with functional materials have attracted more and more interest. By anchoring modifiers onto the membrane surface to directly contact the bacteria/biofilm, the function of the material could be effectively elaborated. Since a thin polyamide layer was maintained during the surface modification process, a proper antibiofouling surface modification not only mitigates biofouling, but also help membranes maintain superior water perm-selectivity [12-14].

1.2 Objectives of this study

As discussed above, growing global water and energy crises urge exploration and development of environmentally sustainable water purification technologies. Membrane-based processes have been considered as some of the most appealing options in this regard. However, membrane biofouling has been one of the main problems inhibiting widespread application of the RO technique. Developing antibiofouling membranes to reduce the adhesion and propagation of bacteria/biofilm would be an effective strategy to solve this problem.

The objective of this study is to propose environmentally friendly, yet effective bacteria/biofilm-"defending" and -"attacking" polymeric/nano- materials, as well as the corresponding facile and controllable modification methods, to modify a commercial RO membrane and improve its antibiofouling performance.

The surface modified commercial membrane would not only maintain its distinctly superior water purification qualities but also suffer from less irreversible fouling caused by microorganismal breeding and colonization that occurs during operation. The developed antibiofouling membrane is expected to increase the lifespan of the membrane used in the RO process and decrease the energy consumption during the water filtration. Finally, these advantages would contribute to an overall decrease in operational costs of the RO technique and increase the ability for the membrane process to relief the global fresh water crisis in the future.

To achieve this goal, this study proposes three types of surface modification strategies with different antibiofouling mechanisms. The specific objectives and research plan are listed as following:

- To select effective, low cost, and environmentally friendly modifiers that possess biocidal/anti-fouling properties for membrane surface modification;

- To propose the corresponding surface modification methods that could stably anchor modifiers while exhibiting little impact on the distinct water purification qualities of the membrane;
- To investigate the potential of fabricating antibiofouling membranes with combined fouling-resistant and biofilm inhibiting strategies.

1.3 Outline of thesis

Chapter 2 is a comprehensive literature review. It introduces the principles of RO technique, physiochemical properties of TFC polyamide membrane, how biofouling occurs, the widely used methods for prevention of biofouling, and well-studied materials/strategies for biofouling control. This information helps to understand why biofouling happens in the membrane process, why physiochemical properties are important for biofouling control on the membrane surface and what is the current research trends are in terms of solving biofouling in membrane processes.

Chapter 3 presents a study which applies the bacteria-"defending" strategy to fabricate an antibiofouling membrane. Two types of functional polymers which have fouling-resistant and fouling-release functions were grafted (by themselves and in combination) on polyelectrolytes mediated membrane to prevent biofouling. It is the first time that the effect of horizontal patterning of these two types of polymers has been investigated.

Chapter 4 and Chapter 5 introduce two studies which apply a bacteria-"attacking" strategy in the fabrication of antibiofouling membrane. CuNPs have been proposed as cost-effective biocides in both two studies; however, two methods to render monolayer and multi-layer CuNPs have been proposed. For the first time, automatic spray- and spin-assisted LbL processes were used in membrane surface modification to offer a uniform NPs layer.

Chapter 6 proposes a modification method which could easily and controllably load different types of polymeric modifiers to fabricate antibiofouling membrane with bacteria/biofilm-"defending" and "attacking" properties. For the first time, GO has been proposed as a modification media for polymeric modification on membrane surface via this method; furthermore, this is the first investigation of the potential of applying this method to fabricate a poly (amino acid) layer on a polyamide membrane to mitigate biofouling.

Chapter 7 is a summary of the contributions and conclusions of this thesis. The limitations and possible future work identified in this thesis have also been discussed.

Chapter 2. Literature review

2.1 Principles and applications of RO

2.1.1 RO plays an important role in water reuse and desalination

The global fresh water crisis is considered as one of the most critical challenges currently faced by the international community. Although 70% of the earth's area is covered by water, fresh water available for direct human consumption accounts for only 0.007% of global source water, as the remainder is either found in seas and oceans, or locked in glaciers and snow, none of which are easily and economically accessible. Furthermore, this tiny reserve of source water is unevenly distributed, with 65% of it concentrated in less than 10 countries. Increasing contamination of surface/ground water, along with the rapid growth of the world's population and, along with it, industries, adds further burdens on already insufficient fresh water resources. National Geographic reports [15] that by 2025, nearly 1.8 billion people will live in areas that are water-scarce, and two-thirds of the world's population will live in areas that are water-stressed. This water crisis not only hinders sustainable societal and economic development but increases global environmental damage and leads to human health risks.

Wastewater reuse and seawater desalination have been considered as highly feasible ways to alleviate water scarcity. Reverse osmosis (RO) has proven to be a competitive technology for various types of waste water reclamation and brackish/seawater desalination due to its superior efficiency in the removal of small-sized contaminants (salt, metal ions, pharmaceuticals, organic colloid, etc.), its smaller physical footprint requirements, and lower construction costs [2] in comparison to traditional treatment methods such as thermal distillation and electro dialysis. In industry, the RO technique is applied to ensure that effluent discharge, such as boiler feed [16], electronic industry effluent [17], and pharmaceutical waters [18], meet established government restrictions and quality standards [19], or to achieve "zero liquid discharge wastewater" industrial processes. In desalination processes, the cost of sea water reverse osmosis (SWRO) desalination is reported to be one-half to one-third of the cost of thermal distillation [2]. At present, RO processes are employed by approximately 60% of the world's desalination plants, and this number continues to increase while total RO energy consumption decreases [3]. Aside from application in industry wastewater treatment and desalination, small RO based setups for domestic usage have been

gradually appearing in the commercial market. These small drinking water purification systems installed in conjunction with water tanks can remove scale deposit and metal ions, such as Pb^{2+}, Ca^{2+}, Mg^{2+}, Cu^{2+}, etc., accumulated in the water distribution process. Therefore, it should be noted that RO is already poised to play an important role in the fresh water supply of the future.

2.1.2 RO membrane process and materials

Reverse osmosis (RO) is a high-pressure, membrane-based process which utilizes a dense membrane to separate water from molecular sized contaminants, such as dissolved organic compounds, colloids, and monovalent ions (e.g., Na^+, Cl^-) [20]. In microfiltration (MF) and ultrafiltration (UF) processes, membrane pore structure is designed to remove containments based upon their size (size exclusion mechanism) [21], and only the contaminants with a size larger than the membrane pore can be retained. The pore size range of different types of membranes and examples of their applications in removing contaminants are illustrated in Figure 2.1. The pore size of RO membranes, however, needs to be about 0.1 nm. It is also claimed that there are no distinct pores in RO membranes and water transport through the membrane follows a 'solution-diffusion' mechanism [22]. In this hypothesis, molecular water on the feed side is absorbed on the polymer surface of membrane via hydrogen bonding, then diffuses through the cave of polymeric molecules due to the concentration gradient, finally desorbing from the membrane and becomes available in the bulk permeate solution [23] (Figure 2.2). Due to its super-highly water-selective nature, reverse osmosis is considered an advanced water purification processes and it is applied as a point-of-use water treatment unit.

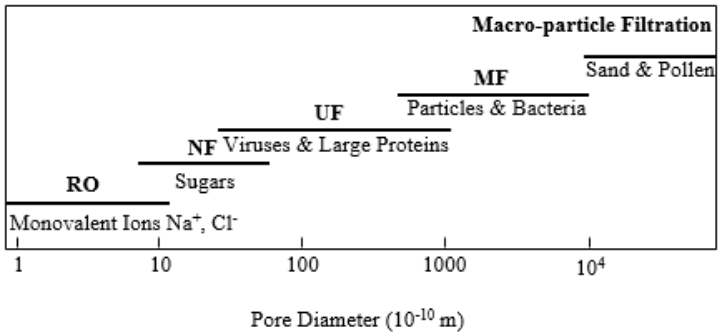

Figure 2. 1 Range of nominal pore diameters of commercially available membranes [21].

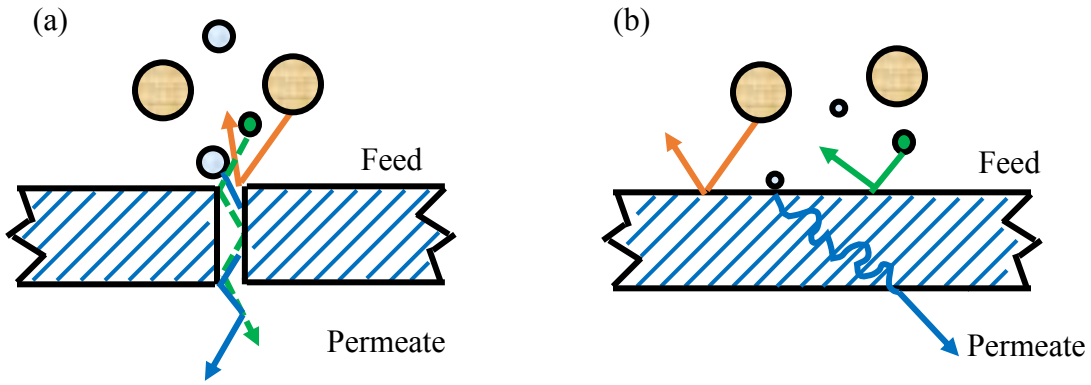

Figure 2. 2 Contaminants transport via (a) size exclusion (macro filtration, MF, UF, etc.) and (b) solution diffusion (NF, RO) mechanisms in a membrane process.

The semi-permeable membrane is the core component of the RO process. The first generation of commercialy available RO membranes were developed by Loeb and Sourirajan in the 1960s using cellulose acetate (CA) via phase inversion [4]. After this, more and more studies related to advanced membrane fabrication materials and optimized membrane structures were conducted to improve the RO process, focused on higher water permeation and salt rejection. In the early 1980s, a polyamide (PA) casted membrane with a thin film composite structure (TFC) was introduced by the Film Tec corporation [24]. Compared with CA membranes, TFC membranes displayed higher water permeability and could be operated at relatively higher temperatures and pressures over a wider range of pH values (pH 4-7 for CA, pH 3-11 for PA). Thin film composite is still regarded as a "state-of-art" material in RO process [4] and has gradually become the predominant form of commercial RO membrane.

A typical TFC reverse osmosis membrane is fabricated from three types of materials (Figure 2.3) [25], (1) a dense top layer, (2) a porous polysulfone support layer in middle, and (3) a non-woven fabric bottom layer. The top layer plays a critical role in separation, whereas the middle layer offers water permeation benefits and the bottom layer provides mechanical strength.

Figure 2. 3 Thin film composite structure of RO membrane with TFC structure [25].

Water permeation and salt rejection of the membrane seem to have a "trade-off" type of relationship. To achieve effective water separation performance at low energy costs, the top layer of RO membrane needs to be very thin, in order to reduce hydraulic resistance. Furthermore, the material needs to be highly crosslinked to retain ultra-fine contaminants.

Polyamide (PA) is a widely used material for the fabrication of commercial TFC membranes. PA active layers are formed through cross-linking between trimesoyl chloride (TMC) and m-phenylene diamine (MPD) (Figure 2.4). Due to the hydrolysis of unreacted TMC in aqueous solutions, membrane surfaces possess negative charges at neutral pH conditions [26]. The PA layer formed is relatively hydrophobic and shows a contact angle of approximately 70°. In order to improve the water affinity of the membrane surface and achieve greater water permeation flux, most commercial membranes are now coated with a hydrophilic polymer layer, such as poly(acrylic alcohol) (PAC) or poly(ethylene glycol) (PEG), which can lead to an improved contact angle range of 40°-50°.

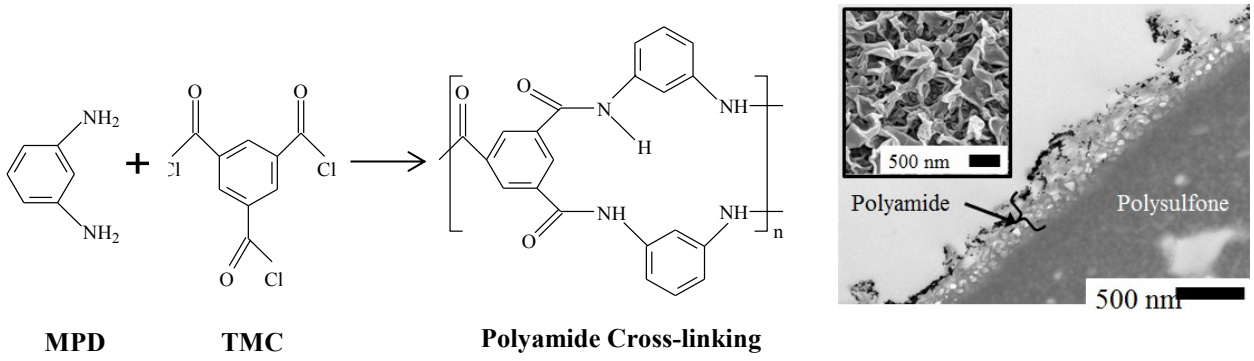

Figure 2. 4 Polymerization of MPD and TMC to form polyamide thin film [3].

2.2 Biofouling is a severe challenge of the RO process

2.2.1 Formation and consequences of biofilms

Feed water in RO systems generally contain four main types of contaminants: inorganic compounds (salts, metal hydroxide, metal carbonate, etc.), natural organic matter (NOM), gel-colloids, and bacteria. During long operational periods, these contaminants may be retained on the membrane surface and form an additional "foulant" layer, affecting membrane performance (Figure 2.5). Periodic physical/chemical cleaning is necessary [27] to maintain the desired flux of the RO membrane. Inorganic fouling, such as scaling and precipitates, can be removed by acid washing or hydraulic cleaning [28]. Selecting an effective pre-treatment can reduce the organic fouling caused by NOM; however, biofouling, resulting from bacterial growth, cannot be easily controlled by any of these methods. Biofouling accounts up to 35-45% of all fouling in the RO process [29].

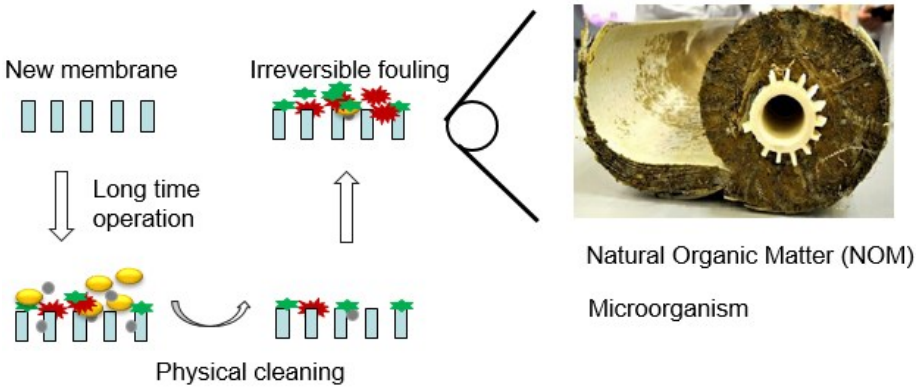

Figure 2. 5 Formation of irreversible fouling on polyamide membrane.

The development of biofilms on membrane surfaces usually follows four steps [30] (Figure 2.6): (1) attachment of bacteria on the membrane surface; (2) bacterial adhesion and growth of new cells; (3) formation of bacterial colonies; and (4) release of cells to form new colonies in other places. Biological substances are unavoidable in any water treatment environment. Even if 99.9% of the bacteria are destroyed in the pretreatment process, those entering the RO system may deposit on the membrane surface and start the formation of a biofilm. Due to the non-porous layer, almost all organic molecules (organic acids, proteins, polysaccharides, etc.) can be retained on the membrane surface during the filtration process. The adhered bacteria may utilize these organic compounds as a source of nutrients and multiply further forming more bacterial colonies.

Extracellular polysaccharide substances (EPS) are the metabolites generated during the cell growth process; consisting mainly of polysaccharides, proteins, lipids, humic substances, and DNA [31]. It is reported that EPS accounts for 50-90% of the organic compounds in a biofilm [32]. The EPS encases cells into its polymeric structure and changes the physical-chemical properties (hydrophilicity, zeta potential, surface energy, roughness, etc.) of a membrane surface, which in turn may cause more settlement and deposition of organic containments. Accumulated bacteria may be further released from the colony and relocate onto other parts of the membrane surface, starting a new bacterial colony, and further spreading the biofilm.

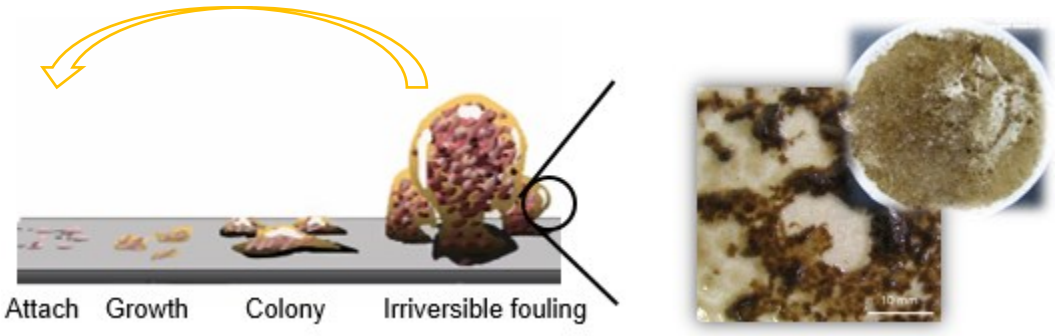

Figure 2. 6 Bacteria cell deposition and multiplication on a membrane surface.

The gradual growth of bacterial colonies within the EPS polymer eventually forms an intact and stable bio-layer across the membrane surface. EPS not only enhances the adhesion of the biofilm, but also shields the microorganism from the biocidal components of the cleaning process [33]. Long-term growth of the biofilm can degrade membrane materials and cause irreversible fouling of the RO membrane [29]. Research also shows that the commonly used disinfectant sodium hypochlorite was only effective against free bacterial cells and exhibited only slight inactivation ability against biofilm capsuled cells [33]. Biofouling not only affects the membrane's lifespan but also adds an energy burden and consequently inhibits widespread application of RO technique [30].

2.2.2 Biofilm prevention and mitigation

Biofouling cannot be completely controlled. However, proper pretreatment, chemical washing, and development of anti-biofouling membranes are effective ways to mitigate biofouling and improve membrane lifespan [3].

(1) Pretreatment

E.coli bacteria range from 800 nm to 3 μm in size, therefore, microfiltration (0.1 to 10 μm) and ultrafiltration (10 nm - 1μm) can be applied as pretreatment processes to reduce the quantity of bacteria. It has been claimed that 90-100% of these pathogens can be removed through the UF process. Nonetheless, biofouling of UF membranes is a major challenge.

Applying an oxidizing agent to pre-disinfect the feed solution can halt the growth of bacteria in the feed solution. Due to the longer residual time and lower cost, chlorine based detergents (typically 0.2-1 mg/L of OCl^- solution) [28] are widely used cleaning chemicals in industry; however, resulting from the N-chlorination reaction of amide linkages (-CONH-) and the corresponding ring-chlorination reaction via "Orton-rearrangement" of aromatic polyamide chains (figure 2.7) [34], the cross-linked polyamide net-working of the membrane is vulnerable to the chlorine-based oxidative attack and causes a decline in salt rejection after chlorine exposure.

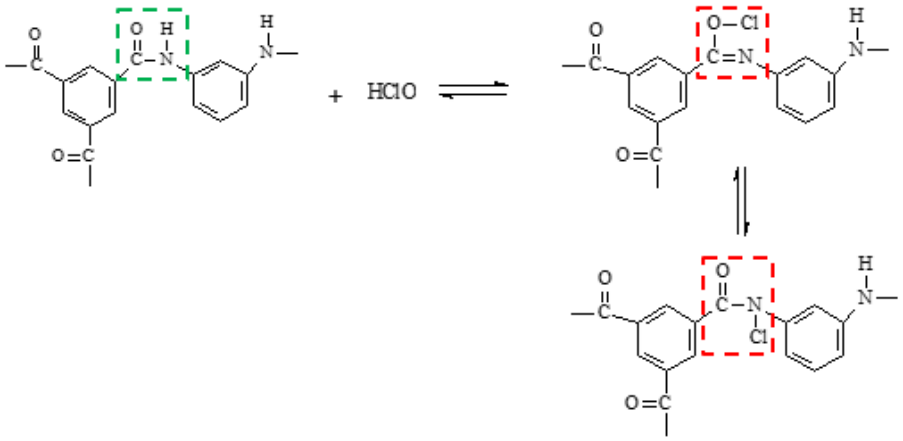

Figure 2. 7 Chlorine attack on polyamide structure.

(2) Membrane cleaning

Frequent membrane cleaning is another important way to mitigate irreversible fouling and it is suggested by most commercial RO membranes (Lennetch, Dow Filmtec™, GE, etc.,) when one or more of the following signs are exhibited: (1) a normalized water permeate flux decrease of 10%; (2) a normalized salt transportation increase of 5 - 10%; (3) a normalized trans-membrane pressure (TMP) increase of 10 - 15%.

In practical cleaning-in-place (CIP) processes, different chemicals and procedures are required to effectively clean the biofouling-contaminated membranes. Typical CIP steps combine alkali, surfactant, acid, enzyme, surfactant, and sanitizer washing [35].

(a) Since calcium ions (Ca^{2+}) are one of the main causes of EPS formation [31], alkali solutions (soda) are applied to dissolve the calcium deposition in the EPS metrix and loosen the biofilm structure;
(b) Surfactants [35] (Tween-80, SDS, dobanic acid, etc.) can enhance the wettability of the organic biofilm and thereby increase the contact between cleaners and the biofilm structure;
(c) Acid solutions remove most of the salt ions encapsulated in biofilm;
(d) Enzyme based cleaners composing of proteases, phosphatases, amylase, and phospholipase. The combination of different functionalized enzymes helps to remove proteins, DNA, lipids, and polysaccharide substances in the biofilm. The cleaning mechanism of the enzyme cleaners is introduced in subsection 1.3.2.
(e) Oxidizing sanitizers, such as sodium hypochlorite, are effective in the freeing/dissociation of cells. They generate reactive oxygen species (ROS) that attack thiol groups containing moieties and unsaturated fatty acids. As a result, bacterial cells are gradually unable to multiply by themselves. Quaternary ammonium based sanitizers are effective against both dissociated and EPS metric capsuled cells[35]. The sanitizers mostly attack ammo acid substances (proteins, nucleic acid), which causes cell membrane breakdown, followed by leakage of intracellular substances.

Membrane washing unavoidably increases the operational costs of the RO process. Another concern related to chemical cleaning is that, according to recent research, a NaClO washed membrane is more vulnerable to biofouling, which may be attributed to the fact that suspended bacteria tend to attach to the membrane surface in order to reduce the exposure to damage potential[36].

(3) Developing anti-biofouling membrane

Development of novel fouling resistant membranes is considered to be a promising method to reduce the energy consumption of the RO process. New materials with high water affinity, such as graphene oxide[37], carbon nanoparticle tubes [38], and aquaporin [39] are being tested to replace polyamides for the fabrication of ultra-high water-permeable membranes, thereby improving water purification efficiency. According to the research, these novel membranes showed three to six times more water flux as compared to the current TFC membrane [3]. However, problems with these

new materials, such as inadequate salt rejection, high costs and unstable membrane physiochemical properties weaken their potential to be used in practical applications [3].

Modifying polyamide surfaces of TFC membranes with anti-fouling and biocidal agents to reduce bacterial cell attachment and viability is yet another way to develop anti-biofouling membranes. Recent studies and literature related to this topic are introduced in section 2.3.

2.3 Developing anti-biofouling membranes

Recent research related to the production of anti-biofouling surfaces is mainly based on modifying membrane surface properties with functionalized polymers and nanoparticles (NPs). According to different biofouling control mechanisms, these studies could be divided into three types: (1) "defending", making membranes more hydrophilic and less active (low surface energy), to resist the adhesion of relatively hydrophobic bacteria; (2) "attacking", improving the anti-bacterial properties of TFC membranes through grafting and anchoring of biocidal agents, (biocidal polymers, metal nanoparticles, organic peptides, enzymes, etc.); and (3) combinations of "defending" and "attacking" modifications.

2.3.1 Anti-biofouling membranes via a "defending" strategy

The modifiers applied in the "defending" modification are mainly polymers and functionalized nanoparticles. Since the physical-chemical properties of the surface are closely related to cell attachment rates, modifications of the RO membrane to reduce bacterial adhesion are generally aimed at making the surface relatively hydrophilic and less active (lower surface energy). By reducing the adhesion of the organic foulants, biofilm formation can be reduced.

1. Hydrophilic surface

Polymers used for membrane surface modification usually contain functional groups of high water affinity or those that are easily hydrolysable, such as hydroxyl (-OH), carboxyl (-COOH), and amine ($-NH_2$).

(a) Hydroxyl (-OH) group-based polymers

High levels of -OH functional groups can increase the hydrophilicity of the membrane, thereby repelling hydrophobic bacterial cells. It has been reported that -COOH groups of polyamide chains

can react with the -OH of the polymer and form a strong hydrogen bond, weakening the dissociative ability of the pendent -COOH, and reducing the surface charge of the polyamide membrane at high pH conditions. Both the increase in hydrophilicity and the reduction of charges on the membrane surface could significantly improve the membrane's resistance to organic foulants.

Polyethylene glycol (PEG) has been the benchmark anti-fouling polymer for many years, applied to membrane surfaces to reduce organic fouling. According to the literature, the attachment of organic proteins on membrane surfaces leads to a compression of PEG chains and resulting in a repulsive elastic force [40]. The longer the PEG chain, the greater the protein and bacterial resistance of the membrane surface [41].

Polyamide membrane surfaces could be easily coated with Poly(vinyl) alcohol (PVA) via physiochemical adsorption within a short time (around 5 min) [42]. In order to improve the stability of PVA coating, researchers have also immobilized the PVA layer via using a thermally initiated free radical grafting method [34]. The contact angle of the membrane is reduced from 60° to 40° and the zeta potential of the polyamide membrane is reduced from -55 mV to -20 mV after PVA grafting [34]. The grafted PVA layer also improves the chlorine resistance of the polyamide membrane via occupation of the N-chlorination reaction sites in aromatic polyamide chains.

(b) carboxyl (-COOH) and amine ($-NH_2$) groups-based polymers (polyelectrolytes)

Polyelectrolytes are polymers that carry ions on the chain, which dissociate as polycations/polyanions in water. Polyelectrolyte solutions possess similar properties to both polymers and salts, being both viscous and electrically conductive. Although polyelectrolyte coatings show an affinity to water, they may attract contaminants (protein, metal ions, microorganism) of the opposite charge. Therefore, instead of a single type of polyelectrolyte coating, a neutral-polyelectrolyte layer, produced by self-assembly of polycations and polyanions, can be applied as an anti-biofouling modification.

Polyethyleneimine/poly(acrylic acid) (PEI/PAA) and poly(allylamine) hydrochloride/ poly(sodium- 4-styrene sulfonate) (PSS/PAH) are commonly used polyelectrolyte coatings for membrane surface modifications. Due to their opposite charge, polycations and polyanions can be alternatively deposited on the substrate through electrostatic force [13]. As no harsh chemical

reactions occur during the procedure, the properties of the original membrane would not be affected by multiple film modifications[43].

Polyelectrolyte coatings attracts water molecules via ion moieties and they can decrease the contact angle of TFC membrane from 52° to 20° [44]. Moreover, some polyelectrolytes, such as PEI, also show certain antimicrobial properties [45, 46] (the mechanism is explained in section 2.3.2), which enhance the anti-fouling properties of the RO membrane. Although possessing the advantages mentioned above, concerns related to the stability of multiple layers in various pH and saline solutions have been noted by researchers.

(c) Polyzwitterions

Different from polyelectrolytes which contain only negative/positive moieties, polyzwitterions contain dipolar ions, resulting in a neutral molecule with both positively and negatively charged units across the polymer chain. It is also known as an "inner salt". The charged groups on polyzwitterionic chains are ideal hydrogen bond acceptors/contributors, leading to a unique water affinity in polyzwitterionic compounds [47]. A layer of strongly bound water molecules at the interface of a polyzwitterion layer offers a repulsive force to hydrophobic contaminants and limits the adhesion of organic species [48].

Zwitterionic coatings, such as poly(carboxybetaine) (PCB), poly(sulfobetaine) (PSB), or poly(phosphorbetain) (PPB), have been shown to be highly resistant to nonspecific protein adsorption, bacterial adhesion, and biofilm formation on TFC membrane surface [49]. These three polymers offer hydrophilic layers on the membrane surface via the same mechanism, while demonstrating differing anti-biofouling performances due to their varied negatively charged units. PPB was reported to show the highest anti-biofouling performance and stability under various water qualities; however, the price of PPB is relatively high in comparison to the others [50]. The ability to resist protein adsorption for PCB is highly dependent on pH (5-9), in contrast, PSB and PPB polymers are less pH sensitive (PSB, 3-10; PPB, 1-10) [51]. Among these polyzwitterions, PSB is both highly availability and offers stable anti-biofouling performance; therefore, it has been the most studied material for membrane surface modification in terms of improving anti-biofouling properties. According to studies, after grafting pSB polymer to the TFC membrane surface, the contact angle significantly decreased from 55° to 25°. After a 48 h filtration test, a 57% decrease in protein attachment was observed as compared to the unmodified membrane [52].

By increasing the length of the polymer chain, the bonded water layer would be correspondingly thicker. This type of polymer is what is called a "polymer brush" (Figure 2.8). The coated anti-fouling polymer coating, such as PEG or PSB, is also called an "anti-fouling polymer brush".

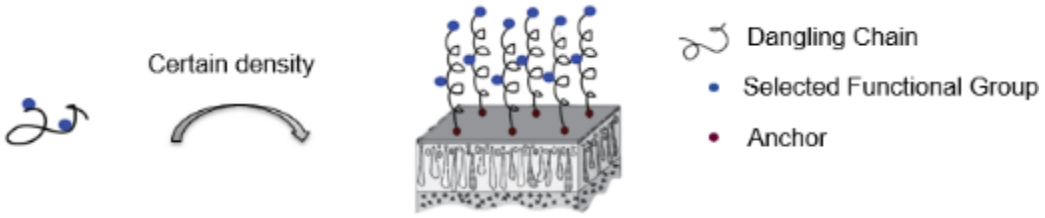

Figure 2. 8 Grafting polymer brush on membrane surface to reduce biofouling.

(d) Hydrophilic nanoparticles

Even though the functionalization of various polymers offered significant improvements to membrane hydrophilicity, it is difficult to decrease the membrane contact angle much below 40° [53]. Hydrophilic nanoparticles (NPs) are another potential material for coating. According to different application purposes, NPs are usually modified with polymers to achieve the selected functional units. Resulting from their ultra-small size, the functional units, free energy, and active reaction sites of NPs can be amplified thousands of times [54]. Therefore, compared with functionalized polymers and polyelectrolytes, NPs now attract more and more interest from the membrane community for their function in anti-bacterial membrane coatings. Many types of nanoparticles with hydrophilic or super-hydrophilic properties, such as silicon [55,53], functionalized carbon nanotubes (CNT)[56], graphene oxide (GO), zeolite [57, 58] and chitosan [59], have been applied to improve the water affinity properties of a membrane. Since they are naturally porous and negatively charged in water system, they not only contribute to the hydrophilicity of the membranes but also act as additional water channels to improve water flux and fouling rejection.

2. Low-energy surface

Membrane surface energy refers to intermolecular bonds between the membrane surface and other species (water, contaminants). Low surface energy indicates weak foulant/surface adhesion, and as a result, dead bacterial cells or organic foulants that settle to the membrane surface can be easily washed off [60]. Surface energy closely relates to the physiochemical properties of surface materials (roughness, hydrophilicity, charge). "Fouling release polymer brushes", such as

Poly(dimethylsiloxane) (PDMS) and perfluorinated, are traditional modifiers used to create low-surface energy membranes [60].

In a previous study, a near 25% reduction of surface energy was observed on a polyamide membrane after PDMS grafting [61]. Although PDMS is a relatively hydrophobic material and showed little contributions toward prevention of bacterial cell deposition, the attached cell quantity significantly decreased after rigorous washing.

2.3.2 Anti-biofouling membranes via an "attacking" strategy

Different from the "defending" strategy, which aims to reduce the attachment of bacteria to the membrane surface, the "attacking" strategy employs a biocidal surface that prevents the multiplication of bacteria. Biocidal polymers, metal nanoparticles, organic peptides, and enzymes are frequently used as coating materials for membrane surface modification to "attack" bacteria and reduce biofouling. According to the different bacteria killing mechanisms, microorganism/biofilm "attacking" agents could be divided into two groups: oxidizing based and surfactant based.

1. Oxidizing based agents

Reactive oxygen species (ROS), such as H_2O_2, ·OH, and O_2· [62], are chemically reactive species containing oxygen. Due to the high chemical reactivity and oxidative stress, ROS can lead to oxidative damage of cellular structures and causes intracellular leaking [63], protein degradation [64] and DNA cleavage [65].

Metal (e.g., gold [66], silver [67] and copper [68]) nanoparticles (NPs) and their oxidizing/ionic branches are oxidizing-based anti-biofouling materials. Resulting from the high surface area in water, metal nanoparticles trend to be oxidized and dissociated into metal ions. This process benefits the production of ROS and inhibits the growth of bacteria by increasing the oxidative stress of the system. Once the cell membrane is damaged, metal nanoparticles and ions further transport into the cell body and disable the essential organelles, thereby disturbing the metabolism of a cell [65]. Moreover, the interaction between a metal ion and phosphorus/sulfur-containing biomolecules (protein, DNA) is spontaneous, the dissolved metal ion could combine with phosphorus/sulfur-containing proteins of bacteria and causes distortion of the organism structure and disrupt metabolism processes [69].

In comparison to a biocidal polymer, another advantage of applying a metal nanoparticle coated surface is that, it could not only prevent the growth of cell colonies on the surface via "contact killing", but could also release bacteria-inactivating ions into the feed solution, thus inhibiting the bacteria's ability to breed via "release killing" [33] (Figure 2.9). Silver nanoparticles are the most extensively explored option for membrane bio-fouling mitigation [70]. Blending particles into the membrane material [71] as well as developing a coating on the membrane surface through covalent bonding [72,73] and in situ reduction methods [74] achieve an appreciable fouling resistant effect.

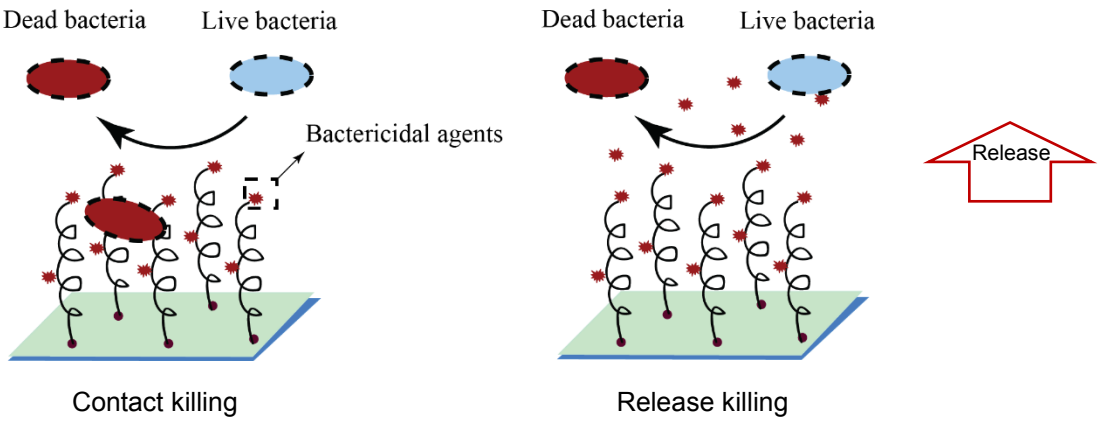

Figure 2.9 Preventing the growth of bacteria on membrane surface via "contact killing" and "release killing" strategies.

Graphene oxide (GO) contains diverse oxygen-rich functional groups (-OH, $-COO^-$, -C-O-C-) which also cause high oxidative stress. The sharp edges of GO potentially may cause damage to the cell membrane and cause the leakage of intercellular substance [75]. Compared to pristine TFC membranes, a 50-60% reduction in live cells was observed on GO coated surfaces [76].

2. Surfactant based agents

The complex mechanism of biocidal polymers, such as quartnary ammonium, peptides, and enzymes, in bacterial cell killing has not been fully elucidated. One of the possible pathways is that the biocidal polymer has similar protein moieties (amino acid, -COOH, $-SO_3$, amide acid, ether, ect.) to that of the cell membrane and cell wall [77]. Once the biocidal polymer surrounds the bacterial cell, interactions between similar moieties loosen the lipid and protein structure of the cell membrane and results in a rupture of the intact cell and leaking of the cytoplasm.

(a) Biocidal polymer

Polymer bearing quaternary ammonium functionalities have been shown to kill or inactivate bacteria [78]. Quartnary ammonium is the traditional biocidal agent used as an anti-bacterial surface coating [60, 79]. Quartnary ammonium contains many positively charged functional groups (-R4N+) which attract and strongly bonds with negatively charged bacteria in aqueous environment. Then, the long alky chain warp around the bacteria cell to disturb its normal metabolism. A longer alkyl chain (or aromatic rings, a more complicated structure) has more chances to lysis bacteria cell structure via a "like dissolve like" mechanism. In one of our preliminary studies, 50% bacteria cell inactivation was observed on the quartnary ammonium brush grafted surface [61]. However, the bacterial inactivation would be weakened over time because of the deposited fouling layer during the "contact killing" process [14].

(b) Peptide

Peptides are common organic species in natural environments which show minor toxicity to mammalian cells. Due to an effective bacterial inactivation ability, cheap price, and low toxicity to the human body, natural and synthesized peptides have been developed and are widely used in industry for cosmetics and food perseveration purposes.

Peptide molecules are formed by two or more amino acids via the interaction between the carboxyl group and amino group (bond: -OC-NH-), which is also an important structure in cell proteins (exist in cell membrane, wall, organelle). By surrounding the bacteria, peptides could gradually lysis cell protein structures; however, the cell inactivation ability of a single peptide is limited [80]. Most peptides are only effective to either gram positive cells (or gram negative) and quite a few types of gram negative (or gram positive) cells, which could be attributed to the different compositions of the cell structure [77].

Based on the structure and composition of cell walls, bacteria can be attributed as either gram positive (G^+) or gram negative (G^-). The former has a thick cell wall (20-80 nm) surrounding an inner cell membrane and 40-95% of the cell wall consists of peptidoglycan [81]. In contrast, gram-negative cells have a thinner cell wall (15-20 nm) but the composition is more complicated (contains an outer membrane and 2-3 nm peptidoglycan). Since the cell wall of gram positive bacteria is mainly formed by peptidoglycan, it could be easily lysed by most peptides via the "like dissolves like" principle and result in cleavage of the pentaglycine cross-bridge in the cell wall

peptidoglycan [77]. However, only certain peptides, such as lysine-based peptides, are effective against gram negative bacteria.

Peptides could be coated to various substrates to create an anti-biofouling surface. Lysostaphin was covalently bonded onto glass and polystyrene via polydopamine coating to prevent the growth of *S. aureus* (G^+) and the results indicate that the newly developed surface can kill bacteria in less than 15 min of incubation [77]. Poly L-Lysine (PLL) and GO were combined and coated on forward osmosis membrane surfaces for biofouling prevention and a 99% live cell reduction was observed on the modified membranes when compared to the pristine membrane [82].

With respect to control of the growth of G^- and G^+ bacteria, various combined peptides have been applied in some research to inactivate bacteria via a synergistic effect. Lauroyl arginate ethyl (LAE), a commercial food preservative was reported to be compatible with the polyamide RO membrane and showed strong antimicrobial properties [83] due to a surfactant-related disruption of cell morphology. When LAE was combined with nisin Z (a natural antimicrobial peptide derived from *Lactococcus lactis*; biocidal to G^+ cells), both the G^- and G^+ bacterial cells in solution were dramatically reduced and inhibited within 1 hour of treatment [84]. Interestingly, a commercial zwitterionic peptide (CRERERE), was reported to show super hydrophilicity via the formation of hydrogen-bond interactions with water molecules. By coating zwitterionic peptides on a gold surface, a strong hydration peptide layer is formed which benefits from the repulsion of proteins and G^- and G^+ bacteria [85]. Another commercially synthetic peptide, CWR11, was reported to show potential antimicrobial functionality to both G^- and G^+ bacteria for at least 21 days [86]; however, the detailed mechanism was not discussed.

3. Indirectly inhibit the biofilm formation

Generally, the oxidizing- and surfactant-based biocides work directly against bacterial cells and prevent biofouling via bacteria inactivation. For some natural amino acids, enzymes and synthetic antibiotics, bacteria/biofilm-"attacking" could be achieved by dispersing proteins which connecting the biofilm, inhibiting the nutrients required metabolism processes or reducing the colony-forming signals produced by bacteria, thereby, preventing the biofilm formation indirectly without bacterial-inactivation. The main attacking objectives are: (i) nutrients for bacteria growth (i.e. polysaccharide); (ii) proteins which connect cell colonies (i.e., EPS, amyloid fibers, etc.); (iii) quorum sensing (QS) signals (oligopeptides, N-acylhomoserine lactones (AHL), and autoinducer-

2 (AI-2) synthesized by the LuxS gene) which regulate the group behavior of bacteria during a biofilm formation.

(a) Enzyme and antibiotic

The anti-microbial mechanisms of enzymes and antibiotics are relatively complicated. Some enzymes could prevent biofilm formation via the same function as that of the surfactant-based peptide. Others work as antibiotics, degrading metabolic products (one or more types of protein, lipid, glycnpeptides), thereby disrupting EPS formation and preventing the maturation of biofilms [87].

A polysaccharide-degrading enzyme, alginate lyase (Alg L), has been covalently linked on cellulose acetate membrane to mitigate the biofouling in the UF process. The result showed that Alg L was able to degrade the polysaccharide on the membrane and prevent bacterial breeding [88]. One enzymatic quorum quenching acylase, in the form of a free enzyme or an immobilized form on a bead, was coated on the NF membrane surface to mitigate biofouling [87]. Results showed that the quorum quenching acylase could effectively degrade the N-acetyl homoserine lactone (AHL) (a class of signaling molecules involved in bacterial quorum sensing) autoinducer of G^+ bacteria and thus prevent biofilm formation [87].

In studies related to the application of antibiotics [89], antibiotic cefotaxime sodium (CS), was coated on a titanium surface to prevent biofouling. According to the result, the CS hindered the synthesis of glycopeptides, which are indispensable for cytoderm (cell wall) formation, therefore resulting in bacterial cell rupture and biofilm prevention. The commercial available vanillin(4-hydroxy-3-methoxybenzaldehyde), was demonstrated to prevent the establishment of biofilm on RO membrane surfaces by inhibiting the QS signals [90].

(b) Amino acid

Similar to the enzymes, the anti-biofouling mechanisms of amino acids are varied. Most amino acids (lysine, glutamic acid [91] and tyrosine [92]) could be functionalized as bacteria/microorganism-"defending" agents to reduce the bacteria/protein adhesion. Amino acid-based polymers, such as peptide, polymeric surfactant which has amino acid moieties, exhibited the potential to not only reduce the attachment of bacteria but also lysis bacteria cells, as introduced above. Furthermore, certain types of amino acids can serve as biofilm "attacking" agents and prevent biofilm formation

by inhibiting the QS signal, releasing the biofilm bridging protein or inhibiting the production of DNA.

In both G (+) and G (-) bacteria, the cell wall is composed of a peptidoglycan which is a polymer that consists of polysaccharides and amino acids. The amino acids in the peptidoglycan structure of a G (-) bacteria are mainly L-alanine, D-glutamic acid, meso-diaminopimelic acid, and D-alanine; while those for a G (+) bacteria are L-alanine, D-glutamine, L-lysine, D-alanine, and glycine. The existence of amino acids (such as tyrosine, tryptophan, leucine, lysine, etc.) in aqueous environments were able to replace components (D-alanine, L-alanine, L-lysine, etc.) of the cell wall and cause the disruption of amyloid fibers (a substance that links cells in the biofilm together) on the cell membrane and release the extracellular matrix connection between the extracellular matrix and the cells [93]. It has been reported that in the presence of a high concentration of amino acids, the bacteria exhibited reduced production of eDNA, extracellular polymeric substance (EPS), and interspecies quorum sensing signal [94]. A high concentration of lysine was observed to completely inhibit the swimming motility and twitching motility (a prerequisite for biofilm formation) of *E. coli BL21* and effectively inhibited biofilm formation [95].

The application of amino acids as an environmentally friendly modifier in membrane biofouling control attracting growing interest; however, its effectiveness in comparison to other commercial materials still requires further investigation.

(c) Nitric oxide (NO)

The NO-based method for membrane biofouling control is a new research topic in recent years. NO is a radical gas and frequently used chemical compounds which could functionalize as NO donors are, sodium nitroprusside, 3-morpholinosydnonimine, sodium nitrite, S-nitroso-N-acetylpenicillamine, diazeniumdiolate, etc[29]. By interacting with NO via a signal-response pathway, the intracellular phosphodiesterase activity of bacteria is stimulated and results in degradation of cyclic di-guanylate monophosphate (c-di-GMP) and changes gene expression in favor of the planktonic state [96, 97]. Therefore, NO donors have been considered as important biofilm cleansers.

Repeated NO treatment has been used to remove biofilm on a fouled industrial RO membrane. Results showed that over 50% of biofilm was dispersed by treatment with 500 μM of NO donor, DETA NONO (diethylenetriamine (DETA) NONOate) [96]. In another study [98], treating biofilm on

RO membrane by 40 M of NO donor, PROLI NONOate, at 24-h intervals exhibited a 48% reduction in polysaccharides, a 66% reduction in proteins, and a 29% reduction in microbial cells as compared to the untreated control.

2.3.3 Anti-biofouling membrane combining "defending" and "attacking" strategy

Although both fouling resistant ("defending") and anti-microbial ("attacking") surfaces exhibited satisfactory anti-biofouling performance within temporally-short experiments as reported in the literature, they all showed unavoidable drawbacks to long-term practical application.

The bacteria/biofilm-"defending" coating mostly relies on the surface physiochemical properties of the membrane to reduce the attachment of organic foulants. However, they gradually are rendered defenseless once deposited bacteria (e.g., due to inhomogeneous coating) grow and form colonies. In case of anti-microbial surfaces, "contact-killing" polymers work based on the contact between biocidal moieties and bacteria and, as such, they cannot control the attachment of cells on the membrane surface. Furthermore, dead cells on the membrane surface inevitably cause additional fouling. Even though "contact- and release-killing" metal nanoparticles inhibit the growth of bacteria, both in the feed solution and on the membrane surface, the biocidal agents become depleted because of gradual dissolution of the metals.

As it is claimed, "it takes walls and knights to defend a castle" [99], the combination of "defending" and "attacking" strategies to develop an anti-biofouling coating may offer a synergistic resistance to biofouling and overcome some of the drawbacks seen with a single type of modification, The research combining "defending" and "attacking" strategies has been summarized in Table 2.1.

It has been shown that in comparison to hydrophilic nanoparticles (SiO_2 and GO), hydrophilic polymers and zwitterionic polymers are more frequently selected as bacteria/biofilm-"defending" moieties in functional coatings. Biocidal silver nanoparticles (especially AgNPs) are preferred over biocidal polymers (such as quartnary ammonium and polydopamine) to serve as bacteria/biofilm-"attacking" moieties for biofouling control.

Table 2. 1 Anti-biofouling surfaces modified via "defending" and "attacking" strategies

Combining	Material and modification method
Zwitterionic polymer & biocidal polymer	PSB & Quartnary ammonium (UV grafting; ATRP) [61, 100]
Zwitterionic polymer & Metal nanoparticle	PSB & silver NPs (polydopamine media, silver *in situ* reduction) [101] PEG & silver NPs (ATRP, silver *in situ* reduction) [102] PAH/PSS & silver NPs & pSB/PDMS (LbL, silver ex- situ fabrication, UV grafting) [72] PAH/PSS & silver NPs & MPC-co-AEMA (LbL, silver *in situ* reduction, dip coating) [103] PSB & silver NPs (ATRP, silver *in situ* reduction) [104]
Hydrophilic nanoparticles & Metal nanoparticle	GO & silver NPs (EDC/NHS cross-linking, silver ex-situ; silver *in situ* reduction) [105]
Hydrophilic polymer & Metal nanoparticle	Polydopamine & silver NPs (dip coating, silver *in situ* reduction)[106, 107]
Biocidal polymer & Hydrophilic NPs and polymer	Polydopamine & SiO_2 & PSB (dip coating, ATRP)[108] Polydopamine & PVP & I_2 (dip coating, UV grafting) [109]
Hydrophilic and biocidal polymer & Metal nanoparticles	Polydopamine + silver NPs (polymerization, silver *in situ* reduction) [107, 110]

2.4 Existing problems in current research

Combining "defending" and "attacking" strategies to develop anti-biofouling coatings could offer a synergistic resistance to biofouling and overcome some of the drawbacks seen with a single type modification strategy. A substantial amount of research related to anti-biofouling membranes via bacteria/biofilm-"defending-attacking" has been reported as listed in Table 2.1. Although appreciable improvements have been reported in laboratory research, few have been applied in a large-scale setup due to the high cost of materials, sophisticated and uncontrollable fabrication procedures, as well the risk of emergence of antibiotic-resistant bacteria.

To develop an effective and practically applicable antibiofouling membrane, the selection of cost-efficient and quality-competitive modifiers and modification methods should be considered.

- Modifiers: cost-effective and environmentally friendly modifiers need to be proposed

AgNPs has been widely used biocidal agents for the modification of the antibiofouling surfaces due to its high effectiveness recently; however, the price of AgNPs is high [14] which may limit their practical application. Furthermore, the antibiofouling-durability of metal NPs-based coatings have not been thoroughly investigated.

Although natural antibiofouling materials, such as peptides, amino acids and enzymes have been proposed as both "green" and effective bacteria/biofilm-"attacking" agents for membrane biofouling control, their application in the fabrication of antibiofouling-coatings are limited in comparison to widely used commercial polymers and nanoparticles.

- Methods: modification methods that can controllably functionalize modifiers on membranes need to be further explored.

UV grafting has been widely used for membrane surface modification with polymeric materials; however, the polyamide skin layer might be damaged under the reaction conditions and may affect the water-perm selectivity of polyamide membranes.

Direct dip coating is the conventional method to functionalize monolayer polymer/NPs on membranes; however, in general, the obtained coating is not uniform, which may weaken the antibiofouling performance of modifiers. Functionalization methods which can stably and controllably anchor materials onto the membrane needs to be investigated.

Chapter 3. Controlling biofouling via "defending" strategy: surface modification via grafting patterned polymer brushes

Abstract

In order to address the fouling problem, we developed novel fouling resistant surface coatings via polyelectrolyte [PAH: poly(allylamine hydrochloride)/PSS: poly(styrene sulfonate)] layer-by-layer self-assembly, functionalized with patterned polymer brushes. Two types of different polymer, poly(sulfobetaine) and fouling-release poly(dimethylsiloxane) (PDMS), were selected and combining patterned in a checkerboard array, with square feature of 25 μm. The successful pattering and incorporation of different polymer brushes on the membrane was confirmed through XPS analysis. Grafting with sulfobetaine and PDMS significantly increased the hydrophilicity and lowered the surface energy of the membrane, respectively. This fouling resistant property of the modified membrane was evaluated via static protein (BSA) deposition and bacterial (*E. coli*) cell adhesion tests. Surface modifications proved to diminish protein adhesion and exhibited 70~93% reduction in bacteria cell attachment. This observation suggests that the modified membranes have strong antifouling properties that inhibit the irreversible adhesion of organic and bio-foulant on the membrane surface.

Keywords: Reverse osmosis membrane, biofouling, surface modification, grafting, polymer brushes

3.1 Introduction

As introduced in Section 2.3.1, the modifiers applied in the "defending" modification are mainly hydrophilic or have a low surface energy (less active) to resist the adhesion of relative hydrophobic bacteria and other organic foulants. In comparison to the "attacking" modifiers, the antibiofouling effect from a bacteria/biofilm-"defending" membrane mainly depends on the physiochemical properties of membrane surface.

Antifouling polymer brushes are conventionally and widely studied for developing bacteria/biofilm-"defending" coatings for membrane surfaces [33, 111]. Since bacterial cell adhesion and their growth on the membrane surface are the governing proponent of biofouling, the coatings are primarily designed either to prevent the settlement of foulants through "antifouling coatings", or to provide weak foulant/surface adhesion thus allowing foulants to be easily washed off, by employing a "fouling release coating". Different polymers have been used to reduce attachment and viability of bacteria on surfaces.

The adhesion strategies for different types of foulants can vary widely, therefore, it is important to combine polymer brushes that contain different functionalities for membrane fouling control [111].

3.1.1 Modifiers: zwitterionic polymer and low-surface-energy polymer

Zwitterionic polymer like poly(sulfobetaine) (PSB) is recently reported as new generation functional material due to its unique zwitterionic charged structure that could significantly bind water molecule to form a water hydration layer close to membrane and offer repulsive force for hydrophobic protein/bacteria adhesion [47]. The number of research studies focusing on the application of zwitterionic polymer to fabricate fouling-resistant surface is growing every year. PSB has already been functionalized on silica nanoparticles to prevent the nonspecific protein fouling in drug carriers [112]; been grafted on stainless steel surface to prevent bacteria adhesion on precise equipment [113]; been functionalized on electrospun nano-fiber to prevent bacteria breeding on wound cloth and been coated on PVDF MF membrane[114], PES UF membranes [115, 116] and TFC RO membrane [117] for mitigate the flux reduction associated with biofilm growth. The mechanism of PSB to resist organic fouling has been introduced in subsection 2.3.1.

In addition, polymer brushes with low surface energy can also be to limit adhesion. They provide the surface with a weak foulant/surface adhesion, and as a result, attached bacterial cells can be

easily washed off from the membrane surface [60]. As a typical low surface energy polymer brushes, poly(dimethylsiloxane), PDMS, and perfluorinated [118], are commonly considered as the "fouling release brushes" [60], but are largely overlooked by the membrane research community.

3.1.2 Modification method: multiple-layer polyelectrolytes mediated surface functionalized with patterned polymer brushes

The widely used method for membrane surface modification with polymers includes physical adsorption via electrostatic attraction with [119], covalently bonding via chemical cross-linker (such as PDA, EDC/NHS, APTES, etc.), radical polymerization and UV/plasma grafting [120]. Except physical adsorption, other methods all rendered a robust and durable functionalization coating on membrane under various aqueous environment [121]. Polymer grafting with the aid of UV or ozone, or plasmas has been considered as the most facile one due to its minor time consumption (few seconds) in modification procedures.

Direct grafting of polymer bushes onto membrane surface may be efficient, but results in a thin active layer (~2 nm), and also may negatively impact structure of TFC layer [43]. Applying a modification media for the polymer grafting on membrane could not only protect the original material and structure of membrane but offer a barrier layer between membrane and foulant, therefore, reduce the chance to have membrane fouling.

The media selected here is polyelectrolytes multiple films formed via layer by layer (LbL) self-assembly process. Since membrane surface is negatively charged, positively charged polycation and polyanion were coated on membrane alternatively. One polycation and one polyanion layer was call it a bilayer. By repeating this circle, a multiply polyelectrolyte-film could be functionalized on membrane surface. Grafting polymer brush on the top of polyelectrolytes media can prevent the direct damage of underlayer membrane and UV. Therefore, the membrane can keep its own material and structure.

Therefore, in this paper, a novel fouling resistant coating for commercial RO membranes is developed. The membrane is first modified with a polyelectrolytes [PAH: poly(allylamine hydrochloride)/PSS: poly(styrene sulfonate)] LbL films, and then the LbL film is functionalized by grafting patterned functional polymer brushes onto the multilayer coating. The proposed functional units, poly(sulfobetaine) (PSB) and PDMS serve as antifouling and fouling-release

brushes, respectively. Modified membrane surface is characterized via X-ray photoelectron spectroscopy (XPS) and scanning electron microscopy (SEM) technique, and their surface properties are assessed through water contact angle and surface energy measurements. Moreover, fouling resistant behavior of modified membrane is evaluated through protein (BSA) deposition and bacterial (*E. coli* K12 MG1655) cell adhesion tests. These novel coatings contain functional units that would serve as promising routes for fouling control of RO membrane.

3.2 Materials and methods

3.2.1 Materials and chemicals

Poly(allylamine hydrochloride) (PAH; Mw = 15 kDa), 18 wt. % Poly(4-styrenesulfonic acid) in water (PSS; Mw=70 kDa), [2-(methacryloyloxy)ethyl]dimethyl-(3-sulfopropyl)ammonium hydroxide, (methacryloyloxy)ethyl trimethylammonium chloride, 4-cyano-4-(phenylcarbonothioylthio)pentanoic acid (CTA), azobisisobutyronitrile (AIBN), 4,4′-azobis(4-cyanovaleric acid) (ACVA), 2,2-dimethoxy-2-phenylacetophenone (DMPA), 2-hydroxy-4′-(2-hydroxyethoxy)-2-methylpropiophenone, propiolic acid, allyl glycidyl ether, methoxymethanol, sodium hydride, dibromoxylene, sodium azide were purchased from Sigma-Aldrich (St. Louis, MO). Methacryloxypropyl terminated PDMS with a viscosity of 3-8 cSt was purchased from Gelest(Morrisville, PA).The commercial TFC polyamide RO membrane (SWC4+) was purchased from Hydranautics Membrane. Deionized (DI) water was obtained from a Milli-Q ultrapure water purification system (Millipore, Billerica, MA).

3.2.2 Preparation of polyelectrolyte LbL films

The commercial RO membranes (SWC4+, hydronautics) were pretreated with 20% isopropyl alcohol solution for 20 min, and rinsed with DI water for 3 times, then stored in DI water at 4℃ until use. Pretreated membrane was spray coated (at 20 psi) alternatively with dilute polymer solutions of positively charged poly(allylamine hydrochloride) (PAH) and negatively charged poly(4-styrenesulfonic acid) (PSS) [Figure 3.1 B]. Excess polymer was rinsed off with a generous amount of water to ensure one layer of absorbed polymer was affixed to the substrate. The number of bi-layers varied from 5 to 10. Top layer of LbL film was composed of a modified polyallylamine

where 30% of the amine groups are substituted with a propiolic acid. The propiolic moieties bear a triple bound used for further grafting reaction.

3.2.3 Coating poly(allyl glycidyl ether) [PAGE] intermediate layer to the LbL films

In order to increase the grafting density and thickness of the polymer brush, 2 wt% N_3-PAGE solution with methanol as solvent was spray-coated on LbL films surface as intermediate layer to procure an abundance of grafting sites (Figure 3.1 C). Triple bonds on the surface of LbL film reacted with azide groups on N_3-PAGE resulting in a tight bind for this PAGE-functionalized layer. The membranes were then immersed in a solution of $CuSO_4$ (1.5 M) and sodium ascorbate (0.5 M) for 8h at room temperature, followed with methanol and water rinse subsequently.

3.2.4 Grafting and patterning of the polymer brushes

The patterning of polymer brushes onto LbL films was performed through Thiol-ene click reaction (Figure 3.1 D). The first solution of thiol-therminated polymer (100 mg/mL) was spray-coated with a radical photoinitiator on the PAGE-functionalized LbL film, and then certain regions of the membrane were exposed for 30s to UV light (3500 uW/cm^2) using a checkerboard patterned photomask with features of 25 μm. Grafting occurred only in the exposed areas, and no reaction was observed in the unexposed areas. After washing with DI water (or hexane in the case of the PDMS brushes), a second polymer was spray-coated with the UV initiator, and the entire membrane was exposed to UV light. This led to the grafting of the second polymer on the previously unexposed regions.

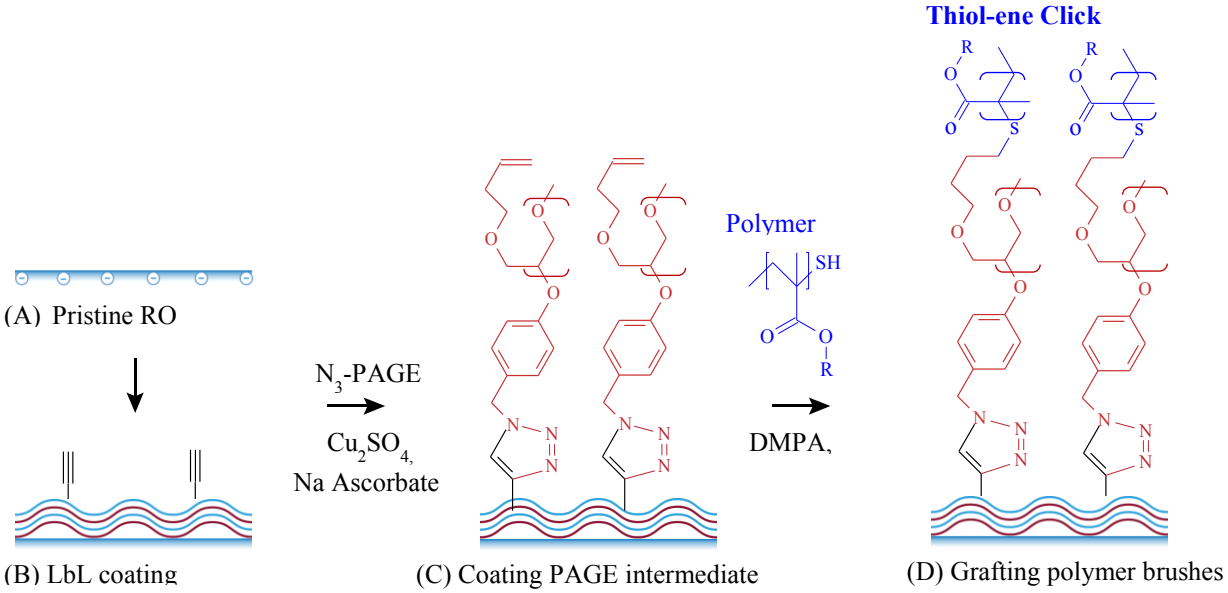

Figure 3. 1 Modification schemes of RO membrane. Polymer brushes with antifouling/fouling release properties are incorporated to commercial RO membranes via LbL (PSS/PAH) self-assembly method and UV grafting technique.

3.2.5 Membrane characterization

X-ray Photoelectron Spectroscopy (XPS) experiments were carried out on Surface Science Instrument (SSI) model SSX-100. The average element contents were calculated from analyzing results of three different spots on membrane surface. Surface wettability was evaluated from contact angle measurements of DI water using the sessile drop method (VCA Video Contact Angle System, AST Products, Billerica, MA). The system was equipped with software to determine the left and right contact angles (VCA Optima XE). Surface energy was calculated from the advancing contact angles of water, ethylene glycol and diiodomethane on the membrane surfaces.

3.2.6 Antifouling activities evaluation

Protein absorption tests were conducted by immersing the membrane for 48 hours in a 0.5 g/L solution of FITC-BSA in 0.1 M phosphate buffer at pH 7.4 containing 3.5% of NaCl. The amount

of protein bounded to the membrane was evaluated by the signal intensity obtained by fluorescence microscopy (Olympus BX41, Japan).

In order to compare bacterial cell adhesion, *E.coli* K12 MG1655 was used to evaluate the antibacterial prosperity of membrane according to the following protocol. Firstly, a single colony of *E. coli* was added into 50 mL LB solution that contained 50 mg/L of ampicillin. The solution was then incubated overnight while shaking (100 rpm) at 37℃. Then 1 mL of overnight bacterial solution was poured into 50 mL fresh LB solution containing 50 mg/L of ampicillin. The bacterial solution was then incubated for another 2.5 h at 37℃ to reach the exponential growth phase. 20 mL of E. coli solution was poured in a sterilized plastic tube and centrifuged at 15,000 rpm for 2 min in 3 cycles. At each time after centrifugation, the supernatant was discarded, and the remaining bacterial cell pellet was resuspended by adding 8 mL of 0.9% saline solution and subsequent vortexing. Finally, adequate amount of 0.9% saline solution was added and mixed with the bacterial cell pellet by vortexing to ensure a final cell concentration of 10^7~10^8 CFU/mL. The cell concentration was estimated by measuring the optical density (OD) of the solution by UV-vis spectroscopy. The desired OD at 600 nm is 0.3. Then, 5 mL of prepared bacteria solution was placed in a sterile plastic vial. A membrane coupon with ¾ inch diameter was placed inside the mouth of the plastic vial with the active side of the membrane facing the bacterial solution. The vial was then inverted and incubated for 1 hour at 37℃. After incubation, the membrane was rigorously rinsed with synthetic wastewater for 5 sec, and then was observed under a fluorescent microscope. At least 10 images were taken across the membrane surface and the average number of cells on the membrane was then normalized across the observed membrane area.

3.3 Results and discussion

3.3.1 Water contact angle and protein adsorption test

The surface wetting phenomena of the membranes modified by LbL films functionalized with different polymer brushes were investigated by contact angle and surface energy measurements. The corresponding organic fouling propensities of the modified surfaces were evaluated via BSA protein adsorption tests. The water contact angle of LbL film remained equal of virgin polyamide membrane (Figure 3.2); however, a distinct reduction in protein deposition was observed on this

LbL surface (Figure 3.3). This resistance to protein adsorption of LbL films may be attributed to the greater charge density caused by PAH/PSS polyelectrolyte bilayers. As mentioned earlier, the zwitterionic units (sulfonate, -SO_3-, and amide, -NH-) of poly(sulfobetaine) resulted in formation of protein repulsive hydration layer on the membrane surface and hence reduced hydrophobic protein adhesion. A membrane grafted with PDMS brushes possessed lower surface energy (30 ± 2 mJ/m^2) when compared to that of virgin polyamide membranes (45 ± 2 mJ/m^2), while showing significant increase in water contact angle. Due to the increased hydrophobicity, PDMS modified membrane surface exhibited the most protein fouling. However, since the PDMS modified membrane offers low adhesion force between proteins and the membrane surface, it is expected that adsorbed proteins would be washed off with moderate rinsing. These obvious changes of membrane surface property further confirmed the success of grafting process. Fabricated polymer brushes severed as functional coating that imparted membrane surface with various fouling rejected units to reduce contamination through combining mechanisms.

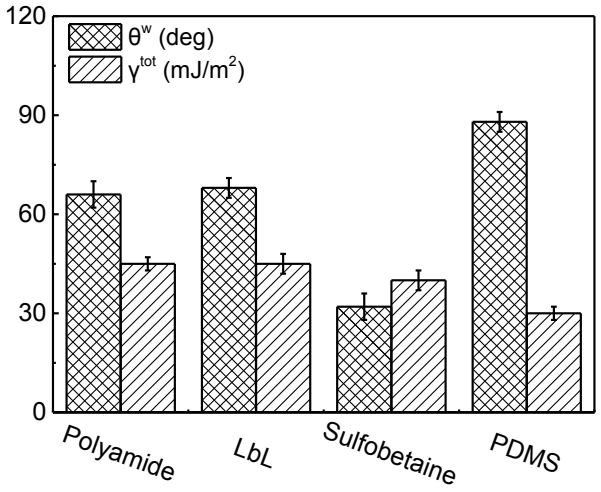

Figure 3. 2 Water contact angle (θ_w) and surface energy (γ^{tot}) of membranes modified with LbL films and grafted with different polymer brushes

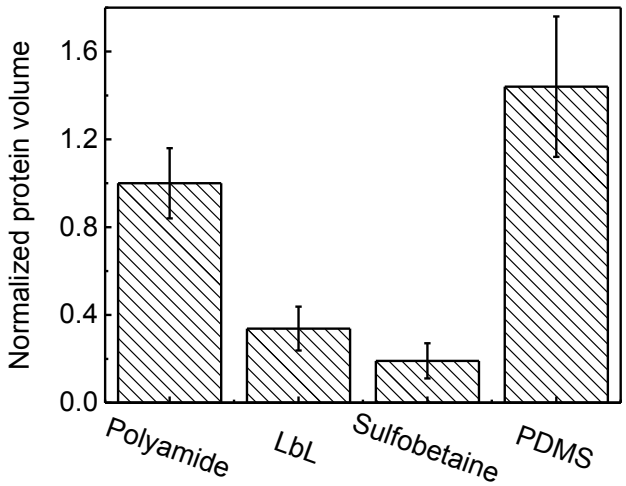

Figure 3. 3 Protein adhesion (adsorption) on membranes modified with individual polymer brushes (unpatterned) in static adhesion tests. Membranes were soaked in a Bovine serum albumin (BSA) solution for 48 hours, and then measured for relative levels of BSA.

3.3.2 Bacterial cell adhesion test

In order to assess the antifouling property of modified membrane, a series of static (no pressure, no flow) bacterial cell adhesion test was performed with *E. coli* K12 MG1655. The results showed that except PDMS polymer brush, LbL polyelectrolyte films and other functional polymer brush patterned layers contributed to a significant reduction of bacterial cell adhesion (Figure 3.4). The massive bacteria cells deposition on PDMS grafted membrane might stem from the low surface energy of modified membrane. Compared with individual polymer brush modified surface, membranes that functionalized with patterned polymer all presented better biofouling resistant property. Normalized cell adhesion in the range of 7 to 30% was investigated on the modified patterned membrane surfaces. This observation suggests that the modified membranes have strong antifouling properties that inhibit bacterial adhesion onto the surface, an irreversible process. This also supports our original hypothesis that the use of low surface energy polymer brushes, in

particular, PDMS patterned with poly(sulfobetaine) brushes, would allow less bacterial cell deposition as well as the near complete ability to remove attached cells with moderate to rigorous rinsing (normalized cell adhesion is less than 10%). The low surface energy brushes, PDMS, offers weak foulant/surface adhesion force and could serve as effective fouling release brushes, whereas sulfobetaine polymer brush acts as an antifouling agent due to their superior hydrophilicity. Both protein and bacteria fouling resistant results suggest a strong potential in using those novel surface coatings for the control of fouling on RO membranes.

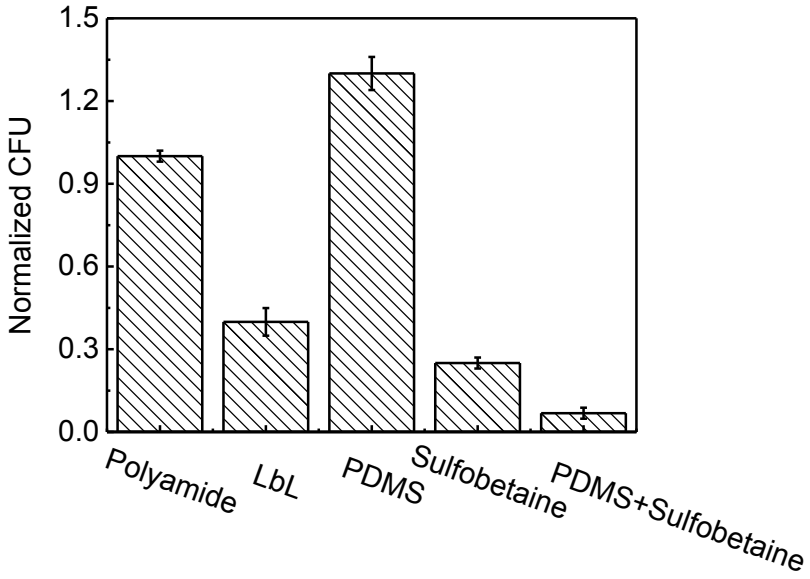

Figure 3. 4 Number of cells (*E. coli K12 MG1655*) attached to the membrane surfaces normalized to that of a control polyamide membrane.

3.3.3 Scanning electron microscopy (SEM) analysis

The changes in surface morphology and the antifouling behavior of the modified membranes were analyzed using SEM (Figure 3.5). As expected, the control polyamide membranes exhibited a uniform ridge-and-valley morphology [5(A)] that is typical for TFC polyamide membranes formed

by interfacial polymerization. The overall surface morphologies of the membranes were not significantly affected after coating with polymer brushes on the LbL film [Figure 3.5 B]. After contact with a bacterial solution and incubation for 1 h, PDMS and poly(sulfobetaine) patterned membrane surfaces showed preferential cell adhesion on the PDMS domains. On the region grafted with PDMS, a considerable cell attachment was observed, while on poly(sulfobetaine) domains, seldom bacteria deposition was found. This may be because of the hydrophobic nature of a PDMS polymer brush that facilitates hydrophobic bonding of the bacterial cells onto the membrane surface. It was also shown in cell adhesion tests that a PDMS polymer brush patterned membrane achieved good fouling release properties as attached bacterial cells were released after being rinsed rigorously with water. The same membrane sample, with different domains showing different anti-fouling property, also supports the successful modification of membrane with patterned polymer brushes.

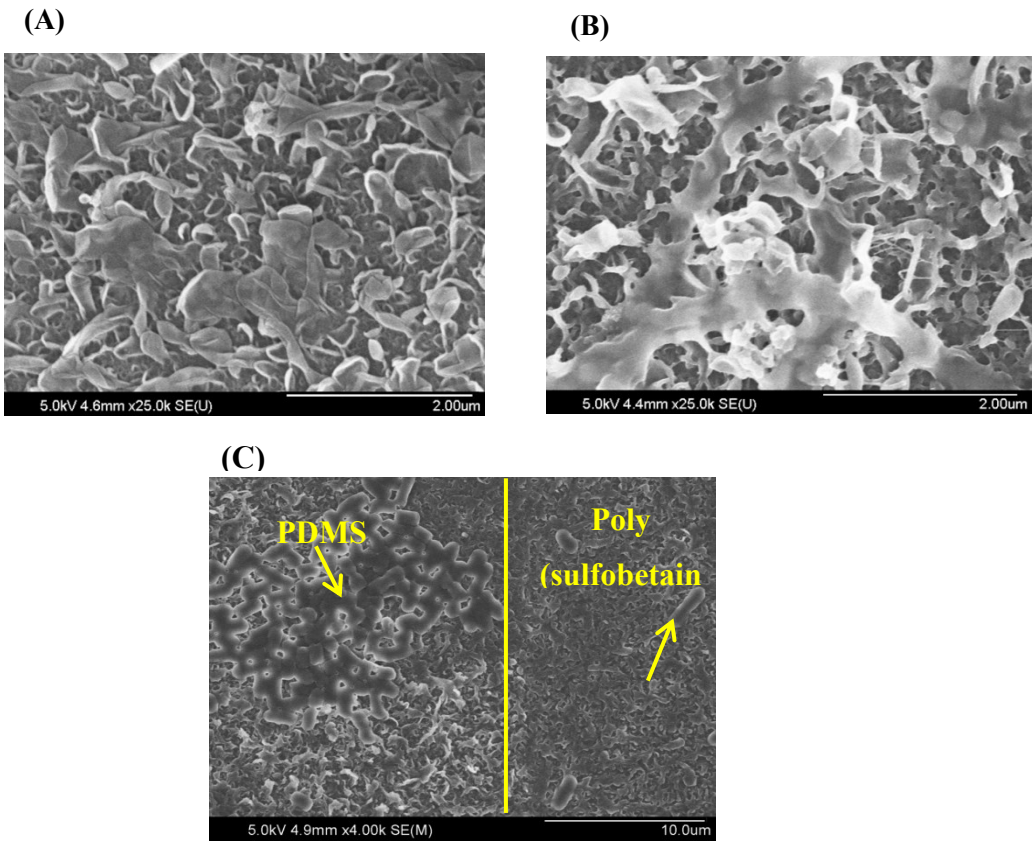

Figure 3. 5 SEM images of (A) Pristine polyamide membrane; (B) Membrane grafted with PDMS and poly(sulfobetaine) polymer brushes on LbL film; (C) Bacterial cell adhesion on the membrane modified with PDMS and poly(sulfobetaine) polymer brushes without rising. Yellow arrows refer to bacteria grow area and yellow line showed the border of PDMS and poly (sulfobeaine).

3.3.4 Implications and challenges

Water scarcity is a critical global concern; water reuse and desalination are currently considered as the only effective ways for increasing water resources beyond the hydrological cycle [122]. Due to its unique separation performance, RO membranes play irreplaceable role in industry of waste water purification and sea water desalination process. However, irreversible fouling caused by NOM and bacteria on membrane surface inhibits their widespread application [43]. Developing a

fouling resistant membrane will greatly contribute to the overall use of RO technique and increase in fresh water supply.

Grafting patterned binary polymer brushes onto the membrane surfaces by using LbL multi-films as media, as demonstrated in this paper, is an effective strategy for mitigating irreversible fouling. Compared with the direct grafting polymers onto the membrane surface [123, 124], the physical intermolecular force of LbL films offers stable binding between a membrane surface and polymer brushes without adversely impacting the membrane barrier layer structure, thus maintains the original outstanding separation performance. Although polymer brushes are universally used for membrane antifouling research, their mono-functionalization on a membrane surface exhibit relatively low efficiency. Poly(sulfobetaine) is widely used polymer to reduce cell deposition on membrane surface through its unique zwitterionic property, where a 50% reduction of cell attachment was reported [125]. In contrast, combined grafting of antibacterial with fouling release/anti-fouling polymer brushes showed excellent antibacterial cell reduction in this paper (71%-85% reduction). Combining patterned polymer brushes can reduce the adhesion of protein and cells from various mechanisms and significantly improve the lifespan of functional units. Polymer brushes grafting also presents advantages on modification process, it needs only few minutes for reaction, and also the price of polymer is significant lower than biocidal nanoparticles, such as silver, gold or carbon nanotubes.

Nonetheless, the stability of LbL multi-films is a big challenge of this novel coating, since salt ions in water may impact the interaction of polyelectrolytes. Even though previous studies [43] have shown that LbL formed by 10 bilayers are stable in saline water for 74 days during reverse osmosis process, further experiment is needed to observe the long time performance of functionalized polymer brush on membrane surface. Effective modification process is another challenge facing grafting method. However, the grafting method used in this study is highly scalable and could be implemented in a roll-to-roll process since the required UV irradiation dose is very low.

3.4 Conclusion

Zwitterionic charged poly(sulfobetaine) brushes significantly lower the contact angle of membrane surface, and subsequently result in the reduction of protein deposition. PDMS modified surface with lower surface energy exhibited an excellent fouling release property.

In general, surface modifications with different types of polymer brushes resulted in a significant reduction of bacterial cell adhesion. However, PDMS and poly(sulfobetaine) polymer brushes patterned surface showed excellent anti-fouling properties (normalized cell attachment 7%, compared to 100% for virgin membrane).

Overall, both antifouling and fouling release results suggest the potential of using this novel surface coating for controlling membrane fouling.

Chapter 4. Controlling biofouling via "attacking" strategy: spray- and spin-assisted layer-by-layer assembly of copper nanoparticles on membrane for biofouling mitigation

Abstract

Copper nanoparticles (CuNPs) have long been considered as highly effective biocides; however, the lack of suitable methods for loading CuNPs onto polymeric membranes is recognized as being one of the primary reasons for the limited research concerning their application in membrane industries. In this study, a highly efficient spray- and spin-assisted layer-by-layer (SSLbL) method was developed to functionalize the TFC polyamide RO membranes with controllable loading of CuNPs for biofouling control. The SSLbL method was able to produce a uniform bilayer of polyethyleneimine-coated CuNPs and poly(acrylic) acid in less than one minute, which is far more efficient than the traditional dipping approach (25-60 min). The successful loading of CuNPs onto the membrane surface was confirmed by XPS analysis. Increasing the number of bilayers from 2 to 10 led to an increased quantity of CuNPs on the membrane surface, from 1.75 to 23.7 μg cm^{-2}. Multi-layer coating exhibited minor impact on the membrane water permeation flux (13.3% reduction) while retaining the original salt rejection ability. Both static bacterial inactivation and cross-flow filtration tests demonstrated that CuNPs could significantly improve anti-biofouling property of a polyamide membrane and effectively inhibit the permeate flux reduction caused by bacterial deposition on the membrane surface. Once depleted, CuNPs can also be potentially regenerated on the membrane surface via the same SSLbL method.

Keywords: Reverse osmosis, biofouling, copper nanoparticles, spray- and spin-assisted layer-by-layer (SSLbL) self-assembly

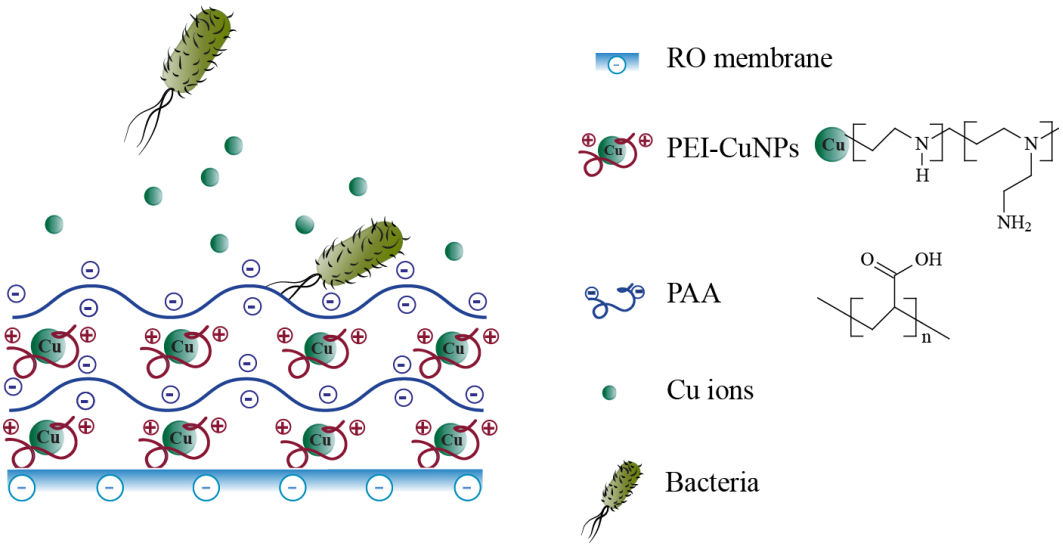

Figure 4. 1 Graphical abstract

4.1 Introduction

As introduced in 2.3.2, an bacteria-/biofilm-"attacking" surface mitigate the biofouling via three possible pathways: (i) releasing reactive oxygen species (ROS) to cause an oxidative damage of cell structures and further intracellular leaking; (ii) warping the cell with polymer which has similar moieties (amino acid, -COOH, $-SO_3$, amide acid, ether, ect.) to that of the protein and lipid in cell membrane and cell wall. Lysis cell structure via "like dissolves like" principle; (iii) degrading/inhibiting metabolic products (protein, lipid, glycopeptides, etc.), thereby disrupting the EPS formation and preventing the maturation of biofilms.

Modifying membrane surfaces with antibacterial materials is an effective technique to prevent the growth of biofilms while maintaining the original water purification qualities of the membrane. Antibacterial polymers [61] are commonly used as coating materials to improve membrane fouling resistance; however, their anti-bacterial activity decreases over time because of a deposited fouling layer duringthe "contact killing" process [14]. With growing interest in nanomaterials, carbon nanotubes (CNT) [38] and graphene oxide (GO) [37] have become widely studied membrane antifouling agents; however, similar to the biocidal polymers, CNT/GO inactive cells via "contact killing," which would gradually compromise the biocidal function within a short time.

4.1.1 Modifier: copper nanoparticle (CuNPs)

Unlike biocidal polymers, metal nanoparticles (NPs) and their oxides/ionic forms, *e.g.*, silver [67] and copper [126], can not only prevent the growth of cell colonies on the contacting surface but also release bacteria-inactivating ions into the feed solution, thus inhibiting bacterial reproduction [33]. These advantages have generated significant interest in membrane fouling control research. In comparison to other metal NPs, silver possesses better stability properties and is less prone to oxidation, thus, it is one of the most extensively explored option for membrane bio-fouling mitigation [127]. However, with a relatively high cost, the financial impact of employing silver significantly limits its widespread application.

Copper is a potential alternative low-cost biocide which has been registered as the first solid antimicrobial material by the U.S. Environmental Protection Agency [128]. Copper ion [129], copper ion-charged polymer [130] and CuNP/CuO-NP containing solutions all showed appreciable performance in bacterial inactivation [131-133]. Dankovich et al. [134] used CuNPs to reduce the cost of

the bioactive paper and found that this new filter had a similar bacterial inactivation capacity as a previously tested AgNP decorated filter. Although plenty of research supports the potential of CuNPs for anti-bacterial surface modification, few of them have focused on applying CuNPs for membrane biofouling control. Ben-Sasson et al. [14] incorporated polyethyleneimine (PEI)-coated copper nanoparticles (CuNPs) onto an RO membrane surface through electrostatic interactions; a significant reduction (80-96%) of live bacteria attached onto the membrane demonstrated the potential of using copper to replace silver for membrane biofouling control. However, despite the aforementioned benefits, the modification method used (*i.e.*, dip-coating) is considerably time consuming [135]. Furthermore, the number of CuNPs loaded onto the membrane surface via the dip-coating method is uncontrollable, and the membrane is likely to lose its antimicrobial functionality through the gradual dissolution of the mono-layered CuNPs. Thus, the development of an efficient method to controllably load the biocide and thereby inhibit biofouling for more sustainable applications is needed.

4.1.2 Modification method: layer by layer self-assembly of CuNPs

Blending metal NPs into the membrane casting solution [71], anchoring NPs into the membrane structure via the cold spray technique [136], and developing a NP coating onto the membrane surface through plasma treatment [137] all appreciably improve the antibacterial activities for some ultrafiltration (UF) and microfiltration (MF) membranes. However, these NP loading methods are not suitable for the surface modification of a RO membrane, since they result in irretrievable damage of the polyamide active layer. Therefore, the salt rejection of the membrane would decrease with the gradual release/consumption of the metal particles. Furthermore, regeneration of the NPs would be challenging.

Layer-by-layer (LbL) self-assembly is an effective strategy for fabricating functionalized multilayers on a membrane surface [138] as introduced in 3.1.1, and the number of functional units can be precisely controlled by manipulating the number of multi-layers [38]. Since no adverse chemical reactions take place during the procedure, the properties of the original membrane are not altered by this multiple film loading modification [139]. Although some researchers have implemented LbL assembly to apply nanoparticles for biofouling control, the manual dipping LbL assembly operation is time consuming, and the coating proves not as uniform as would be expected [135]. These unsatisfactory results present an opportunity to improve the coating efficiency and

quality of the LbL modification method. Automatic spray- and spin-assisted LbL processes have been reported to produce uniform nanotube/nanowire electrodes [140] and polymer coating on glass plates [141]; however, to the best or our knowledge, it has never been used for membrane surface modification

In this study, the highly efficient spray- and spin-assisted layer-by-layer (SSLbL) method was applied to assemble CuNP functionalized anti-bacterial coatings on a commercial RO membrane in a controllable manner. This antifouling coating consists of multi-layers that employ PEI-coated CuNPs as a polycation and PAA as a polyanion. By taking advantage of the negative charge on the polyamide surface, the multi-films are firmly deposited onto the membrane and held in place by the resulting electrostatic interactions. The successful modification of a commercial RO membrane was examined, and the modified membrane surface properties were assessed. The effect of the modification on membrane performance was evaluated through water permeability and salt rejection experiments. Moreover, the biocidal properties of the modified membrane were evaluated through static bacterial cell inactivation and cross-flow cell filtration tests. The SSLbL methodology provides a uniform coating of CuNPs on the membrane surface, offers controllable particle loading and also presents a high modification efficiency (32 sec per bilayer deposition) compared with manual dip-coating LbL modification (25-60 min [139, 142] per bilayer deposition), indicating the potential for its practical application in commercial anti-biofouling membrane modification practices.

4.2 Materials and methods

4.2.1 Chemicals and materials

Copper sulfate ($CuSO_4$), sodium borohydride ($NaBH_4$), nitric acid (HNO_3), polyethylenimine (PEI) (branched, MW=25 kDa), isopropyl alcohol, hydrochloric acid (HCl) and poly(acrylic acid) (PAA) were all purchased from Sigma-Aldrich (Oakville, ON, Canada), and all solutions were prepared in deionized (DI) water. The UTC-82C seawater desalination membrane was obtained from Toray Company (Poway, CA, USA).

4.2.2 Preparation of the PEI-coated copper nanoparticles (CuNPs)

Positively charged PEI-CuNPs were synthesized via the wet chemical reduction method (Figure 4.2 A) following a published protocol [14]. Briefly, 10 mL of 50 mM $CuSO_4$ was added to 30 mL of 0.066 mM PEI solution. After a 5 min reaction with magnetic stirring, 10 mL of 100 mM $NaBH_4$ was gradually added into the solution, reacting for approximately 25 min. The formed CuNPs were subsequently dialyzed for 20 h to remove unreacted ions.

4.2.3 Loading CuNPs on the membrane surface via SSLbL

The RO membrane was stored as received in DI water at 4 ºC. To modify the active layer, the membrane coupon was immersed in 20% isopropanol solution for 20 min. Then, the pretreated membranes were rinsed several times using and soaked into in DI water until use. The Cee® 200XD Model spray/puddle developer (Brewer Science Inc. Rolla, MO, USA) with spray- and spin-assisted coating functionalities was used to achieve uniform layer-by-layer modification. A picture of the coating system is presented in Figure A-1, and the schemes of the spray- and spin-assisted PEI-CuNPs/PAA layer-by-layer coating modification processes are displayed in Figure 4.2 B-C. Briefly, a 10 cm × 10 cm membrane coupon was adhered onto a polycarbonate plate and spun at 2000 rpm while being spray-coated at 2.1 bar (30 psi), alternating between the positively charged PEI-CuNPs (pH 8.3) and negatively charged PAA solution (pH 3, 1 g/L) in increments of 3 s at 5 mL/s. Between each layer deposition, the membrane was rinsed with DI water for 3 s at 5 mL/s and then air-dried for 10 s (with only spinning). This process completed one cycle of LbL deposition to form a single bilayer of PEI-CuNPs/PAA. The same process was then repeated until a desired number of bilayers was achieved.

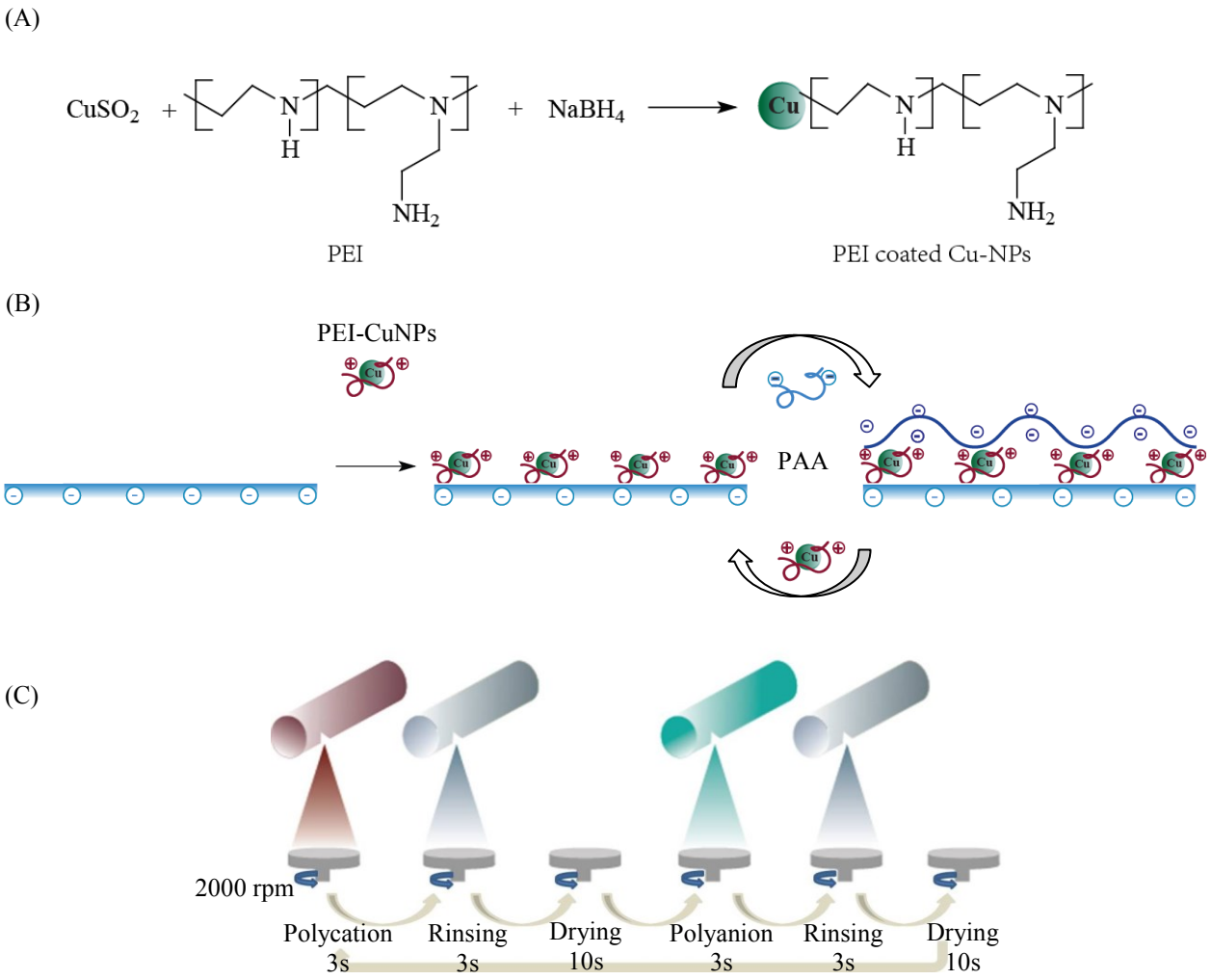

Figure 4. 2 Schemes of **(A)** preparation of PEI-coated CuNPs through the wet chemical reduction method; **(B)** coating CuNPs on the membrane surface via the layer-by-layer self-assembly method; **(C)** spray- and spin-assisted layer-by-layer (SSLBL) self-assembly process.

4.2.4 Membrane characterization

The thickness of the bilayer coating was evaluated by forming exactly the same number of LbL multi-films on the pristine silicon wafer and then analyzed by a profilometer (Dektak XT, Bruker, Germany). X-ray photoelectron spectroscopy (XPS) (ThermoFisher Scientific K-Alpha, Waltham, MA, USA) analysis of the membrane was performed using a monochromatized Al-KαX-ray

source v= 1350 eV with a spot size of 400 μm. The surface zeta potential of the membrane was assessed by an electrokinetic analyzer (EKA) (Anton Paar, Graz, Austria) using 1 mM KCl solution, and the pH was adjusted from 4 to 10 using 1 M NaOH and 1 M HCl. The membrane surface roughness was evaluated using an atomic force microscope (AFM) (NanoINK Inc. Skokie, IL, USA) in tapping mode. The average roughness values were calculated by analyzing the results of three randomly selected scanned positions on the membrane surface (10 μm×10 μm) by using the software 'Gwyddion'. The water contact angle of the membrane was measured by a Video Contact Angle system (VCA, AST Products, Inc., Billerica, MA, USA). At least three position were selected on each membrane surface to obtain the average contact angle value.

To quantify the CuNPs loaded onto the membrane surface, a sample with an area of 3.8 cm^2 was cut from a modified membrane and then immersed into 10 mL solution containing 1% HNO_3 and 0.5% HCl. The total amount of CuNPs released in the acidic solution were quantified by atomic absorption spectroscopy (SpectraAA 220 FS, Agilent Technologies, Inc. Santa Clara, CA, USA).

4.2.5 Evaluation of membrane perm-selectivity

A standard laboratory-scale RO cross flow filtration system was used to test the water permeate flux and salt rejection (Figure A-2). Specifically, a membrane with an effective area of 20.02 cm^2 was compacted overnight at 27.6 bar (400 psi) until a steady water permeate flux was reached. The water permeate flux was monitored with a digital flow meter (Liquid Flow Meter SLI-2000, Sensirion Inc.CA,USA), and the salt rejection was assessed by measuring the rejection of 50 mM NaCl solution using a calibrated conductivity meter (Oakton Instruments, Vernon Hills, IL, USA). All filtration experiments were performed at 20.0 ± 0.5 °C with a cross-flow velocity of 21.4 cm/s.

4.2.6 Observation of membrane antimicrobial property

Static bacterial inactivation tests using three different bacterial strains were performed to evaluate the antimicrobial properties of the membrane. *Enterococcus faecalis* (ATCC 29212) was used as a representative Gram-positive organism, and *Escherichia coli* D21f2 and *Escherichia coli* O157:H7 (ATCC 700927) were used as representative nonpathogenic and pathogenic Gram negative strains, respectively. The static cell inactivation test was performed according to the following protocol. First, a single colony of each bacterial strain was added to 20 mL sterile lysogeny broth (LB) solution and incubated overnight with shaking (70 rpm) at 35℃. Next, the

bacterial suspension was poured in a sterile centrifuge tube and centrifuged at 5000 g (Mandel Multifuge X3R, 75003603) for 10 min in 2 sequential cycles. After each centrifugation cycle, the supernatant was discarded, and the remaining bacterial cell pellet was resuspended by adding 20 mL of 0.9% NaCl and vortexing. Finally, the bacterial suspension was diluted 10 times and 1 mL of the diluted bacterial suspension was placed into each well of a Millicell® 24 well cell culture plate, containing 2.0 cm^2 membrane coupons fixed at the bottom of the wells with the modified side contacting the suspension. The 24 well plate was incubated at 25℃ for different time intervals (0.5 h, 1 h, 2 h, 4 h and 6 h). After incubation, the membrane coupons were gently rinsed twice with 1 mL 0.9% NaCl solution to remove loosely attached bacteria and sonicated with 2 mL 0.9% NaCl solution for 7 min to detach the adhered bacteria. The obtained bacterial suspension was then serially diluted with 0.9% NaCl and 10 µL of each dilution was plated on LB agar for overnight incubation at 35 ℃.

After being exposed to the bacterial suspension, the membrane coupons were also analyzed by FEI Quanta 450 Environmental Scanning Electron Microscope (FE-ESEM) (FEI company, USA) to assess the effects of CuNPs coating on cell morphology of *E. coli* D21f2. For ESEM observation, membrane samples incubated with bacteria were rinsed, and the bacteria attached on the surface were fixed with 2.5% glutaraldehyde (in 0.1 mM sodium cacodylate buffer) at ambient temperature for 15 min. Then, the sample was rinsed with 0.1 mM sodium cacodylate buffer solution for twice, and dehydrated with ethanol/DI water solutions: 30%, 50%, 70%,90%, 100% for 10 min each in trays. Finally, the samples were dried for at least 3 hours and coated with evaporated carbon (Edwards Auto306, UK Crawley) before being analyzed by SEM.

4.2.7 Assessment of anti-biofouling performance of the modified membrane

The anti-biofouling property of the pristine and modified membranes was evaluated using a RO cross-flow filtration system with three types of feed solutions: (i) DI water, (ii) LB solution (containing 0.1% LB in 10 mM NaCl), and (iii) bacterial suspension (containing 10^5-10^6 CFU/mL in LB solution). The filtration tests with DI water and LB solution were conducted as follows: each membrane was compacted with feed solutions (either with DI water or LB solution) for 8 hours at 27.6 bar (400 psi) to achieve a steady water permeate flux; then, the water permeate flux was

continuously monitored for 24 hours with a digital flow meter connected to a personal computer. For the filtration test with bacterial suspension, the LB solution was initially permeated for 8 hours, and then 50 mL of bacterial suspension (*E. coli* D21f2 in 0.9% NaCl, at a concentration of 10^7-10^8 CFU/mL ($OD_{600\ nm}$ = 0.3)) was added and completely mixed with the LB solution to investigate the biofouling propensity of the modified membrane. The normalized flux was obtained by comparing the measured water flux with the initial flux.

4.2.8 Regeneration of CuNPs on the membrane surface

The regeneration potential of the modified membranes was investigated through release-reloading strategy. First, CuNPs needed to be released from the surface of the modified membrane. In order to release the CuNPs, the active side of a freshly modified 10 cm × 10 cm membrane was put into contact with 32 g/L NaCl solution on a shaker under 50 rpm for 7 days which allowed a near complete release of CuNPs from the membrane surface. The salt solution was replaced each day during the releasing process. After the release of CuNPs, the membrane surface was rinsed with DI water three times to remove the loosely bonded salt ions, then the membrane was soaked in DI water, and stored in a refigrerator until the regeneration process was conducted.

In order to regenerate the $(PEI\text{-}CuNPs/PAA)_{10}$ coating, after 7 days of release and subsequent DI water rinse, the membrane was adhered onto a polycarbonate plate, and the same SSLbL coating process was repeated as described in 2.3.

4.3 Results and discussion

4.3.1 Characteristics of PEI-CuNPs

The polyamide active layer of the RO membrane is formed by interfacial polycondensation between trimesoyl chloride (TMC) and m-phenylene diamine (MPD). Due to the hydrolysis of unreacted TMC in aqueous solution, the membrane exhibits a negative charge under general operating pH conditions [26]. To stably anchor CuNPs onto the membrane surface without adverse effects on its separation performance, PEI was used as a capping agent to provide the particles with a positive charge that then assisted in the binding between the CuNPs and the thin active layer through electrostatic interactions. The amine groups of PEI contain lone pair electrons that will attract Cu^{2+} in solution and occupy its outer orbit. By adding $NaBH_4$ into the solution, the copper

ions are reduced into CuNPs within the matrix of the PEI polymer. The reduced metal nanoparticles exhibited better dispersion ability than CuNPs that were prepared by $CuSO_4$ and $NaBH_4$ without the capping agent (Figure A-3).

The average diameter of the synthesized PEI-CuNPs was 39.4±0.3 nm, as observed by DLS and TEM (Figure A-4.A, Figure A-4E). As expected, the PEI-CuNPs remained positively charged in the pH range of 4 to 10 (Figure A-4.B). To confirm that this positive charge was associated with the amine group of PEI, ATR-FTIR spectra was used to investigate the functional units on the CuNP surface (Figure A-4.C). Compared with pure CuNPs, the emerging characteristic peaks of an amine group at 1092 cm^{-1} (C-N stretching), 1594 cm^{-1} (N-H bending) and a broad band at ~3400 cm^{-1} (N-H stretching) indicated the successful functionalization of PEI on the PEI-CuNPs' surface. The percentages of CuNPs and polymers in the PEI-CuNPs were evaluated by TGA (Figure A-4.D) after being washed (three times) through centrifugation and subsequent drying at 105±3℃. The PEI-CuNPs complex began to decrease in weight with an increase in temperature and remained constant after 700℃. The remaining 57.8% of the mass consisted of inorganic CuNPs. It is uncertain, though, how much of the copper was oxidized throughout the process, so the mass percentage of CuNPs in the PEI-CuNPs would be within 46.2-57.8%.

4.3.2 Binding PEI-CuNPs on the membrane surface

CuNPs were incorporated onto the membrane surface through electrostatic interactions [143] with the SSLbL method (Figure 4.2 B-C). The color of the membrane surface changed to a darker and greener shade as the number of PEI-CuNPs/PAA bilayers increased (Figure A-5), and the CuNPs exhibited a uniform distribution on the membrane surface. The freshly synthesized CuNPs were brown, but they were gradually oxidized, turning green, after being exposed to air for approximately five days. The thickness of the LbL films formed on silicon wafers was measured by a profilometer. The thickness was found to increase almost linearly with the increasing number of bilayers, with each PEI-CuNP/PAA bilayer being approximately 60-80 nm (Figure 4.3 A). In the LbL process, the thickness of the coating can be conveniently controlled through the number of bilayers [144].

XPS analyses of both the pristine and modified membrane surfaces were performed to confirm whether the CuNPs were successfully incorporated. In comparison to a pristine PA membrane, additional signals at 89 eV and 931 eV, representing the Cu3p3 orbital and Cu2p/Cu_2O, respectively, appeared on the CuNP-modified surface (Figure 4.3 B). The element contents of Cu on the modified membrane surface, as assessed by XPS, were 0%, 7.3±1.1%, 7.4±0.7% and 6.9±1.5% (Table A-1) for the pristine membrane and the two, six and ten bilayer PEI-CuNP/PAA-modified membranes, respectively. The CuNPs presented very consistent contents on the modified membrane surfaces, and this further suggests that the SSLbL assembly method granted a nearly constant loading of the CuNPs in each bilayer.

The quantity of CuNPs loaded onto the substrate surface increased with each additional PEI-CuNP/PAA bilayer. Two bilayers resulted in 1.75 μg cm^{-2} of copper on the membrane surface, and this number increased to 23.7 μg cm^{-2} for a 10-bilayer modified surface (Figure 4.3 C). By selecting the number of bilayers, the desired quantity of CuNPs on the surface could be achieved. Manual dip-coating was also applied in this study to produce the same PEI-CuNPs/PAA bilayers, while a larger quantity of CuNPs and more uniform bilayers were observed on the membranes modified via SSLbL method in comparison to that manual dipping (Figure A-6, A-7). The stability of the multi-films has always been a concern in the LbL process. To test the stability of the CuNPs, a modified membrane was placed in a vial that contained 20 mL DI water, and then submerged in a bath sonicator (Branson 8510, Branson ultraschall, Germany) for 5 min. The quantity of copper on the modified membrane surface remained nearly unchanged before and after sonication (Figure 4.3 C), indicating a stable binding between the nanoparticles and the membrane surface.

A batch test was performed to further evaluate the amount of released CuNPs and the durability of the 10-bilayer coating. Initially, copper ions were released from the membrane at a rate of 1.25 μg cm^{-2} day^{-1} under DI water, and then the release rate declined with operation time (Figure 4.3 D). After 7 days, the release rate decreased to a level lower than 0.4 μg cm^{-2} day^{-1}. The amount of copper that leached out during 7 days of batch testing (7.0 μg cm^{-2}) accounted for 29.8% of the total amount of copper on the membrane. Since the LbL assembly relies heavily on electrostatic interactions between the oppositely charged PEI-CuNPs and PAA layers, a highly concentrated salt solution (i.e., seawater) may disturb the charge balance between the polyelectrolytes and may cause destabilization of the bilayers resulting in a rapid loss of CuNPs from the membrane.

Therefore, the stability of the modfied membrane with $(PEI\text{-}CuNPs/PAA)_{10}$ coating was further assessed under a higher ionic strength condition (50 mM NaCl). As observed in Figure 4.3 D, the release rate of CuNPs showed a slight increase at the mid-ionic strength condition, and near 39.0% of copper on membrane surface elapsed after seven days. This indicates a comparable stability of the bilayers, even at certain salt concentrations. A slightly increased release rate of Cu ions may be caused by the increased ionic strength of the solution. The release behavior of the CuNPs under a cross-flow filtration (under 400 psi with DI water for overnight compaction and with 50 mM NaCl for 24 h filtration) was also observed (Figure A-8), and the varied release rates of CuNPs from the different parts of the membrane was observed. The stability of LbL films under different solution chemistries was also investigated in the existing literatures. Choi et al. presented the electrostatic interactions between the multifilms provided adequate stability to graphene oxide nanosheet modified RO membranes even at high salt concentration (2000 mg/L NaCl) and harsh pH (pH 4 and pH 10) conditions [145]. In another report it demonstrated that a 10-bilayer PAH/PSS (polyallylamine hydrochloride/poly(sodium 4-styrenesulfonate) coating on a polyamide membrane could remain stable in saline water for more than 74 days [139].

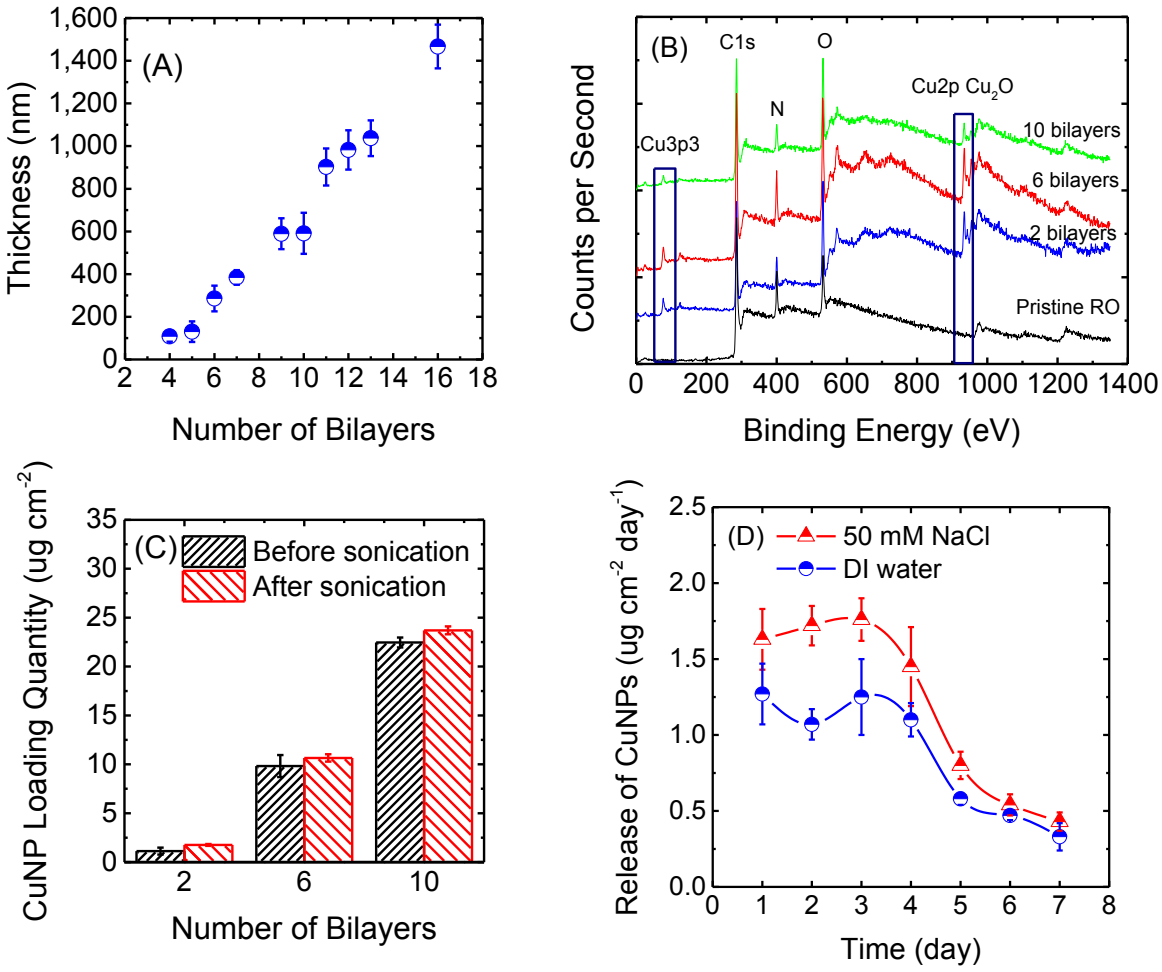

Figure 4. 3 (A) Thickness of PEI-CuNP/PAA coating with different numbers of bilayer. **(B)** XPS spectra of pristine (black) and functionalized PA membrane with different numbers of PEI-CuNP/PAA bilayer coatings. **(C)** The quantity of CuNPs bonded onto the membrane surface before and after 5 min bath sonication. **(D)** Copper ions release from the batch test. During the batch test, a 3.8 cm^2 ten bilayer PEI-CuNP/PAA modified membrane samples were incubated in 40 mL of NaCl solution (50 mM) under 100 rpm, and the NaCl solution was replaced every 24 h.

4.3.3 Characterization of modified membrane

The ability of a membrane to resist fouling is closely related to its surface physico-chemical properties, particularly the roughness, charge and hydrophobicity. Generally, a membrane with a

relatively smooth surface, an electro-neutral and hydrophilic nature presents improved fouling resistance [6]. AFM, EKA and contact angle measurements were conducted to evaluate the surface physico-chemical property changes of the modified membranes.

The effect of the CuNP modification on the membrane surface morphology was investigated by SEM, and the corresponding roughness was evaluated using AFM (Figure 4.4). SEM images presented the characteristic "ridge-and-valley" [146] structure that resulted from the interfacial polymerization could be clearly identified on a pristine PA membrane surface; however, the valley region was partially filled with nanoparticles and the accompanying polymers after two polyelectrolyte bilayers were added, and a $(PEI\text{-}CuNPs/PAA)_{10}$ (ten bilayer coating of PEI-CuNPs/PAA) covered the original morphology of the PA membrane completely. This observation can also be noted in the corresponding AFM analysis. The slight increase in roughness (Table A-2) of the modified membrane may be associated with the incorporation of CuNPs. Although increasing the surface roughness might cause more bacterial cell deposition on the membrane surface, the deposited bacteria may become inactivated through action of the CuNPs.

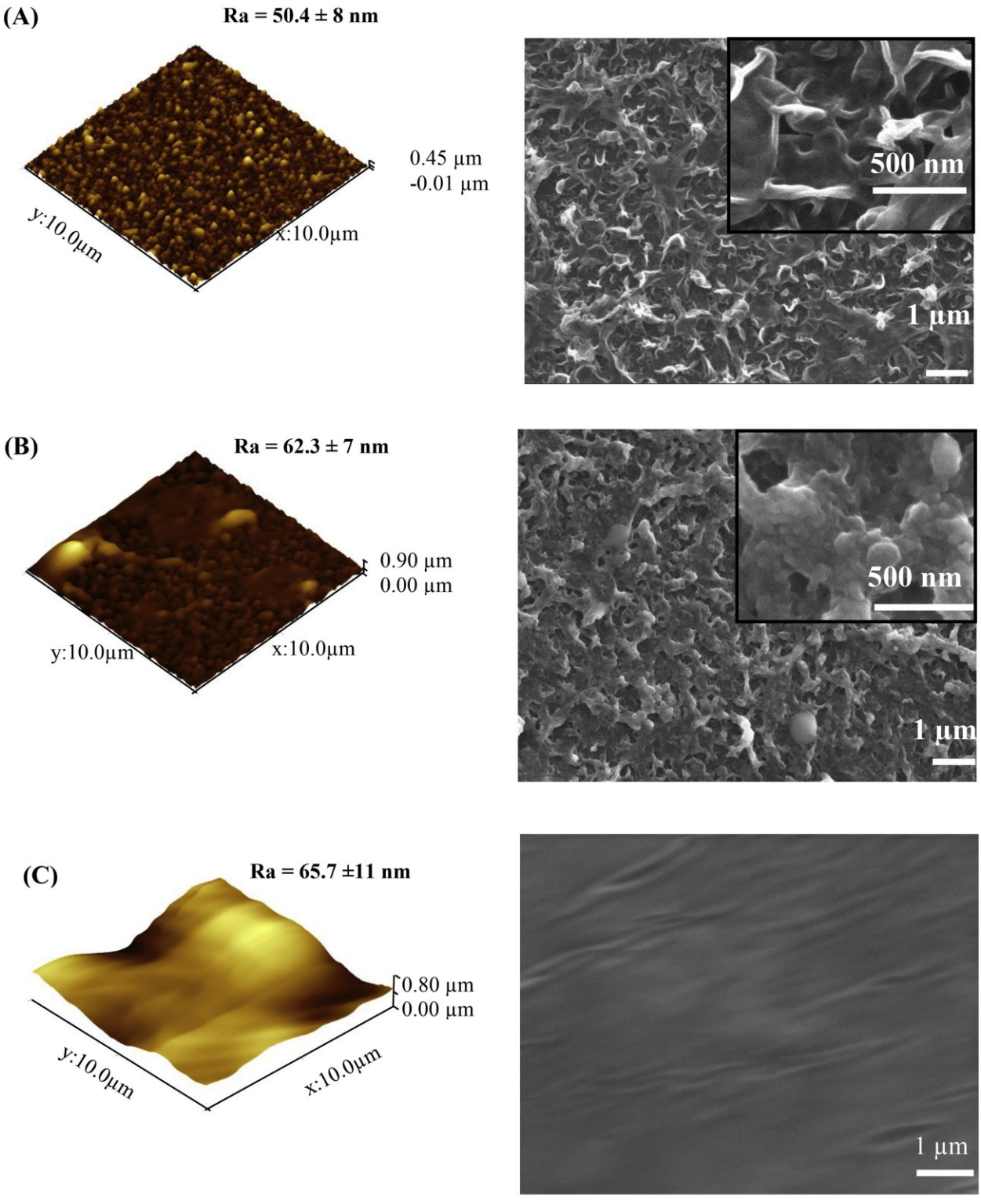

Figure 4. 4 AFM and SEM images of the membrane surface. **(A)** Pristine membrane and **(B)** two bilayer, and **(C)** ten bilayer PEI-CuNP/PAA modified membranes.

The top layer of the modified membrane mainly consists of PAA, which has the same carboxylic (-COOH) groups as the pristine TFC membrane; therefore, both the pristine and modified membranes exhibited negative charges from pH 4.2 to pH 9.9 (Figure 4.5 A). It was hypothesized that compared with the pristine membrane, the added PAA layer would significantly increase the number of carboxylic (-COOH) groups on the surface, which may cause a corresponding decrease in the zeta potential for the modified membrane; however, the results show that after (PEI-CuNPs/PAA)$_{10}$ multi-film coating, only a minor decrease in the membrane surface charge was observed. This may be because of the lone pair electrons on the -NH_2 group of the PEI beneath the PAA layer that tends to attract some of the protons (isoelectric point of PEI is near pH 10 [9], thereby maintaining nearly the same overall surface charge on the modified membrane.

CuNP coatings significantly change the membrane surface wettability (Figure 4.5 B). Because PEI and PAA are naturally hydrophilic, even a ten-bilayer polyelectrolyte modified membrane consisting of only PEI and PAA had a contact angle of approximately 20º; while, adding CuNPs to the PEI matrix resulted in a decrease in the surface hydrophilicity (The contact angle increased from 20º of ten bilayers of PEI/PAA to near 60º of ten bilayers of PEI-CuNPs/PAA). The CuNPs increased the thickness of the coatings, which might cause additional hydraulic resistance towards permeation of water. However, in the RO desalination process, the applied pressure is typically approximately 13.8-55.2 bar (200-800 psi), which is adequately high for water molecules to overcome the hydraulic resistance of the coating layers. Thus, the PEI-CuNP/PAA bilayers would not cause an appreciable negative effect on the membrane's performance. This hypothesis was supported by the results of the performance evaluation (Figure 4.5 C).

Due to higher water flux and excellent salt rejection ability, the TFC membranes are considered to be the 'state-of-the-art' in RO process. Therefore, no significant compromise of membrane performance is deemed after surface modifications. A slight decrease in water permeation flux is observed for the modified membranes with the addition of the coating layers (Figure 4.5 C and A-9). A ten-bilayer coating resulted in only a 13.3% reduction (from 1.54 ± 0.18 L m^{-2} h^{-1} bar^{-1} of pristine membrane to 1.38 ± 0.14 L m^{-2} h^{-1} bar^{-1} of the ten-bilayer modified membrane) in the water permeation flux, which might stem from the additional CuNP coatings on the membrane surface. Because no adverse chemical reaction was taking place between polyamide and the coating layer, the modified membrane still performed well, with a high salt rejection capacity.

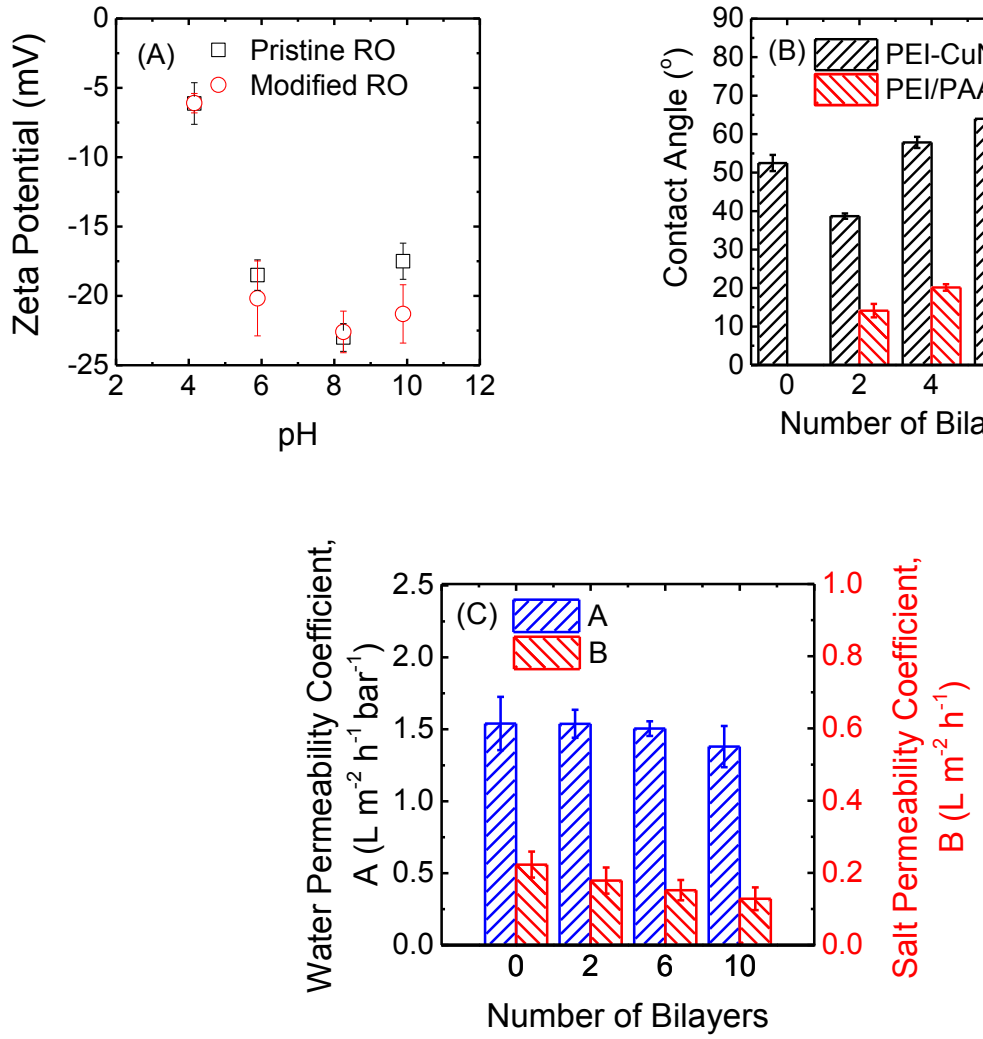

Figure 4. 5 (A) Zeta potential of pristine membrane and ten bilayer modified membrane at different pH values; **(B)** contact angle of pristine membrane and membranes modified with different numbers of (PEI-CuNP/PAA) and (PEI/PAA) bilayers; **(C)** water permeability coefficient, A, and salt permeability coefficient, B, of pristine (0 bilayer) and modified membranes.

4.3.4 Antimicrobial and antifouling activities of modified membrane

To evaluate how the applied surface modification improves the anti-biofouling potential of the membrane, the antimicrobial behavior of different surfaces: pristine, $(PEI/PAA)_{10}$-, $(PEI\text{-}CuNPs/PAA)_2$-, and $(PEI\text{-}CuNPs/PAA)_{10}$-coated membrane, was initially investigated using a model non-pathogenic *E. coli*. Compared with the polyamide pristine membrane, the membrane coated with CuNPs exhibited strong antibacterial property that increased with the amount of loaded CuNPs on the membrane surface (Figure 4.6 A). A considerable decrease in CFU of *E. coli* D21f2 (in the range of 94.3% to nearly 100%) was observed on two, six and ten bilayer PEI-CuNPs/PAA modified membrane surfaces after 1 h of contact. Although PEI was reported to possess a certain antibacterial property as well [45], the pure $(PEI/PAA)_{10}$-modified membrane showed only 14% inactivation of the bacterial cells attached on the membrane surface. Thus, it could be concluded that the CuNPs played the decisive role in the increase of bacterial cell inactivation. FE-ESEM was used to observe the morphology of the bacterial cells on the pristine and $(PEI\text{-}CuNPs/PAA)_2$ modified surface. The bacaterial inactivation could possibly be evidenced by slight morphological changes (from the regular rod shape) of the deposited bacteria as displayed in Figure 4.6 B-C, a similar observation was reported in the literature [74, 147]. However, these slight changes in the shape of the bacteria on the SEM images provide only a possible indirect evidence of bacterial inactivation.

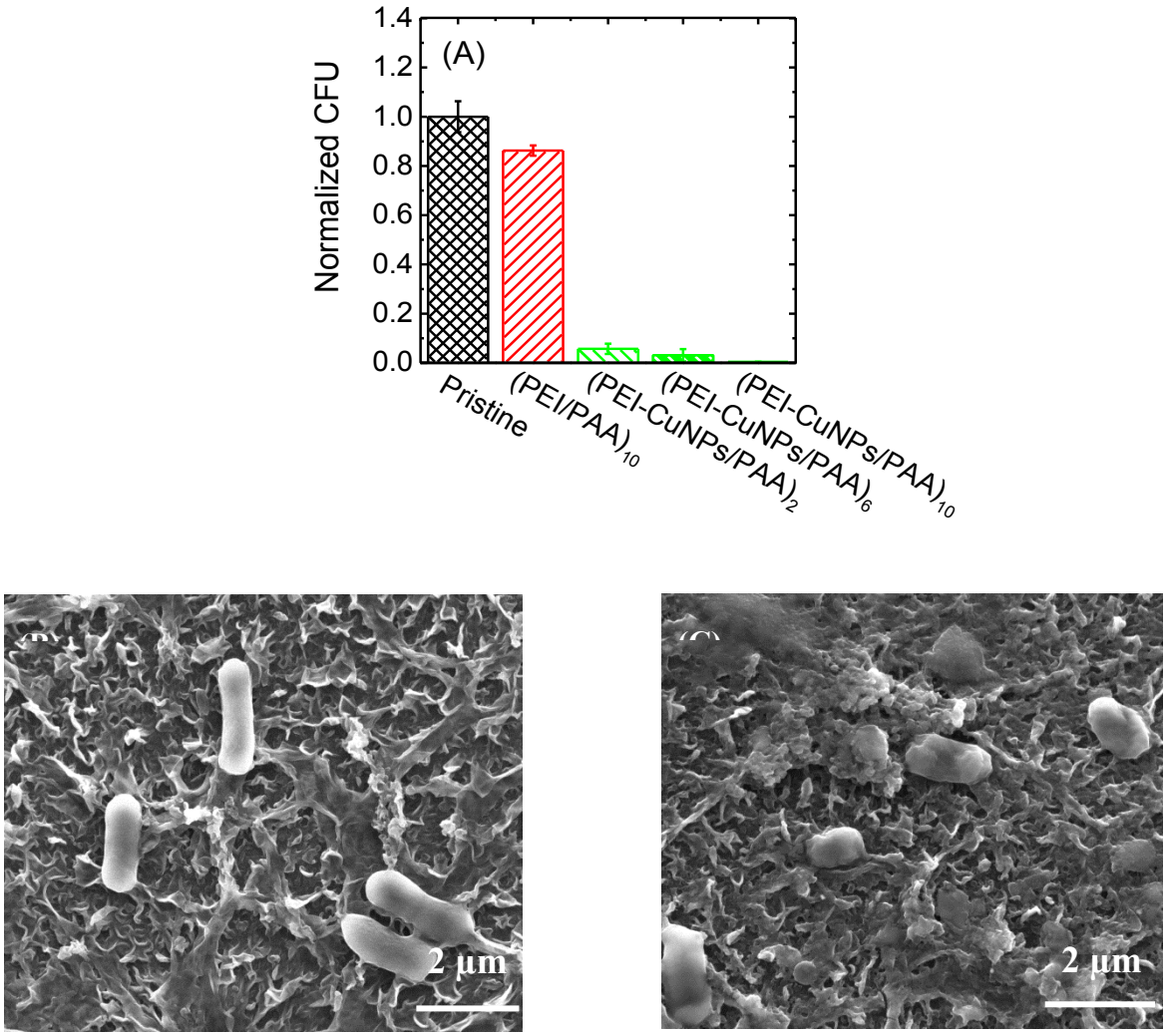

Figure 4. 6 (A) The number of live cells attached to the pristine and CuNPs modified membrane surfaces after 1-hour static contact. In the samples preparation process, the membrane coupons with the surface areas of 2.0 cm^2 were contacted with 1 mL of the E. coli D21f2 solution ($OD600_{nm}$= 0.1) for 1 h. SEM images of cells (*E. coli D21f2*) after contacting with **(B)** pristine polyamide membrane and **(C)** $(PEI\text{-}CuNPs/PAA)_2$-modified membrane for 1 h.

To further evaluate the antimicrobial behavior of the modified membrane, time-dependent static (no pressure, no flow) bacterial inactivation tests were performed using three different strains of bacteria; namely, *E. coli* D21f2 (Gram negative and non-pathogenic), *E. coli* O157:H7 (Gram negative and pathogenic) and *E. faecalis* (Gram positive and pathogenic). The results showed that the $(PEI\text{-}CuNPs/PAA)_{10}$-modified membrane exhibited strong anti-bacterial effect to all tested bacteria whereas on the pristine membrane, bacteria remained viable with increasing number of CFU over time (Figure 4.7 A-C). The top layer of the pristine membrane, polyamide, was non-toxic and exhibited relatively rough surface; therefore, the number of bacteria that deposited on the pristine membrane increased significantly with the extension of the contact time between the bacterial suspension and the membrane from 0.5 to 6 hours.

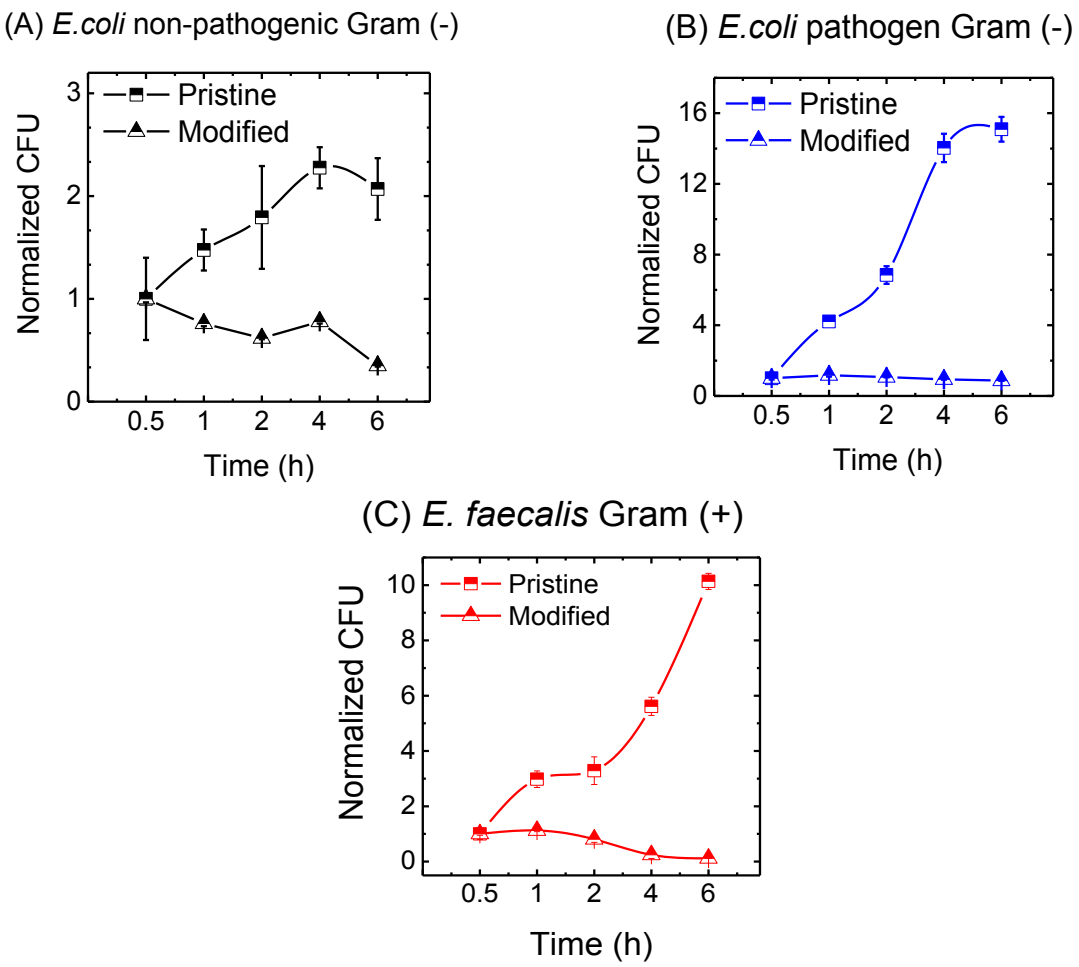

Figure 4. 7 The number of live cells on the pristine and $(PEI\text{-}CuNPs/PAA)_{10}$ modified surface over 0.5-6 hours contact with **(A)** *E. coli D21f2*, **(B)** *E. coli O157:H7* and **(C)** *E. faecalis (ATCC 29212)* bacterial suspensions.

The strong antimicrobial behavior of the modified membrane is linked to the presence of biocidal CuNPs. The complex mechanism of CuNP action in bacterial cell killing is not fully understood, while some possible cell killing pathways of copper are reported and widely accepted: (1) the appearance of trace amounts of CuNPs depolarizes the cell membrane and causes the anomalous growth of bacteria [148]; (2) the oxidation of CuNPs results in a release of electrons and motivates the production of ROS (reactive oxygen species) [62], which leads to oxidative damage of the cellular structures; (3) the spontaneous interaction between Cu^{2+} and phosphorus/sulfur-containing biomolecules (protein, DNA) causes distortion of the organism structure and disruption of metabolism processes [149]. It was also reported [148] that the interaction between CuNPs and bacterial cells was active, and the binding of the Cu^{2+} to DNA caused more ion release from CuNPs and led to more DNA damage. This suggests that the interaction between CuNPs and bacterial cells has certain influence on the dissolution rate of the CuNPs. Therefore, one may conclude that a greater number of bilayers should be taken into consideration for the membrane to be effective in bacterial inactivation for longer time periods.

The anti-biofouling property of the modified membrane was also studied through dynamic RO cross-flow filtration tests using *E. coli* D21f2 as a model bacterium. The permeate flux reductions of the pristine and $(PEI\text{-}CuNPs/PAA)_{10}$ coated membranes associated with biofouling are presented in Figure 4.8 A-B, and the corresponding normalized flux reductions were reported in Figure A-10 A. Both the pristine and modified membranes exhibited stable water flux under the DI water condition; but showed a gradual decrease in permeate flux with the LB solution (containing 0.1% LB in 10 mM NaCl), which is likely caused by deposition of proteins and other constituents of the LB onto the membrane surface. When bacteria were added to the LB solution, the permeate flux of the pristine membrane significantly decreased (66% reduction after 24 hours of filtration); by contrast, the flux reduction of the CuNP-modified membrane was slower under the same experimental conditions. After 24 hours, a 43% reduction of permeate flux was observed for the CuNP-modified membrane, which was very close to the control LB solution without bacteria (38% reduction of the permeate flux). Compared with polyamide surface, this reduced flux decline supported the hypothesis that the CuNPs effectively mitigated the growth of bacterial cells on the membrane surface.

The biofilms formed on both the pristine and the modified membranes after 24 hours filtration in a cross-flow RO cell were visualized via FE-SEM (Figure A-10 B-C). Consistent with that observed during the static bacterial inactivation tests, more vegetative cells (with regular rod shape) were visualized on the pristine membrane; while cells with slightly changed morphologies appeared on modified surface. The structures of the biofilm mat produced on the two surfaces also seemed to be different. A thicker matrix and higher concentration of extracellular polymeric substances (EPS) between *E.coli* cells on the pristine membrane surface may imply that the bacterial communities were embedded within an EPS matrix [150, 151]. In comparison, the individual cells on the modified surface were relatively clear, which likely indicates less production of EPS on the CuNPs coated surface. The EPS produced by bacteria on membranes usually reinforces the adhesion between cells and membrane material, and results in the gradual reduction of water flux.

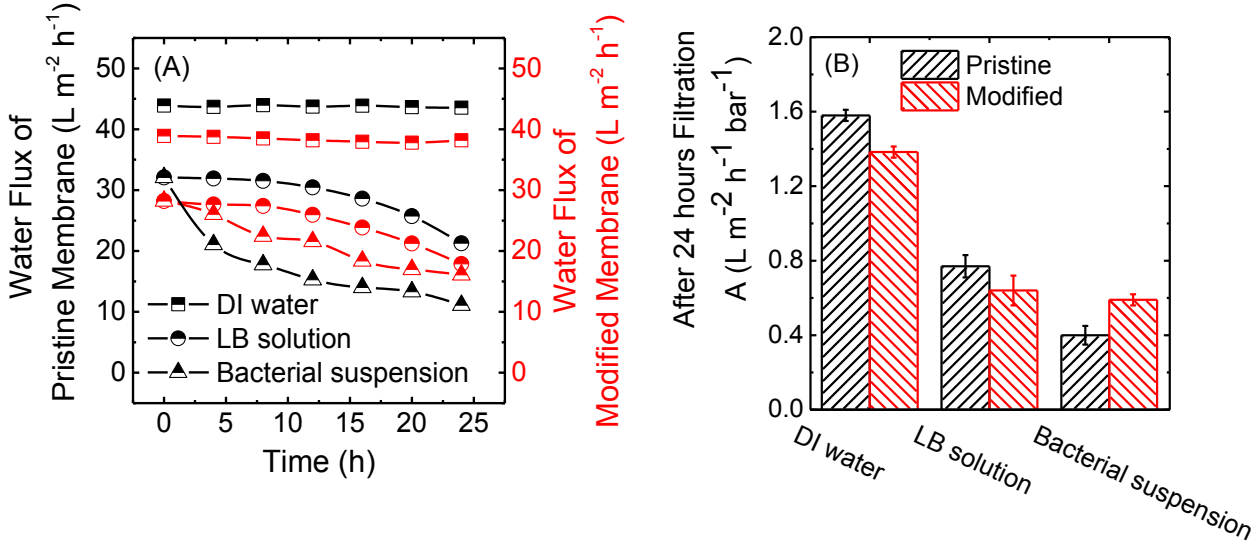

Figure 4. 8 (A) The water flux changes of pristine (black color) and $(PEI\text{-}CuNPs/PAA)_{10}$ modified membranes (red color) tested with three different feed solutions: (i) DI water, (ii) LB solution (containing 0.1% LB in 10 mM NaCl), and (iii) bacterial suspension (10^5-10^6 CFU/mL in LB solution). **(B)** The water permeability coefficients of the pristine and $(PEI\text{-}CuNPs/PAA)_{10}$ modified membrane after 24 hours filtration with three different feed solutions.

Both static bacterial adhesion and cross-flow filtration tests demonstrated that CuNPs could significantly improve anti-biofouling property of a polyamide membrane and effectively reduce the permeate flux decline caused by bacterial deposition on the membrane surface. However, it remains unclear whether CuNPs on the membrane surface or dissolved copper ions in solution mainly contributed to this anti-bacterial activity. The interaction between CuNPs/Cu^{2+} and bacterial cells and the release rate of CuNPs from the membrane surface requires further study.

4.3.5 Regeneration of CuNPs coating on the membrane surface

Due to the biochemical reactions and the applied shear force during the filtration process, the depletion of biocidal NPs from membrane surface became inevitable for most of the modification method with metallic NPs. Therefore, a convenient and effective method of regeneration of biocidal agents after their discharge should also be taken into consideration. Since the CuNPs were fastened to the membrane through electrostatic interactions, the original structure of the membrane surface was not irreversibly changed. Furthermore, LbL has fewer requirements as relating to substrate surface properties, and it could be successfully produced on different substrates such as silicon, glass or quartz plates [152 153]. Thus, it is expected that the PEI-CuNPs/PAA multi-film could easily be regenerated by the same SSLbL technique once CuNPs are completely depleted from the modified membrane.

To confirm the regeneration of PEI-CuNPs/PAA bilayers after their depletion, a freshly modified membrane was immersed in 32 g/L NaCl solution for seven days to allow a near-complete release of CuNPs, and then multi-film was regenerated via the same SSLbL method. It was observed that the quantity of CuNPs after $(PEI\text{-}CuNPs/PAA)_{10}$ regeneration was even higher than the freshly modified membrane (Figure 4.9 A), which may be because of the incomplete release of CuNPs after seven days. Owing to the high quantity of CuNPs content, the regenerated membrane exhibited excellent antimicrobial properties (Figure 4.9 B), and almost complete inactivation (nearly 100% decrease in CFU when compared with that of pristine membrane) was observed with the regenerated membranes. This observation supports that the potential anti-biofouling properties of the modified membrane could be maintained during long-term operation through a process of regeneration of the CuNPs coating after being depleted.

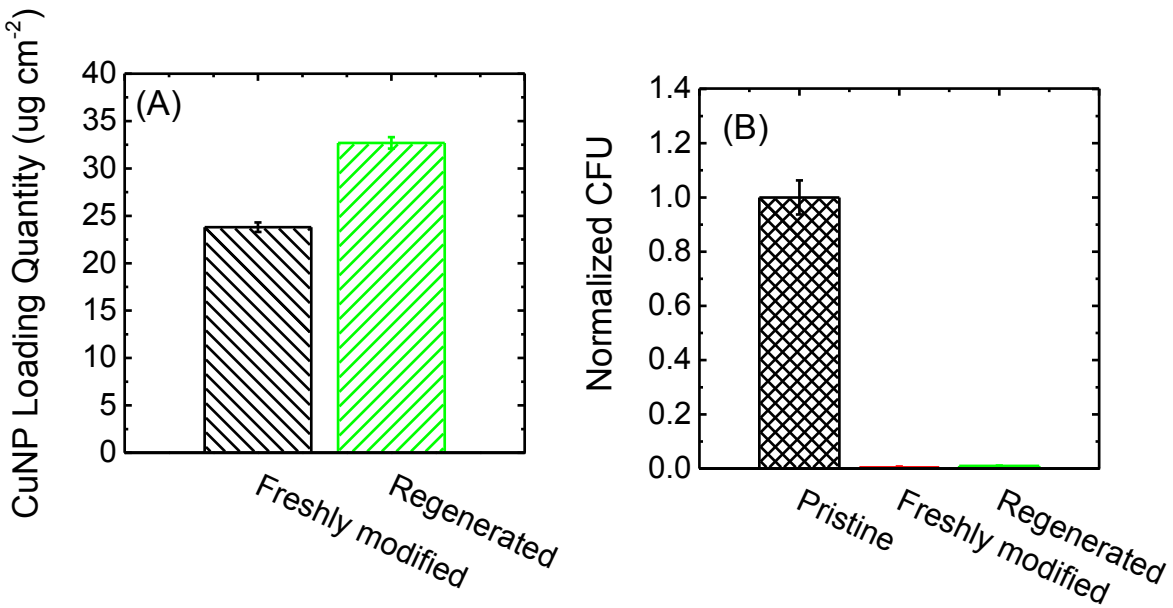

Figure 4. 9 (A) The quantity of CuNPs on the freshly $(PEI\text{-}CuNPs/PAA)_{10}$ modified membrane and $(PEI\text{-}CuNPs/PAA)_{10}$ regenerated membrane. **(B)** The number of live cells attached to the pristine, freshly $(PEI\text{-}CuNPs/PAA)_{10}$ modified membrane and $(PEI\text{-}CuNPs/PAA)_{10}$ regenerated membrane surfaces after 1-hour static contact.

4.3.6 Implications

There is no denying that the CuNPs are more prone to oxidation and release when compared with AgNPs; however, the LbL process benefits from the increased number of CuNPs on the membrane surface, and the $(PEI\text{-}CuNPs/PAA)_{10}$ modified membrane shows a comparable antimicrobial performance and NP durability in comparison to that of AgNPs modified surfaces, according to our previous work [72] [127]. The released CuNPs could also potentially serve as bacteria-inactivating NPs/ions in the feed solution, inhibiting the reproduction of bacteria.

Compared with manual LbL process reported in several references, the SSLbL process introduced in this study could produce a more uniform layer on the membrane surface within a very short period. Even though the spinning process is difficult to apply in large scale membrane modification, it could be easily replaced by a rolling spiral axis, or the static spray nozzles could be changed into

moving ones to produce a uniform layer for industrial applications. Therefore, the scaling up of this technique for large-scale industrial production would not be an issue. In the case of membranes in a spiral wound module, the combining the SSLbL coating of CuNPs at the beginning, and reduction of Cu ions or the dipping LbL process for the regeneration of CuNPs in situ could be a feasible way to improve the anti-biofouling performance of the RO membrane with the lower cost when compared with the one with the AgNPs as the modifier.

Furthermore, the LbL process is a facile method for surface modification, and it does not have critical requirements for the substrates. Thus, even though NPs deplete after long-time use, the functional units could be conveniently reproduced on the membrane surface via the same method.

4.4 Conclusions

To improve the antimicrobial properties of RO membrane surfaces, CuNPs were used as biocides and deposited on a membrane via 'spray- and spin-assisted layer-by-layer' self-assembly. This rapid (32 sec per bilayer) and efficient method improved the uniformity of the CuNPs distribution on a modified membrane's active layer compared to conventional dip coating techniques.

In general, the LbL modification did not adversely affect the membrane's separation performance and maintained the same level of salt rejection after modification. However, additional bilayers reduced the surface's hydrophilicity and resulted in a 13.3% reduction in water permeation flux.

The CuNP-functionalized membrane exhibited a significant inactivation ability to model Gram positive and Gram-negative bacteria. The inactivation of bacteria increased with increasing CuNP loading on the membrane surface. The CuNP-modified membrane exhibited ability to inhibit bacterial growth on the membrane surface and thus reduce the permeate flux decline (caused by biofouling) considerably.

The quantity of CuNPs and the bacterial inactivation properties of the membrane could be maintained through regeneration of PEI-CuNPs/PAA multi-films via the same SSLbL method after the depletion of CuNPs.

Overall, both the effective and time-saving modification process along with the promising anti-microbial results demonstrate the potential for this novel surface coating in practical applications for membrane biofouling control.

Chapter 5. Controlling biofouling via "attacking" strategy: cysteamine- and graphene oxide-mediated copper nanoparticle decoration on membrane for enhanced anti-microbial performance

Abstract

In this work, copper nanoparticles (CuNPs) were decorated onto the polyamide RO membranes via *in-situ* reduction for biofouling mitigation. To increase CuNPs loading and improve anti-microbial properties of the membrane, cysteamine (Cys) and graphene oxide (GO), which contain different functional groups with high metal affinity, were applied as bridging agents between CuNPs and membrane surface via covalent bonding. The functionalization of Cys and GO linkers on membrane was confirmed by XPS and SEM analysis. By applying the linkers, the loading quantity of copper, in particular on Cys-modified membrane, was significantly improved and the particle size of CuNPs appeared smaller and had more uniform distribution. The GO medium increased the hydrophilicity of CuNP-decorated membranes, leading to an increase in water permeation with minor impact on membrane's salt rejection. Bacterial inactivation of the Cys-Cu- and GO-Cu-functionalized membranes was over 25% higher than that of the bare CuNP-coated surface, indicating enhanced bacterial inactivation benefiting from the application of linkers. After a CuNPs' release test, the membranes modified with Cys and GO retained larger quantities of CuNPs and showed better antimicrobial performance than that of bare CuNP-modified membranes. The successful regeneration of CuNPs after their depletion demonstrated the modified membranes' potential for long-term application.

Keywords: copper nanoparticles; biofouling; thin-film composite membrane; cysteamine, graphene oxide; linker

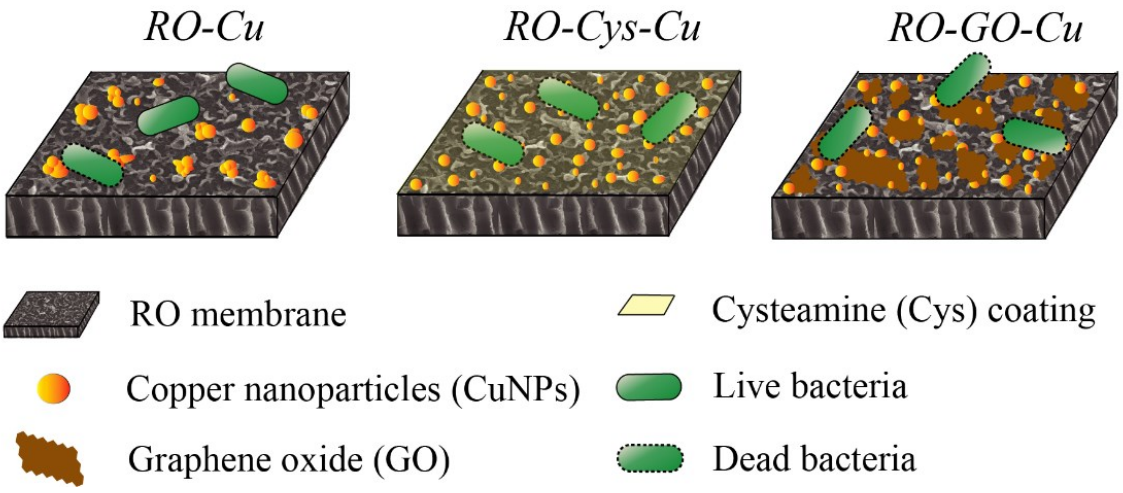

Figure 5. 1 Graphical Abstract

5.1 Introduction

Copper is a potential alternative low-cost biocide which has been registered as the first solid antimicrobial material by the U.S. Environmental Protection Agency [128]. Copper ion [129], copper ion-charged polymer [130] and CuNP/CuO-NP containing solutions all showed appreciable performance in bacterial inactivation [131-133]. Dankovich et al. [134] used CuNPs to reduce the cost of the bioactive paper and found that this new filter had a similar bacterial inactivation capacity as a previously tested AgNP decorated filter. Although plenty of research supports the potential of CuNPs for anti-bacterial surface modification, few of them have focused on applying CuNPs for membrane biofouling control. Ben-Sasson et al. [154] prepared polyethyleneimine (PEI) coated CuNPs and bonded them onto a polyamide membrane surface through electrostatic interaction. Even though the modified RO membrane exhibited significant bacterial inactivation (80-96%), the preparation and binding process of the CuNPs was considerably time-consuming (two days).

The spray- and spin-assisted layer-by-layer self-assembly method was applied in Chapter 4 to load multiple layers of CuNPs onto the membrane surface within a short time; however, regeneration of CuNPs within a spiral wound module would be difficult to achieve. A method to fabricate CuNPs anchored membrane with a durable biocidal performance is required.

In-situ reduction of metal ions to form NPs was reported as an efficient method to load AgNPs on polymer surfaces within a short time (15 min) [155]; however, CuNPs aggregate more easily than AgNPs [156]. Direct *in situ* fabrication of CuNPs may result in an insufficient loading or a non-uniform distribution of NPs on the membrane surface and lead to a poor anti-biofouling performance. Applying linkers of high metal affinity as fabrication media is a potential way to overcome this problem [157]. Carrying zwitterionic units, -SH and $-NH_2$, Cys is a frequently used cross-linker between the metal surface and other molecules [158]. In our previous work, the quantity of bonded AgNPs on the forward osmosis membrane surface was significantly improved by Cys coating due to the thiol-metal bond [105]. Graphene oxide (GO) is another material reported to improve the loading of NPs [159]. GO contains diverse oxygen-rich functional groups (-OH, $-COO^-$, -C-O-C-), which are capable of attracting positively charged ions. With high oxidative stress and sharp edges, GO shows significant potential for bacterial inactivation [75, 160]. Furthermore, GO nanosheets show water affinity and have been applied in many studies to fabricate highly

permeable membranes by taking advantage of their rapid water transportation properties. Therefore, metal nanoparticles, such as gold (Au) [161, 162], TiO_2, and Ag [163, 164] have been combined with GO nanosheets to obtain enhanced biocidal property and improve the water affinity of the substrate surface. Due to their function on improving the loading of metal NPs, both Cys and GO present great potential to develop a cost-efficient, quality-competitive biocidal coating on membranes in the application of metal NPs. However, the application of Cys and GO for improvement of loading of CuNPs to mitigate membrane biofouling, as well as the comparison of their effects, have not been reported. Furthermore, the regeneration of CuNPs and potential recovery of anti-microbial performance after the elapsing of NPs have not been investigated.

In this study, CuNPs were formed onto the polyamide membrane surface via a facile, *in situ* chemical reduction method for biofouling mitigation. For the first time, Cys and GO were functionalized on the membrane surface to serve as functionalization media for CuNPs to improve its loading quantity and enhance the antibacterial properties of the membrane surface. After modification, the number of NPs, membrane surface morphology and water transportation properties were evaluated and compared to investigate the influences of different linkage layers on the CuNP formation. Moreover, the antibacterial performance of the membrane was evaluated using a static bacterial inactivation test; and the live/dead status of bacteria on the membrane surface was observed under confocal microscopy. To study the durability of the modified biocidal membranes, the release rate of CuNPs was assessed and the possibility of regenerating the NPs after their dissolution was investigated further.

5.2 Materials and methods

5.2.1 Chemicals and materials

Copper sulfate ($CuSO_4$), sodium borohydride ($NaBH_4$), cysteamine (Cys), nitric acid (HNO_3), sodium chloride (NaCl), isopropyl alcohol, sodium hydroxide (NaOH), hydrochloric acid (HCl), glutaraldehyde, ethanol, N-(3-dimethylaminopropyl)-N′-ethylcarbodiimide hydrochloride (EDC), N-Hydroxysuccinimide (NHS), Ethylenediamine (ED), 2-(N-morpholino)ethanesulfonic acid (MES) buffer and 4-(2-hydroxyethyl)-1-piperazineethanesulfonic acid (HEPES) buffer were purchased from Sigma-Aldrich (Oakville, ON, Canada). Single layer graphene oxide (GO) nanosheets with a thickness of 0.7-1.2 nm and length of 300-800 nm were purchased from Cheap

Tubes Inc. (Grafton, VT, USA). All samples were prepared with deionized (DI) water produced by a Milli-Q ultrapure water purification system (Millipore, Billerica, MA). The Dow Filmtec SW30XLE seawater desalination membrane was purchased from Dowchem (Midland, MI, USA).

5.2.2 Fabrication of the CuNPs on the membrane surface via *in situ* reduction

Before their modification, the RO membrane samples were immersed in 30% isopropanol for 20 min to remove any coatings on the surface. The pretreated membranes were then rinsed several times and stored in DI water at 4 °C until their use. The rinsed membrane was placed on a plate and covered by a polyester frame with only 6 cm × 11 cm of the active side exposed for modification. The plate and the frame were then tightly clamped with clips to prevent any leakage (Figure A-11). The whole modification process was conducted at room temperature on an orbital shaker with a speed of 50 rpm.

To synthesize the CuNPs *in situ* on the membrane surface without any media, 30 mL of 5 mM $CuSO_4$ was poured onto the exposed membrane surface and contacted for 10 min to allow the adsorption of copper ions. Loosely bound Cu^{2+} was then removed by gently rinsing the membrane with DI water and the active layer was subsequently exposed to 30 mL of 10 mM $NaBH_4$ for 5 min to reduce the remaining Cu^{2+} into CuNPs (Figure 5.2).

In order to synthesize CuNPs on the membrane surface with the Cys linker, the isopropanol treated membrane was contacted with 30 mL of 20 mM Cys solution (dissolved in 70% ethanol) for 4 hours then rinsed 3 times with DI water. The CuNPs were then reduced *in situ* on the membrane surface using the identical process as described above (Figure 5.2).

Covalently binding GO to the PA TFC membranes was conducted according to a published protocol [38, 159] (Figure 5.3). Both the membrane and GO surfaces were modified with an EDC-NHS cross-linker (the amine-reactive intermediates) to convert the carboxyl groups into intermediate amine-reactive esters; then, an amine carrying chemical, ED, was applied to bridge GO onto the membrane surface via amid coupling. Specifically, the isopropyl pretreated membrane was fixed on the frame with the active layer immersed in 30 mL the EDC-NHS solution (consisting of 4 mM EDC, 10 mM NHS and 0.5 mM NaCl in 10 mM MES buffer) for 1 hour. The

EDC-NHS modified membrane was then rinsed with DI water and contacted with 30 mL of the ED solution (consisting of 10 mM ED, 10 mM HEPES buffer and 0.15 mM NaCl) for 30 min.

To prepare an EDC-NHS-ED-GO-modified membrane, 0.05% GO, 2 mM EDC, 5 mM NHS and 0.15 mM NaCl were added in 10 mM MES buffer and sonicated for 10 min to obtain uniformly dispersed GO nanosheets. Finally, the sonicated GO suspension was cooled to room temperature and contacted with the aforementioned EDC-NHS-ED-modified RO surface for 4 hours. After the covalent linking of GO, the CuNPs were reduced *in-situ* on the membrane surface using the aforementioned process (Figure 5.2).

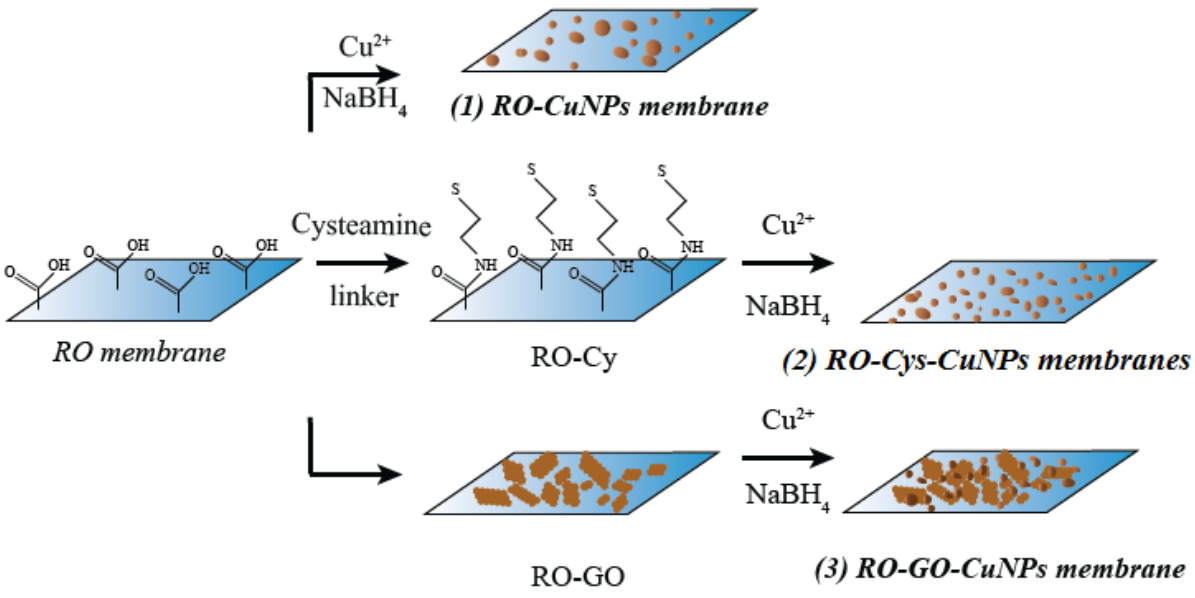

Figure 5. 2 Fabrication of CuNPs modified membranes with GO and Cys as media.

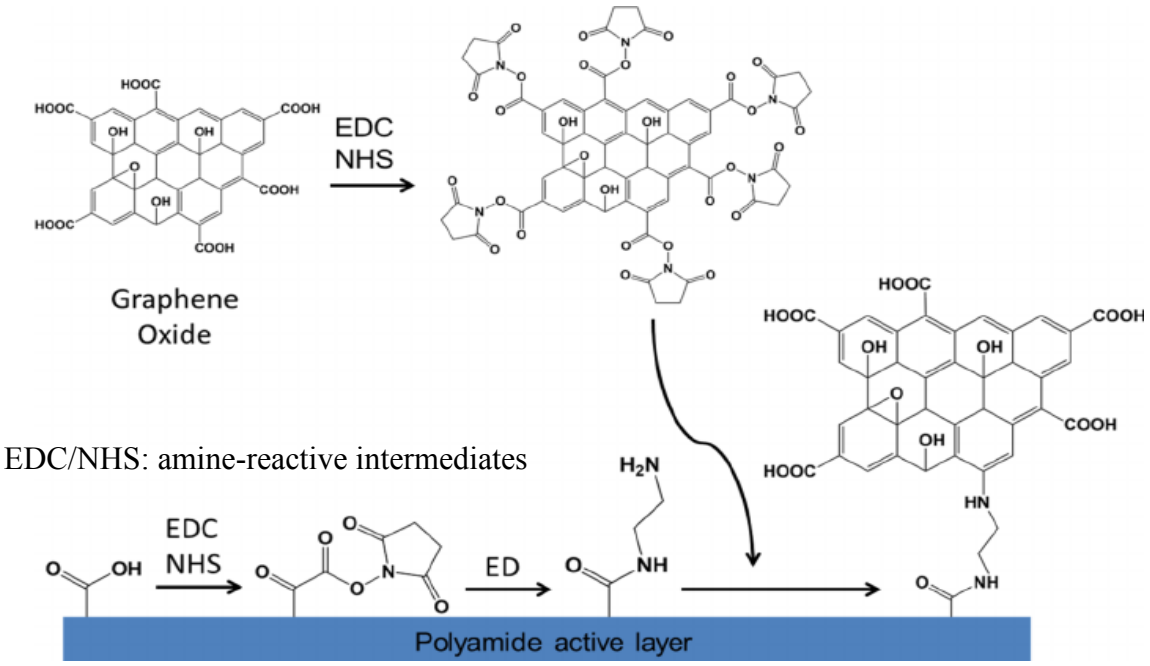

Figure 5. 3 Covalent binding of GO to the native functional groups of the polyamide membrane membrane [40, 123].

5.2.3 Membrane surface characterization

X-ray photoelectron spectroscopy (XPS) (ThermoFisher Scientific K-Alpha, Waltham, MA, USA) analysis of the membrane surfaces was performed using a monochromatized Al-KαX-ray source v= 1350 eV with a spot size of 400 μm. The FEI Quanta 450 field emission environmental scanning electron microscope (FE-ESEM) (FEI Company, OR, USA) was used to analyze the surface morphology. Before FE-ESEM observation, the membrane samples were dried at ambient temperature and coated with evaporated carbon (Edwards Auto306, Sussex, UK). The size of CuNPs on the membrane surface is measured by the SEM imaging software on-board ruler-tool. An atomic force microscope (AFM) (NanoINK Inc. Skokie, IL, USA) was used to measure the membrane surface roughness using the tapping mode. Three representative samples (5 μm×5 μm) from each membrane were randomly selected and scanned to obtain the topographic images of the membrane, the images were then analyzed using the software "Gwyddion" (supported by Department of Nanometrology, Czech Metrology Institute, Okružní, Brno, Czech Republic). The water contact angle of the membrane was measured using a video contact angle system (VCA, AST Products, Inc., MA, USA) via sessile method and at least three points were selected on each membrane surface to obtain the average contact angle value. The surface energy was evaluated by measuring the contact angle of the membrane surface with three different liquids: DI water, diiodomethane, and glycerol. The surface energy value was then calculated with the system's SE-2500 software via the acid-base theory model. The surface charge of the membrane under different pH (4, 7, 9) was assessed by an electrokinetic analyzer (EKA) (Anton Paar, Graz, Austria) using 1 mM NaCl solution (pH was adjusted by 1 M NaOH and 1 M HCl).

To quantify the amount of CuNPs formed on the membrane surface, three 3.8 cm^2 sample coupons were cut from the modified membrane, and each was placed into a sealed tube containing 40 mL of 1% HNO_3. The tubes with the membranes were agitated for 24 hours to dissolve the CuNPs completely. The total amount of CuNPs was evaluated by quantifying the concentration of Cu^{2+} in the acidic solution using inductively coupled plasma mass spectroscopy (ICP-MS, Perkin Elmer NexION 300X, Waltham, MA, USA).

5.2.4 Evaluation of the membrane transportation properties

Membrane transport properties were evaluated using a standard bench-scale RO cross flow filtration system following the method described in a previous study [165]. The membrane had an effective area of 33 cm^2 and was compacted with pure DI water overnight under a pressure of 27.6 bar to achieve a steady permeation flux. The water flux was monitored and recorded with the SLI-1000 digital flow meter (Sensirion AG, Staefa, Switzerland). Salt rejection was calculated by measuring the rejection of a 50 mM NaCl solution under 27.6 bar using a calibrated conductivity meter (Oakton Instruments, Vernon Hills, IL, USA). All filtration experiments were performed at 20 ± 1 °C with a cross-flow velocity of 21.4 cm/s and all permeation was recycled into the feed tank.

5.2.5 Observation of the membrane antimicrobial property

Bacterial inactivation of the membrane was evaluated by comparing the colony forming units (CFU) of the bacterial strain, *Escherichia coli* (PGEN-GFP (LVA) ampR), on the membrane surface after 2 hr of contact. In order to prepare the bacterial suspension, a 25 mL LB (Luria-Bertani) solution was inoculated with a single colony of *E. coli* and the solution was cultured overnight while shaking at 50 rpm under 35°C. Then, 1 mL of the incubated suspension was injected into 25 mL of fresh LB and incubated for another 3 hr to grow bacteria exponentially. The suspension was centrifuged at 5000 g (Fiberlite F15-8*50cy, Thermo Fisher Scientific, MA, USA) for 3 min in 3 cycles to purify the bacteria. After each centrifugation cycle, the supernatant was discarded, and the remaining bacterial cell pellet was resuspended in 20 mL of 0.9% NaCl. Finally, the bacterial pellet was diluted by 0.9% NaCl to reach a cell concentration of 10^7-10^8 CFU/ mL (optical density at $\lambda_{600\,nm} = 0.3 \pm 0.01$). In order to evaluate the bacterial inactivation, 1 mL of the prepared bacterial suspension was placed into every well of a Millicell® 12 well cell culture plate each containing 3.8 cm^2 membrane coupons fixed at the bottom with the modified side exposed to the suspension. The well plate was incubated at 35°C for 2 hr to allow the deposition and growth of the cells on the membrane surface. To evaluate the quantities of live cells on the membrane surface, the incubated membrane coupons were gently rinsed with 0.9% NaCl and then sonicated in 4 mL 0.9% NaCl for 7 min to detach all the cells on the membrane surface. The obtained bacterial solution was diluted by 0.9% NaCl to obtain the 1, 10, 10^2, 10^3, 10^4 and 10^5 dilutions.

Finally, 20 μL of each diluted solution was placed on LB agar plates to incubate overnight, and the number of colony-forming units (CFU) on the plate was then counted to determine the number of live bacterial cells. The normalized CFU was calculated by comparing the CFU on the modified membrane plates with the pristine membrane plate.

The live/dead cells on the membrane surface after 2 hr of contact were also observed under confocal microscopy (Nikon Eclipse TiE inverted C2 confocal microscope, Nikon Instruments Inc., NY, USA) with SYTO® 9 and propidium iodide (PI) (LIVE/DEAD® BacLight™ Bacterial Viability Kits L7012, Invitrogen Detection Technologies, MA, USA) applied as green and red fluorescent nucleic acid stains, respectively. The stain solution was prepared according to the method described in the product manual. 100 μL of both SYTO® 9 and PI were mixed thoroughly and then diluted 100 times with DI water. 300 μL of the prepared solution was added onto the surface of the 3.8 cm^2 bacteria-contacted sample. The strain reaction took place in the dark for 20 min and the dyed membrane sample was then loaded on a glass slide with a thin cover to be observed under confocal microscopy using a TIRF 40×oil lens. SYTO® 9 and PI dyes were excited with 488 nm argon and 561 nm diode-pumped solid-state lasers, respectively. At least 5 images were taken of each sample, and these were analyzed using Image J software to calculate the volumes of the live and dead bacteria cells.

5.2.6 The release of CuNPs from membrane surface

In order to examine the release rate of CuNPs from the membrane surface, membrane coupons with 3.8 cm^2 areas were cut and incubated in 40 mL of DI water or synthetic wastewater and continuously rotated on a shaker (360° rotation, Labquake Rotisserie Shaker, 415110, Barnstead Thermolyne, MN, USA). Every 24 hours, the membrane coupon was removed and placed into a freshly prepared 40 mL of DI water or synthetic wastewater for incubnation under the same conditions. After removing the membrane coupon, 400 μL of HNO3 was added to the 40 mL solution to dissolve the released CuNPs, forming Cu^{2+}. The concentration of copper ions in the solution was then evaluated by ICP-MS to determinate the quantity of of CuNPs released each day from the membrane surface.

The synthetic wastewater was prepared by inoculating DI water with 0.1% glucose, 0.8 mM NH_4Cl, 0.2 mM KH_2PO_4, 0.2 mM $CaCl_2$, 0.5 mM $NaHCO_3$, 8.0 mM NaCl and 0.15 mM $MgSO_4$.

5.2.7 The regeneration of CuNPs

After seven days of CuNP release, the aforementioned *in-situ* formation method was carried out to regenerate CuNPs on the surface of "CuNPs-elapsed" membrane.

5.2.8 Statistical Analysis

The data was analyzed via the Student's t test (Excel) assuming a two tailed and homoscedastic/heteroscedastic distribution (determined by the F-test, $p< 0.05$) to determine any statistically significant differences. Asterisks (*) indicate a statistically significant difference ($p < 0.05$).

5.3 Results and discussion

5.3.1 Fabrication of the CuNPs on the membrane surface

The top active layer of the TFC membrane with a thickness of 100 nm - 300 nm plays pivotal role for contaminant removal. This active layer is formed via interfacial polymerization of trimesoyl chloride (TMC) and m-phenylene diamine (MPD); therefore, the TFC membrane showed a "ridge and valley" topography and showed a relatively high surface energy. Due to the hydrolysis of unreacted TMC in the aqueous solution, the innate membrane surface has negatively charge originated from carboxyl groups ($-COO^-$) [166, 167], which could serve as reaction sites for functionalization [168]. When Cu^{2+} contacted with the membrane surface, shaking promoted the diffusion of the metal ions within the membrane rough structure; furthermore, the surface charge benefited the adsorption and bonding of the Cu^{2+} via the electrostatic attraction. When the reducing agent ($NaBH_4$) was added, metal nucleant formed *in-situ* on the membrane's active sites and gradually grew into large CuNPs over time. The *in-situ* CuNPs modified membrane exhibited a non-uniformly light brown color after 5 min of reduction (Figure A-12 B) and 0.8 0.2 μg cm^{-2} of CuNPs was formed on the modified RO surface (Figure 5.4 A).

Cys was selected as a Cu^{2+} binding media with the expectation to increase the CuNP loading on the membrane surface. During contact with the polyamide surface, the amino groups ($-NH_2$) from the Cys covalently bond with carboxylic units on the membrane surface [157] and resulted in the exposure of a thiol derivative surface. When Cu^{2+} was added to the surface, the thiol groups from

the Cys reacted with Cu^{2+} and formed firm metal-sulphur bonds. The RO-Cys-Cu membrane showed a more uniform brown color (Figure A-12 C) as compared to RO-Cu samples indicating a higher and more consistent loading of CuNPs. ICP-MS results showed that the quantities of loaded CuNPs were doubled (from 0.8 to 1.60.2 μg cm^{-2}) when Cys was used as media (Figure 5.4 A).

After the EDC-NHS functionalization, the ED treatment turned the unreacted -COOH on the top surface of the membrane into the $-NH_2$ [38], thus benefitting the covalent binding of EDC-NHS functionalized GO. After 4 hr of contact with the GO suspension, the membrane surface showed a yellowish-brown color and the brown color became more intense (Figure A-12 D) following the formation of CuNPs. The quantity of the CuNPs on the GO-modified surface was around 1.1 μg cm^{-2} (Figure 5.4 A) indicating that the GO-coated layer offers more reactive sites for the binding of Cu^{2+} than the pristine RO membranes.

XPS analysis was conducted to investigate the surface functional groups and elemental composition of the pristine and modified membranes (Figure 5.4 B). In comparison to the spectra of a pristine membrane, new Cu3p3 and Cu2p/Cu2O peaks at 89 eV and 931 eV, respectively, were clearly observed on the modified RO-Cu, RO-Cys-Cu, and RO-GO-Cu membrane surfaces. The atomic percentages of Cu the RO-Cys-Cu (4.3 ± 0.8 %) was higher than that of RO-Cu (2.7± 0.4 %) and RO-GO-Cu surfaces (3.8 ± 0.3 %), indicating a higher CuNPs coverage on the membrane surface. After 4 hr contact with Cys, the S2p peak at 163.9 eV appeared on the spectra; this new signal confirming the presence of thiol groups (-SH) after Cys treatment. The atomic percentage of S decreased from 2.57 ± 0.3 % to 1.87 % ± 0.1 % when the CuNPs were fabricated on the Cys-coated surface. This decrease in signal intensity is associated with the reaction between thiol groups and the CuNPs. The peak spectra of C was analyzed to evaluate the change in functional groups on the membrane surface after GO modification (Figure A-13). Due to the oxygen-containing functional groups on GO nanosheets, the content of the C-O (286.4 eV) and C=O (288.5 eV) bonds on the GO-coated surface increased approximately 14% (Table A-3) above the value for the pristine membrane. When the CuNPs formed, they hindered the formation of C-C (284.6 eV) bonds on the membrane surface, reducing the content from 51.8% ± 1.1% to 22.4% ± 0.4%. The appearance of Cu and S2p peaks, along with the increased oxygen-containing states of C indicated the successful functionalization of Cys/GO media and the presence of CuNPs on membrane surface.

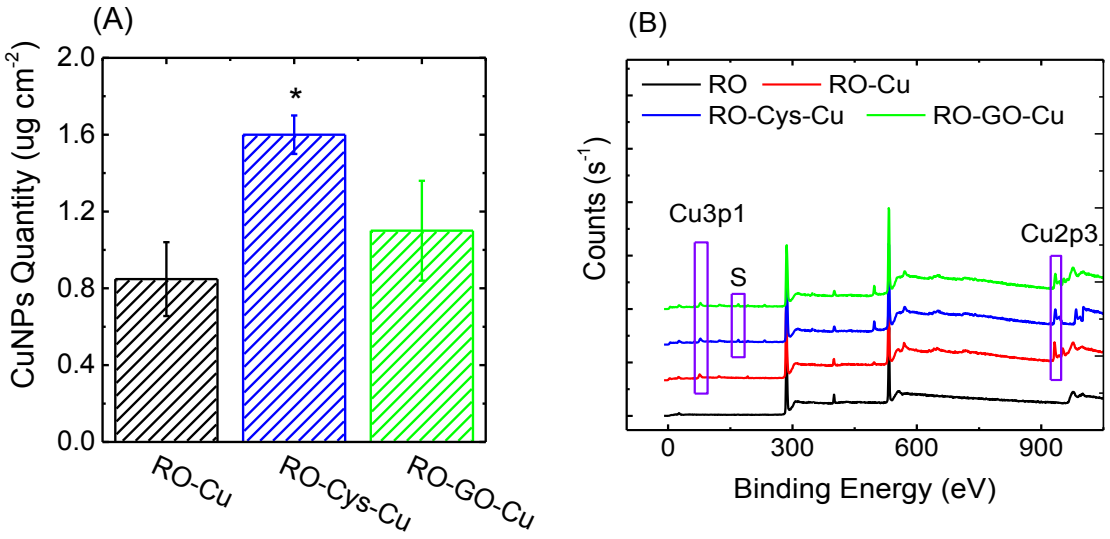

Figure 5. 4 (A) The quantity of CuNPs bonded onto the membrane surface measured by ICP-MS. **(B)** XPS spectra of pristine (black) and CuNP-functionalized PA membranes.

5.3.2 Surface characterization and performance evaluation of the modified membranes

The surface morphology of the modified membranes was observed by FESEM (Figure 5.5) and the influence of different modifications on the surface roughness was evaluated by AFM (Figure A-14, Table A-4). As observed on the RO-Cu surface, particles with a size of 30-80 nm appeared mainly on the typical "ridge-and-valley" structure while the relatively smooth area showed fewer NPs formation (Figure 5.5 D). The particles showed an irregular shape which looked like three or four particles aggregated together. The Cys coating showed a minor impact on the membrane morphology (Figure 5.5 B); however, the CuNPs presented less aggregation on the Cys-treated surface in comparison to those formed on the pristine membrane (Figure 5.5 E). The size of the particles decorated on Cys surface ranged from 20 to 60 nm, which might infer that Cys treatment imparted more reaction sites on the membrane surface for the nucleation of the Cu^{2+}. The GO nanosheets filled the valleys of the membrane, rendering a relatively flat surface (Figure 5.5 C). The decoration of CuNPs on the GO-coated surface was not as uniform as it was on the Cys medium; furthermore, a smaller quantity of CuNPs appeared on the smooth area than on the edge of the GO sheet. This might be due to the edge of the GO nanosheets having higher free energy, which would attract more Cu^{2+} to stabilize the energy potential. Also, according to another study

[169], the basal plane of the GO was mostly covered by epoxide groups, while the edges of GO were covered by carboxyl and hydroxyl groups which are more favorable sites for ion attraction and nucleation. The GO-coated surface had a smaller CuNP than the Cys surface which could be a result of the uneven distribution of CuNPs across the GO surface. The size of CuNPs on the GO-coated surface ranged from 20-60 nm. The presence of both Cys and GO increases the functionality of the membrane surface, providing more nucleation sites and governing the size and distribution of the NPs. The larger loading quantity and smaller particle size of CuNPs ascribed to the Cys and GO media might equip the membrane with a greater bacterial inactivation potential.

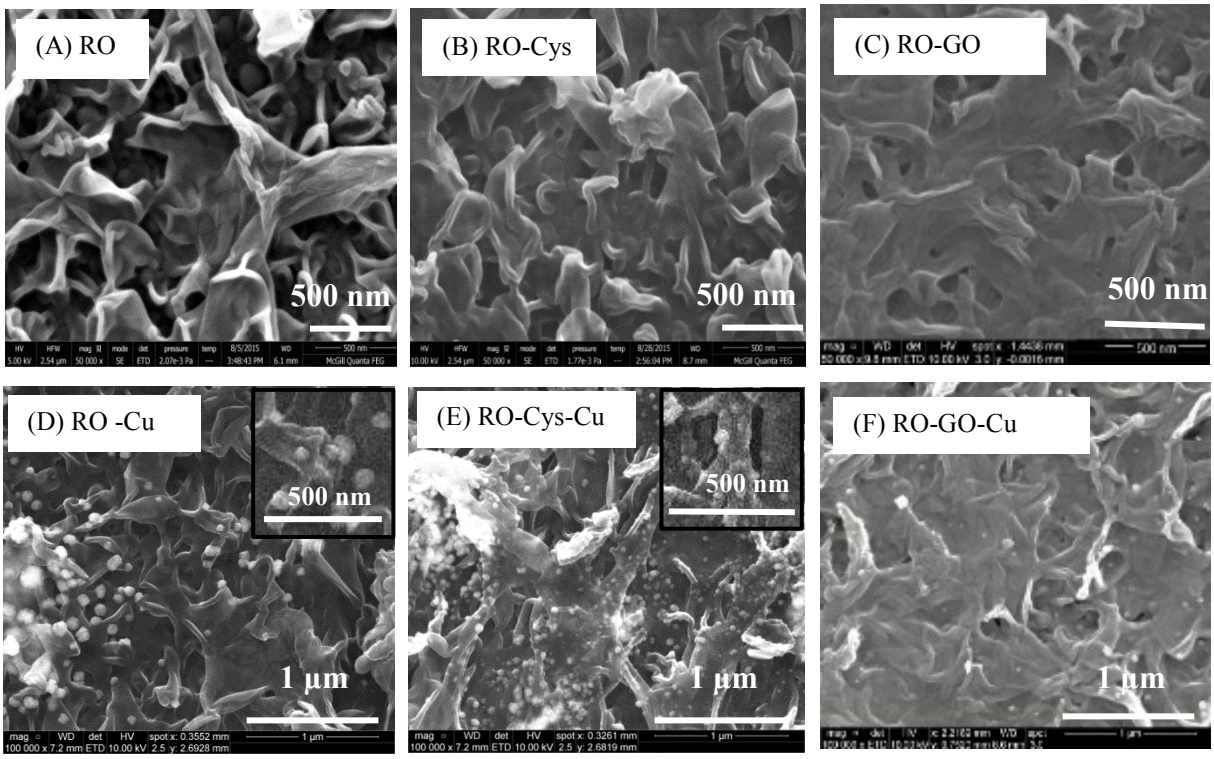

Figure 5. 5 SEM images of the pristine and modified membrane surfaces.

Besides the surface morphology, the physio-chemical properties of a membrane, expecially the charge, hydrophilicity and wetting ability, are closely related to the fouling resistant ability of a membrane. Therefore, the zeta potential, the water contact angle and surface energy of the pristine and modified membranes are measured to observe the influence of different modification method on the physio-chemical properties change of membrane.

Surface hydrophilicity is a critical parameter that affects the biofouling of the membrane. Since most microorganism are hydrophobic, the modification increases hydrophilicity thus aiding the preferential adsorption of water molecules and forming a water layer as an energy barrier on the surface, further reducing biofouling [167]. The hydrophilicity of each membrane was evaluated by the water contact angle (Figure 5.6 A). *In-situ* Cu decoration of pristine membranes led to a decrease in hydrophilicity (the contact angle increased from 52.7± 2.5º to 62.4 ± 1.5º). Stemming from the hydrophobic nature of thiol groups, the Cys linker did not significantly improve the

membrane hydrophilicity; while the presence of hydrophilic GO layers (16.0 ± 3.3º of RO-GO) led to a decrease in the water contact angle of CuNPs decorated membranes from 62.4 ± 1.5º to 45 ± 6º.

In comparison to that of the pristine polyamide membrane (-6.1±1.00 mV ~ -25.6±3.00 mV), the zeta potential of surfaces with direct in-situ and Cys-mediated CuNPs fabrication (-12.6±6.90 mV ~ -22.6 ± 4.00 mV) were more resistant to variation in pH (Figure A-15 A). While, with a GO media the RO-GO-Cu membrane was more negatively affected than other membranes under pH 4~9 (-20.3 ± 0.67 mV ~ -34.5 ± 0.95 mV). The difference in zeta potential was closely related to the diverse oxygen-rich functional groups on the surface. The more stable surface charge might attribute to less exposure of COO- and OH- groups of polyamides on RO-Cu and RO-Cys-Cu surfaces. Generally, bacterial cells are negatively charged in a pH range of 4-9 (*E.coli*, -10 mV~ -60 mV [170, 171]). Although the more negative charge on the RO-GO-Cu membrane could offer a stronger electrostatic repulsion to bacteria and reduce their deposition, it may also attract more similarly and oppositely charged ions.

The wetting ability of the membrane measured by surface energy is another parameter to evaluate the cohesive force between the membrane surface and the contaminant. The lower surface energy usually indicates a weaker foulant/surface adhesion, and as a result, cells or organic foulants that settle on the membrane can be easily washed off. The Cys coating showed a slight influence on the membrane surface energy (42 ± 1.7 dyne/cm of RO and 36 ± 1.3 dyne/cm of RO-Cys-Cu) (Figure A-15 B); while with GO media, the surface energy of the CuNPs decorated membane increased by 40% (from 35.9 ± 1.5 dyne/cm of RO-Cu to 62.5 ± 0.5 dyne/cm of RO-GO-Cu). Surface energy is related to many factors, such as charge, roughness, and hydrophilicity of a membrane. The GO media renders the membrane with a smoother and more negatively charged surface, which is unfavorable to the attachment of bacteria; however, the higher surface wetting ability may still lead to the attraction of bacteria.

The influence of the metal NPs modification on the intrinsic transport properties of the modified membranes was evaluated using a cross-flow cell in RO mode (Figure 5.6 B). Even though the coated CuNPs layer caused additional hydraulic resistance for water transport, the water flux and salt rejection of the CuNP-modified membrane remained similar to the performance of the pristine membrane under the same operating pressure. When Cys and GO were applied as linkers, the water

permeation flux increased slightly; the reasons attributed to the increase in water permeation were different because of their different physiochemical properties. Cys was dissolved in a 70% ethanol solution; therefore, the increase in water flux should be attributed to the swelling of the active layer after contacting with ethanol solution for four hours. The increase in water permeation led to a slight decrease of the salt rejection. The same results for Cys-treated membranes were observed in another study [157]. GO, however, contains diverse functional groups with an affinity for water that benefits the preferential adsorption and quicker transport of water molecules. Since the GO treatment did not destroy the original structure of PA underlayer, the RO-GO and RO-GO-Cu membranes maintained a high salt rejection. In general, both the Cys and GO coating did not show significant compromises on membrane performance.

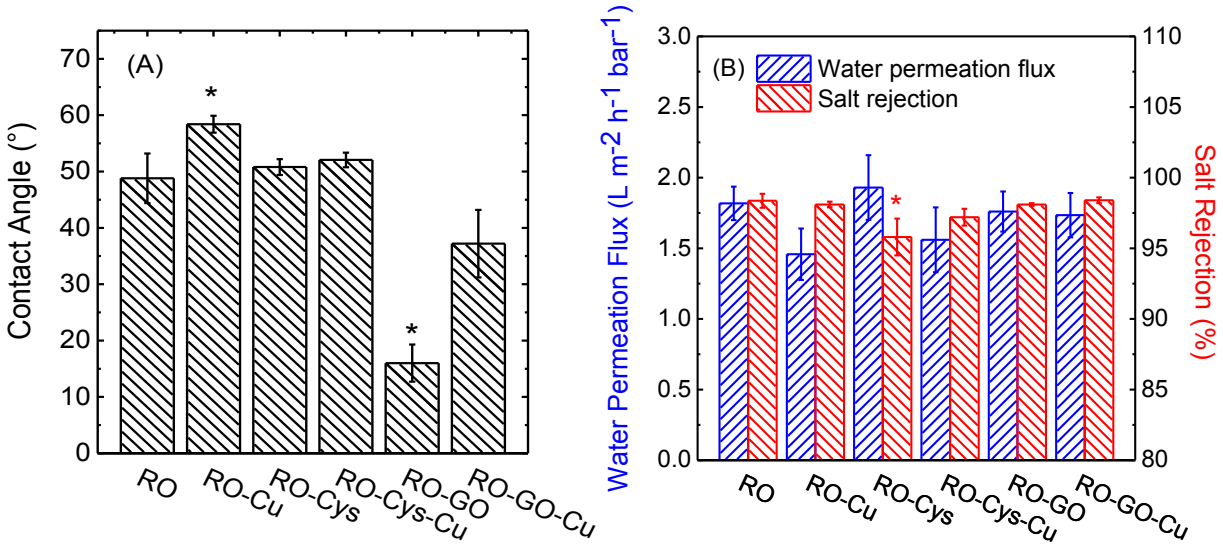

Figure 5. 6 (A) Water contact angle and **(B)** water permeability and salt rejection of the pristine and modified membranes (tested under 27.5 bar).

5.3.3 The antimicrobial activities of the modified membranes

A static bacterial inactivation test was performed with *E. coli* (gram-negative, non-pathogenic) to assess the antimicrobial properties of the modified membranes (Figure 5.7 A, Figure A-16). The *in situ* CuNP-modified membrane exhibited appreciable antibacterial performance showing a

normalized CFU reduction that was 64% above the capability of the pristine membrane. There is no theoretical model that clearly explains the bacterial inactivation by CuNPs. Some studies claim that the antimicrobial property of CuNPs could be caused by the depolarization of the cell structure as a result of CuNPs/Cu^{2+} attachment and following degradation of the cell membrane due to the interaction between phosphorus/sulfur-containing protein and CuNPs/Cu^{2+} [65]. It is also reported that reactive oxygen species (ROS) [62] produced in metal NPs releasing process may cause the oxidation damage of cell, result in cell membrane rupture and metabolism processes disruption [64], which finally lead to the death of bacteria.

Cys alone did not show any bacterial inactivation; however, the RO-Cys-Cu was nearly twice as effective as the RO-Cu membrane in inactivating bacteria (Figure 5.7 A). The higher anti-bacterial property of the RO-Cys-Cu membrane could be attributed to a larger amount of CuNPs bonded to the surface by the Cys linkers.

It was reported that GO coating exhibited certain antibacterial property [172]. The redox potential caused by the large quantity of oxygen-containing functional groups is the main reason for the antibacterial potential of GO. Contact between the cell membrane and the GO surface could lead to lipid peroxidation as well as the production of ROS in the liquid, which would cause severe oxidative damage to cellular structures [173]. It was also noted that the sharp edges of GO could rupture the cell membrane and cause intracellular leaking [159]. When decorating CuNPs onto the GO-modified membranes, the inactivation performance was higher than both the CuNP and the pure GO-modified membranes. The enhanced bacterial inactivation could be attributed to the synergetic anti-bacterial effect [174] of CuNPs and GO. Even though the CuNPs would inevitably release during the operation, the remaining GO would still serve as an antimicrobial coating to mitigate the biofouling of the membrane surface. In comparison to a Cys-Cu-modified surface, the RO-GO-Cu membrane with a lower quantity of CuNPs showed lower anti-biofouling performance, which indicate that the mainly bacterial inactivation of the modified membrane can be attributed to the CuNPs rather than GO.

The status of the live/dead bacteria deposited on the pristine and modified membrane after 2 hr of contact was observed by a confocal microscopy (Figure 5.8 A-F). The red fluorescent nucleic acid stain, PI (propidium iodide), penetrated the only damaged cell membrane, therefore it could be inferred that the Cu, Cys-Cu and GO-Cu-modified surfaces all impacted the integrity of the *E.coli*

cell membranes. The volume of live and dead *E.coli* cells was measured using image-analyzing software and the result further supported the CFU count tests (Figure 5.7 B). Contrary to our expectation, more bacterial cells were deposited on the RO-GO-Cu surface in comparison with other membranes. This result possibly due to the diverse functional groups and high surface energy of GO that capture bacteria [174]. Many bacteria were still alive on the pristine membrane while almost half were dead on the CuNPs modified surface; the RO-GO-Cu and RO-Cys-Cu achieved nearly 83% and 97% bacteria' inactivation, respectively. Contrary to the expectations, the number of cells deposited on the RO-GO and RO-GO-Cu surface did not show a significant reduction in comparison with other membranes (Figure 5.8 B, 5.8 E), although their more hydrophilic and negatively charged surfaces (Figure A-15 A) were expected to offer a stronger repulsive force to bacteria. To further investigate the attachment behavior of *E.coli* cells, the surface morphology of pristine and GO-mediated membranes was observed under SEM after contact with bacteria (Figure A-18). In comparison to the bacteria deposited on the pristine membrane, some of the cells on RO-GO surface presented a slightly altered morphology and were likely stuck on the surface. A similar observation was reported by Liu et al. noting that GO nanosheets could wrap bacteria cells [175]. It was also demonstrated that in comparison with CNT, planar graphene monolayers with diverse functional groups exhibited a stronger ability for hybridization with the lipid bilayers of a cellular membrane [176]. The high surface energy (Figure A-15 B) and potential interaction with the cellular membrane indicated greater influence than the surface charge and hydrophilicity did on cellular attachment to a RO-GO surface. This may be a possible explanation to the non-reduced cell deposition and the "capture-killing" anti-microbial properties of a GO-mediated surface.

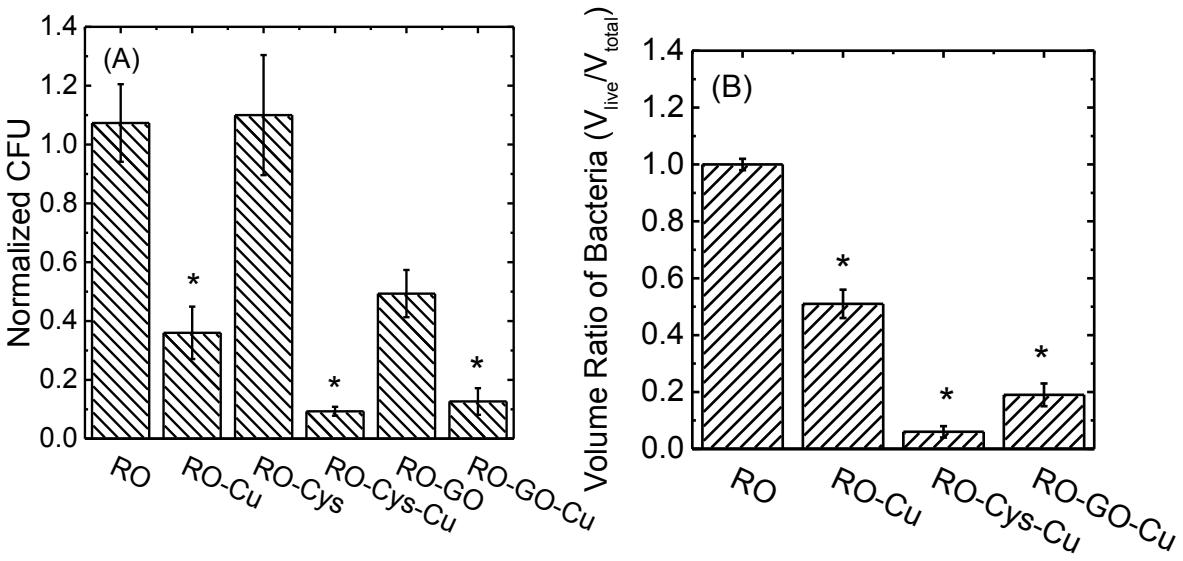

Figure 5. 7 (A) The number of attached live cells on the pristine and modified membrane surfaces after 2 hours of static contact. The values are normalized to the number of attached live bacteria colonies on the pristine membrane ($N/N_{pristine}$) **(B)** The volume of the attached live bacteria on the membrane samples. The value is normalized to the volume of total bacteria (live and dead) on the same sample.

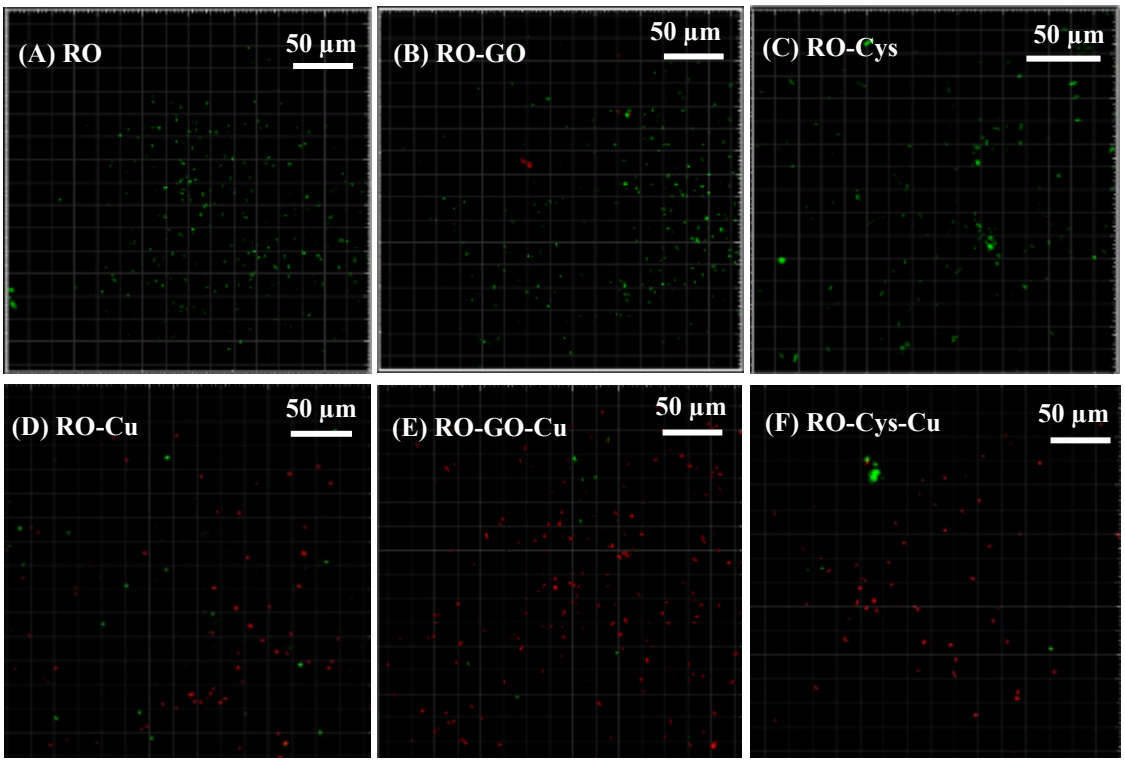

Figure 5. 8 Representative confocal microscope images of *E.coli* on pristine and modified membranes after 2 hours of static contact. The bacteria on membrane surface is stained with PI and SYTO 9 fluorescent nucleic acid stains before observation.

5.3.4 The release and regeneration of the CuNPs coating on the membrane surface

The nanoparticle modification imparted the membrane with an increased biocidal property; however, the stability of the particles and the durability of the membrane's anti-biofouling performance has always been a concern.

In order to evaluate the release behavior of CuNPs from the surface of the modified membranes, batch tests were conducted for seven days with the RO-Cu, RO-Cys-Cu, and RO-GO-Cu samples. The release rate of the CuNPs was proportional to the total quantity released from the membrane surface. The daily amount of CuNPs released from the surface gradually reduced over time (Figure 5.9 A). CuNPs, CuO-NPs [177] and Cu^{2+} [129] all show a potential for antimicrobial applications; the released NPs are therefore expected to serve as bacteria-inactivating NPs/ions in the feed solution, inhibiting the overall growth of bacteria. Although higher release rates of CuNPs were observed

from the RO-Cys-Cu and RO-GO-Cu samples, the remaining Cu content was still larger than that on the RO-Cu surface (Figure 5.9 B). This observation indicates durable bacterial inactivation performance imparted by the Cys and GO linker.

To confirm that the Cys and GO linkers helped retain higher amounts of CuNPs on the surface, the static bacterial inactivation test was conducted to measure the antibacterial performance of the modified membranes after seven days of Cu release (Figure 5.9 C). Due to the depletion of CuNPs, the three CuNP-decorated membranes all showed a certain decrease in bacterial inactivation over time; the RO-Cys-Cu and RO-GO-Cu samples maintained 72% and 65% bacteria inactivation, respectively, which is still higher than that of the fresh RO-Cu membrane. The quantity of CuNPs remaining on RO-GO-Cu surface after release was smaller than that of the fresh RO-Cu sample, yet the former still showed greater antimicrobial performance indicating the existence of the covalently bonded GO layer even after 7 days. The durability of the membrane coating was improved by the Cys-Cu modification because it retained a larger amount of CuNPs; the GO-Cu modification retained lower amount than Cys-Cu modified membrane but instead allowed the GO substrate to inactivate the bacteria.

The release behavior of CuNPs was also observed in a synthetic wastewater. The appearance of organic and inorganic contaminants increased the ionic strength of the water (from 20 μs of DI water to around 2600 μs) and boosted the release of CuNPs from membrane surface (Figure A-17 A). Almost all of the CuNPs dissolution occurred on the RO-Cu membrane (Figure A-17 B) and the membrane nearly lost all anti-bacterial properties (Figure A-17 C) after a 7-day release. With a small quantity of biocides left on surface, the RO-Cys-Cu membrane retained 23% bacterial inactivation.

The regeneration of NPs after their gradual depletion was reported as an ideal method to maintain the biocidal ability of the substrates [154, 155]. Because of the effective and convenient fabrication process, the *in-situ* regeneration of CuNPs is feasible for improvement of biocidal-durability. After the 7-day release, the XPS spectra of the S2p peak on the RO-Cys-Cu sample confirmed the existence of thiol groups (Figure 5.9 D). The presence of GO on the polyamide surface after the NP release was also confirmed by XPS and Raman spectroscopy analysis in a previous study, with the released RO-GO-Cu sample also showing a greater antibacterial property than the fresh RO-Cu sample. Therefore, the CuNPs were regenerated on the three released samples via the same *in-*

situ reduction method following the 7 days CuNPs release without re-coating the linkers, and then the quantity of CuNPs, as well as the antibacterial property of the re-modified membranes, were evaluated after the regeneration process. All membranes showed higher quantities of CuNPs on their surface after regeneration than the initial values (Figure 5.9 B). This is likely due to the incomplete release of CuNPs and the existence of unsaturated Cu^{2+} reaction sites on the membranes, which enhanced the antimicrobial properties of the regenerated membranes (Figure 5.9 C). The regenerated RO-Cys-Cu and RO-GO-Cu surfaces achieved nearly 95% and 92% of bacterial inactivation, respectively, which is comparable to that of the AgNPs regenerated on the polyamide membrane in our previous study (98% for freshly modified AgNPs membrane and 95% for regenerated AgNPs membrane) [76]. These observations showed the possibility to maintain the anti-microbial property of RO membranes in long-term operation.

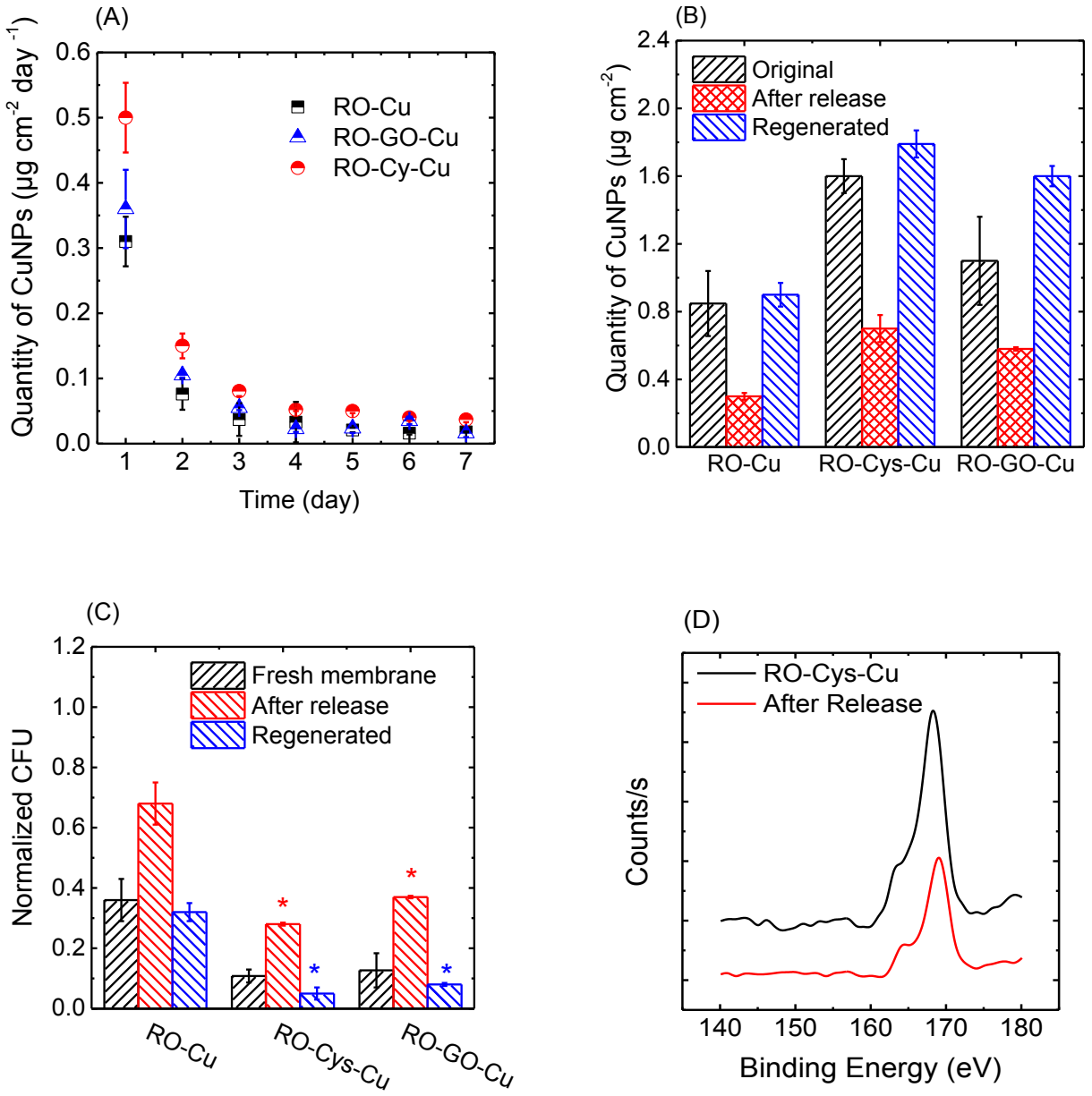

Figure 5. 9 (A) The release rate of CuNPs from membrane surface. During the batch test, a membrane coupon (3.8 cm^2) was incubated in 40 mL DI water under rotation and the solution was replaced every 24 h. **(B)** The quantity of CuNPs remaining on the membrane surface after 7-day release and the quantity of CuNPs after regeneration. **(C)** The number of attached live bacterial colonies (CFU) on the membranes (compared to that on a pristine membrane, $N/N_{pristine}$). **(D)** The XPS peak spectra of S on the RO-Cys-Cu membrane before and after the 7-day copper release.

In order to confirm whether the absorption of unsaturated Cu^{2+} was one of the reasons leading to the higher quantity of CuNPs after regeneration, the contact time between Cu^{2+} and the membrane surface was increased from 10 min to 30 min (reduction time still kept as 5 min) (Figure A-19). As expected, the quantity of the CuNPs proportionally increased with that of the Cu^{2+} concentration. Furthermore, in another report [168], 50 mM of $CuSO_4$ (10 times of the concentration applied in this study) was applied to decorate the TFC membrane surface with CuNPs, which further supported the existence of the unsaturated reaction sites of Cu^{2+}. However, the increased number of CuNPs on the membrane surface could cause an increase in surface hydrophobicity. The number of CuNPs should be optimized with consideration to both the antibacterial property and the hydrophobicity of the membrane.

Although the gradual release and consumption of metal NPs added a burden to the antimicrobial application of the membrane, the released CuNPs/Cu^{2+} from the membrane surface could still benefit the process through inactivation of microorganisms in the feed solution via the "release killing" process [154]. Furthermore, in comparison to that of a biocidal polymer modified anti-biofouling membrane, the effective biocidal function, and the durable fouling resistant performance of the metal NPs decorated membrane could be achieved by facile regeneration of metal nanoparticles. This an incomparable advantage for a metal nanoparticle decorated anti-biofouling membrane as compared to that of a polymer fabricated one. Ouyang et al. [128] prepared a poly-l-lysine/reduced graphene oxide/copper nanoparticles (PLL–rGO–CuNPs) hybrid that could extend the stability and antibacterial effect of CuNPs in a solution. Although this super hydrophobic coating was not suitable for membrane modifications, it showed the potential of modifying CuNPs to delay oxidation as an effective approach for maintaining long-term anti-biofouling performance. Moreover, the preparation of copper based NPs with greater stability than Cu are being more widely investigated for the development of anti-microbial materials [178, 179]. It could be inferred that a medium to alleviate the oxidation of CuNPs (e.g., chitosan, ascorbic acid) and more stable copper based nanoparticle (e.g., CuS) are potential candidates for the development of novel low-cost anti-biofouling membranes in future..

5 Conclusions

Metal nanoparticles, especially AgNPs, are attracting more and more attention for membrane biofouling control, while the unavoidable release of NPs adds challenges to the practical

application of highly-priced AgNPs. Here, *in-situ* decoration of CuNPs onto a membrane surface by using a media with an affinity to metal is proposed as a cost-efficient and quality-competitive strategy for controlling membrane biofouling.

Both of the well-studied media of high metal affinity, Cys and GO, offered a membrane surface with more reactive sites for Cu^{2+} binding and led to the formation of smaller CuNPs with a more uniform distribution on the membranes. However, the membrane with a thiol-derivative surface (Cys) was more effective in terms of improving the CuNPs loading quantity than that with a diverse oxygen-contain layer (GO). The quantity of CuNPs synthesized on the Cys coated membrane increased by 100%, which resulted in a 33% improvement in bacterial inactivation in comparison to that of a bare CuNP modified membrane. Due to the higher CuNPs loading, the Cys-Cu-modified membranes showed more robust and durable biocidal properties than that of the bare Cu- or Ag-/GO-Ag-decorated [76] [155] membranes. Decoration of *In-situ* CuNPs with Cys media exhibited excellent potential for fabrication of membranes with comparable anti-microbial performance as those modified by more expensive AgNPs.

GO media shows a 38% improvement in CuNPs loading and a 14% improvement in anti-microbial performance; however, it increases membrane surface energy and may result in increased deposition of foulant. GO improved the hydrophilicity of CuNPs decorated membranes. GO media is more suitable for water affined membrane fabrication rather than for its application in an anti-microbial purpose.

Overall, the economic nature and effective anti-microbial performance demonstrate the potential of the copper-based nanoparticle as a promising candidate for development of novel biofouling-resistant membranes in future.

Chapter 6. Controlling biofouling via "defending and attacking" combining strategy: surface modification with fouling-resistant/biofilm inhibition polymer

Abstract

In this study, GO was applied as a modification media to functionalize fouling-resistant (poly(sulfobetaine methacrylate), PSBMA, bacteria-"defending" agent) and biofilm controlling (poly methacryloyl-L-Lysine, PLysMA, biofilm-"attacking" agent) polymers on membranes to improve their anti-biofouling properties. The polymers were controllably generated on GO-coated polyamide membranes via the activators regenerated by electron transfer-atom transfer radical polymerization (ARGET-ATRP) technique. The successful polymerization of copolymers on the GO-coated membrane was examined by FTIR and SEM observation. Both PSBMA and PLysMA grafting significantly increased the hydrophilicity of the membrane and reduced its surface roughness and charge density. Less cell deposition was observed on PSBMA and PLysMA coated surfaces with an increase in coating thickness during a short time contact. Combined PSBMA and PLysMA grafting offered membrane surfaces with a bacterial-"defending" and -"attacking" coating, reducing the biofouling caused by gram positive (G+) bacteria, *B. Subtilis,* via a synergistic effect. However, no obvious inactivation of the attached gram positive (G-) bacteria, *E.coli*, was observed. The "defending" function played an important role in controlling biofouling caused by *E.coli.* When PSBMA was grafted to the surface of the membrane and directly exposed to the *E.coli*-containing suspension, the membrane exhibited lowest deposition of bacteria after 48 h of contact. With a strong water affinity and fouling-resistance, the M-PLysMA-*b*-PSBMA membrane exhibited less flux reduction (27%) associated with biofilm growth in comparison to that of PA (80%) under the same condition. 100% flux recovery was observed on the M-PLysMA-*b*-PSBMA membrane after two cycles of a "fouling-cleaning" procedure; while only 94% recovery of flux was observed on the control membrane.

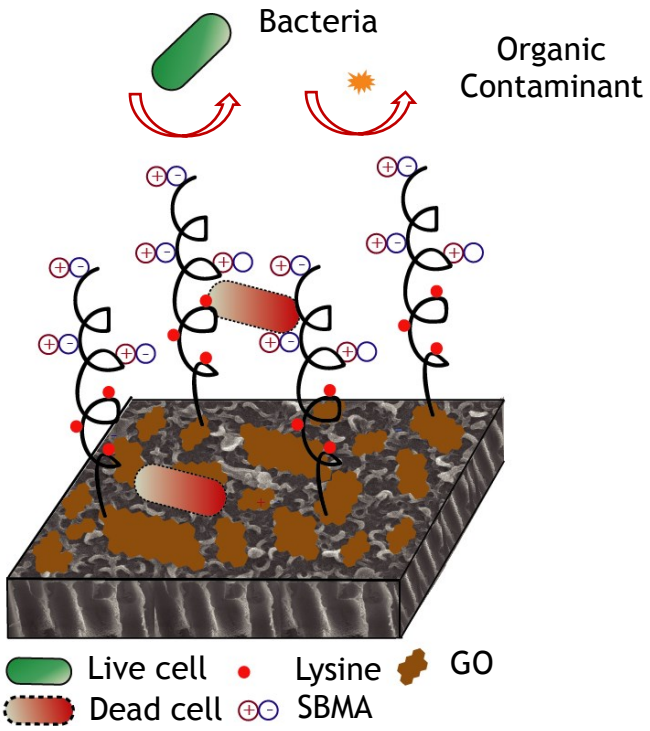

Figure 6. 1 Graphical abstract

6.1 Introduction

As discussed in 2.3.3, Combining "defending" and "attacking" strategies to develop anti-biofouling coatings could overcome some of the drawbacks seen in a single type modification and offer an enhanced antibiofouling performance. In this chapter, anti-biofouling membrane was fabricated with a combination of microorganism-"defending" and -"attacking" agents to mitigate membrane biofouling via a synergistic effect.

6.1.1 Modifiers: zwitterionic polymer and poly(amino acid)

As discussed in Chapter 2, zwitterionic polymers containing zwitterionic units (such as carboxylic ($-COO^-$), sulfonate ($-SO_3^-$), phosphoric ($-PO_4^-$), and ammonium (R_4N^+)) are ideal hydrogen bond acceptors/contributors [49] as they can significantly bind water molecules and form protein/bacteria repulsive hydration layers on the membrane surface [49]. Among polyzwitterions, poly(sulfobetaine) (PSB) is highly available and it offers stable anti-biofouling performance in various qualities of water [50, 51]. Therefore, in this chapter, PSB is selected for the "defending" agent for anti-biofouling surface modification.

Even though it has been shown that CuNPs effectively mitigate membrane biofouling via a bacterial-"contact- and release-killing" manner, these biocidal agents depleted as a result of gradual dissolution of the metals, which might cause secondary contamination in water purification. Furthermore, continuous regeneration of CuNPs on the membrane would increase the cost of membrane process due to the large volume of membrane filtration system. Other biocidal agents (e.g., quaternary ammonium [180], metal NPs, graphene oxide [147, 181]), have all been applied in the design of anti-biofouling membranes. Although appreciable improvements have been reported in laboratory research, few of them have been applied in a large-scale setup due to the high price of materials, sophisticated fabrication procedures, potential appearance of antibiotic-resistant bacteria, and general health and environmental concerns. An environmentally friendly material with effective biofilm control properties was expected when selecting the "attacking" agent.

Natural occurring biomolecules which have antibiofouling properties, such as bacteriophages [182], enzymes, peptides [77, 87] and polysaccharides, are attracting growing interest in the fabrication of anti-biofouling membranes as bacteria/biofilm "attacking" agents, due to their effective anti-

microbial properties, low cost, and low toxicity to humans. Amino acid is another attractive option [183]. In comparison to long chain polymers, amino acids containing protonated primary amino groups ($-NH_3^+$) or deprotonated carboxyl groups (-COO-) can render a very thin hydrophilic surface and reduce the attachment of organic foulants on a substrate [92]. Furthermore, certain types of amino acids, such as tyrosine, tryptophan, leucine, etc., are able to replace components in cell walls and cause the release of amyloid (a substance that links cells in the biofilm together) fibers on the cell membrane and disrupt the extracellular matrix connection between the extracellular matrix and the cells [93]. It has been reported that in the presence of a high concentration of amino acids, bacteria exhibited reduced production of eDNA, extracellular polymeric substance (EPS) and interspecies quorum sensing signal [94].

Although systematical mechanisms regarding biofilm inhabitation function of these amino acids are still not elucidated, potential amino acid based antifouling applications have been widely reported. Inoculating D-tyrosine in the feed strongly prevented biofouling [94] and removed the biofilm [94] from the membrane during the nanofiltration (NF) process. D-tyrosine has also been loaded on zeolite and then bonded to NF membrane via EDC/NHS crosslinker to reduce biofouling on the membrane. L-cysteine has been functionalized on RO membrane via thiol-ene reaction to prevent protein deposition [184]. A high concentration of lysine was observed to completely inhibit the swimming motility and twitching motility (a prerequisite for biofilm formation) of *E. coli BL21* and effectively inhibit biofilm formation [95]. Lysine has been functionalized on silica mesoporous nanoparticles to prevent protein adhesion [185], been anchored on multi wall carbon nanotubes (MWCNT) to enhance its antibacterial potential [186], and been coated on hydrophobic silicon wafers and UF, RO membranes via self-assembly to prevent biofouling [91]. However, amino acids-based materials exhibit dosage-dependent functions on biofouling mitigation. An incorporation of a large amount of amino acids to bulk feed water is costly. Instead, anchoring amino acids on a surface would mitigate the dilution effect due to the bulk volume.

Most previous studies only applied monolayer amino acids for the fouling resistance which offered a low quantity of fouling resistant function groups. Applying multiple layers of fouling resistant amino acid or poly(amino acid) brushes to reduce biofouling on polyamide membranes has not yet been investigated.

Combining zwitterionic polymers with the biofilm-controlling poly(amino acid) is expected to develop anti-biofouling coatings which offer a bacterial/protein-"defending" and bacterial/biofilm-"attacking" synergistic resistance to prevent biofouling on the membrane. In this study, zwitterionic polymer, PSBMA and biofilm controlling (amino acid)-based polymers, were functionalized on RO membrane to mitigate biofouling in the RO filtration process.

6.1.2 Modification method: activators regenerated by electron transfer-atom transfer radical polymerization atom (ARGET-ATRP)

To conveniently functionalize zwitterionic and biofilm-controlling polymers to the membrane, the activators regenerated by electron transfer-atom transfer radical polymerization atom (ARGET-ATRP) technique was selected for controllable polymer grafting via the "graft-from" approach.

ATRP is one of the most widely used controlled radical polymerization (CRP) methods for polymer fabrication [187]. Four components are required in a normal ATRP process: monomer, an initiating species (usually is alkyl halide, -X), a metal catalyst (Mt^n, usually it is Cu^+) and a metal ligand (L). ATRP relies on an equilibrium between the alkyl halide-initiated species, P_n-X, and radicals that are produced by the cleavage of the C-X bond by a redox-active, metal/ligand complex (Mt^n/L to X-Mt^{n+1}/L) [91]. In the activation step, the Mt^n/L is oxidized and bonds with the halide to form the X-Mt^{n+1}/L (the deactivator), and produced radicals react with an initiated substrate (P_n*), allowing the monomer to grow into a long chain polymer (P_n- P_n). The reversible deactivation (X-Mt^{n+1}/L to Mt^n/L) causes a dormant period for polymer propagation, therefore, polymers functionalized via ATRP have a uniform chain length (molecular weight) distribution.

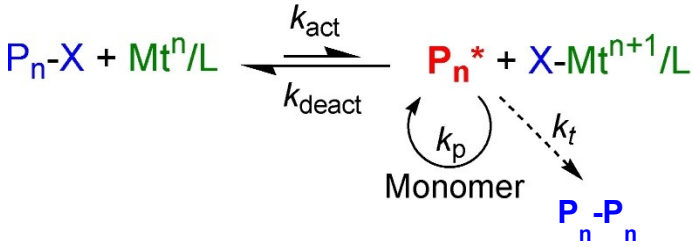

Figure 6. 2 Illustration of a basic ATRP process [91].

The ATRP reaction is very robust and it is highly tolerant of monomer functional groups (such as, amino, epoxy, hydroxy groups); therefore, it is convenient for the fabrication of new copolymers containing different functional units. By controlling the reaction parameters (including reaction time, monomer concentration, and monomer addition sequence), macromolecular chain parameters, including the molecular weight (chain length), grafting density, and functional units (polymer architecture) of grafted copolymers can be precisely controlled. These controlled parameters are critical for material functionalization as they are directly related to water absorption and foulant repelling abilities of the polymer. Furthermore, control of the thickness of polymer coating greatly affected the water-perm-selectivity of the membrane.

The initiation of polymer grafting via ATRP requires special functional groups on the membrane surface, mainly a -OH or a $-NH_2$ group. To offer a membrane fabrication media convenient to polymer grafting, GO, which has an abundance of -OH groups, was used as the anchoring sites for tethering bromoester initiators to the membrane for subsequent grafting of polymer brushes.

The functional polymer with varied grafting density and polymeric chain lengths on membrane surface was examined and the physiochemical properties of functionalized membrane were also characterized. The effects of fouling-resistant polymeric coating on the membrane surface properties and water-selective performance were also assessed. The fouling-resistance performance of the nanocomposite membranes was investigated via static contact experiment using *Bacillus subtilis* (*B. subtilis*) and *Escherichia coli* (*E.coli)* as the model gram positive (G+) and gram negative (-) bacteria. The antibiofouling performance of modified membrane was also investigated in a dynamic crossflow filtration mode. This study demonstrates that modifying membrane surface with zwitterionic polymer/biofilm controlling coatings is an effective approach to mitigate biofouling in membrane processes.

This is the first time that GO has been applied as a modification media for membrane surface modification via ATRP method. Furthermore, this is the first investigation into the potential of applying ATRP to fabricate a poly (amino acid) layer on polyamide membrane in order to mitigate biofouling.

6.2 Materials and methods

6.2.1 Chemicals

N-(3-dimethylaminopropyl)-N'-ethylcarbodiimide hydrochloride (EDC), N-Hydroxysuccinimide (NHS), ethylenediamine (ED), 2-(N-morpholino)ethanesulfonic acid (MES) buffer, 4-(2-hydroxyethyl)-1-piperazineethanesulfonic acid (HEPES) buffer, ethylenediaminetetraacetic acid (EDTA) (≥99%), sodium dodecyl sulfate (SDS) (≥98.5%), [2-(Methacryloyloxy)ethyl]dimethyl-(3-sulfopropyl)ammonium hydroxide (sulfobetaine methacrylate, SBMA) (95%), tris(2-pyridylmethyl)amine (TPMA) (98%), L-ascorbic acid (≥99%), disodium phosphate (Na_2HPO_4) (NIST SRM 2186II), potassium dihydrogen phosphate (KH_2PO_4) (anhydrous, HPLC LiChropur®), ammonium chloride (NH_4Cl) (≥99.5%), magnesium sulphate ($MgSO_4$) (≥99.5%) and Luria Bertani (LB) (microbiologically tested) were purchased from MilliporeSigma (Oakville, ON, Canada). Methanol (peroxide-free/sequencing), isopropanol (≥99%) 2-bromo-2-methylpropionyl bromide (BiBB) (98%), calcium chloride ($CaCl_2$) (anhydrous, ≥96.0%), hexanes (Certified ACS), copper bromide ($CuBr_2$) (≥95%), and sodium chloride (NaCl) (≥99.5%) were purchased from Thermo Fisher Scientific (St Laurent, QC, Canada). Methacryloyl-L-Lysine was purchased from Cedarlane Laboratories (Burlington, ON, Canada). All chemicals were used, as received, without any further purification. Single layer graphene oxide (GO) nanosheets (with thickness of 0.7–1.2 nm and length of 300–800 nm) were purchased from Cheap Tubes Inc. (Grafton, VT, USA). Deionized (DI) water (produced by a Milli-Q ultrapure water purification system, Millipore, Billerica, MA, USA) was used to prepare all aqueous solutions.

6.2.2 Preparation of PSBMA- and PLysMA-grafted membranes

The commercial polyamide RO membrane, UTC-82V, was obtained from Toray Company (Poway, CA, USA) and stored as received, refrigerated at 4 °C. Before surface characterization and modification, the membrane samples were immersed in 30% isopropanol for 20 min to remove any chemical coatings and were then rinsed several times with DI water.

The polymeric modification of the polyamide RO membrane consisted of two steps: functionalizing GO on the PA surface via covalent binding and growing polymers on GO-coated PA membrane via ARGET- ATRP method.

Covalently binding GO to the PA TFC membranes via EDC/NHS crosslinker was conducted according to published protocols [38, 159]. This technique has been successfully applied in previous studies as a bridging agent to anchor copper nanoparticles onto membrane [188]. In this work, the GO-coated PA membrane is referred to as M.

To functionalize the polymers on the membrane, the initiator was first tethered onto the surface of GO-coated PA membrane (obtained M-Br), and then the polymer was grown "bottom-up" on the membrane via the surface initiated ATRP (SI-ATRP) method. The synthesis procedure is demonstrated in Figure 6.3.

Before preparing the surface-initiated membrane (M-Br), the GO-coated PA (M) was dried in desiccator overnight. Then, the membrane was placed on a plate (13 cm × 13 cm) and covered by a nylon frame with 9.5 cm × 9.5 cm of the active side exposed for modification. On the top of the frame, another plate with two holes (diameter of 1 cm) sealed with septa was covered. The whole setup was tightly clamped to prevent any leakage. The nitrogenic environment inside the frame was created by vacuum and then back-flushing with nitrogen gas for three cycles, then maintained with a nitrogen balloon. Then, 50 mL of hexane and 0.4 mL (~3%, wt%) of BiBB were injected into the setup through the septum in sequence. The whole setup was put on orbital shaker with a speed of 100 rpm and the reaction was conducted at room temperature for varied times. After reaction, the solution was discharged, and the membrane was washed for five cycles with hexane for three rounds and 50% methanol for two rounds. Finally, the obtained M-Br membrane was stored in DI water at 4 °C for at least 12 h before use.

The polymer grafting onto the M-Br was conducted via the ARGET-ATRP method modified from published protocols where polydopamine was applied as surface modification media [100, 104]. In brief, the M-Br membrane was compacted on the setup as described above. Then, the SBMA dissolved in a 1:1 isopropyl: DI water mixture (50 mL, v/v) of various strengths (1.7, 3.5, 7, 14, 28 mmol) was injected into the nylon container. The reactor was degassed by N_2 purging for 10 min, then a nitrogen balloon was inserted on one of the septa. A stock solution of $CuBr_2$ (0.146 mmol/mL) and TPMA (0.05 mmol/mL) in 1:1 methanol :DI water were then injected into the container, followed by the addition of ascorbic acid (1 mol/mL 1:1 methanol: water v/v). The initial chemical concentration in the reactor, monomer :$CuBr_2$:TPMA :ascorbic acid were

maintained at 700 :1 :3 :20. The polymerization process was undertaken on an orbital shaker at a speed of 100 rpm and the reaction was conducted at room temperature for 20-60 min. The obtained M-PSBMA was washed with a 1:1 methanol/DI water mixture (50 mL, v/v) three times and was stored in DI water in a refrigerator at 4 °C.

The PLysMA-grafted membrane (M-PLysMA) was prepared with the same procedure used across the whole study with the lysine concentration of ~1.7 mmol. The ratio of monomer, $CuBr_2$, TPMA and ascorbic acid in the reactor was maintained at the same as that of the PSBMA grafting process.

When preparing the M-PSBMA-*b*-PLysMA (M-PLysMA-*b*-PSBMA) membrane, the M-PSBMA- as prepared above was compacted into the setup and the polymerization of PLysMA was conducted with the same procedure.

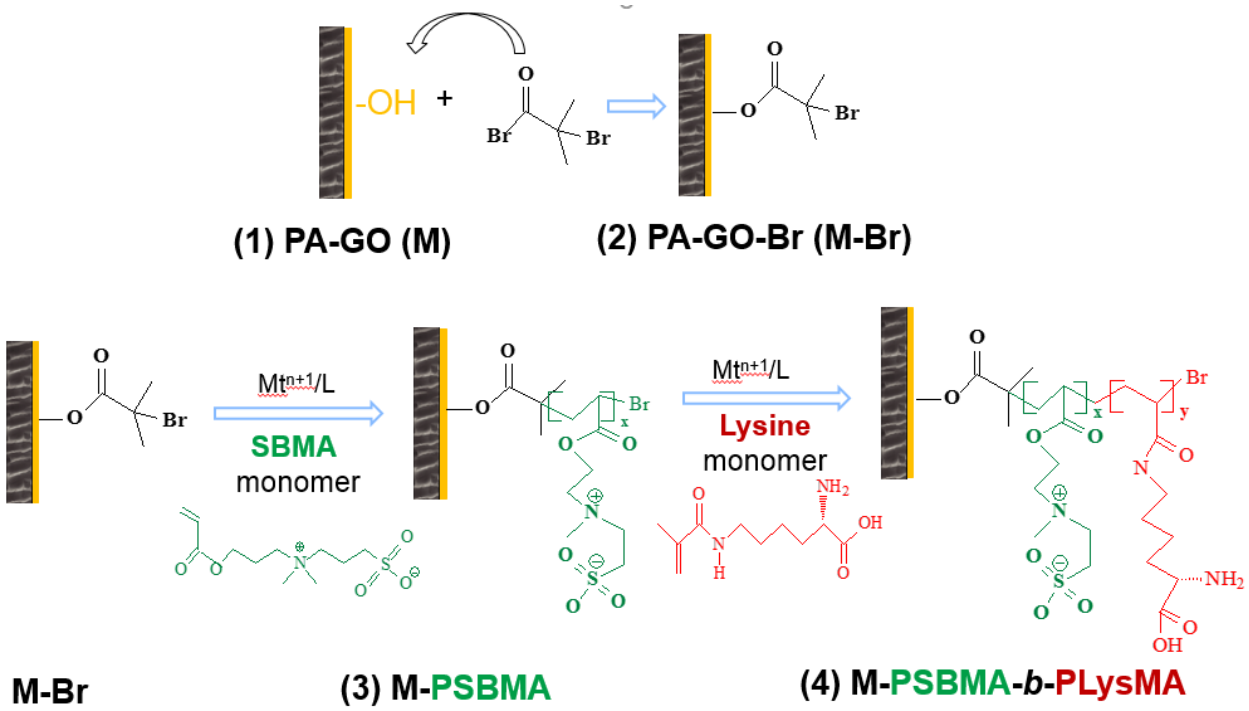

Figure 6. 3 Scheme of the SI-ATRP reaction for grafting PSBMA and PLysMA on a polyamide RO membrane after GO pretreatment.

6.2.3 Characterization of the polymer modified membranes

To estimate the hydrophilicity of the fabricated membranes, membrane coupons were dried in a desiccator overnight. The water contact angle of the membrane was measured by a Video Contact Angle system (VCA, AST Products, Inc., Billerica, MA, USA). At least three positions were selected on each sample to obtain the average contact angle value. The surface free energy was evaluated by measuring the contact angle of the membrane surface with three different liquids: DI water, diiodomethane, and glycerol. The surface energy value was calculated with the system's SE-2500 software via the geometric theory model. The functional groups on the membrane surface were measured via Fourier transform infrared (FT-IR) spectroscopy on a Nicolet 6700 / Smart iTR (Thermo Scientific, Waltham, MA, USA) equipped with an attenuated total reflectance single logic accessory (ATR). Membrane morphology was observed via a FEI Quanta 450 environmental scanning electron microscope (FE-ESEM) (FEI company, USA) after adding a platinum

nanoparticle (~4 nm) coating. Membrane topography was investigated using an atomic force microscope (AFM) (NanoINK Inc. Skokie, IL, USA) in tapping mode. Roughness was measured using the "Gwyddion" statistical software. The average membrane surface (10 μm×10 μm) value was reported. The surface charge of the nanocomposites was determined by a zeta potential analyser (ZetaPlus/Bl-PALS, BrookHaven Instrument Corp., Holtsville, NY, USA) at different pH conditions adjusted using 100 mM HCl and 10 mM KOH.

6.2.4 Evaluation of membrane perm-selectivity

A bench-scale cross flow filtration system was used to test water permeate flux and salt rejection. Specifically, a membrane with an effective area of 33 cm^2 was compacted for 5-8 hr at 13.8 bar (400 psi) until a steady water flux was reached. The permeation flux was monitored with a digital flow meter (Liquid Flow Meter SLI-2000, Sensirion Inc. CA, USA) and salt rejection was assessed by measuring the rejection of 50 mM NaCl solution using a calibrated conductivity meter (Oakton Instruments, Vernon Hills, IL, USA). All filtration experiments were performed at 20.0 ± 0.5 °C (maintained by a chiller) with a cross-flow rate of 0.5 litre per minute (LPM).

6.2.5 Evaluation of bacteria-resistance and -inactivation performance of membrane

Bacterial resistance of the membrane was evaluated by comparing the quantity of bacterial cells, *Escherichia coli* (*E.coli*) (PGEN-GFP (LVA) ampR) (a model of gram negative bacterium) and *Bacillus subtilis* (*B. subtilis,* ATCC6633) (a model of gram positive bacterium), on the membrane surface after 2 h of contact. First, the bacterial suspension was prepared with an optical density of λ_{600} nm = 0.3 ± 0.01 (*E.coli* concentration of 10^7-10^8 CFU/ mL in 0.9% NaCl described in detail in previous work [44, 182]. To evaluate bacterial deposition, 2 mL of the prepared bacterial suspension was placed into every well of a Millicell® 12 well plate (Thermo Fisher Scientific, Waltham, MA, USA) with each containing 3.8 cm^2 membrane coupons fixed to the bottom with the top surface exposed to the suspension. The well plate was incubated at 35 °C under 100 rpm shaking for 2 h. Then, the bacterial suspension was discarded, and each well was refilled with 2 mL 0.9% NaCl followed by 5 min shaking under 100 rpm to remove the loosely attached bacterial cells.

The live/dead cells on the membrane surface after 2 h of contact were observed under confocal laser scanning microscopy (CLSM) (Nikon Eclipse TiE inverted C2 confocal microscope, Nikon

Instruments Inc., NY, USA) with SYTO® 9 and propidium iodide (PI) (LIVE/DEAD® BacLight™ Bacterial Viability Kits L7012, Invitrogen Detection Technologies, MA, USA) applied as green and red fluorescent nucleic acid stains, respectively. The stain solution was prepared according to the method described in the product manual. 100 µL of both SYTO® 9 and PI were mixed thoroughly and then diluted at a 1:100 ratio with DI water. 300 µL of the prepared solution was added to the surface of the 3.8 cm^2 bacterial-contacted membrane sample. The strain reaction took place in the dark for 20 min and the dyed membrane sample was washed with 1 mL of 0.9% NaCl solution and loaded on a glass slide with cover glass to be observed under confocal microscopy using a TIRF 40× oil lens. SYTO® 9 and PI dyes were excited with 488 nm argon and 561 nm diode-pumped solid-state lasers, respectively. At least 10 images were taken of each sample, and these were analysed using Fiji ImageJ software to calculate the number of the live (stained by STYO® 9, green colour) and dead bacteria cells (stained by both STYO® 9 and PI, red colour).

The durability of membrane fouling resistance was evaluated by comparing the volume of bacterial cells grown on membranes after 48 h of culturing. Different from the 2 h contact experiment in which only *E.coli* and 0.9% NaCl were in suspension, the 48 h bacterial culturing applied carbon resources and multiple salts in suspension to promote the formation of biofilms on the membrane surface. In brief, *E.coli* (10^7-10^8 CFU/ mL), LB, and multiple salt stocks (concentrated salt stocks should be prepared separately to prevent the precipitation) were added to DI water to prepare the synthetic wastewaters according to a published protocol by Ben-Sasson et al. [74] The final bacterial suspension was composed of: *E.coli* 10^5-10^6 CFU/mL, 0.1% LB, 0.2 mM KH_2PO_4, 0.8 mM NH_4Cl, 8 mM NaCl, 0.15 mM $MgSO_4$, 1.2 mM $Na_3C_6H_5O_7$, 0.5 mM $NaHCO_3$, and 0.2 mM $CaCl_2$. To evaluate the biofilm formation, 2 mL of the prepared bacterial suspension was placed into every well of a Millicell® 12 well plate and put into contact with 3.8 cm^2 membrane coupons fixed to the bottom. The well plate was incubated at 35 °C under 100 rpm shaking for 48 h. The membrane coupons were washed and prepared for CLSM observation as described above. Five images were taken of each sample and these were analysed using Imaris 8 software to calculate the volume of the live (green colour) and dead bacteria cells (red colour).

6.2.6 Assessment of anti-biofouling performance of the modified membrane

The influence of biofilm growth (model bacteria: *E.coli*) on membrane flux was investigated by using two fouling/cleaning cycles under the cross-flow filtration system as described above in section 6.2.4. The same membrane was used during the entire experiment. First, the water permeation flux of membrane was obtained after compacting the membrane with 5 L of DI water for 5-8 h under 27.3 bar (400 psi) at 25.0 ± 1.0 °C.

The fouling cycle began by adding 50 mL of *E.coli* stock (10^7-10^8 CFU/ mL) and 50 mL of nutrient solution into the feed tank without stopping the filtration, to achieve a final concentration of 10^5-10^6 CFU/ mL *E.coli*, 0.1% LB, 0.2 mM KH_2PO_4, 0.8 mM NH_4Cl, 8 mM NaCl, 0.15 mM $MgSO_4$, 1.2 mM $Na_3C_6H_5O_7$, 0.5 mM $NaHCO_3$, and 0.2 mM $CaCl_2$. The filtration continued for 4 h to allow bacteria to deposit on the membrane surface. Then, the feed solution was changed to DI water inoculated with nutrient solution and filtration was continued for 12 h to promote the growth of biofilm and membrane flux was evaluated. The feed solution had an initial pH of 6.5 ± 0.2, calculated ionic strength of 25.8 mM, and a measured conductivity of 860±34 μS/cm (OAKTON conductivity meter, CON 11 series, Vernon Hills, IL USA). After the biofouling test, the feed solution was discarded and replaced with DI water for 30 min of membrane cleaning. The pressure of the cross-flow system was maintained at 25 psi and flow rate was increased to 1 LPM during the washing process. Membrane flushing of the system was conducted with a sequence of 10 L tap water, 10 L 0.2 mM EDTA (pH 8), 10 L tap water, 10 L of 5 mM SDS, 10 L tap water and 10 L DI water without circulation. After cleaning, the membrane was again compacted with DI water to measure the recovered water permeation flux and determine the flux recovery ratio of the membranes.

Without stopping filtration, *E.coli* and nutrient stock were inoculated into the feed to start the second cycle of the fouling experiment as described above.

6.3 Results and discussion

6.3.1 The surface initiation of polyamide membrane

The "bottom-up" growth of the functional polymer on the membrane via ATRP started with the initiator monolayer deposition. In anhydrous environment, the α-bromoisobutyryl bromide (BiBB) initiating species reacted with hydroxyl groups (-OH) on GO via substitution and formed α-bromoester on the GO coated membrane. Since -OH groups are the important hydrogen bond donor and acceptor, the gradual conversion of -OH into α-bromoester groups would lead to the reduced hydrophilicity of GO. The quantity of activator controls the density of the resulting polymer chain. Dense polymeric grafting was expected to form strong steric repulsive force between polymers, therefore causing the swelling of polymer chains to favour their fouling resistant/biocidal function.

In this study, initiator density was controlled by varying the contact time between -Br initiator and membrane and was evaluated by measuring the surface hydrophilicity of the corresponding obtained initiator tethered membrane (M-Br). The influence of initiator density on polymer grafting was investigated by evaluating the membrane water permeation flux of the polymer grafted membranes. Finally, the influence of polymer density on anti-bacterial performance of the membrane was evaluated by observing the bacterial attachment on different membranes.

As expected, functionalizing hydrophilic GO nanosheets decreased the water contact angle of the PA membrane from 54.9±1.6° to 27.8±1.1° (Figure 6.4 A). The contact-angle of the membrane increased after contacting with 3 wt% (n-hexane) BiBB, indicating the gradual loss of -OH due to the activator species tethering. After 20 min of reaction time, the contact angle of M-Br became stable, which might infer the near complete substitution of -OH on GO with α-bromoester groups. To evaluate whether the quantity of -Br initiator affects the grafting density of polymers, the PSBMA was functionalized on M-Br membranes under the same experimental condition and the corresponding water permeation flux of fabricated M-PSBMA membranes were evaluated (Figure 6.4 B). Consistent with the water contact angle test, the more flux reduction caused by polymer coating was obtained on membrane with the larger amount of initiator anchoring, indicating a higher density of polymer grafting. Notably, membranes without initiator anchoring performed with a similar water permeation flux as that of the pristine PA, inferring unsuccessful

functionalization of polymer coating on PA surface with the absence of an initiator. According to the static bacterial contact test, the membrane exhibited an increased bacterial-resistance and less CFU was observed on membrane with a higher polymer density (Figure 6.4 C). The observed result confirmed that the density of grafted polymer on membrane can be controlled by varying the activator reaction time. Furthermore, higher density of PSBMA brush reduced bacterial deposition on membrane. Since further increases in initiator reaction time exhibited little influence on membrane hydrophilicity and bacterial resistance, the surface initiation with 3 wt% BiBB (in n-hexane) for 20 min of contact time was selected for further polymer functionalization study.

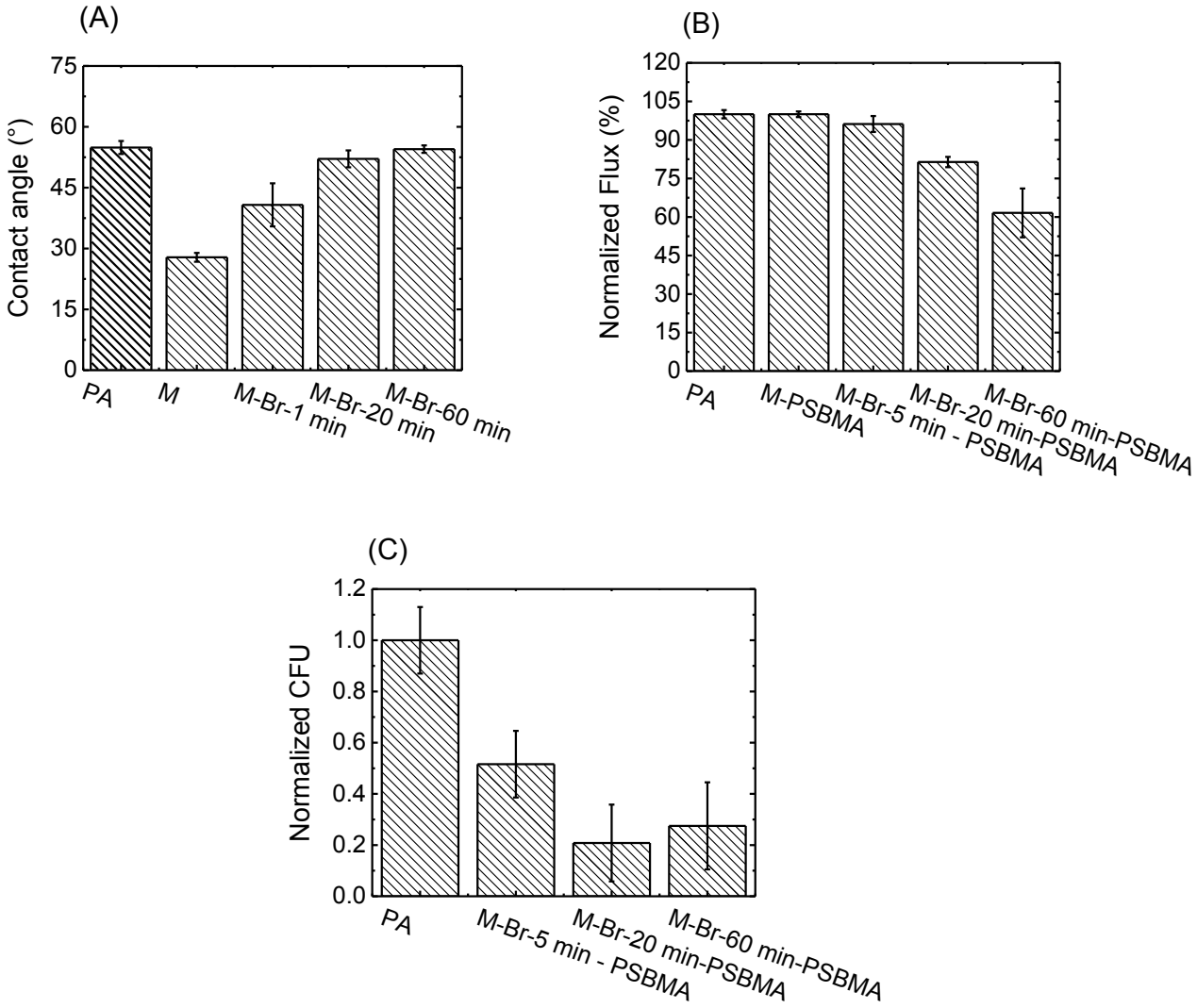

Figure 6. 4 (A) The water-contact angle of pristine PA, GO-coated PA (M) and different time of -Br initiated (M-Br) membranes; **(B)** The water permeation flux of of PA, M and different M-Br membranes after 30 min of PSBMA (3.5 mmol) polymerization; **(C)** The bacteria colony forming units (CFU) on the pristine and modified membrane surfaces after 2 h of static contact. The values are normalized to the number of attached live bacteria colonies on the pristine PA membrane (N/N_{PA}).

6.3.2 Optimizing the experiment condition for the PSBMA and PLysMA grafting via ATRP

In an oxygen-free environment with the existence of Cu^{+}, polymerization of monomer starts from the initiator anchored position. The concentration of monomer, as well as polymerization time, affects the thickness of the resulting polymeric layer. Although a thick polymeric coating is expected to offer a membrane with a stronger antibiofouling performance, the extra coating on membrane will also increase the hydraulic resistance force for water permeation. To achieve satisfactory fouling resistance with minor scarification of water permeation flux, monomer concentration and polymer grafting time were optimized by observing the water permeation flux of the modified membrane.

Within the same polymerization time, the hydrophilicity of the obtained M-PSBMA was proportional to the initial concentration of the monomer in reactor (Figure 6.5 A). A 30 min grafting with an initial SBMA concentration of 3.5 mmol resulted in a membrane with a water contact angle of 14.6±1.8°. Further increase of monomer concentration showed little influence on membrane hydrophilicity. The decrease of water contact angle indicated an increase in hydrophilic functional groups on the membrane which might be caused by more uniform grafting of PSBMA layers on the membrane. The corresponding water permeation flux of M-PSBMA was shown in Figure 6.5 B. The gradual deposition of PSBMA blocked the polymeric structure of the membrane and resulted in a reduction in water permeation flux. Opposite of expectations, the salt rejection of the PSBMA grafted membrane did not exhibit a "trade-off" with reduced water flux. With near 60% reduction in water permeation flux, the salt rejection of 28 mmol PSBMA grafted membrane was reduced from 96.3% to 92.6% ($p<0.05$). Reduced salt rejection may be due to the PSBMA attracting a larger quantity of salt ions to the membrane surface, enhancing the concentration polarization. The lower quantity of polymer grafting (SBMA<7 mmol) showed minor influence on salt rejection.

Since a harsh reduction in flux was observed when monomer concentration increased from 1.7 mmol to 3.5 mmol, the M-PSBMA functionalized under these two monomer-concentrations with varied grafting time were further optimized. According to these results (Figure 6.5 C), increasing monomer concentration and extending the polymerization time exhibited similar effects on the "bottom-up" growth of PSBMA. A similar flux reduction was observed on the M-PSBMA

functionalized with 1.7 mmol of SBMA after 60 min of reaction time and the one modified with 3.5 mmol SBMA after 30 min polymerization. To maintain the level of initiator activity for the next step of polymerization, SBMA of 3.5 mmol were selected for further study.

The grafting of zwitterionic PSBMA onto PA surface has been previously reported for the fabrication of antibiofouling PA membrane via different modification media. The functionalization time and influence of PSBMA grafting on membrane water permeation flux, as well as the bacterial resistance, were compared with results in the literature (Table 6.1). In comparison to the literature, GO-mediated PSBMA grafting exhibited less flux scarification than the (3-Aminopropyl)triethoxysilane (APTES) media [117] and offered more reaction sites for polymer growth than polydopamine (PDA) [100] did due to the *in-situ* initiation process. Therefore, GO mediated polymer grafting exhibited greater potential for use in functional surface modification.

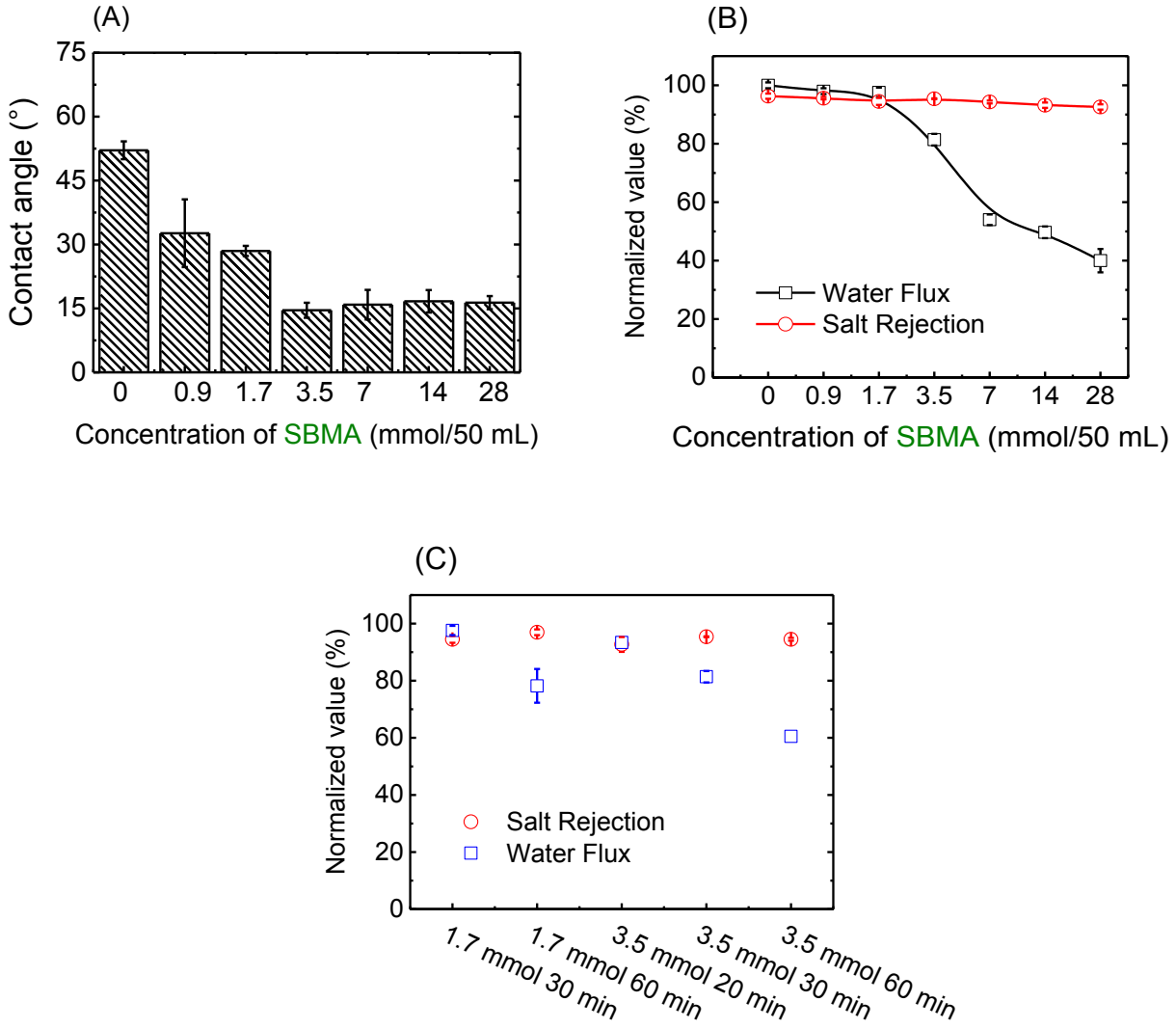

Figure 6. 5 The water-contact angle **(A)** and the water perm-selectivity **(B)** of M-Br membranes after 30 min of PSBMA polymerization with varied initial concentration of monomer. **(C)** The water perm-selectivity of M-Br membranes after PSBMA polymerization with varied initial concentration of monomers and polymerization time.

Table 6. 1 The influence of different modification media on PSBMA functionalized polyamide membrane via ARGET ATRP.

Media	Area (cm^2)	Polymerization Time (min)	Monomer (mmol)	Flux Reduction	Reduced bacteria adhesion	Ref.
PDA	375	60	28	~8%	73%	[100]
APTES	35	20	10	~40%	60%	[117]
GO	**90**	**20**	**3.5**	**~8%**	**60%**	**This work**

The optimization of grafting "attacking" units, PLysMA, conducted with a fixed monomer concentration of 1.7 mmol and varied polymerization times. As with that of PSBMA, the PLysMA coating improved membrane hydrophilicity and the water contact angle of M-PlySMA was maintained around 27~33° (Figure 6.6 A). However, the PLysMA coating-layer exhibited a higher influence on membrane flux (Figure 6.6 B). The flux of PLysMA modified membranes reduced by 7% and 80% after 20 and 60 min of polymerization, respectively; while the flux of the membrane with PSBMA functionalization under the same experimental conditions were reduced by only 2.4% and 21.6% (Figure 6.5 C). The more significant influence of PLysMA coatings on membrane flux might affect reaction rate of different solvents on ARGET ATRP. Considering the solubility of the lysine monomer, the polymerization of PLysMA was performed in water, while SBMA monomer was performed in 50% methanol (v/v in water). Metal ions showed more affinity to the halide in a water solvent, and therefore, promoted the polymerization process.

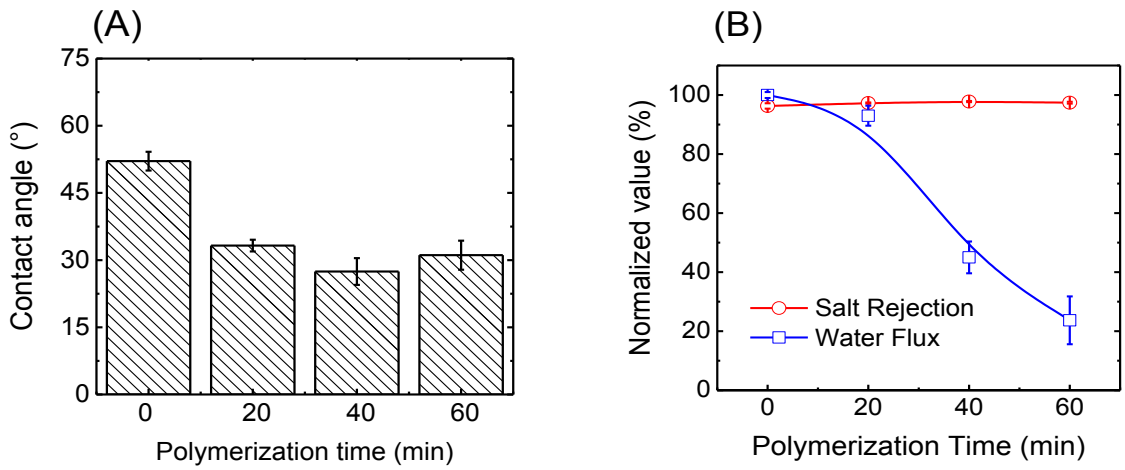

Figure 6. 6 The water-contact angle **(A)** and the water perm-selectivity **(B)** of M-PLysMA membranes modified with 1.7 mmol initial monomer concentration under varied polymerization time. The water permeation flux and salt rejection values are normalized to the value of pristine membrane (N/N_{PA}).

Since the water contact angle of PSBMA $_{3.5\ mmol}$ and PLysMA $_{1.7\ mmol}$ grafted membranes stabilized after 20 min of polymerization, it was inferred that a uniform covering of PSBMA/PLysMA appeared around this time. To confirm this hypothesis, the surface morphology of PSBMA- and PLysMA-modified membranes were observed via SEM (Figure 6.7). In comparison to the rough surface of the PA membrane which was formed by "ridge and valley", the bonding of GO nanosheets partially covered the "valleys" and membranes exhibited a reduced surface roughness. Bromide initiation showed little influence on membrane morphology. After 20 min of PSBMA polymerization, the "ridges" of the membranes became broadened and almost completely shaded the "valley" morphology; while in the PLysMA modified membranes, the polymer grafting felt denser and the filling of "valleys" with polymer was more clearly observed. The relative uneven grafting of PLysMA was probably caused by the differences in polymerization rate between PSBMA and PLysMA as explained above. After 40 min of polymerization, the original "ridge and valley" morphology of the pristine PA was completely covered by the polymer coating.

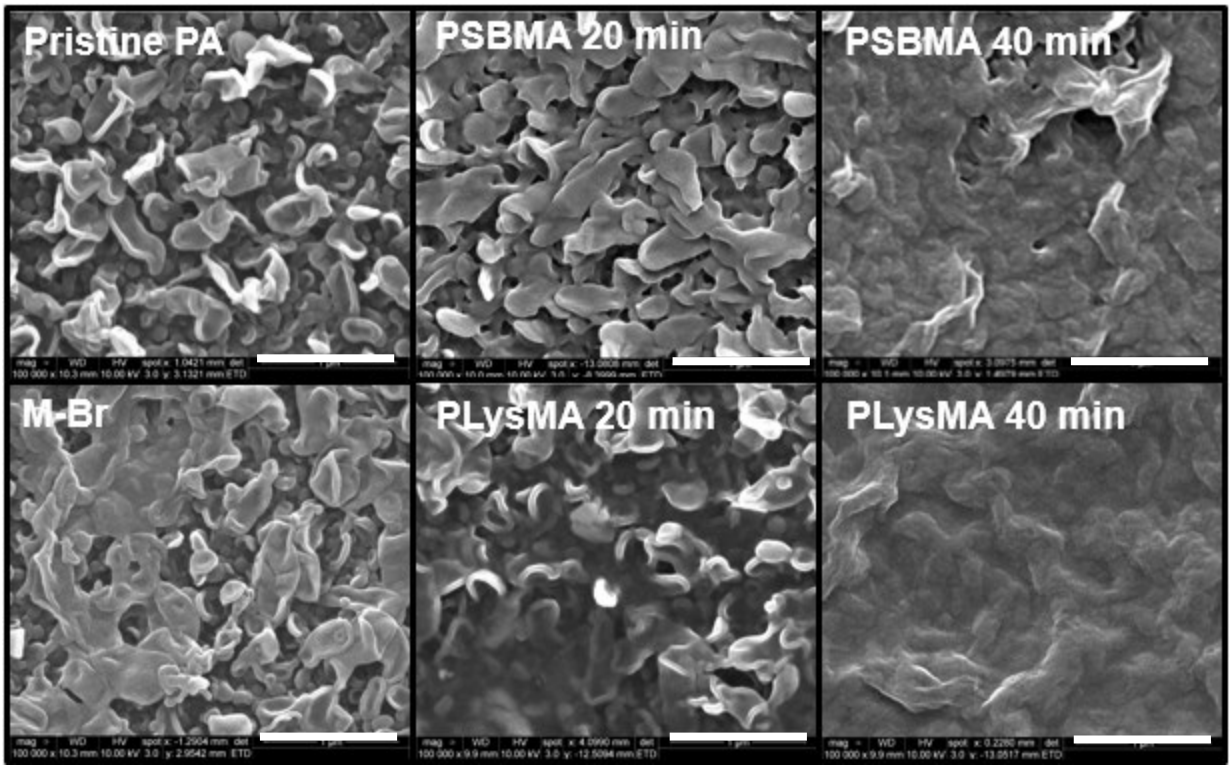

Figure 6. 7 SEM images of the PA, PSBMA (3.5 mmol)- and PLysMA (1.7 mmol)-modified membranes with varied polymerization time. The scale bar on image indicates 1 μm.

A thin polymeric coating does not offer sufficient fouling-resistance to repel the bacteria; however, the thicker polymer grafting is usually accompanied with a sacrifice in water permeation flux. To select a suitable compromise polymer grafting time with moderate water flux while also maintaining a high fouling resistance, the influence of PSBMA and PLysMA grafting on membrane antimicrobial performance was investigated by plate counting with *E.coli* as the model bacteria (Figure 6.8). Results demonstrated that the bacterial cells attached to the polymer-modified membranes was reduced in concert with the increase of polymerization time, especially on the PSBMA-grafted membranes. Compared to the control PA (number of CFU was normalized as "1"), the modified membrane with 20 min of PSBMA-grafting showed a 40% reduction in bacterial attachment. After 30 min polymerization, the CFU on M-PSBMA exhibited an 80% reduction in comparison to PA. However, further increasing the polymerization time to 60 min,

showing little influence on the bacteria attachment. The quantity of bacteria on PLysMA-functionalized membrane was relative stable at 60-70% reduction in CFU after 20-60 min modification.

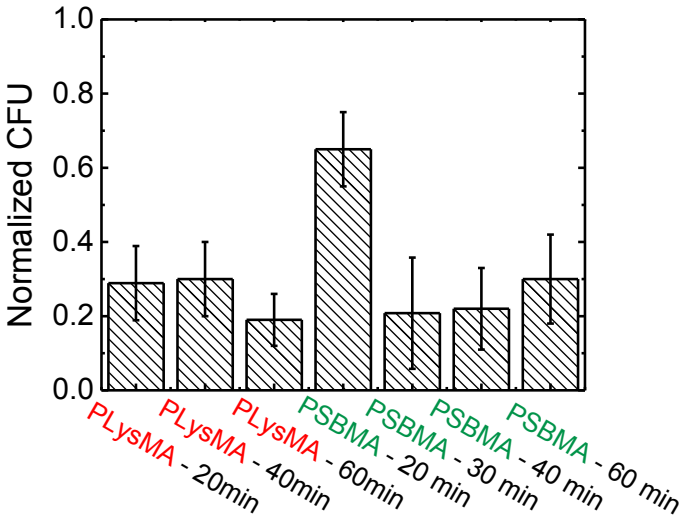

Figure 6. 8 The influence of polymer length on bacterial adhesion. The normalized value was obtained by comparing the colony forming units (CFU) on modified membrane with that of the pristine PA membrane (N/N_{PA}).

6.3.3 The fabrication of PSBMA and PLysMA copolymer grafted membrane

Since increasing the polymerization time of PLysMA after 20 min and PSBMA after 30 min did not cause significant change in the antimicrobial or the fouling resistance performance (Figure 6.9), the ratio of the polymers was optimized to further select an effective copolymer grafting. In comparison to the M-PSBMA $_{30\ min}$, M-PSBMA $_{20\ min}$-*b*-PLysMA $_{10\ min}$ exhibited a similar reduction in normalized bacteria CFU. Increasing the polymerization of PSBMA and PLysMA, the normalized bacteria CFU on M-PSBMA $_{30\ min}$-*b*-PLysMA $_{10\ min}$ and M-PSBMA $_{20\ min}$-*b*-PLysMA $_{20\ min}$ surfaces reduced to 90% and 91%, respectively; while the former exhibited a larger standard deviation, which might be due to the uneven grafting of PLysMA within the short 10 min

timeframe. Improved reduction in CFU further supported the hypothesis that the quantity of PSBMA and PLysMA affected the antimicrobial performance of polymer modified membrane. Exchanging the grafting order of PLysMA $_{20\ min}$ and PSBMA $_{20\ min}$, the membrane (M- PLysMA $_{20\ min}$ -PSBMA $_{20\ min}$) showed similar rates of CFU formation. Therefore, M-PLysMA $_{20\ min}$-*b*-PSBMA $_{20\ min}$ and M-PSBMA $_{20\ min}$-*b*- PLysMA $_{20\ min}$ were selected for further copolymer grafting tests.

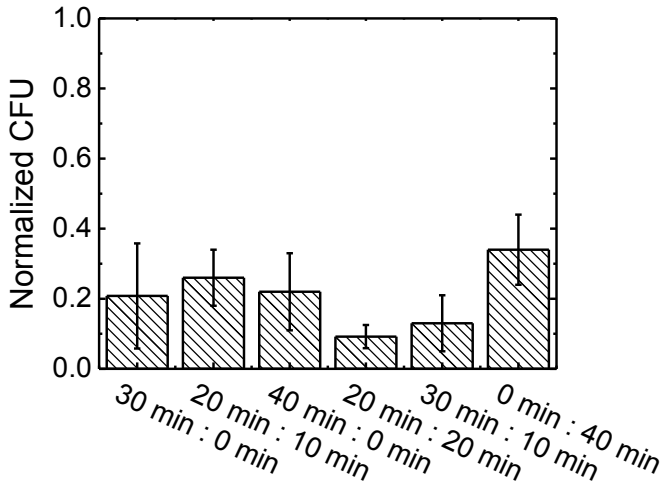

Figure 6. 9 The influence of grafting time of PSBMA: PLysMA on bacterial attachment on membranes.

6.3.4 Surface characterization and performance evaluation of the copolymer modified membranes

The membrane surfaces were evaluated via FTIR-ATR to investigate functional group change before and after polymer grafting (Figure 6.10). In comparison to the control PA, the characteristic peaks of PSBMA appeared on M-PSBMA at 953, 1039 and 1072 cm^{-1}, ascribed to R_4N^+ (quaternary amine), SO_3^- (sulfonate) and C=O (carbony) functional groups. PLysMA mainly consists of N-C=O (amide), NH_2 (primary amine) and COOH (carboxylic) functional groups. The

signal of primary amines (C-N at 1550 cm^{-1} and -NH_2 at 3300 cm^{-1}) on membrane became stronger and broader after PLysMA grafting. However, since the penetration depth of FTIR (1-5 μm) is larger than the thickness of polyamide membrane (150~300 nm), the combined signals of the polymer and polyamide (PA) from the support layer were detected. Therefore, the spectra of N-C=O exhibited little change with PLysMA modification. On the copolymer grafted surface, the characteristic peaks of PSBMA and PLysMA with reduced intensities (probably due to the reduced percentage when more types functional groups appeared) were all observed. This result further supported the successful grafting of PSBMA-*b*-PLysMA and PLysMA-*b*-PSBMA.

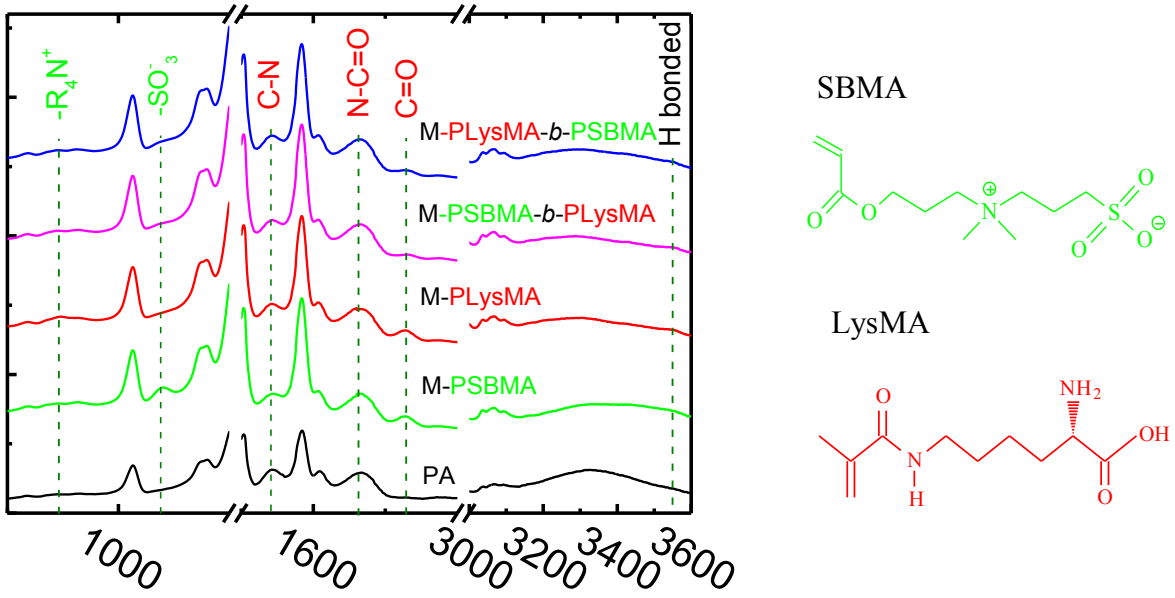

Figure 6. 10 FTIR of the control PA membrane and PA membranes modified by different polymers.

The surface morphology of the copolymer grafted membranes was further observed via AFM and SEM (Figure 6.11), and then compared with the PSBMA- or PLysMA-modified ones (Fig. 5). With different architectures, the copolymers (PSBMA-*b*-PLysMA and PLysMA-*b*-PSBMA) grafted membrane exhibited similar surface morphologies and the "ridge-valley" structure of PA

substrate was completely covered by the coating. In comparison to the M-PLysMA $_{40\ min}$, the polymer coating on M-PLysMA $_{20\ min}$-PSBMA $_{20\ min}$ were less dense which further confirmed the different polymerization rate of PLysMA and PSBMA. Due to a thicker polymeric coating, the M-PSBMA $_{20\ min}$-*b*-PLysMA $_{20\ min}$ and M-PLysMA $_{20\ min}$-*b*-PSBMA $_{20\ min}$ membranes exhibited a reduced surface roughness (Ra ranges from 44~55 nm) in comparison to those of M-PSBMA $_{20\ min}$ and M-PLysMA $_{20\ min}$ (Ra was ~90 nm). The smoother seen with the copolymer modified membranes was expected to reduce cell deposition.

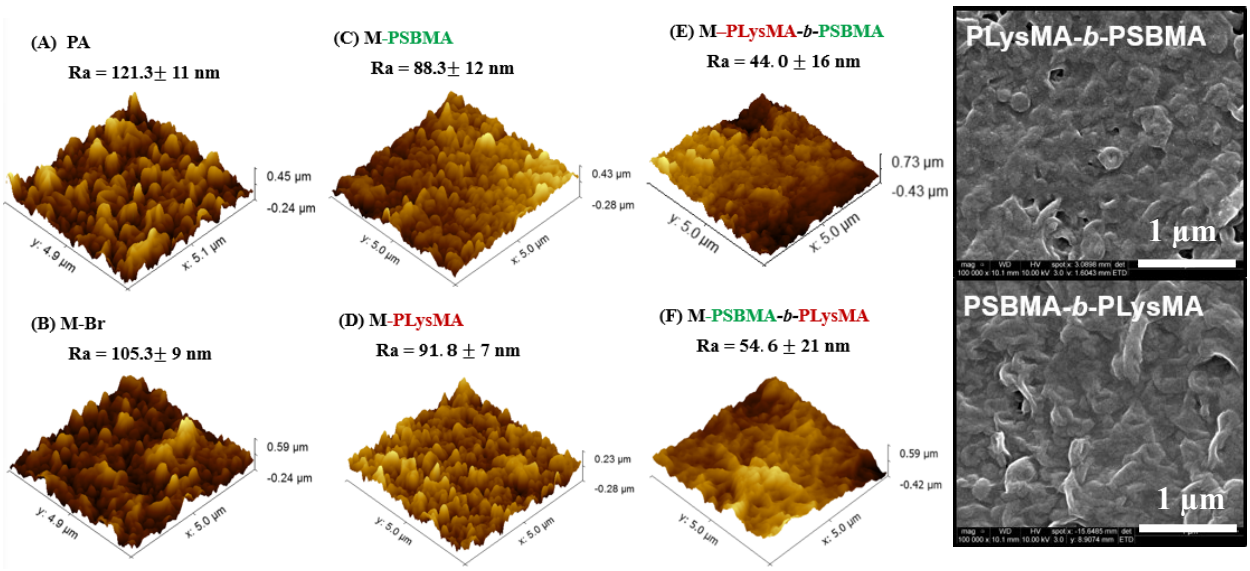

Figure 6. 11 The AFM and SEM images of pristine PA and different polymer modified membranes.

The charge densities of polymer grafted membranes were evaluated via zeta potential analysis (Figure 6.12 A). Less of a charge density might reduce any nonspecific interactions between membrane and contaminant. With abundant oxygen-containing functional groups on GO, the GO coating significantly increased the negative-charge density of the PA membrane (the zeta potential of PA and PA-GO membranes were -22.9±4.1 mV, -46.3 ±1.7 mV, respectively). Due to the substitution of -OH groups on GO by bromoester, the zeta potential of the M-Br membrane increased to -28.5 ±4.2 mV. Both the single polymer and the copolymer grafting resulted in a reduction in membrane charge density. Since both PSBMA and PLysMA can be considered neutral polymers due to the zwitterionic functional groups (the zeta potential of PSBMA were less than -5 mV under pH 3~9), reduced charge densities on the M-PSBMA and M-PLysMA appeared. However, due to the existence of the GO substrate, the differences in the charge density between PA and polymer modified surfaces were not as considerable as expected. The results indicate that both "defending" and "attacking" coatings mitigate the charge densities of the PA surface.

Wetting ability is important for the adhesion of foulant to membrane. A membrane with a high surface free energy (SFE) is prone to interact with the contaminate (wetted). To evaluate the wetting ability of membrane, three types of liquids with different surface tensions: DI water (H_2O), diiodomethane (CH_2I_2) and glycerol ($C_3H_8O_3$) were used to evaluate the contact angle of different liquid drops on pristine and polymer modified membranes. The corresponding SFEs were calculated by the software in a geometric model (Table 6.2). Like the PSBMA and PLysMA coating, the copolymer-modification significantly increased the hydrophilicity of the PA membrane (inferred from a >30° reduction in water-contact-angles). The PSBMA- and PLysMA-based modifications exhibited little influence on the membrane diiodomethane-contact-angle. However, incorporating PLysMA on the surface slightly improved the affinity of the membrane towards glycerol, as indicated by the ~10° reduction in glycerol-contact-angles on the surface of M-PLysMA, M-PSBMA-*b*-PLysMA and M-PLysMA-*b*-PSBMA. These observations implied that, in comparison to the PA polymer modified membranes showed more affinity to water. Although the incorporation of PLysMA also slightly increased the hydrophobic interaction between membrane and contaminant in aqueous environments, the improvements in hydrophilic interactions were much stronger. With the improved affinity towards water and glycerol, the SFEs of polymer and copolymer modified membranes correspondingly increased. Notably, the increase in SFEs predominantly contributed by the polar force component, was mainly ascribed to the large

H bond and ionic bond interaction, instead of dispersive-force component which mainly exists between the interaction of non-polar molecules. The SFE observation further supported that all PSBMA- and PLysMA-based polymeric coatings significantly increased the water affinities of the membrane.

The influence of copolymer grafting on the membrane perm-selective was evaluated (Figure 6.12 B). After 20 min of PSBMA and PLysMA-grafting, the membranes flux was maintained at 93.4 ± 3.3% and 95.1±2.6, respectively, without significant differences between two types of polymer. Further polymerizing a different type of polymer on the surface, the flux of M-PSBMA-*b*-PLysMA and M-PLysMA-*b*-PSBMA decreased to 73.5±0.8% and 82.9±1.5%. In comparison to M-PLysMA-*b*-PSBMA, the more flux reduction (~5%) on M-PSBMA-*b*-PLysMA might be because 20 min of PSBMA polymerization offered a flat substrate which favored PLysMA grafting in the second step. While, when PLysMA was directly grafted on the PA surface, the coating was not uniform (as observed by SEM) and some of the initiator might be hindered or might lose their activity due to the fast polymerization rate of PLysMA, therefore, the polymerized PSBMA layer on PLysMA-derivated surface was not as thick and dense as directly coated on Br initiated membrane surface.

Table 6. 2 The water, diiodomethane and glycerol contact angles for pristine and polymer modified membranes. Surface energy calculations are based on the geometric model.

Membrane	Contact angle (Deg.)			Surface energies (mJ/m^2)		
	H_2O	CH_2I_2	$C_3H_8O_3$	Dispersive	Polar	Total
PA	54.2±0.8	31.4±6.9	40.4±1.0	27.3±4.6	26.9±5.3	54.2±2.6
M (PA-GO)	28.7±0.6	38.0±2.1	21.5 ±1.6	24.8±3.2	38.2±6.3	63.0±1.9
M-Br	52. 4± 0.6	30.2±2.9	42.4±3.3	37.4±3.6	20.9±2.1	58.3±1.3
M-PSBMA	8.0±1.2	35.1±0.9	39.4 ± 3.0	16.4± 9.2	54.9± 8	71.4± 17.4
M-PLysMA	17.2±1.3	29.4±1.5	28.1 ± 1.4	22.9±10.1	44.9±25	67.8±8.2
M-PSBMA-co-PLysMA	9.6±3.6	27.4±3.3	31.8±14.3	22.4±12.8	48.6±28.1	71±14
M-PLysMA-co-PSBMA	10.7±3.5	29.8±3.1	35.9±4.1	22.3±13.5	50.2±14.1	72.5±18.5

Note: The surface tension of the liquid used in experiment: (A) H_2O (SFE_{total}=72.8 mJ/m^2, $SFE_{dispersive}$=21.8 mJ/m^2, SFE_{polar}=51 mJ/m^2); (B) CH_2I_2 (SFE_{total}=50.8 mJ/m^2, $SFE_{dispersive}$=50.8 mJ/m^2, SFE_{polar}=0 mJ/m^2); (C) $C_3H_8O_3$ (SFE_{total}=64 mJ/m^2, $SFE_{dispersive}$=34 mJ/m^2, SFE_{polar}=30 mJ/m^2).

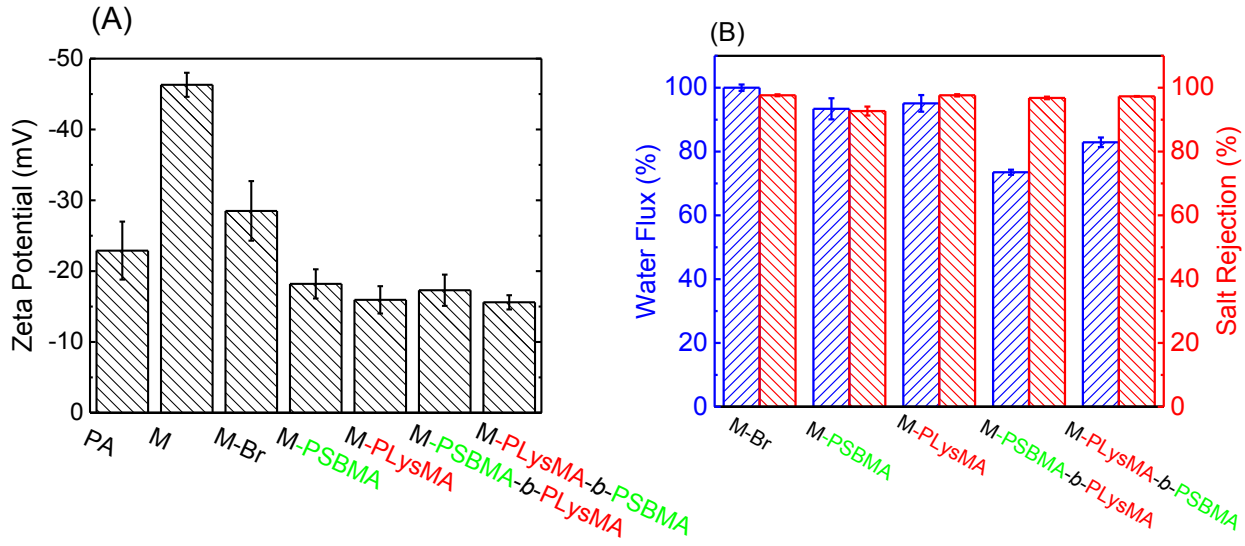

Figure 6. 12 The zeta potential **(A)** and the water perm-selectivity **(B)** of pristine and modified membranes.

6.3.5 The antimicrobial and antibiofouling performance of copolymer grafted membranes

To investigate the influence of copolymer modification on the antibacterial performance of the membrane, the cell-adhesive and antimicrobial behavior of pristine and modified membranes were evaluated by contacting the membrane with model bacteria, *B. Subtilis* (G+) and *E.coli* (G-), for 2 h and then observing the live/dead status of bacteria by fluorescence microscope (Figure 6.13).

According to observation, both single type of polymer and block copolymer coatings significantly reduced the *B. Subtilis* (G+) attachment, which might result from the reduced roughness, hydrophilicity and charge density of the polymeric coating. The viability of *B. Subtilis* (G+) on the PSBMA-coated surface was higher than those on the PLysMA-grafted ones, indicating the inactivation potential of PLysMA towards *B. Subtilis* (G+) bacteria. It was interesting to observe that on the M-PSBMA-PLysMA where PLysMA was predominantly exposed to bacteria, near 100% inactivation of cells was observed as with the M-PLysMA; however, when PSBMA was exposed to bacteria, the cell viability increased. Results inferred that copolymer modification effectively controlled the biofouling caused by deposition and propagation of *B. Subtilis* (G+).

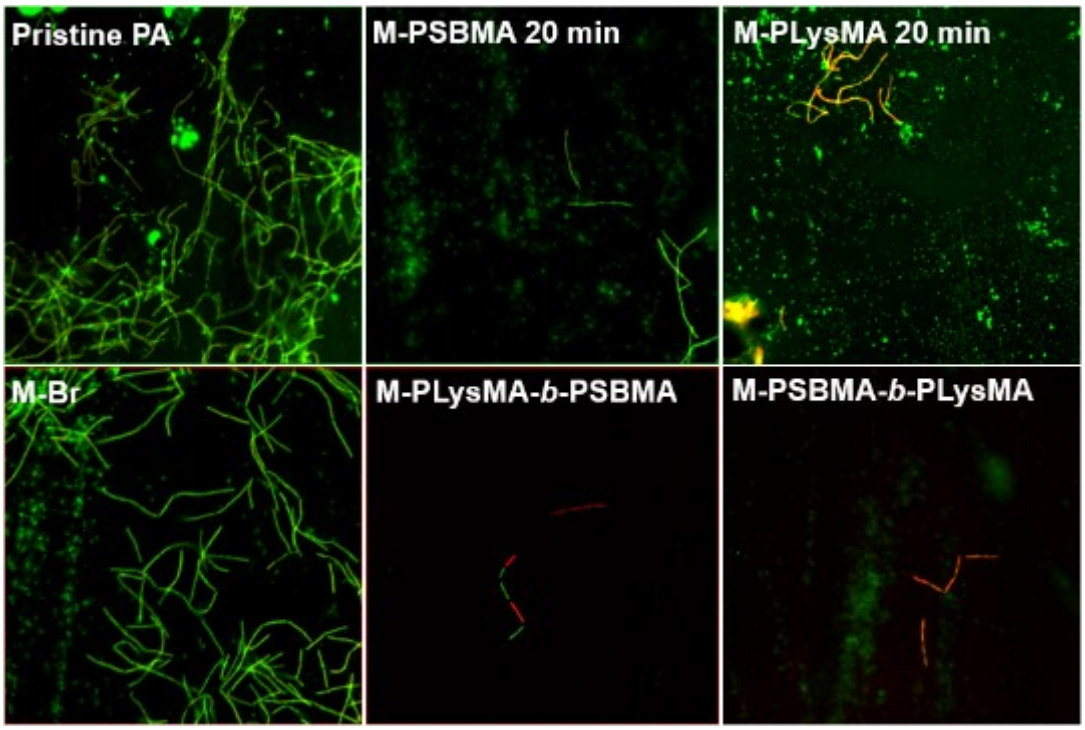

Figure 6. 13 Representative confocal microscope images of B. Subtilis (G+) on pristine and modified membranes after 2 h of static contact. The bacteria on the membrane surface was stained with PI (indicating dead cell, red color) and SYTO 9 (indicating live cell, green color) fluorescent nucleic acid stains before observation. Each image shows an area of 105.67 μm×105.67 μm.

As with *B. Subtilis* (G+), both PLysMA-*b*-PSBMA- and PSBMA-*b*-PLysMA-modified membrane considerably repelled deposition of *E.coli* (G-) (Figure 6.14 A1-C1). However, the inactivation performance of PLysMA towards *E.coli* was not observed. The differing cell inactivation performance of PLysMA coating to *B. Subtilis* and *E.coli* could be attributed to the different cell structures of G+ and G- bacteria. G+ bacteria has a thick cell wall (20-80 nm) surrounding an inner cell membrane, with 40-95% of the cell wall consisting of peptidoglycan [81]. In contrast, gram-negative cells have a thinner cell wall (15-20 nm) but the composition is much more complicated

(containing an outer membrane and 2-3 nm peptidoglycan). Since the cell wall of G+ bacteria is mainly formed by peptidoglycan, it could be more easily lysed by most amoni-acids/peptides via the "like dissolves like" principle and result in cleavage of the pentaglycine cross-bridge in the cell wall peptidoglycan [77]. The results indicate that the "defending" strategy played a predominant role in the reduction of *E.coli* causing fouling.

The stability of the copolymer coating in preventing bacterial breeding was further evaluated by contacting membranes with the bacteria-nutrient suspension (containing 0.1% LB as a carbon resource and multiple salts to promote biofilm formation) for 48 h (Figure 6.14 A2-C2), and the volume of bacteria cell attachment on the membranes were evaluated (Figure 6.15). Compared with the PA surface, the copolymer-modified membrane with a "defending"-moiety dominated surface maintained superior anti-deposition performance (total bacterial volume on M-PLysMA-*b*-PSBMA was 39.6% of that on the PA membrane) towards *E.coli*. When exposing biofilm-"attacking" moieties to bacteria, the M-PSBMA-*b*-PLysMA exhibited less bacterial repulsion and the bacterial volume was 59.8% of that of the control PA surface. The viability of *E.coli* on pristine PA, M-PSBMA-*b*-PLysMA and M-PLysMA-*b*-PSBMA surfaces were 92.3%, 87.5% and 80%, respectively. Result showed that biofilm-"attacking" moieties did not play a significant role reducing the biofouling caused by *E.coli*.

Aside from the different cell wall structure as discussed above, the relative high SFEs of PLysMA in comparison to PSBMA layer might be another reason for the low-antibiofouling-performance of M-PSBMA-*b*-PLysMA. The PLysMA coated trends to be more easily wetted by organic contaminant (LB, citric acid) and gradually lost their biofilm-"attacking" potential due to organic foulant covering. Furthermore, it has been reported that zwitterionic moieties in PSBMA were able to "swell" (enhanced intra- and intermolecular forces and stiffness) in salt-containing solutions while it "collapsed" in pure water [24]. Therefore, when PSBMA was grafted on the top, the membrane was able to offer strong repulsive forces towards contaminants.

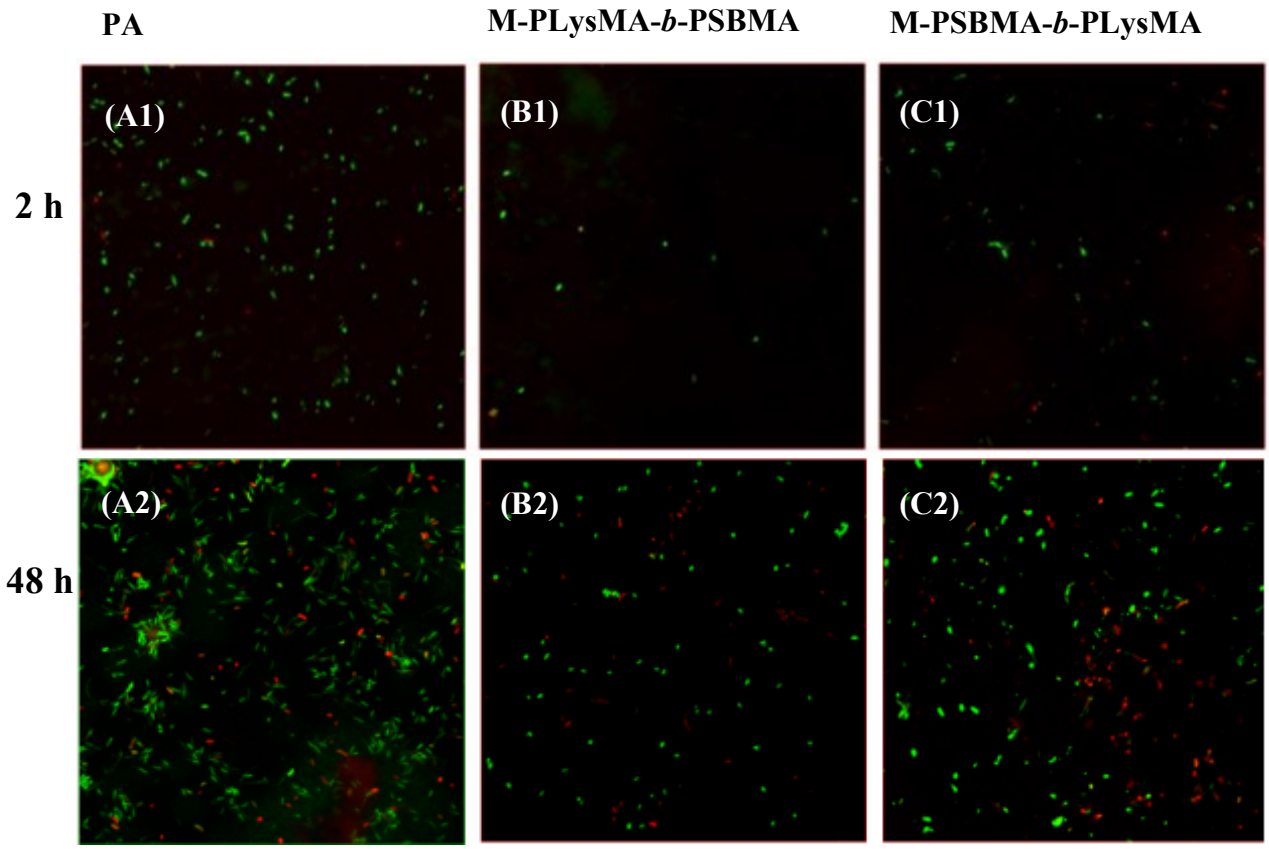

Figure 6. 14 Representative florescence microscopy images of E. coli on control PA, M-PLysMA-b-PSBMA and M-PLysMA-b-PSBMA membranes after 2 h **(A1, B1, C1)** and 48 h **(A2, B2, C2)** of contact. The experiment condition was described in section 2.5. The bacteria on membrane surface was stained with PI (indicating dead cell, red color) and SYTO 9 (indicating live cell, green color) fluorescent nucleic acid stains before observation. Each image shows an area of 105.67 μm×105.67 μm.

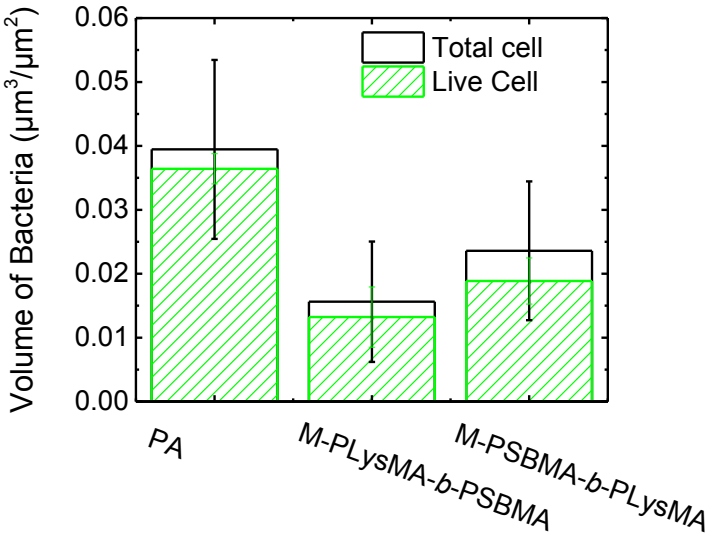

Figure 6. 15 The volume of the attached bacteria on the membrane samples after 48 h contact.

The influence of copolymer modification on the antibiofouling performance of membranes was further investigated in a dynamic filtration system (Figure 6.16). The experiment was conducted by continuous filtration of bacteria-containing synthetic wastewater (0.1% LB as carbohydrate source and multiple salts) for 4 h to let *E.coli* cells attach to the membrane. Then, the feed solution was changed to synthetic wastewater only and filtration continued for 12 h to promote the breeding of those bacteria that attached to the membrane to form biofilms. During the filtration process, the flux change of membranes associated with the biofilm was recorded. Then, the biofouled membrane was cleaned with EDTA (0.2 mM) and SDS (5 mM) in sequence to observe the flux recovery rate. The experiment was conducted in two cycles.

In the first cycle of the "fouling-cleaning" process, the water permeation flux of pristine PA rapidly declined during the 0-4 h bacteria filtration and continued decreasing linearly further in the biofilm culturing process. On the contrary, the copolymer modified membranes maintained most of the initial flux. The flux reduction of M-PSBMA-*b*-PLysMA was slightly more severe than that of M-PLysMA-*b*-PSBMA and reached to stability at around 7 h of biofilm culturing. After 4 h of bacterial attachment and 12 h of biofilm culturing, the PA, M-PLysMA-*b*-PSBMA and M-

PSBMA-*b*-PLysMA membranes maintained 20%, 65%, and 73% of the initial flux, respectively. The flux decline during the filtration process should be a result of gradual deposition and propagation of bacteria as well as binding of organic compounds (yeast in LB) and salt on the membrane due to the adsorption and interactions, which gradually blocked the membrane pores. In a cross-flow filtration environment, the hydraulic shear force could peel off loosely bonded contaminants; therefore, the membrane shows steady flux after certain time when the adsorption/desorption of contaminants on the membrane reaches an equilibrium. The mitigated flux reduction after copolymer modification indicated the less quantity of cell and other contaminant on membrane, which caused by the weak interaction between contaminant (bacteria, carbohydrate substance and salt) and the low potential of biofilm formation due to the "defending and attacking" moieties of modified membranes. After cleaning, 100% of flux was recovered on all these three types of membranes.

The slightly severe flux reduction on pristine and modified membranes was observed in the second cycle of biofouling testing. After 12 h of biofilm culturing, 73% of initial flux was maintained on the M-PLysMA-*b*-PSBMA and the flux was fully recovered after EDTA and SDS cleaning. With a different polymeric architecture, the M-PLysMA-*b*-PSBMA maintained ~62% of initial flux and 98% recovery of flux was observed after the second cleaning cycle. With the control, PA, only 16% of initial flux was maintained and the flux recovery rate decreased to 94%, indicating the appearance of irreversible fouling on the pristine PA after only two filtration cycles.

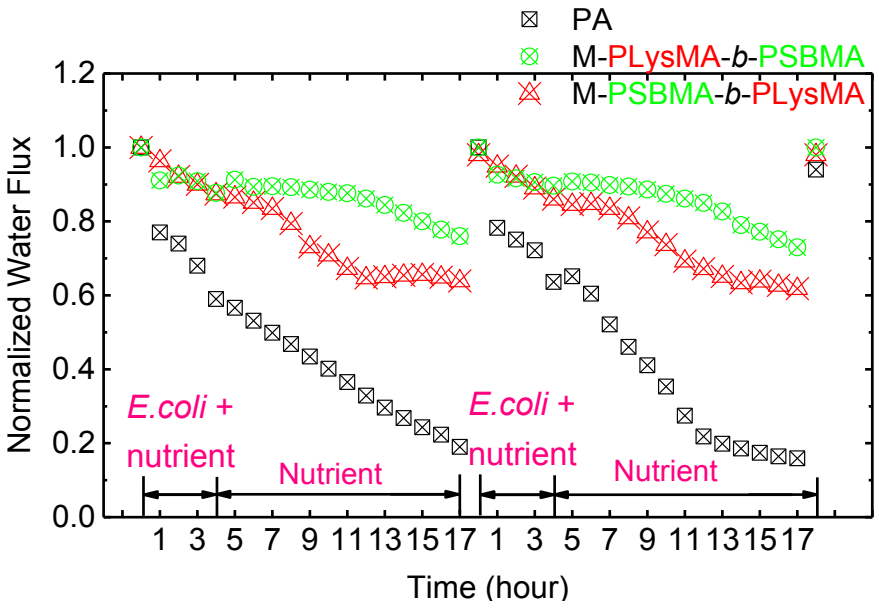

Figure 6. 16 The water flux reduction of the control PA and block copolymer modified membranes, M-PLysMA-b-PSBMA and M-PSBMA-b-PLysMA, associated with biofilm growing in filtration process. The value was normalized to the initial flux of membrane at time 0 of the first fouling cycle.

The investigation of static bacterial attachment and dynamic cross-flow filtration demonstrated that GO mediated dual functional copolymer (zwitterionic polymer PSBMA and biofilm controlling polymer PLysMA) modification could significantly improve fouling resistance of a polyamide membrane and effectively reduce the water flux decline caused by deposition of contaminant and formation of biofilm on the membrane surface. The copolymer modification reduced the biofouling caused by *B. Subtilis* (G+) via a synergistic "defending" and "attacking" strategies. However, in case of biofouling caused by *E.coli* (G-), "defending" functions which resulted from the strong affinity of polymers, played an important role. When the "defending" -PSBMA was grafted on the top and directly exposed to bacteria-containing suspensions, the membrane exhibited the lowest bacterial attachment and maintained a high water-permeation-flux along with biofilm growth.

Although no obvious biofilm-control function toward *E.coli* (G-) was observed with the PLysMA-modified membrane, PLysMA coating functionalized as a weak "defender" and exhibited moderate antibiofouling (~60%) performance, due to the improved hydrophilicity and the reduced surface charge density and roughness of membrane. GO mediated dual functional polymer grafting via ARGET ATRP presents to be a potential method for robust and convenient surface modification. To improve the antibiofouling performance of the membrane further via "defending-attacking" strategies, a material with a stronger bacterial/biofilm-"attacking", such as poly-L-lysine and $_{D}$-tyrosine, should be considered in future work.

6.4 Conclusion

In this study, a zwitterionic polymer (PSBMA) and a biofilm controlling polymer (PLysMA) have been selected as functional materials to mitigate the biofouling on a membrane via a combined-"defending and attacking" strategies. It is the first time that GO has been applied as modification media to facilitate polymeric modification on membranes in order to reduce the scarification of flux. Furthermore, the potential of applying poly(amino acid) brushes to reduce biofouling on PA membranes has been investigated for the first time.

PSBMA and PLysMA grafting both significantly enhanced water affinity, reduced roughness of and slightly neutralized the charge density of polyamide membrane. However, due to the extra coating on membrane, the copolymer modification compromised 20~25% of water permeation flux.

Due to the changed physiochemical properties, membranes modified with both copolymers (M-PSBMA-*b*-PLysMA and M-PLysMA-*b*-PSBMA) reduced the attachment of *B. Subtilis (G+)* and *E.coli (G-)*. The PLysMA dominated surface exhibited inactivation ("attacking") functions toward *B. Subtilis (G+)*; however, no obvious inactivation towards the attached *E.coli (G-)* was observed.

The "defending" function played an important role in controlling biofouling caused by *E.coli*. When PSBMA was grafted on the surface and directly exposed to the bacteria-containing suspension, the membrane exhibited extremely low bacterial deposition, even after 48 h of contact.

In the cross-flow filtration experiment, the M-PLyMA-*b*-PSBMA mitigated the harsh decline in flux caused by *E.coli* deposition and propagation on the membrane surface. During the two cycles

of the “fouling-cleaning” experiment, the membrane maintained 73% initial water flux after 12 biofilm culturings and saw a 100% flux recovery after cleaning. However, only 20% of initial flux was maintained for a control PA membrane under the same experimental conditions and only 94% flux recovered after cleaning.

Overall, the facile and convenient modification process, enhanced water affinity and led to promising antifouling results, demonstrating the potential of the novel copolymer grafted membranes in practical applications for energy efficient water purification in relieving water shortages in future.

Chapter 7 Conclusions and future work

7.1 Conclusion

The RO technique plays an irreplaceable role in waste water purification and sea water desalination industries. However, irreversible fouling, caused by bacterial adhesion and propagation on the membrane surface, inhibits widespread application. Developing an antibiofouling membrane will greatly contribute to the overall use of the RO technique and increase its contribution in relieving the global water crisis into the future.

To address the membrane biofouling problem, this study proposes three types of membrane-surface modifications as potential strategies to mitigate biofouling in the RO process; namely: (i) coating with zwitterionic and low-surface-energy polymer to "defend" the membrane from microorganism/protein deposition; (ii) anchoring CuNPs to "attack" microorganisms and prevent their propagation; (iii) grafting both polymers and natural antibiofouling materials to not only "defend" the membrane from foulant deposition but potentially inhibit ("attack") the biofilm formation.

The conclusions and contributions of this study can be summarized through three different aspects: the modification strategy, antibiofouling modifiers, and modification methods.

- The physiochemical properties of the membrane affect the membrane anti-biofouling performance.

Surface hydrophilicity has been found to be critical with the biofouling-"defending" zwitterionic polymer, PSB, with modification significantly reducing the water contact angle of the membrane and the modified membrane achieving a near 70%~80% reduction in protein and cell attachment.

Combining modifiers with different antibiofouling mechanisms could achieve enhanced antibiofouling performance via a synergistic effect. Combined PDMS (fouling-release polymer) and PSB (fouling-resistant polymer) grafted surfaces showed improved antibacterial-adhesion performance than the individual PDMS and PSB modified ones. The copolymer (PLysMA-*b*-PSBMA) functionalized membrane effectively decreased cell attachment and inhibited the propagation *of G(+)* bacteria.

- High-quality, effective, cost-efficient and environmentally-friendly modifiers for the fabrication of antibiofouling-membranes have been proposed.

CuNPs exhibited great potential to replace AgNPs in the development of cost-efficient and quality-competitive biocidal coatings for membrane biofouling control. CuNPs control biofouling in a dose-dependent manner. A membrane decorated with a mono-layer of CuNPs via *in-situ* reduction exhibited a greater than 90% antimicrobial performance; while increasing the quantity of CuNPs via SSLbL method acheived near 100% bacterial-inactivation. Durable antibiofouling performance of modified membranes could be achieved by CuNPs regeneration.

Graphene oxide (GO) can be effectively functionalized as modification-media in the fabrication of antibiofouling coatings on membrane surfaces. Due to their nanometer thickness, GO media exhibited minor effects on membranes in terms of water perm-selectivity. GO coatings render more reaction sites for the anchoring of metal NPs and polymers. GO functionalization improved membrane hydrophilicity, which might reduce organic foulant adhesion, and GO coated membranes exhibited 40% bacterial inactivation.

Natural antibiofouling materials have been shown as promising option for membrane biofouling control in an environmentally friendly manner. Poly (amino acid) brush, PLysMA, is functionalized as a "weak" zwitterionic polymer and effectively reduces the attachment of both G(+) and G(-) bacteria. Furthermore, PLysMA exhibited potential for inactivating and controlling the propagation of G(+) bacteria attached on membrane; however, the same function to G(-) bacteria has not been observed.

- The controllable functionalization of nanoparticle- and polymer-based materials for membrane biofouling control has been proposed.

In-situ decoration of CuNPs onto a membrane surface using a medium with an affinity to metal could be used to control aggregation and increase the loading quantity of CuNPs modifiers. The CuNPs can also be conveniently regenerated to maintain a durable antibiofouling performance.

A spray- and spin-assisted layer-by-layer (SSLbL) method was developed to controllable load and functionalize the membrane with CuNPs for biofouling control. This method was able to produce

a uniform bilayer of PEI-CuNPs/PAA in less than 1 min, which is far more efficient than the traditional dipping approach (25-60 min).

The activators regenerated by electron transfer-atom transfer radical polymerization (ARGET-ATRP) technique has been applied to controllably grow polymeric modifiers on the membrane. This method provided insights into the influence of polymer density, length, and architecture to the antibiofouling performance of modified membrane.

7.2 Future work

- Metal nanoparticles are effective biocides for the prevention of biofilm formation; however, their gradual dissolution in aqueous environments does increase the cost. Mediums that alleviate the oxidation of CuNPs (e.g., chitosan, ascorbic acid) and provide stability for copper-based nanoparticles (e.g., CuS) are potential candidates for the development of novel low-cost anti-biofouling membranes in future.
- The potential strategies of applying natural antibiofouling materials to mitigate biofouling or remove biofilms in an environmentally friendly manner are worth further investigation.
- This research is a proof-of-concept study; therefore, the modifier selections were limited to the modification methods. ARGET ATRP is a facile and effective method for membrane surface modification with polymers; however, the material used in ATRP needs to be functionalized with a vinyl terminated bond. By cooperating with researchers in the field of organic chemistry, a natural material with a strong bacteria/biofilm-"attacking" function, such as poly-L-lysine and D-tyrosine, could be incorporated on the membrane surface alongside the zwitterionic polymer to effectively reduce biofouling.

7.3 Publications

Journal paper published

[J1] **Ma, W.,** Chen, T., Nanni, S., Yang, L., Ye, Z., Rahaman, M.S., Thin film nanocomposite (tfn) membrane based on zwitterion functionalized graphene oxide (GO) with improved water affinity and antifouling properties, *Langmuir*, 2018, (revision submitted, la-2018-02044t.R1).

[J2] Tabrizian, P., **Ma, W.,** Bakr, A., Rahaman, M.S., pH-sensitive and magnetically separable Fe/Cu bimetallic nanoparticles supported by graphene oxide (GO) for high-efficiency removal of tetracyclines, *J. Colloid Interface Sci.,* 2019, 534, 549-562 (**co-first author**).

[J3] **Ma, W.,** Panecka, M., Rahaman, M. S., Tufenkji, N., Bacteriophage-based strategies for biofouling control in ultrafiltration: in situ biofouling mitigation, biocidal additives and biofilm cleanser, *J. Colloid Interface Sci*., 2018, 523, 254-265.

[J4] **Ma, W.,** Soroush, A., Tran V.A.L, Rahaman, M.S., Cysteamine- and Graphene Oxide-Mediated Copper Nanoparticle Decoration on Reverse Osmosis Membrane for Enhanced Anti-Microbial Performance, *J. Colloid Interface Sci.* 2017, 50, 330-340.

[J5] **Ma, W.,** Soroush, A., Tran V.A.L, Brennan, G., *Rahaman, M.S., Asadishad, B., Tufenkji, N., Spray- and spin-assisted layer-by-layer assembly of copper nanoparticles on thin-film composite reverse osmosis membrane for biofouling mitigation, *Water Res.,* 2016, 99, 188-199.

[J6] **Ma, W.,** Rahaman, M.S., and Therien-Aubin, H., Controlling biofouling of reverse osmosis membranes through surface modification via grafting patterned polymer brushes, *J. Water Resue Desal.,* 2015.

[J7] Soroush, A., **Ma, W.,** Cyr, M., Rahaman, M.S., Asadishad, B., Tufenkji, N., In situ silver decoration on graphene oxide-treated thin film composite forward osmosis membranes: Biocidal properties and regeneration potential, *Environ. Sci. Technol. Lett.,* 2015, 3 (1), 13-18.

[J8] Soroush, A., **Ma, W.,** Silvino, Y., Rahaman, M.S., Surface modification of thin film composite forward osmosis membrane by silver-decorated graphene-oxide nanosheets, *Environ. Sci. Nano,* 2015, 2 (4), 395-405.

Manuscript under preparation

1. **Ma, W.,** Chen, T., Ye, Z., Rahaman, M.S., Grafting zwitterionic polymer and poly (amino acid) on polyamide membranes: “defending and attacking” strategies for biofouling control.

Applied Patent

Rahaman, M.S., Islam, M.S., Chen, T., Ma, W. "Membranes for forward osmosis and membrane distillation and process for treating fracking wastewater", US provisional patent application, 62/732,781, 2018.

Attended conference

[C1] **Ma, W.,** Chen, T. Nannni, S., Rahaman, M. S., Grafting zwitterionic polymer and poly (amino acid) on polyamide membranes: "defending and attacking" strategies for biofouling control, Membranes: Materials & Processes – Gordon Research Conference, 2018, New London, NH, USA, Discussion leader, Poster presentation.

[C2] **Ma, W.,** Nannni, S., Chen, T. Rahaman, M. S., Tiraferri, Grafting fouling-resistant polymer brush on go-coated membranes: defending and attacking strategies for biofouling control, 2017 Association of Environmental Engineering and Science Professors (AEESP) research and education conference, 2017, Anh Arbor, MI, USA, Oral presentation. (Obtained the Carollo Student Scholarship Award)

[C3] **Ma, W.,** Panecka, M., Wong, K., Tufenkji, N., Rahaman M. S., 2016 Gordon Research Conference on Membranes: Materials & Processes, New London, NH, USA. 2016, Poster.

[C4] **Ma, W.,** Soroush, A., Tran V.A.L, Rahaman, M.S., Improving the antibiofouling property of polyamide membrane by copper nanoparticles modification via cysteamine and graphene oxide as media, 251st ACS (America Chemistry Society) National Meeting & Exposition, 2016. San Diego, CA, USA,. Oral.

[C5] **Ma, W.,** Soroush, A., Tran V.A.L, Rahaman, M.S., Comparison of the effectiveness of silver nanoparticles (AgNps) and copper nanoparticles (CuNps) for thin-film composite (TFC) reverse osmosis (RO) membrane biofouling control, 4th Annual Conference Sustainable Nanotechnology Organization (SNO), 2015, Portland, OR, USA. Poster.

[C6] **Ma, W.,** Soroush, A., Tran V.A.L, Brennan, G., Rahaman, M.S., Asadishad, B., Tufenkji, N., Functionalization of TFC polyamide membrane with copper nanoparticles using spray- and spin-assisted layer-by-layer assembly, North American Membrane Society (NAMS) 25th Annual Meeting, 2015, Boston, MA, USA. Poster.

[C7] **Ma, W.,** Rahaman, M.S., and Therien-Aubin, H., Controlling biofouling of reverse osmosis membranes through surface modification via grafting patterned polymer brushes, the Canadian Society for Civil Engineering (CSCE) Annual Conference, 2014, Halifax, NS, Canada. Oral Presentation & Paper.

References

1. Rahaman, M. S.; Vecitis, C. D.; Elimelech, M., Electrochemical carbon-nanotube filter performance toward virus removal and inactivation in the presence of natural organic matter. *Environ. Sci. Technol.* **2012,** *46*, (3), 1556-1564.

2. Greenlee, L. F.; Lawler, D. F.; Freeman, B. D.; Marrot, B.; Moulin, P., Reverse osmosis desalination: water sources, technology, and today's challenges. *Water Res.* **2009,** *43*, (9), 2317-2348.

3. Elimelech, M.; Phillip, W. A., The future of seawater desalination: energy, technology, and the environment. *Science* **2011,** *333*, (6043), 712-717.

4. Lee, K. P.; Arnot, T. C.; Mattia, D., A review of reverse osmosis membrane materials for desalination—Development to date and future potential. *J. Membr. Sci.* **2011,** *370*, (1-2), 1-22.

5. Kang, G. D.; Cao, Y. M., Development of antifouling reverse osmosis membranes for water treatment: A review. *Water Res.* **2012,** *46*, (3), 584-600.

6. Rana, D.; Matsuura, T., Surface modification for antifouling membrane. *Chem. Rev.* **2011,** *110*, 2448-2471.

7. Mi, B.; Elimelech, M., Organic fouling of forward osmosis membranes: Fouling reversibility and cleaning without chemical reagents. *J. Membr. Sci.* **2010,** *348*, (1-2), 337-345.

8. Yu, D.; Lin, W; Yang, M., Surface modification of poly(L-lactic acid) membrane via layer-by-layer assembly of silver nanoparticle-embedded polyelectrolyte multilayer. *Bioconjugate Chem.* **2007,** *18*, (5), 1521-1529.

9. Elimelech, M.; Zhu, X.; Childress, A. E.; Hong, S., Role of membrane surface morphology in colloidal fouling of cellulose acetate and composite aromatic polyamide reverse osmosis membranes. *J. Membrane Sci.* **1997**, (127), 101-109.

10. Masuelli, M.; Marchese, J.; Ochoa, N. A., SPC/PVDF membranes for emulsified oily wastewater treatment. *J. Membrane Sci.* **2009,** *326*, (2), 688-693.

11. Richards, H. L., Metal nanoparticle modified polysulfone membranes for use in wastewater treatment: a critical review. *J. Surf. Eng. Mater. Adv. Technol.* **2012,** *02*, (03), 183-193.

12. Mo, J.; Son, S.-H.; Jegal, J.; Kim, J.; Lee, Y. H., Preparation and characterization of polyamide nanofiltration composite membranes with TiO2 layers chemically connected to the membrane surface. *J. Appl. Polym. Sci.* **2007,** *105*, (3), 1267-1274.

13. Tiraferri, A.; Vecitis, C. D.; Elimelech, M., Covalent binding of single-walled carbon nanotubes to polyamide membranes for antimicrobial surface properties. *ACS Appl. Mater. Interfaces* **2011,** *3*, (8), 2869-2877.

14. Ben-Sasson, M.; Zodrow, K. R.; Genggeng, Q.; Kang, Y.; Giannelis, E. P.; Elimelech, M., Surface functionalization of thin-film composite membranes with copper nanoparticles for antimicrobial surface properties. *Environ. Sci. Technol.* **2014,** *48*, (1), 384-393.

15. Council, N. I., Global Trends 2025: A Transformed World. *Washington DC: U.S. Government Printing Office* **2008**.

16. Koo, C. H.; Mohammad, A. W.; Suja, F., Recycling of oleochemical wastewater for boiler feed water using reverse osmosis membranes - A case study. *Desalination* **2011,** *271*, 178-186.

17. Ndiaye, P. I.; Moulin, P.; Dominguez, L.; Millet, J. C.; Charbit, F., Removal of fluoride from electronic industrial effluentby RO membrane separation. *Desalination* **2005,** *173*, (1), 25-32.

18. Radjenovic, J.; Petrovic, M.; Ventura, F.; Barcelo, D., Rejection of pharmaceuticals in nanofiltration and reverse osmosis membrane drinking water treatment. *Water Res.* **2008,** *42*, (14), 3601-3610.

19. Aman, T.; Kazi, A. A.; Sabri, M. U.; Bano, Q., Potato peels as solid waste for the removal of heavy metal copper(II) from waste water/industrial effluent. *Colloids Surf. B* **2008,** *63*, 116-121.

20. Fritzmann, C.; Löwenberg, J.; Wintgens, T.; Melin, T., State-of-the-art of reverse osmosis desalination. *Desalination* **2007,** *216*, (1-3), 1-76.

21. Green, D. W.; Perry, R. H., Perry's Chemical Engineers' Handbook. *McGraw-Hill: New York,* **1997**.

22. Lonsdale, H. K.; Merten, U.; Riley, R. L., Transport properties of cellulose acetate osmotic membranes. *J. Appl. Polym. Sci.* **1965,** *9*, (4), 1341-1362.

23. Paul, D. R., Reformulation of the solution-diffusion theory of reverse osmosis. *J. Membrane Sci.* **2004,** *241*, 371-386.

24. Mattson, M. E.; Lew, M., Recent advances in reverse osmosis and electrodialysis membrane desalting technology. *Desalination* **1982,** *41*, (1), 1-24.

25. Guo, K. W., Membranes coupled with nanotechnology for daily drinking water: an overview. *Petrol. Environ. Biotechnol.* **2011,** *2*, (3), 1-21

26. Xie, W.; Geise, G. M.; Freeman, B. D.; Lee, H.-S.; Byun, G.; McGrath, J. E., Polyamide interfacial composite membranes prepared from m-phenylene diamine, trimesoyl chloride and a new disulfonated diamine. *J. Membrane Sci.* **2012,** *403-404*, 152-161.

27. Johnson, J. http://www.waterworld.com/articles/iww/print/volume-6/issue-1/features/membrane-cleaning-fundamentals-cleaning-criteria-and-normalization-of-reverse-osmosis-systems.html

28. Charles, L.; Caothien, S.; Hayes, J.; Caothuy, T.; Otoyo, T.; Ogawa, T. In membrane chemical cleaning: from art to science, American Water Works Association, 2001; 2001.

29. Nguyen, T.; Roddick, F. A.; Fan, L., Biofouling of water treatment membranes: a review of the underlying causes, monitoring techniques and control measures. *Membranes (Basel)* **2012,** *2*, (4), 804-840.

30. Rendueles, O.; Ghigo, J. M., Multi-species biofilms: how to avoid unfriendly neighbors. *FEMS Microbiol. Rev.* **2012,** *36*, (5), 972-989.

31. Herzberg, M.; Kang, S.; Elimelech, M., Role of extracellular polymeric substances (EPS) in biofouling of reverse osmosis membranes. *Environ. Sci. Technol.* **2009,** *43*, 4393–4398.

32. Karimi, A.; Karig, D.; Kumar, A.; Ardekani, A. M., Interplay of physical mechanisms and biofilm processes: review of microfluidic methods. *Lab Chip.* **2015,** *15*, (1), 23-42.

33. Mansouri, J.; Harrisson, S.; Chen, V., Strategies for controlling biofouling in membrane filtration systems: challenges and opportunities. *J. Mater. Chem.* **2010,** *20*, (22), 4567-4586.

34. Liu, M.; Chen, Q.; Wang, L.; Yu, S.; Gao, C., Improving fouling resistance and chlorine stability of aromatic polyamide thin-film composite RO membrane by surface grafting of polyvinyl alcohol (PVA). *Desalination* **2015,** *367*, 11-20.

35. Parkar, S. G.; Flint, S. H.; Brooks, J. D., Evaluation of the effect of cleaning regimes on biofilms of thermophilic bacilli on stainless steel. *J. Appl. Microbiol.* **2004,** *96*, (1), 110-116.

36. Cai, W.; Liu, Y., Enhanced membrane biofouling potential by on-line chemical cleaning in membrane bioreactor. *J. Membrane Sci.* **2016,** *511*, 84-91.

37. He, L.; Dumée, L. F.; Feng, C.; Velleman, L.; Reis, R.; She, F.; Gao, W.; Kong, L., Promoted water transport across graphene oxide–poly(amide) thin film composite membranes and their antibacterial activity. *Desalination* **2015,** *365*, 126-135.

38. Tiraferri, A.; Vecitis, C. D.; Elimelech, M., Covalent binding of single-walled carbon nanotubes to polyamide membranes for antimicrobial surface properties. *ACS Appl. Mater. Interfaces* **2011,** *3*, (8), 2869-2877.

39. Busch, M.; Mickols, W. E., Reducing energy consumption in seawater desalination. *Desalination* **2004,** *165*, 299-312.

40. Banerjee, I.; Pangule, R. C.; Kane, R. S., Antifouling coatings: recent developments in the design of surfaces that prevent fouling by proteins, bacteria, and marine organisms. *Adv. Mater.* **2011,** *23*, (6), 690-718.

41. Miller, D. J.; Araujo, P. A.; Correia, P. B.; Ramsey, M. M.; Kruithof, J. C.; van Loosdrecht, M. C.; Freeman, B. D.; Paul, D. R.; Whiteley, M.; Vrouwenvelder, J. S., Short-term adhesion and long-term biofouling testing of polydopamine and poly(ethylene glycol) surface modifications of membranes and feed spacers for biofouling control. *Water Res.* **2012,** *46*, (12), 3737-3753.

42. Dražević, E.; Košutić, K.; Dananić, V.; Pavlović, D. M., Coating layer effect on performance of thin film nanofiltration membrane in removal of organic solutes. *Sep. Purif. Technol.* **2013,** *118*, 530-539.

43. Chen, L.; Thérien-Aubin, H.; Wong, M. C. Y.; Hoek, E. M. V.; Ober, C. K., Improved antifouling properties of polymer membranes using a 'layer-by-layer' mediated method. *J. Mater. Chem. B* **2013,** *1*, (41), 5651-5658.

44. Ma, W.; Soroush, A.; Van Anh Luong, T.; Brennan, G.; Rahaman, M. S.; Asadishad, B.; Tufenkji, N., Spray- and spin-assisted layer-by-layer assembly of copper nanoparticles on thin-film composite reverse osmosis membrane for biofouling mitigation. *Water Res.* **2016,** *99*, 188-199.

45. Wong, S. Y.; Han, L.; Timachova, K.; Veselinovic, J.; Hyder, M. N.; Ortiz, C.; Klibanov, A. M.; Hammond, P. T., Drastically lowered protein adsorption on microbicidal hydrophobic/hydrophilic polyelectrolyte multilayers. *Biomacromolecules* **2012,** *13*, (3), 719-726.

46. SY, W.; Q, L.; J, V.; BS, K.; AM, K.; PT, H., Bactericidal and virucidal ultrathin films assembled layer by layer from polycationic N-alkylated polyethylenimines and polyanions. *Biomaterials* **2010** *31*, (14), 4079-4087.

47. Li, Q.; Bi, Q.-y.; Lin, H.-H.; Bian, L.-X.; Wang, X.-L., A novel ultrafiltration (UF) membrane with controllable selectivity for protein separation. *J. Membrane Sci.* **2013,** *427*, 155-167.

48. Jiang, S.; Cao, Z., Ultralow-fouling, functionalizable, and hydrolyzable zwitterionic materials and their derivatives for biological applications. *Adv. Mater.* **2010,** *22*, (9), 920-32.

49. Khung, Y. L.; Narducci, D., Surface modification strategies on mesoporous silica nanoparticles for anti-biofouling zwitterionic film grafting. *Adv. Colloid Interface Sci.* **2015,** *226*, (Pt B), 166-186.

50. Kojima, M.; Ishihara, K.; Watanabe, A.; Nakabayashi, N. I., Interaction between phospho-lipids and biocompatible polymers containing a phosphorylcholinemoiety. *Biomaterials.* **1991,** *12*, 121-124.

51. Li, L.; Marchant RE.; Dubnisheva, A., Roy, S., Fissell, WH., Anti-biofouling sulfobetaine polymer thin films on silicon and silicon nanopore membranes. *J. Biomater. Sci. Polym. Ed.* **2011,** *22*, 91-106.

52. Chen, L.; Thérien-Aubin, H.; Wong, M. C. Y.; Hoekcde, E. M. V.; Ober, C. K., Improved antifouling properties of polymer membranes using a 'layer-by-layer' mediated method. *J. Mater. Chem. B* **2013,** *1*, 5651-5658.

53. Zhu, L.-J.; Zhu, L.-P.; Jiang, J.-H.; Yi, Z.; Zhao, Y.-F.; Zhu, B.-K.; Xu, Y.-Y., Hydrophilic and anti-fouling polyethersulfone ultrafiltration membranes with poly(2-hydroxyethyl methacrylate) grafted silica nanoparticles as additive. *J. Membrane Sci.* **2014,** *451*, 157-168.

54. Dasari, A.; Quirós, J.; Herrero, B.; Boltes, K.; García-Calvo, E.; Rosal, R., Antifouling membranes prepared by electrospinning polylactic acid containing biocidal nanoparticles. *J. Membrane Sci.* **2012,** *405-406*, 134-140.

55. Liang, S.; Kang, Y.; Tiraferri, A.; Giannelis, E. P.; Huang, X.; Elimelech, M., Highly hydrophilic polyvinylidene fluoride (PVDF) ultrafiltration membranes via postfabrication grafting of surface-tailored silica nanoparticles. *ACS Appl. Mater. Interfaces* **2013,** *5*, (14), 6694-6703.

56. Zhao, H.; Qiu, S.; Wu, L.; Zhang, L.; Chen, H.; Gao, C., Improving the performance of polyamide reverse osmosis membrane by incorporation of modified multi-walled carbon nanotubes. *J. Membrane Sci.* **2014,** *450*, 249-256.

57. Han, R.; Zhang, S.; Liu, C.; Wang, Y.; Jian, X., Effect of NaA zeolite particle addition on poly(phthalazinone ether sulfone ketone) composite ultrafiltration (UF) membrane performance. *J. Membrane Sci.* **2009,** *345* (1-2), 5-12.

58. Lind, M. L.; Ghosh, A. K.; Jawor, A.; Huang, X.; Hou, W.; Yang, Y.; Hoek, E. M., Influence of zeolite crystal size on zeolite-polyamide thin film nanocomposite membranes. *Langmuir* **2009,** *25*, (17), 10139-10145.

59. Kumar, R.; Isloor, A. M.; Ismail, A. F.; Rashid, S. A.; Matsuura, T., Polysulfone–Chitosan blend ultrafiltration membranes: preparation, characterization, permeation and antifouling properties. *RSC Adv.* **2013,** *3*, (21), 7855-7861.

60. Coneski, P. N.; Weise, N. K.; Fulmer, P. A.; Wynne, J. H., Development and evaluation of self-polishing urethane coatings with tethered quaternary ammonium biocides. *Prog. Org. Coat.* **2013,** *76*, (10), 1376-1386.

61. Ma, W.; Rahaman, M. S.; Therien-Aubin, H., Controlling biofouling of reverse osmosis membranes through surface modification via grafting patterned polymer brushes. *J. Water Reuse Desal.* **2015,** *5*, (3), 326-334.

62. Valko, M.; Morris, H.; Cronin, M. T. D., Metals, toxicity and oxidative stress. *Curr. Med. Chem.* **2005,** *12*, 1161-1208.

63. Zhang, Y.; Rock, C. O., Membrane lipid homeostasis in bacteria. *Nat. Rev. Microbiol.* **2008,** *6*, 222-233.

64. Berlett, B. S.; Stadtman, E. R., Protein oxidation in aging, disease, and oxidative stress. *J. Biol. Chem.* **1997,** *272*, 20313-20316.

65. Chatterjee, A. K.; Chakraborty, R.; Basu, T., Mechanism of antibacterial activity of copper nanoparticles. *Nanotechnology* **2014,** *25*, (13), 135101.

66. Glisic, B. D.; Djuran, M. I., Gold complexes as antimicrobial agents: an overview of different biological activities in relation to the oxidation state of the gold ion and the ligand structure. *Dalton T.* **2014,** *43*, (16), 5950-5969.

67. Das, M. R.; Sarma, R. K.; Saikia, R.; Kale, V. S.; Shelke, M. V.; Sengupta, P., Synthesis of silver nanoparticles in an aqueous suspension of graphene oxide sheets and its antimicrobial activity. *Colloids Surf. B.* **2011,** *83*, (1), 16-22.

68. Subhankari, I.; P.L.Nayak, Antimicrobial activity of copper nanoparticles synthesised by ginger (zingiber officinale) extract. *World J. Nano Sci. Technol.* **2013,** *2*, (1), 10-13.

69. Raffi, M.; Mehrwan, S.; Bhatti, T. M.; Akhter, J. I.; Hameed, A.; Yawar, W.; ul Hasan, M. M., Investigations into the antibacterial behavior of copper nanoparticles against Escherichia coli. *Ann. Microbiol.* **2010,** *60*, (1), 75-80.

70. Yang, H. L.; Lin, J. C.; Huang, C., Application of nanosilver surface modification to RO membrane and spacer for mitigating biofouling in seawater desalination. *Water Res.* **2009,** *43*, (15), 3777-3786.

71. Liu, Y.; Rosenfield, E.; Hu, M.; Mi, B., Direct observation of bacterial deposition on and detachment from nanocomposite membranes embedded with silver nanoparticles. *Water Res.* **2013,** *47*, (9), 2949-2958.

72. Rahaman, M. S.; Thérien-Aubin, H.; Ben-Sasson, M.; Ober, C. K.; Nielsen, M.; Elimelech, M., Control of biofouling on reverse osmosis polyamide membranes modified with biocidal nanoparticles and antifouling polymer brushes. *J. Mater. Chem.* **2014,** *2*, (12), 1724-1732.

73. Yin, J.; Yang, Y.; Hu, Z.; Deng, B., Attachment of silver nanoparticles (AgNPs) onto thin-film composite (TFC) membranes through covalent bonding to reduce membrane biofouling. *J. Membrane Sci.* **2013,** *441*, 73-82.

74. Ben-Sasson, M.; Lu, X.; Bar-Zeev, E.; Zodrow, K. R.; Nejati, S.; Qi, G.; Giannelis, E. P.; Elimelech, M., In situ formation of silver nanoparticles on thin-film composite reverse osmosis membranes for biofouling mitigation. *Water Res.* **2014,** *62*, 260-270.

75. Perreault, F.; Faria, A. F. D.; Nejati, S.; Elimelech, M., Antimicrobial properties of graphene oxide nanosheets: why size matters. *ACS nano* **2015,** *9*, (7), 7226-7236.

76. Soroush, A.; Ma, W.; Cyr, M.; Rahaman, M. S.; Asadishad, B.; Tufenkji, N., In situ silver decoration on graphene oxide-treated thin film composite forward osmosis membranes: biocidal properties and regeneration potential. *Environ. Sci. Technol. Lett.* **2016,** *3*, (1), 13-18.

77. Yeroslavsky, G.; Girshevitz, O.; Foster-Frey, J.; Donovan, D. M.; Rahimipour, S., Antibacterial and antibiofilm surfaces through polydopamine-assisted immobilization of lysostaphin as an antibacterial enzyme. *Langmuir* **2015,** *31*, (3), 1064-1073.

78. Kenawy, E.-R.; Worley, S. D.; Broughton, R., The chemistry and applications of antimicrobial polymers: a state of the art review. *Biomacromolecules* **2007,** *8*, (5), 1359 -1384.

79. Jia, Z.; shen, D.; Xu, W., Synthesis and antibacterial activities of quaternary ammonium salt of chitosan. *Carbohydr. Res.* **2001,** *333*, 1-6.

80. Costa, F.; Carvalho, I. F.; Montelaro, R. C.; Gomes, P.; Martins, M. C., Covalent immobilization of antimicrobial peptides (AMPs) onto biomaterial surfaces. *Acta Biomater.* **2011,** *7*, (4), 1431-1440.

81. Ghuysen J.-M., Hakenbeck R., *Bacterial Cell Wall*. Elsevier Science: 1994.

82. Hegab, H. M.; ElMekawy, A.; Barclay, T. G.; Michelmore, A.; Zou, L.; Saint, C. P.; Ginic-Markovic, M., Fine-tuning the surface of forward osmosis membranes via grafting graphene oxide: performance patterns and biofouling propensity. *ACS Appl. Mater. Interfaces* **2015,** *7*, (32), 18004-18016.

83. Kim, T.-S.; Park, H.-D., Lauroyl arginate ethyl: An effective antibiofouling agent applicable for reverse osmosis processes producing potable water. *J. Membrane Sci.* **2016,** *507*, 24-33.

84. Pattanayaiying, R.; H-Kittikun, A.; Cutter, CN., Effect of lauric arginate, nisin Z, and a combination against several food-related bacteria. *Int. J. Food Microbiol.* **2014,** *188*, 135-146.

85. Ye, H.; Wang, L.; Huang, R.; Su, R.; Liu, B.; Qi, W.; He, Z., Superior antifouling performance of a zwitterionic peptide compared to an amphiphilic, non-ionic peptide. *ACS Appl. Mater. Interfaces* **2015,** *7*, (40), 22448-22457.

86. Lim, K.; Chua, R. R.; Bow, H.; Tambyah, P. A.; Hadinoto, K.; Leong, S. S., Development of a catheter functionalized by a polydopamine peptide coating with antimicrobial and antibiofilm properties. *Acta Biomater.* **2015,** *15*, 127-138.

87. Kim, J. H.; Choi, D. C.; Yeon, K. M.; Kim, S. R.; Lee, C. H., Enzyme-immobilized nanofiltration membrane to mitigate biofouling based on quorum quenching. *Environ. Sci. Technol.* **2011,** *45*, (4), 1601-1607.

88. Meshram, P.; Dave, R.; Joshi, H.; Dharani, G.; Kirubagaran, R.; Venugopalan, V. P., Biofouling control on ultrafiltration membrane through immobilization of polysaccharide-degrading enzyme: optimization of parameters. *Desal. Water Treat.* **2016,** *57*, (55), 26861-26870.

89. He, S.; Zhou, P.; Wang, L.; Xiong, X.; Zhang, Y.; Deng, Y.; Wei, S., Antibiotic-decorated titanium with enhanced antibacterial activity through adhesive polydopamine for dental/bone implant. *J. R. Soc. Interface* **2014,** *11*, (95), 20140169.

90. Kappachery, S.; Paul, D.; Yoon, J.; Kweon, J. H., Vanillin, a potential agent to prevent biofouling of reverse osmosis membrane. *Biofouling* **2010,** *26*, (6), 667-672.

91. Piatkovsky, M.; Acar, H.; Marciel, A. B.; Tirrell, M.; Herzberg, M., A zwitterionic block-copolymer, based on glutamic acid and lysine, reduces the biofouling of UF and RO membranes. *J. Membrane Sci.* **2018,** *549*, 507-514.

92. Xing, S. F.; Sun, X. F.; Taylor, A. A.; Walker, S. L.; Wang, Y. F.; Wang, S. G., D-amino acids inhibit initial bacterial adhesion: thermodynamic evidence. *Biotechnol. Bioeng.* **2015,** *112*, (4), 696-704.

93. Kolodkin-Gal, I.; Romero, D.; Cao, S.; Clardy, J.; Kolter, R.; Losick, R., D-amino acids trigger biofilm disassembly. *Science* **2010,** *328*, 627-629.

94. Xu, H.; Liu, Y., Reduced microbial attachment by D-amino acid-inhibited AI-2 and EPS production. *Water Res.* **2011,** *45*, (17), 5796-5804.

95. Goh, S.-N.; Fernandez, A.; Ang, S.-Z.; Lau, W.-Y.; Ng, D.-L.; Cheah, E. S. G., Effects of different amino acids on biofilm growth, swimming motility and twitching motility in *Escherichia Coli BL21*. *J. Biol. Life Sci.* **2013,** *4*, (2), 103-115.

96. Oh, H.-S.; Constancias, F.; Ramasamy, C.; Tang, P. Y. P.; Yee, M. O.; Fane, A. G.; McDougald, D.; Rice, S. A., Biofouling control in reverse osmosis by nitric oxide treatment and its impact on the bacterial community. *J. Membrane Sci.* **2018,** *550*, 313-321.

97. Arora, D. P.; Hossain, S.; Xu, Y.; Boon, E. M., Nitric oxide regulation of bacterial biofilms. *Biochemistry* **2015,** *54*, (24), 3717-3728.

98. Barnes, R. J.; Low, J. H.; Bandi, R. R.; Tay, M.; Chua, F.; Aung, T.; Fane, A. G.; Kjelleberg, S.; Rice, S. A., Nitric oxide treatment for the control of reverse osmosis membrane biofouling. *Appl. Environ. Microbiol.* **2015,** *81*, (7), 2515-2524.

99. Zou, P.; Hartleb, W.; Lienkamp, K., It takes walls and knights to defend a castle – synthesis of surface coatings from antimicrobial and antibiofouling polymers. *J. Mater. Chem.* **2012,** *22*, (37), 19579-19589.

100. Ye, G.; Lee, J.; Perreault, F.; Elimelech, M., Controlled architecture of dual-functional block copolymer brushes on thin-film composite membranes for integrated "defending" and "attacking" strategies against biofouling. *ACS Appl. Mater. Interfaces* **2015,** *7*, (41), 23069-23079.

101. Liu, C. Y.; Huang, C. J., Functionalization of polydopamine via the aza-michael reaction for antimicrobial interfaces. *Langmuir* **2016,** *32*, (19), 5019-5028.

102. Sileika, T. S.; Kim, H. D.; Maniak, P.; Messersmith, P. B., Antibacterial performance of polydopamine-modified polymer surfaces containing passive and active components. *ACS Appl. Mater. Interfaces* **2011,** *3*, (12), 4602-4610.

103. Karkhanechi, H.; Razi, F.; Sawada, I.; Takagi, R.; Ohmukai, Y.; Matsuyama, H., Improvement of antibiofouling performance of a reverse osmosis membrane through biocide release and adhesion resistance. *Sep. Purif. Technol.* **2013,** *105*, 106-113.

104. Liu, C.; Lee, J.; Ma, J.; Elimelech, M., Antifouling thin-film composite membranes by controlled architecture of zwitterionic polymer brush layer. *Environ. Sci. Technol.* **2017,** *51*, (4), 2161-2169.

105. Soroush, A.; Ma, W.; Silvino, Y.; Rahaman, M. S., Surface modification of thin film composite forward osmosis membrane by silver-decorated graphene-oxide nanosheets. *Environ. Sci.: Nano* **2015,** *2*, (4), 395-405.

106. Zhang, R.; Su, Y.; Zhou, L.; Zhou, T.; Zhao, X.; Li, Y.; Liuab, Y.; Jiang, Z., Manipulating the multifunctionalities of polydopamine to prepare high-flux anti-biofouling composite nanofiltration membranes. *RSC Adv.* **2016,** *6*, 32863–32873.

107. Yang, E.; Chae, K.-J.; Alayande, A. B.; Kim, K.-Y.; Kim, I. S., Concurrent performance improvement and biofouling mitigation in osmotic microbial fuel cells using a silver nanoparticle-polydopamine coated forward osmosis membrane. *J. Membrane Sci.* **2016,** *513*, 217-225.

108. Yu, B. Y.; Zheng, J.; Chang, Y.; Sin, M. C.; Chang, C. H.; Higuchi, A.; Sun, Y. M., Surface zwitterionization of titanium for a general bio-inert control of plasma proteins, blood cells, tissue cells, and bacteria. *Langmuir* **2014,** *30*, (25), 7502-7512.

109. Jiang, J.; Zhu, L.; Zhu, L.; Zhang, H.; Zhu, B.; Xu, Y., Antifouling and antimicrobial polymer membranes based on bioinspired polydopamine and strong hydrogen-bonded poly(N‑vinyl pyrrolidone). *ACS Appl. Mater. Interfaces* **2013,** *5*, 12895−12904.

110. Tang, L.; Livi, K. J. T.; Chen, K. L., Polysulfone membranes modified with bioinspired polydopamine and silver nanoparticles formed in situ to mitigate biofouling. *Environ. Sci. Technol. Letters* **2015,** *2*, (3), 59-65.

111. Rahaman, M. S.; Therien-Aubinb, H.; Ben-Sasson, M.; Oberd, C. K.; Nielsena, M.; Elimelechc, M., Control of biofouling on reverse osmosis polyamide membranes modified with biocidal nanoparticles and antifouling polymer brushes. *J. Mater. Chem. B* **2014,** *2*, 1724-1732.

112. van Andel, E.; de Bus, I.; Tijhaar, E. J.; Smulders, M. M. J.; Savelkoul, H. F. J.; Zuilhof, H., Highly specific binding on antifouling zwitterionic polymer-coated microbeads as measured by flow cytometry. *ACS Appl. Mater. Interfaces* **2017,** *9*, (44), 38211-38221.

113. Sin, M. C.; Sun, Y. M.; Chang, Y., Zwitterionic-based stainless steel with well-defined polysulfobetaine brushes for general bioadhesive control. *ACS Appl. Mater. Interfaces* **2014,** *6*, (2), 861-873.

114. Li, M.-Z.; Li, J.-H.; Shao, X.-S.; Miao, J.; Wang, J.-B.; Zhang, Q.-Q.; Xu, X.-P., Grafting zwitterionic brush on the surface of PVDF membrane using physisorbed free radical grafting technique. *J. Membrane Sci.* **2012,** *405-406*, 141-148.

115. Kang, S.; Asatekin, A.; Mayes, A.; Elimelech, M., Protein antifouling mechanisms of PAN UF membranes incorporating PAN-g-PEO additive. *J. Membrane Sci.* **2007,** *296*, (1-2), 42-50.

116. Sun, Q.; Su, Y.; Ma, X.; Wang, Y.; Jiang, Z., Improved antifouling property of zwitterionic ultrafiltration membrane composed of acrylonitrile and sulfobetaine copolymer. *J. Membrane Sci.* **2006,** *285*, (1-2), 299-305.

117. Yang, Z.; Saeki, D.; Matsuyama, H., Zwitterionic polymer modification of polyamide reverse-osmosis membranes via surface amination and atom transfer radical polymerization for anti-biofouling. *J. Membrane Sci.* **2018,** *550*, 332-339.

118. Liu, G.; Wei, W.; Wu, H.; Dong, X.; Jiang, M.; Jin, W., Pervaporation performance of PDMS/ceramic composite membrane in acetone butanol ethanol (ABE) fermentation–PV coupled process. *J. Membrane Sci.* **2011,** *373*, (1-2), 121-129.

119. Bruening, M. L.; Adusumilli, M., Polyelectrolyte-multilayer-films-and-membrane-functionalization. *Aldrich Mater. Sci.* **2013,** *6*, (3), 5.

120. Kobayashi, M.; Terayama, Y.; Yamaguchi, H.; Terada, M.; Murakami, D.; Ishihara, K.; Takahara, A., Wettability and antifouling behavior on the surfaces of superhydrophilic polymer brushes. *Langmuir* **2012,** *28*, (18), 7212-7222.

121. Zhou, S.; Xue, A.; Zhao, Y.; Li, M.; Wang, H.; Xing, W., Grafting polyacrylic acid brushes onto zirconia membranes: Fouling reduction and easy-cleaning properties. *Sep. Purif. Technol.* **2013,** *114*, 53-63.

122. Shannon, M. A.; Bohn, P. W.; Elimelech, M.; Georgiadis, J. G.; Marinas, B. J.; Mayes, A. M., Science and technology for water purification in the coming decades. *Nature* **2008,** *452*, (7185), 301-10.

123. Kang, G.; Liu, M.; Lin, B.; Cao, Y.; Yuan, Q., A novel method of surface modification on thin-film composite reverse osmosis membrane by grafting poly(ethylene glycol). *Polymer* **2007,** *48*, (5), 1165-1170.

124. Lin, N. H.; Kim, M.-m.; Lewis, G. T.; Cohen, Y., Polymer surface nano-structuring of reverse osmosis membranes for fouling resistance and improved flux performance. *J. Mater. Chem.* **2010,** *20*, (22), 4642-4652.

125. Chen, S.; Li, L.; Zhao, C.; Zheng, J., Surface hydration: Principles and applications toward low-fouling/nonfouling biomaterials. *Polymer* **2010,** *51*, (23), 5283-5293.

126. Subhankari, I.; P.L.Nayak, Antimicrobial activity of copper nanoparticles synthesised by ginger (Zingiber officinale) extract. *World J. Nano Sci. Technol.* **2013,** *2*, (1), 10-13.

127. Soroush, A.; Ma, W.; Silvino, Y.; Rahaman, M. S., Surface modification of thin film composite forward osmosis membrane by silver-decorated graphene-oxide nanosheets. *Environ. Sci.: Nano* **2015,** *2*, 395 - 405.

128. Ouyang, Y.; Cai, X.; Shi, Q.; Liu, L.; Wan, D.; Tan, S.; Ouyang, Y., Poly-L-lysine-modified reduced graphene oxide stabilizes the copper nanoparticles with higher water-solubility and long-term additively antibacterial activity. *Colloids Surf. B* **2013,** *107*, 107-114.

129. Dwidjosiswojo, Z.; Richard, J.; Moritz, M.; Dopp, E.; Flemming, H.-C.; Wingender, J., Influence of copper ions on the viability and cytotoxicity of Pseudomonas aeruginosa under conditions relevant to drinking water environments. *Int. J. Hyg. Environ. Health* **2011,** *214*, (6), 485-492.

130. Hong, R.; Kang, T. Y.; Michels, C. A.; Gadura, N., Membrane lipid peroxidation in copper alloy-mediated contact killing of Escherichia coli. *Appl. Environ. Microbiol.* **2012,** *78*, (6), 1776-1784.

131. Deryabin, D. G.; Aleshina, E. S.; Vasilchenko, A. S.; Deryabina, T. D.; Efremova, L. V.; Karimov, I. F.; Korolevskaya, L. B., Investigation of copper nanoparticles antibacterial mechanisms tested by luminescent Escherichia coli strains. *Nanotechnol. Russ.* **2013,** *8*, (5-6), 402-408.

132. Gilbertson, L. M.; Albalghiti, E. M.; Fishman, Z. S.; Perreault, F.; Corredor, C.; Posner, J. D.; Elimelech, M.; Pfefferle, L. D.; Zimmerman, J. B., Shape-dependent surface reactivity and antimicrobial activity of nano-cupric oxide. *Environ. Sci. Technol.* **2016,** *50*, (7), 3975-3984.

133. Chatterjee, A. K.; Sarkar, R. K.; Chattopadhyay, A. P.; Aich, P.; Chakraborty, R.; Basu, T., A simple robust method for synthesis of metallic copper nanoparticles of high antibacterial potency against E. coli. *Nanotechnology* **2012,** *23*, (8), 085103.

134. Dankovich, T. A.; Smith, J. A., Incorporation of copper nanoparticles into paper for point-of-use water purification. *Water Res.* **2014,** *63*, 245-251.

135. Morton, S. W.; Herlihy, K. P.; Shopsowitz, K. E.; Deng, Z. J.; Chu, K. S.; Bowerman, C. J.; Desimone, J. M.; Hammond, P. T., Scalable manufacture of built-to-order nanomedicine: spray-assisted layer-by-layer functionalization of PRINT nanoparticles. *Adv. Mater.* **2013,** *25*, (34), 4707-4713.

136. Dumée, L. F.; He, L.; King, P. C.; Moing, M. L.; Güller, I.; Duke, M.; Hodgson, P. D.; Gray, S.; Poole, A. J.; Kong, L., Towards integrated anti-microbial capabilities: Novel bio-fouling resistant membranes by high velocity embedment of silver particles. *J. Membr. Sci.* **2015,** *475*, 552-561.

137. Mauter, M. S.; Wang, Y.; Okemgbo, K. C.; Osuji, C. O.; Giannelis, E. P.; Elimelech, M., Antifouling ultrafiltration membranes via post-fabrication grafting of biocidal nanomaterials. *ACS Appl. Mater. Interfaces* **2011,** *3*, (8), 2861-2868.

138. Rajesh, S.; Yan, Y.; Chang, H.-C.; Gao, H.; Phillip, W. A., Mixed mosaic membranes prepared by layer-by-layer assembly for ionic separations. *ACS Nano* **2014,** *8*, (12), 12338-12345.

139. Chen, L.; Thérien-Aubin, H.; Wong, M. C. Y.; Hoek, E. M. V.; Ober, C. K., Improved antifouling properties of polymer membranes using a 'layer-by-layer' mediated method. *J. Mater. Chem. B* **2013,** *1*, (41), 5651-5658.

140. Gittleson, F. S.; Hwang, D.; Won-Hee Ryu; Hashmi, S. M.; Hwang, J.; Goh, T.; Taylor, A. D., Ultrathin nanotube/nanowire electrodes by spin spin–spray layer-by-layer assembly: a concept for transparent energy storage 2015. *ACS Nano* **2015,** *9*, (10), 10005-10017.

141. Gittleson, F. S.; Kohn, D. J.; Li, X.; Taylor, A. D., Improving the assembly speed,quality, and tunability of thin conductive multilayers. *ACS Nano* **2012,** *6*, (5), 3703-3711.

142. Merrill, M. H.; Sun, C. T., Fast, simple and efficient assembly of nanolayered materials and devices. *Nanotechnology* **2009,** *20*, 1-7.

143. Decher, G., Fuzzy nanoassemblies: toward layered polymeric multicomposites. *Science* **1997,** *277*, 1232-1237.

144. Hu, M.; Mi, B., Enabling graphene oxide nanosheets as water separation membranes. *Environ. Sci. Technol.* **2013,** *47*, (8), 3715-3723.

145. Choi, W.; Choi, J.; Bang, J.; Lee, J. H., Layer-by-layer assembly of graphene oxide nanosheets on polyamide membranes for durable reverse-osmosis applications. *ACS Appl. Mater. Interfaces* **2013,** *5*, (23), 12510-12509.

146. Elimelech, M.; Zhu, X.; Childress, A. E.; Hong, S., Role of membrane surface morphology in colloidal fouling of cellulose acetate and composite aromatic polyamide reverse osmosis membranes. *J. Membrane Sci.* **1997,** *127*, 101-109.

147. Perreault, F.; Tousley, M. E.; Elimelech, M., Thin-film composite polyamide membranes functionalized with biocidal graphene oxide nanosheets. *Environ. Sci. Technol. Lett.* **2014,** *1*, (1), 71-76.

148. Chatterjee, A. K.; Chakraborty, R.; Basu, T., Mechanism of antibacterial activity of copper nanoparticles. *Nanotechnology* **2014,** *25*, (13), 1-12.

149. Raffi, M.; Mehrwan, S.; Bhatti, T. M.; Akhter, J. I.; Hameed, A.; Yawar, W.; ul Hasan, M. M., Investigations into the antibacterial behavior of copper nanoparticles against Escherichia coli. *Ann. Microbiol.* **2010,** *60*, (1), 75-80.

150. Dawson, L. F.; Valiente, E.; Faulds-Pain, A.; Donahue, E. H.; Wren, B. W., Characterisation of clostridium difficile biofilm formation, a role for Spo0A. *PLoS One* **2012,** *7*, (12), e50527.

151. Shailesh Kumar, M. C., Role of cse1034 in escherichia coli biofilm destruction. *J. Micro. Biochem. Technol.* **2013,** *05*, (03).

152. Hyder, M. N.; Hammond, P. T.; Lee, S. W.; Cebeci, F. C.; Schmidt, D. J.; Shao-Horn, Y.; Hammond, P. T., Layer-by-layer assembled polyaniline nanofiber/multiwall carbon nanotube thin film electrodes for high-power and high-energy storage applications. *ACS Nano* **2011,** *5*, (11), 8552-8561.

153. Nogueira, G. M.; Banerjee, D.; Cohen, R. E.; Rubner, M. F., Spray-layer-by-layer assembly can more rapidly produce optical-quality multistack heterostructures. *Langmuir* **2011,** *27*, (12), 7860-7867.

154. Ben-Sasson, M.; Zodrow, K. R.; Genggeng, Q.; Kang, Y.; Giannelis, E. P.; Elimelech, M., Surface functionalization of thin-film composite membranes with copper nanoparticles for antimicrobial surface properties. *Environ. Sci. Technol.* **2014,** *48*, (1), 384-393.

155. Ben-Sasson, M.; Lu, X.; Bar-Zeev, E.; Zodrow, K. R.; Nejati, S.; Qi, G.; Giannelis, E. P.; Elimelech, M., In situ formation of silver nanoparticles on thin-film composite reverse osmosis membranes for biofouling mitigation. *Water Res.* **2014,** *62*, 260-270.

156. Wuithschick, M.; Witte, S.; Kettemann, F.; Rademann, K.; Polte, J., Illustrating the formation of metal nanoparticles with a growth concept based on colloidal stability. *Phys. Chem. Chem. Phys.* **2015,** *17*, (30), 19895-19900.

157. Yin, J.; Yang, Y.; Hu, Z.; Deng, B., Attachment of silver nanoparticles (AgNPs) onto thin-film composite (TFC) membranes through covalent bonding to reduce membrane biofouling. *J. Membr. Sci.* **2013,** *441*, 73-82.

158. Song, P.; Guo, X.-Y.; Pan, Y.-C.; Shen, S.; Sun, Y.; Wen, Y.; Yang, H.-F., Insight in cysteamine adsorption behaviors on the copper surface by electrochemistry and Raman spectroscopy. *Electrochim. Acta* **2013,** *89*, 503-509.

159. Perreault, F.; Tousley, M. E.; Elimelech, M., Thin-film composite polyamide membranes functionalized with biocidal graphene oxide nanosheets. *Environ. Sci. Technol. Lett.* **2014,** *1*, 71-76.

160. Mangadlao, J. D.; Santos, C. M.; Felipe, M. J.; de Leon, A. C.; Rodrigues, D. F.; Advincula, R. C., On the antibacterial mechanism of graphene oxide (GO) Langmuir-Blodgett films. *Chem. Commun.* **2015,** *51*, (14), 2886-2889.

161. Zhang, N.; Qiu, H.; Liu, Y.; Wang, W.; Li, Y.; Wang, X.; Gao, J., Fabrication of gold nanoparticle/graphene oxide nanocomposites and their excellent catalytic performance. *J. Mater. Chem.* **2011,** *21*, (30), 11080-11083.

162. Bei, F.; Hou, X.; Chang, S. L.; Simon, G. P.; Li, D., Interfacing colloidal graphene oxide sheets with gold nanoparticles. *Chemistry* **2011,** *17*, (21), 5958-5964.

163. Perreault, F.; Jaramillo, H.; Xie, M.; Ude, M.; Nghiem, L. D.; Elimelech, M., Biofouling mitigation in forward osmosis using graphene oxide functionalized thin-film composite membranes. *Environ. Sci. Technol.* **2016,** *50*, (11), 5840-5848.

164. Li, J.; Liu, X.; Lu, J.; Wang, Y.; Li, G.; Zhao, F., Anti-bacterial properties of ultrafiltration membrane modified by graphene oxide with nano-silver particles. *J. Colloid Interface Sci.* **2016,** *484*, 107-115.

165. Hegab, H. M.; ElMekawy, A.; Barclay, T. G.; Michelmore, A.; Zou, L.; Saint, C. P.; Ginic-Markovic, M., Single-step assembly of multifunctional poly(tannic acid)-graphene oxide coating to reduce biofouling of forward osmosis membranes. *ACS Appl. Mater. Interfaces* **2016,** *8*, (27), 17519-17528.

166. Tiraferri, A.; Elimelech, M., Direct quantification of negatively charged functional groups on membrane surfaces. *J. Membr. Sci.* **2012,** *389*, 499-508.

167. Tiraferri, A.; Kang, Y.; Giannelis, E. P.; Elimelech, M., Superhydrophilic thin-film composite forward osmosis membranes for organic fouling control: fouling behavior and antifouling mechanisms. *Environ. Sci. Technol.* **2012,** *46*, (20), 11135-11344.

168. Ben-Sasson, M.; Lu, X.; Nejati, S.; Jaramillo, H.; Elimelech, M., In situ surface functionalization of reverse osmosis membranes with biocidal copper nanoparticles. *Desalination* **2016,** *388*, 1-8.

169. Bao, Q.; Zhang, D.; Qi, P., Synthesis and characterization of silver nanoparticle and graphene oxide nanosheet composites as a bactericidal agent for water disinfection. *J. Colloid. Interface Sci.* **2011,** *360*, (2), 463-470.

170. Novak, S.; Maver, U.; Peternel, Š.; Venturini, P.; Bele, M.; Gaberšček, M., Electrophoretic deposition as a tool for separation of protein inclusion bodies from host bacteria in suspension. *Colloids Surf. A.* **2009,** *340*, (1-3), 155-160.

171. Schwegmann, H.; Feitz, A. J.; Frimmel, F. H., Influence of the zeta potential on the sorption and toxicity of iron oxide nanoparticles on S. cerevisiae and E. coli. *J. Colloid Interface Sci.* **2010,** *347*, (1), 43-48.

172. Perreault, F.; Fonseca de Faria, A.; Elimelech, M., Environmental applications of graphene-based nanomaterials. *Chem. Soc. Rev.* **2015,** *44*, (16), 5861-5896.

173. Castrillón, S. R.-V.; Perreault, F.; Faria, A. F. d.; Elimelech, M., Interaction of graphene oxide with bacterial cell membranes: insights from force spectroscopy. *Environ. Sci. Technol. Lett.* **2015,** *2*, (4), 112–117.

174. Xu, W.; Zhang, L.; Li, J.; Lu, Y.; Li, H.; Ma, Y.; Wang, W.; Yu, S., Facile synthesis of silver@graphene oxide nanocomposites and their enhanced antibacterial properties. *J. Mater. Chem.* **2011,** *21*, (12), 4593-4597.

175. Liu, S.; Zeng, T. H.; Hofmann, M.; Burcombe, E.; JunWei; Jiang, R.; Kong, J.; Chen, Y., Antibacterial activity of graphite, graphite oxide, graphene oxide, and reduced graphene oxide: membrane and oxidative stress. *ACS Nano* **2011,** *5*, (9), 6971-6980.

176. Titov, A. V.; l, P. K.; Pearson, R., Sandwiched graphene - membrane superstructures. *ACS Nano* **2010,** *4*, (1), 229 - 234.

177. Ahamed, M.; Alhadlaq, H. A.; Khan, M. A. M.; Karuppiah, P.; Al-Dhabi, N. A., Synthesis, characterization, and antimicrobial activity of copper oxide nanoparticles. *J. Nanomater.* **2014,** *2014*, 1-4.

178. Kent, R. D.; Vikesland, P. J., Dissolution and persistence of copper-based nanomaterials in undersaturated solutions with respect to cupric solid phases. *Environ. Sci. Technol.* **2016,** *50*, (13), 6772-6781.

179. Gilbertson, L. M.; Albalghiti, E. M.; Fishman, Z. S.; Perreault, F.; Corredor, C.; Posner, J. D.; Elimelech, M.; Pfefferle, L. D.; Zimmerman, J. B., Shape-dependent surface reactivity and antimicrobial activity of nano-cupric oxide. *Environ. Sci. Technol.* **2016,** *50*, 3975-3984.

180. Ye, G.; Lee, J.; Perreault, F.; Elimelech, M., Controlled architecture of dual-functional block copolymer brushes on thin-film composite membranes for integrated "defending" and "attacking" strategies against biofouling. *ACS Appl. Mater. Interfaces* **2015,** *7*, (41), 23069-23079.

181. Perreault, F.; Jaramillo, H.; Xie, M.; Ude, M.; Nghiem, L. D.; Elimelech, M., Biofouling mitigation in forward osmosis using graphene oxide functionalized thin-film composite membranes. *Environ. Sci. Techno.l* **2016,** *50*, (11), 5840-5848.

182. Ma, W.; Panecka, M.; Tufenkji, N.; Rahaman, M. S., Bacteriophage-based strategies for biofouling control in ultrafiltration: In situ biofouling mitigation, biocidal additives and biofilm cleanser. *J. Colloid Interface Sci.* **2018,** *523*, 254-265.

183. Yu, C.; Wu, J.; Zin, G.; Di Luccio, M.; Wen, D.; Li, Q., D-Tyrosine loaded nanocomposite membranes for environmental-friendly, long-term biofouling control. *Water Res.* **2018,** *130*, 105-114.

184. Azari, S.; Zou, L., Fouling resistant zwitterionic surface modification of reverse osmosis membranes using amino acid l-cysteine. *Desalination* **2013,** *324*, 79-86.

185. Villegas, M. F.; Garcia-Uriostegui, L.; Rodriguez, O.; Izquierdo-Barba, I.; Salinas, A. J.; Toriz, G.; Vallet-Regi, M.; Delgado, E., Lysine-grafted mcm-41 silica as an antibacterial biomaterial. *Bioengineering (Basel)* **2017,** *4*, (80), 1-13.

186. Wang, S. Y.; Sun, X. F.; Gao, W. J.; Wang, Y. F.; Jiang, B. B.; Afzal, M. Z.; Song, C.; Wang, S. G., Mitigation of membrane biofouling by d-amino acids: Effect of bacterial cell-wall property and d-amino acid type. *Colloids Surf. B.* **2018,** *164*, 20-26.

187. Lee, S. H.; Dreyer, D. R.; An, J.; Velamakanni, A.; Piner, R. D.; Park, S.; Zhu, Y.; Kim, S. O.; Bielawski, C. W.; Ruoff, R. S., Polymer brushes via controlled, surface-initiated atom transfer radical polymerization (ATRP) from graphene oxide. *Macromol. Rapid Commun.* **2010,** *31*, (3), 281-288.

188. Ma, W.; Soroush, A.; Luong, T. V. A.; Rahaman, M. S., Cysteamine- and graphene oxide-mediated copper nanoparticle decoration on reverse osmosis membrane for enhanced anti-microbial performance. *J. Colloid Interface Sci.* **2017,** *501*, 330-340.

Appendices

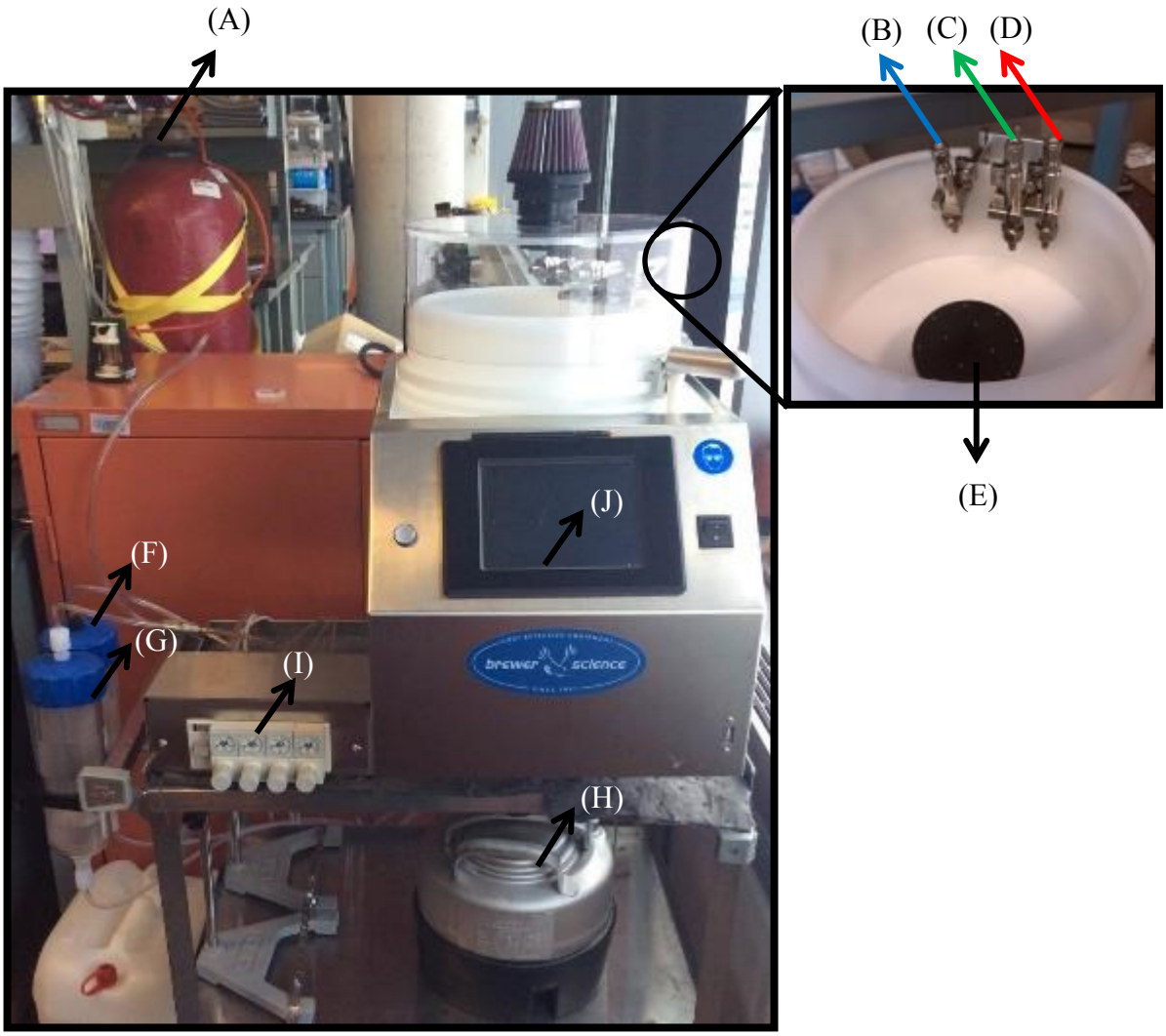

Figure A- 1. Cee® Model 200XD spray/puddle developer (Brewer Science Inc. USA). (A) Nitrogen tank; (B) spray nozzle for polycation solution; (C) spray nozzle for DI water; (D) spray nozzle for polyanion solution; (E) spinning substrate; (F) polycation container; (G) polyanion container; (H) DI water container; (I) pressure controller; (J) computer screen.

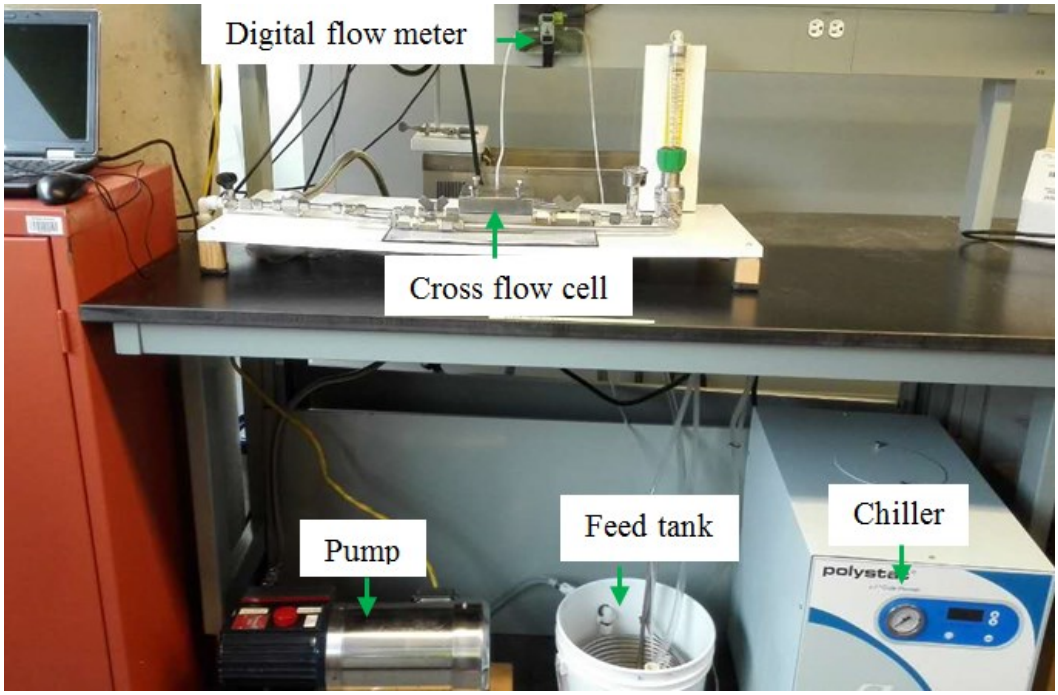

Figure A- 2. Image of the laboratory-scale RO cross flow filtration setup. The setup consisted of a diaphragm pump (1.8 GPM, 230V, 60Hz, 3 PH motor, Sterlitech Corporation, WA, USA), a stainless steel water permeation cell, a panel-mount flow meter (0.25~1.5 gpm, purchased from McMaster-CARR, Canada), a digital flow meter (Liquid Flow Meter SLI-2000, Sensirion Inc.CA,USA), and a 10 L feed solution tank. The whole system was connection by stainless tubes and PVC tubes.

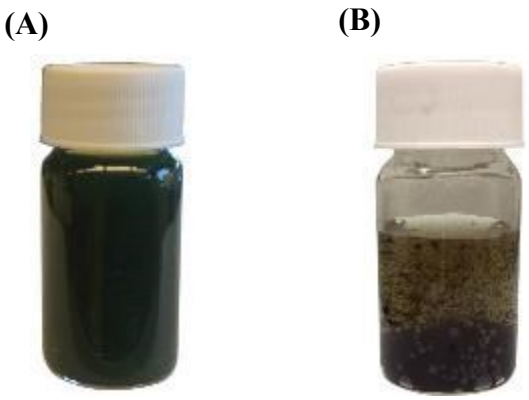

Figure A- 3. Prepared copper nanoparticles with **(A)** and without **(B)** PEI as a capping agent. It was observed that the former could be stable for at least a week, whereas the latter easily aggregates and settles within 15 min.

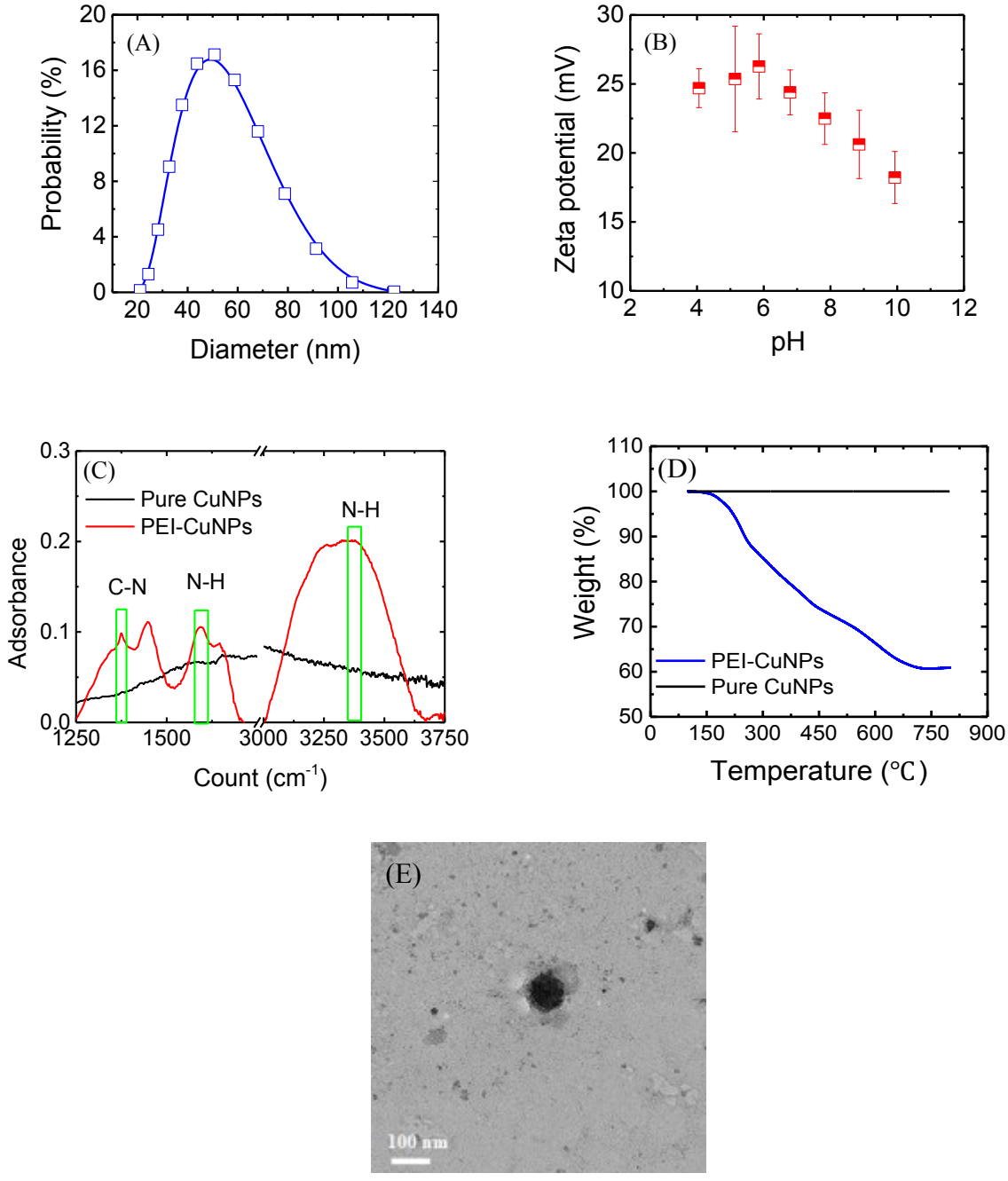

Figure A- 4 Characterization of PEI-CuNPs: **(A)** particle size distribution; **(B)** zeta potential of particles at different pH conditions; **(C)** ATR-FTIR spectra of pure CuNPs and PEI-CuNPs; **(D)** TGA analysis of PEI-CuNPs. **(E)** TEM images of the PEI-CuNPs.

The size of the copper nanoparticles was measured using a ZetaSizer Nano S90 (Malvern, UK) particle size analyzer. Fourier transform infrared spectroscopy (FT-IR) was performed with a Nicolet 6700 / Smart iTR (Thermo Scientific, Waltham, MA, USA) equipped with an attenuated total reflectance single logic (ATR) accessory. The percentage of Cu-NPs and capping agent (PEI) was evaluated using thermogravimetry coupled with mass spectrometry (TGA-MS) (TA Instruments, Q500/ Discovery MS, New Castle, DE, USA). Measurement was carried out by heating 3 mg Cu-NPs for 15 min at 100 ℃ in a N_2 gas stream (25 mL min^{-1}) and then increasing the temperature to 900 ℃ at a rate of 10 ℃ min^{-1}. The surface charge of the CuNPs was determined by a zeta potential analyzer (ZetaPlus/Bl-PALS, BrookHaven Instrument Corp., Holtsville, NY, USA) at different pH conditions obtained using 100 mM HCl and 10 mM NaOH. The transmission electron microscope (TEM) images (Tecnai G2 F20, USA) were obtained using a carbon coated copper micro-grid as substrate.

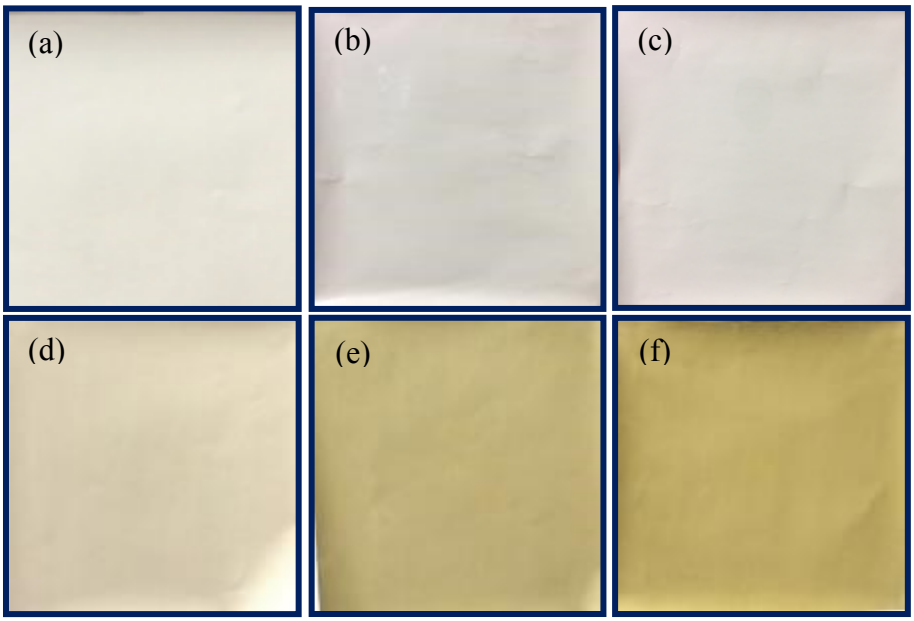

Figure A- 5 Images of (a) pristine membrane; (b) $(PEI/PAA)_{10}$-; (c) $(PEI\text{-}CuNP/PAA)_{2}$-; (d) $(PEI\text{-}CuNP/PAA)_{6}$-; (e) $(PEI\text{-}CuNP/PAA)_{10}$ - and (f) $(PEI\text{-}CuNP/PAA)_{14}$- modified membrane.

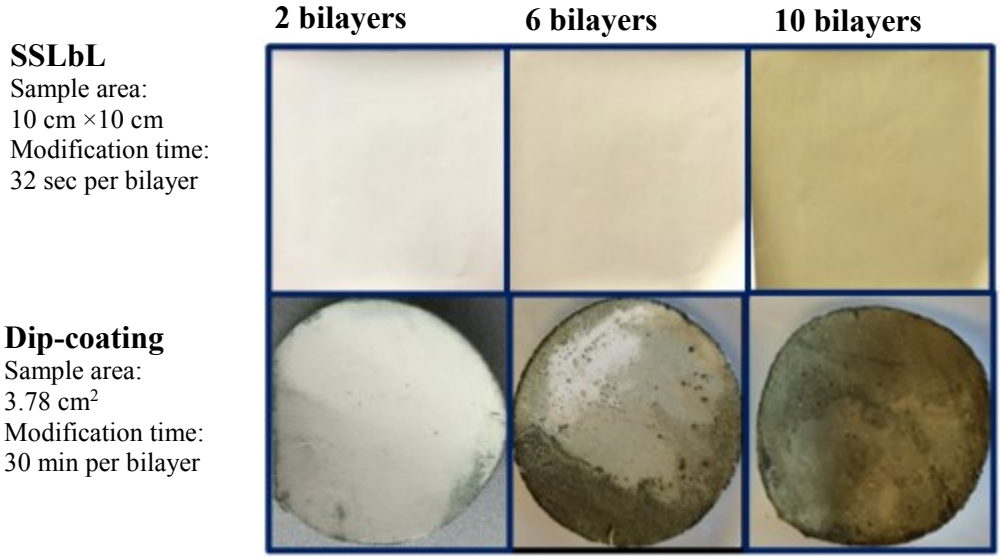

Figure A- 6 The images of different number of (PEI-CuNPs/PAA) bilayers modified membranes via SSLbL and dip-coating methods.

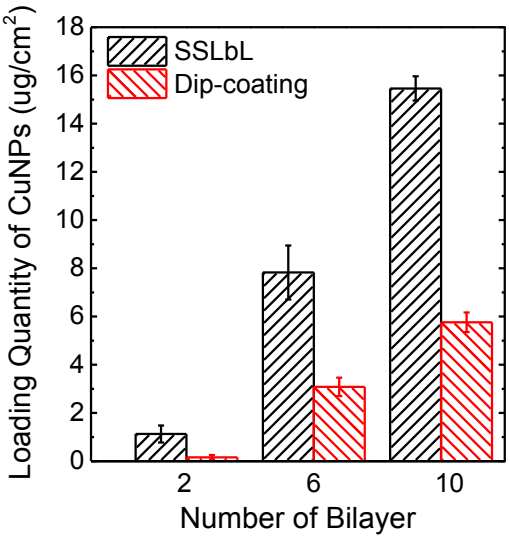

Figure A- 7 The quantity of CuNPs bonded onto the membrane surface via SSLbL and dip-coating method.

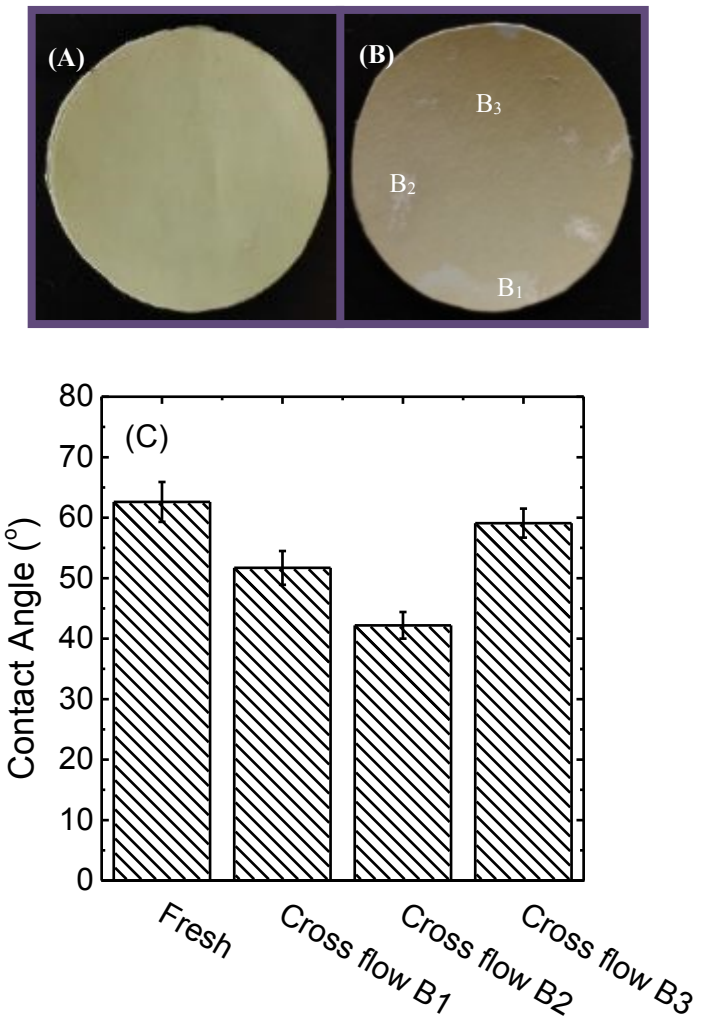

Figure A- 8 Images of the **(A)** freshly modified $(PEI\text{-}CuNPs/PAA)_{10}$ membrane; **(B)** membranes after cross-flow filtration under 400 psi with DI water for overnight compaction and with 3000 mg/L NaCl for 24 h filtration. **(C)** The contact angles of different membranes.

After the cross-flow filtration, the surface of the $(PEI\text{-}CuNPs/PAA)_{10}$-modified membrane showed uneven color which indicated a varied release rate of CuNPs from the different parts of the membrane in the salt solution. The relatively white part of the membrane showed a decreased contact angle (42.2±2.2º at point B2 and 51.7±2.4º at point B1) in comparison to the freshly modified membrane (62.6±3.3º), which was caused by the elapse of the CuNPs. Since the surfaces remained more hydrophilic than the pristine RO membrane (52.5±2.1º), it was possible that the PEI/PAA remained on the membrane surface even after the release of CuNPs.

Table A- 1 Content of main elements on pristine and different numbers of (PEI-CuNPs/PAA) bilayer modified membrane surfaces as measured by XPS.

Membrane	Carbon (%)	Oxygen (%)	Nitrogen (%)	Copper (%)
Pristine	75.8 ± 0.4	13.4 ± 0.3	10.8 ± 0.1	0.0 ± 0
2 bilayers	62.6 ± 1.0	20.2 ± 0.3	9.3 ± 0.3	7.3 ± 0.3
6 bilayers	63.5 ± 1.9	19.4 ± 0.8	11.6 ± 0.6	7.4 ± 0.7
10 bilayers	64.1 ± 2.5	19.1 ± 1.8	10.6 ± 1.4	6.9 ± 1.5

Table A- 2 Surface roughness of pristine and different numbers of (PEI-CuNPs/PAA) bilayer modified membranes, determined by AFM analyses.

Membrane	R_a(nm)	RMS (nm)	R_{max}(nm)	SAD (%)
Pristine	50.4 ± 8	62.9 ± 9	454 ± 14	58.4 ± 14.2
2 bilayers	62.3 ± 7	50.1 ± 18	528 ± 26	20.9 ± 7.8
10 bilayers	65.7 ± 11	89.9 ± 13	672 ± 71	1.52 ± 3.7

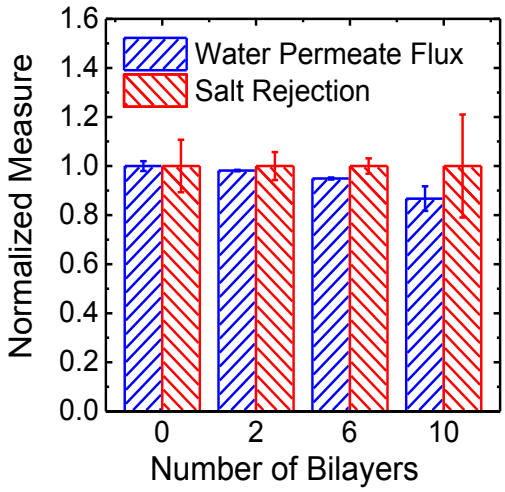

Figure A- 9 Normalized water permeability and salt rejection of pristine (0 bilayer) and modified membranes. The pristine RO membrane showed the water-permeate-flux of 1.59 ± 0.18 L m^{-2} h^{-1} bar^{-1}.

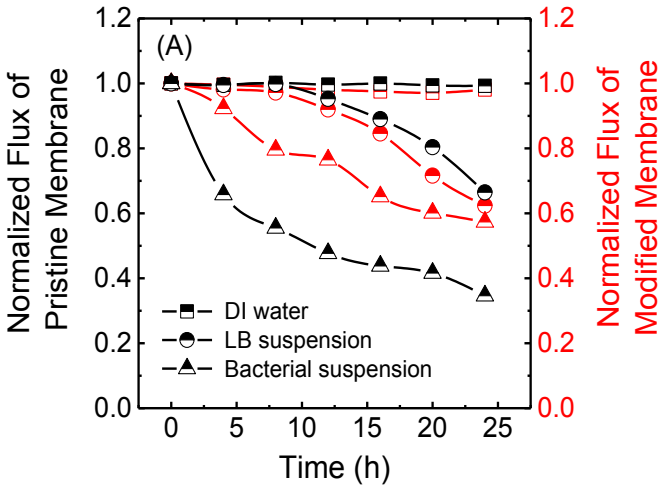

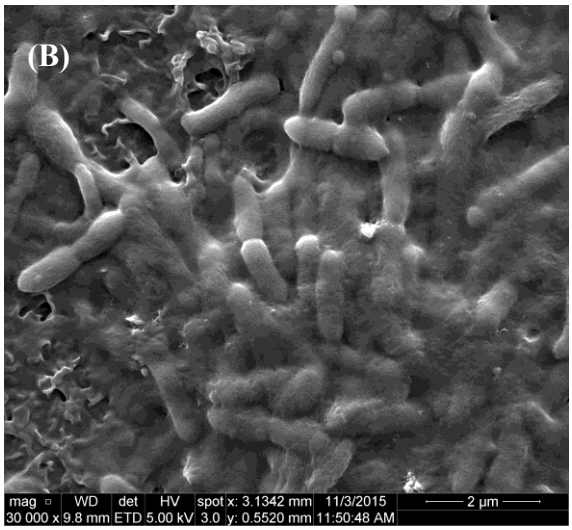

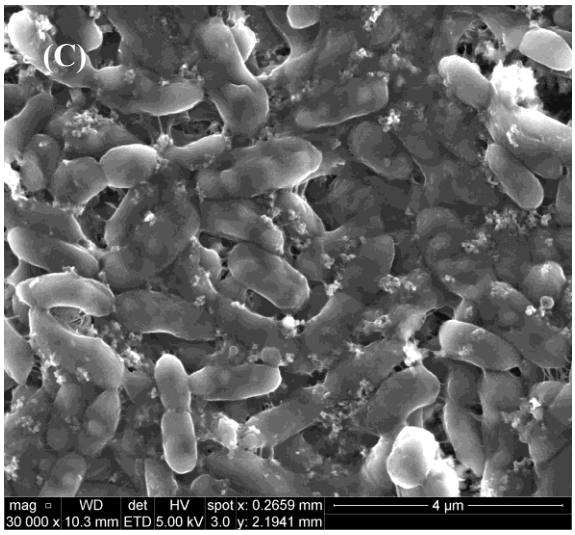

Figure A- 10 (A) The normalized water flux changes of pristine (black color) and (PEI-CuNPs/PAA)$_{10}$ modified membranes (red color) tested with three different feed solutions: (i) DI water, (ii) LB solution (containing 0.1% LB in 10 mM NaCl), and (iii) bacterial suspension (10^5-10^6 CFU/mL in LB solution). SEM images of **(B)** pristine and **(C)** (PEI-CuNPs/PAA)$_{10}$ modified membrane surfaces after 24 hours filtration under bacteria suspension without rinse.

Figure A- 11 Membrane modification frame.

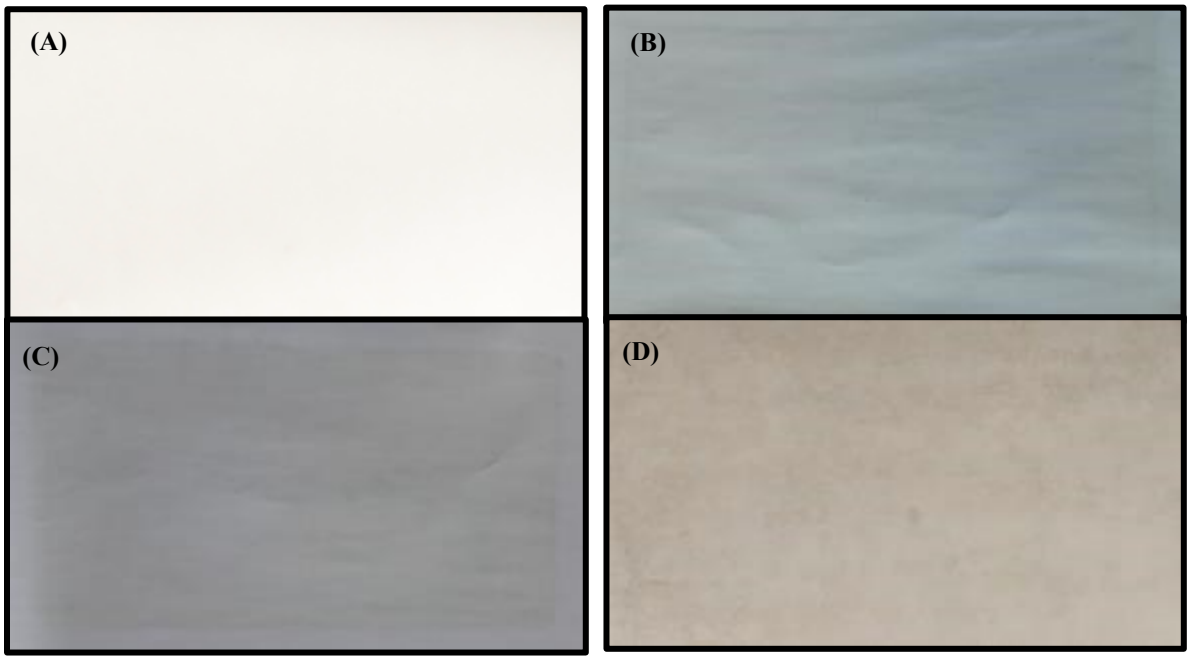

Figure A- 12 Images of (A) pristine RO, (B) RO-Cu, (C) RO-Cys-Cu and (D) RO-GO-Cu.

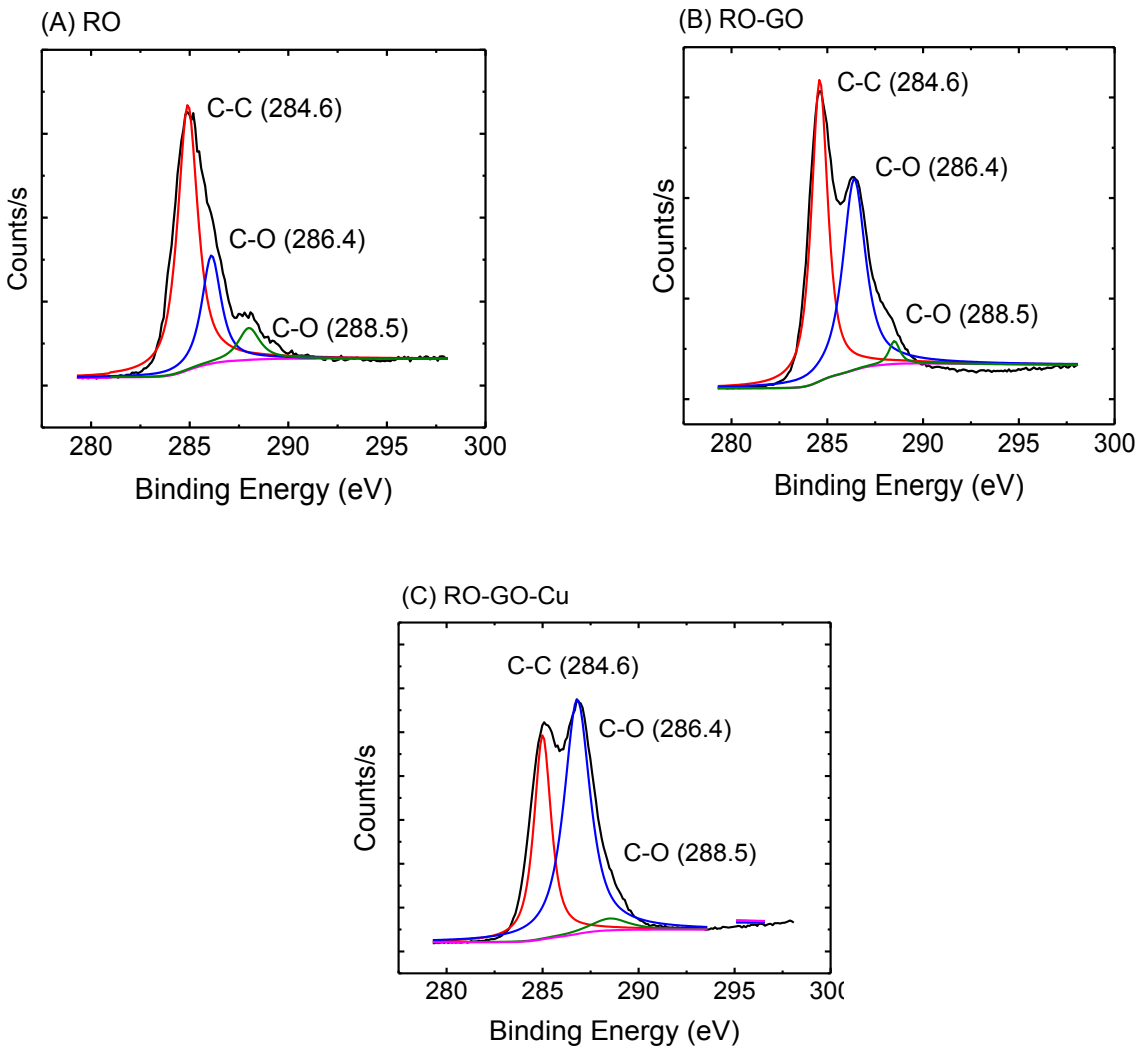

Figure A- 13 XPS analysis for carbon spectra on the (A) Pristine RO, (B) RO-GO and (C) RO-GO-Cu surface.

Table A- 3 Percentage of the chemistry bond of C spectra

	C-C (284.6)	C-O (286.4) & C= O (288.5)
RO	65.8 ± 2.1%	34.2 ± 0.8%
RO-GO	51.8 ± 1.1%	48.2 ± 1.7%
RO-GO-Cu	22.4 ± 0.4%	79.6 ± 3.3%

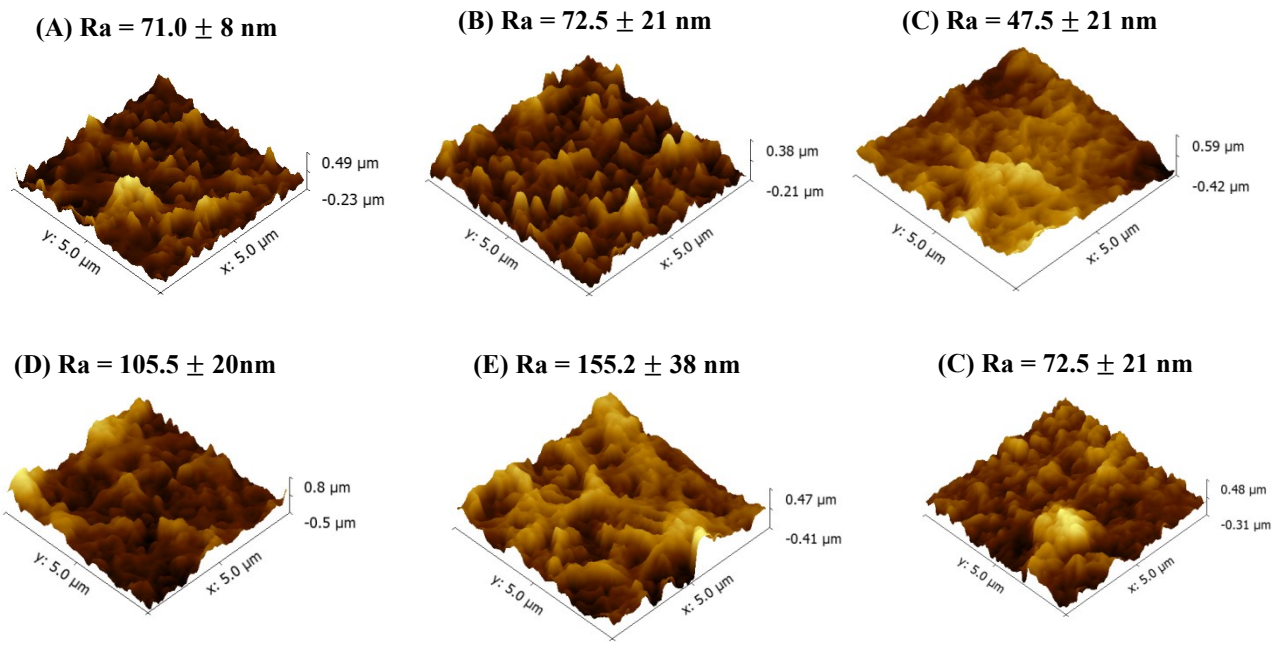

Figure A- 14 AFM images of the membrane surfaces for (A) Pristine RO, (B) RO-Cys, (C) RO-GO, (D) RO-Cu, (E) RO-Cys-Cu and (F) RO-GO-Cu.

Table A- 4 Surface roughness of the pristine and modified membranes

Membrane	R_a(nm)	RMS (nm)	R_{max}(nm)	SAD (%)
RO	71.0 ± 8	91.1 ± 10	382.5 ± 40	44 ± 4.2
RO-Cu	105.5 ± 20	206.2 ± 16	690 ± 179	77.8 ± 5.2
RO-Cys	72.5 ± 21	92.4 ± 23	396.1 ± 101	59.1 ± 2.9
RO-Cys-Cu	155.2 ± 38	305.9 ± 23.7	696.3 ± 91	85.3 ± 2.9
RO-GO	47.5 ± 11	61 ± 6	269 ± 79	27 ± 2.1
RO-GO-Cu	93 ± 5	122 ± 8	475 ± 102	71.5 ± 8.1

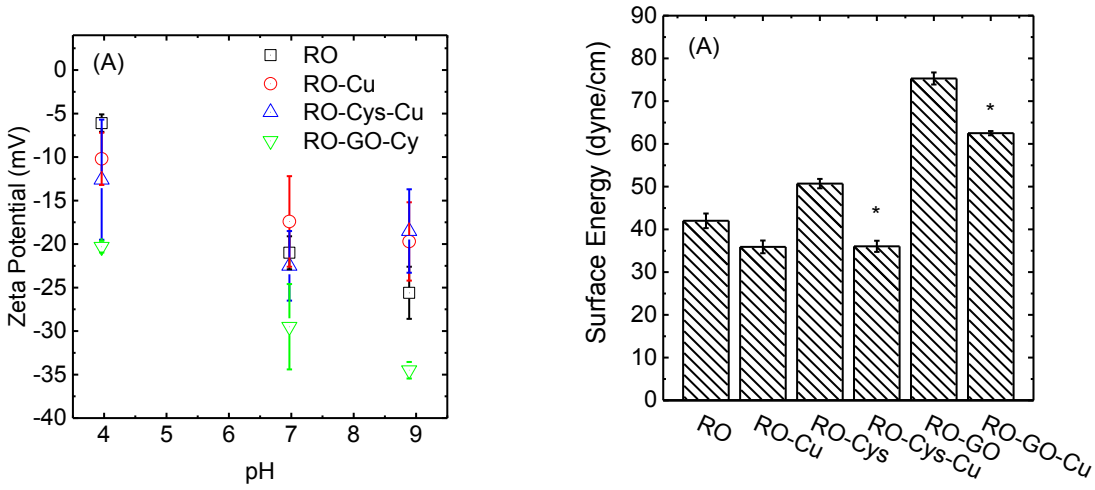

Figure A- 15 (A) Zeta potential of pristine membrane and CuNPs modified membranes under different pH conditions; **(B)** surface energy of the pristine and modified membranes. Asterisks (*) indicate a statistically significant difference between the RO-Cu and RO-Cys-Cu/RO-GO-Cu memrbanes ($p < 0.05$).

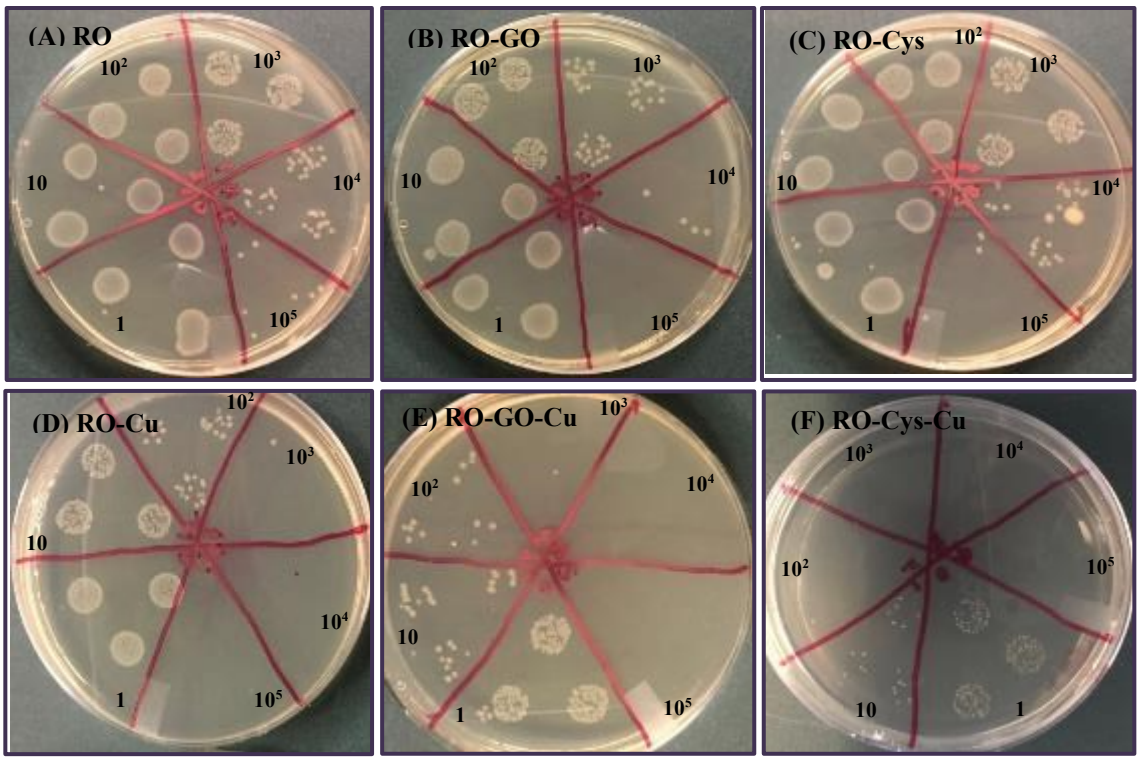

Figure A- 16 Images of the attached live bacteria colonies (CFU) on the pristine and modified membranes. During the experiment, the 3.8 cm^2 membrane sample contacts with 1 mL of 10^7 ~ 10^8 CFU/mL bacteria for 2 hours. Each petri-dish is divided into 5 zones and represents the bacteria solution is diluted 1, 10^2, 10^3, 10^4, 10^5 times.

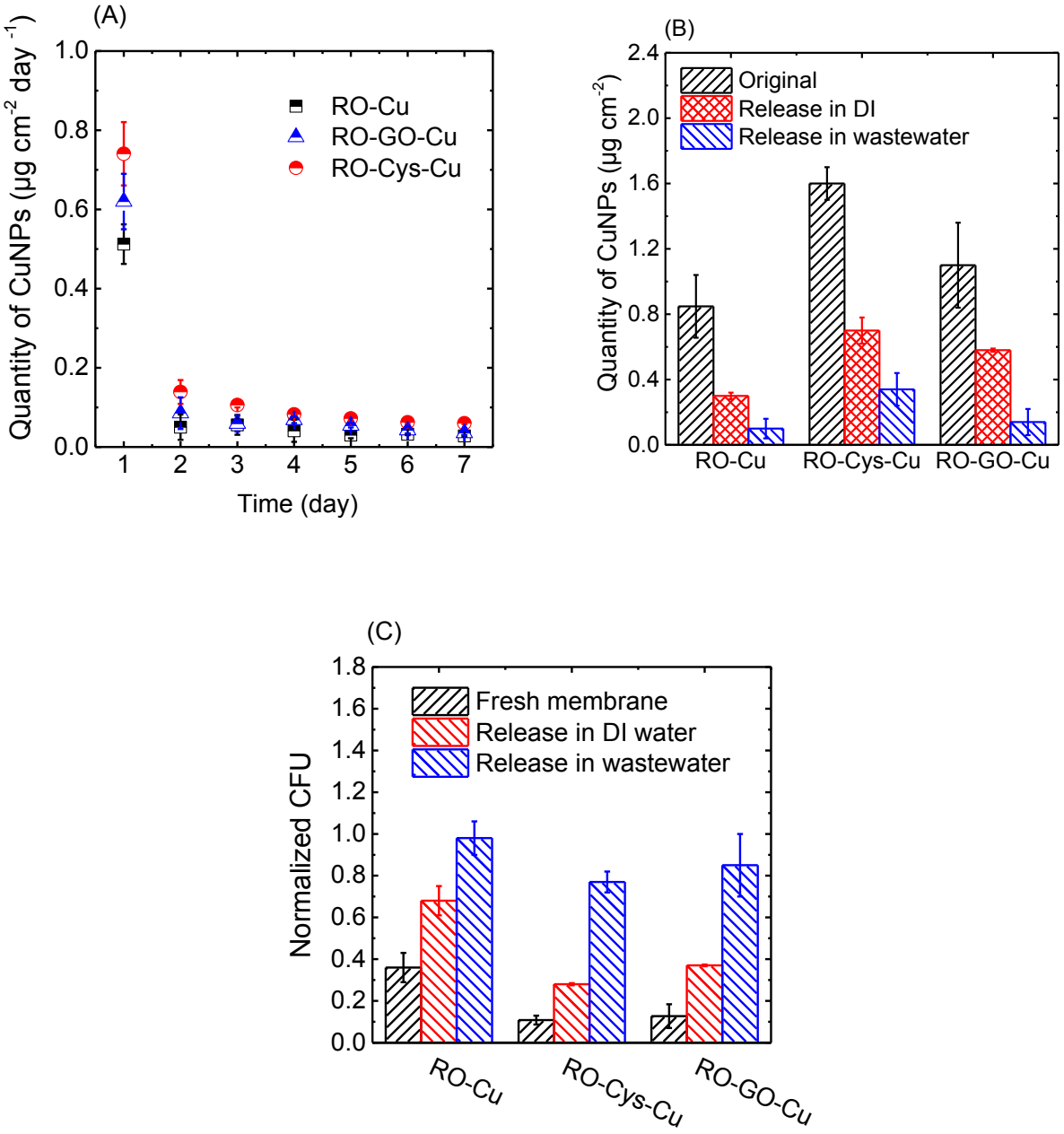

Figure A- 17 (A) The release rate of CuNPs on membrane. During the batch test, a 3.8 cm^2 membrane coupon was incubated in 40 mL DI water and synthetic wastewater under rotation. The solution was replaced every 24 h. **(B)** The quantity of CuNPs remaining on the membrane surface before and after the 7-day release in DI water and synthetic wastewater. **(C)** Number of attached

live bacteria colonies (CFU) on modified membranes after 7-days' release test (the value is compared to that on a pristine membrane under a same batch test, $N/N_{pristine}$).

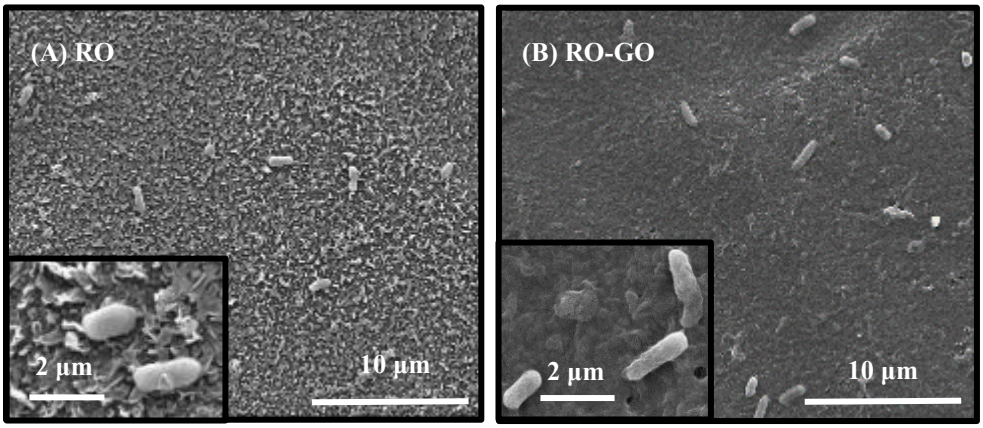

Figure A- 18 SEM images of bacteria cells (*E. coli*) on a **(A)** pristine polyamide membrane and **(B)** GO-modified membrane. Membrane samples contacted with 1 mL of $10^7 \sim 10^8$ CFU/mL *E.coli* solution for 2 hours.

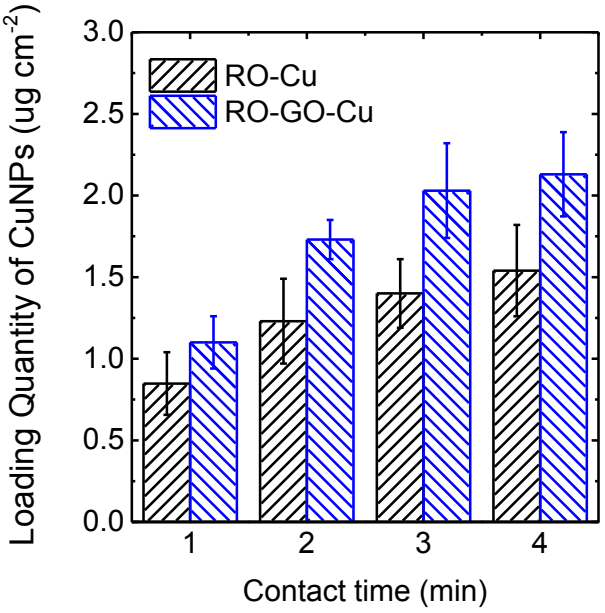

Figure A- 19 Quantity of CuNPs loaded on the pristine membrane surface and GO-coated membrane surface with different contact time between Cu^{2+} and the membrane.